

Università Ca' Foscari Venezia

Dottorato di Ricerca in Scienze Ambientali, Ciclo XXII

(A. A. 2006/2007 – A.A. 2008/2009)

COASTAL PLAIN IN NORTHEASTERN BUENOS AIRES PROVINCE:
HYDROGEOLOGICAL CHARACTERISTICS

SETTORE SCIENTIFICO DISCIPLINARE DI AFFERENZA: GEO/05

Tesi di dottorato di Jerónimo Enrique Ainchil, matricola 955399

Coordinatore del dottorato
Prof. Bruno Pavoni

Tutore del dottorando
Prof. Giovanni Maria Zuppi

Co-tutore del dottorando
Dr. Andrea Mazzoldi

RIASSUNTO

I concetti di sviluppo sostenibile, gestione integrata delle aree costiere, iniziative come la “Ramsar Convention”, e più in generale tutti gli sforzi indirizzati alla conservazione ed al recupero ambientale richiedono molteplici informazioni per un’attività decisionale. In questo contesto è essenziale comprendere il comportamento delle componenti ambientali e la loro interazione.

L’acquisizione di dati e la elaborazione delle informazioni sono generalmente processi costosi. Inoltre, possono richiedere lunghi tempi di esecuzione. La tesi qui di seguito esposta prevede una sequenza di passi successivi, in cui ogni passo porta ad una maggiore comprensione dei differenti aspetti della idrologia nella zona costiera in NE di Buenos Aires (Argentina), convergendo in una proposta di modello concettuale idrogeologico. Questo modello è la base necessaria per l’assunzione delle decisioni relative allo sviluppo economico e sociale dell’area in esame.

Partendo da una indagine geofisica, è necessaria la realizzazione di perforazioni per verificare la litologia del sistema acquifero. In seguito, viene costruita una rete di monitoraggio per mezzo della quale i dati di livello portano alla conoscenza delle condizioni di flusso e delle relazioni nella dinamica tra i livelli degli acquiferi. Questi pozzi per misure freatiche permettono di ottenere campioni d’acqua che, analizzati, caratterizzano le acque del sistema. Inoltre, è possibile ricostruire la storia delle acque attraverso gli isotopi ambientali.

Le conclusioni evidenziano il contributo di ogni tecnica adottata alla costruzione di un modello ed i vantaggi derivanti dall’integrazione delle informazioni ottenute.

Alla fine, si può concludere che è fondamentale conoscere le caratteristiche delle risorse naturali per indirizzare le politiche di sviluppo regionale.

ABSTRACT

The concepts of sustainable development, integrated management of coastal zones, initiatives such as the Ramsar Convention, and in general all the efforts aimed at environmental conservation and recovery require information for decision-making. In this context, it is essential to understand the behaviour of environmental components and their interrelation.

Data acquisition and information processing are usually expensive processes. Besides, they can last long periods of time. This thesis involves a sequence in which each step makes it possible to advance in better understanding of the different aspects of the coastal zone in NE of Buenos Aires (Argentina) hydrogeology, concluding in the proposal of a model. This model is the necessary basis for decision-making related to economic and social development of the analysed area. This area has an important industry activity.

Starting from a geophysical survey, the construction of boreholes is undertaken in order to verify the lithological sequence of the aquifer system. Afterwards, a monitoring network is constructed, and data of levels enabling knowledge of flow conditions and the dynamic relation of aquifer levels are collected. These boreholes also enable us to obtain samples to be analysed and that characterise waters in the system. Moreover, it is possible to reconstruct the history of waters with environmental isotopes.

The conclusions highlight the contribution of each technique to the construction of a model and the advantages of constructing a model integrating the information processed by the methodologies used.

Finally, it should be noted that it is significant to know the features of natural resources in order to establish regional development policies.

ACKNOWLEDGMENTS

The author wishes to thank the following people and institutions:

Professors Giovanni Maria Zuppi and Bruno Pavoni, Università Ca' Foscari di Venezia

Dr Andrea Mazzoldi, ISMAR-CNR - Venezia

Dr Luigi Tosi, Dra Federica Rizzetto and Dr Maurizio Bonardi, ISMAR-CNR - Venezia

Professor Eduardo Kruse, Universidad Nacional de La Plata, Argentina

Dr Sebastián Pera, DACD-IST-SUPSI - Switzerland

Dr Daniel Nieto Yabar, OGS - Trieste

Marco Giada, Morgan S.r.L. – Venezia

Dra Cristina Dapeña, INGEIS, Universidad de Buenos Aires, Argentina

Nicoletta, Eloissa and Samanta

All the CNR – ISMAR – Venezia - SS Apostoli's staff

ALFA – Europe Aid – Co operation office

INDEX

1. INTRODUCTION AND SCOPE	1
2. GENERAL CHARACTERISTICS OF THE AREA	6
2.1 Location	6
2.2 Social and economic aspects	7
2.3 Climate	10
2.4 Soil	16
2.5 Surface water resources	17
3. GEOLOGICAL SETTING	19
3.1 Regional and structural geology	19
3.2 Geomorphology	21
3.3 Stratigraphy	27
3.4 Hydrogeology	28
4. MATERIALS AND METHODS. RESULTS	33
4.1 Geophysical survey	34
4.1.1. Vertical Electrical Sounding	35
4.1.2 Electrical Imaging	42
4.2 Geological profile	49
4.3 Monitoring network	55
4.4 Level variation	63
4.5 Groundwater flux	66
4.6 Groundwater chemical features	70
4.6.1 Chemical characteristics of the phreatic layer	71
4.6.2 Chemical characteristics of Pampeano and Puelche aquifers	82
4.6.3 Minor ions and trace elements	89
4.7 Environmental isotope results	95
4.7.1 Stable isotopes	97
4.7.2 Tritium	103

5. DISCUSSION	107
6. CONCLUSIONS	111
7. THEORETICAL BACKGROUND	116
8. BIBLIOGRAPHY	182
9. ANNEXES	195

1. INTRODUCTION AND SCOPE

It is known that water is one of the bases of life as well as a resource of primary importance for the socioeconomic development of a region and the preservation of its environmental characteristics. Understanding how water behaves and conducting a relevant follow-up is becoming more important every day, not only to correctly plan the use of water but also to anticipate any quali-quantitative alteration of this resource.

Problems derived from the pollution of water resources have led to acknowledge the need to advance in the scientific knowledge of global hydrological aspects with an interactive view from all the disciplines involved in the study of this resource (Eagleason 1991).

Regions with less socioeconomic development, which are more frequent in new countries like Argentina, are usually characterised by deficiency in the understanding of groundwater behaviour. This is especially due to a lack of information about the physical media related to the subsoil (deep drilling) and about measurements of the hydrodynamic and hydrochemical system. It is assumed that, because of its recent history and natural conditions, a new country is one in which man is being faced with an incipient "crisis" with natural resources, becoming aware of the importance of knowing more about them (Room et al 1983).

The previous concepts applied to our country cannot be considered without the hydrological issue of big plains. Generally, the less known characteristics in flat environments are:

- a) predominance of water vertical movements (evapotranspiration - infiltration) over horizontal ones (runoffs)
- b) a strong relationship between surface water and groundwater in every hydrological process.

The most recent advances focused on this (Kruse and Zimmermann, 2002) because groundwater is an important element in environmental

matters due to the quantification of processes of infiltration, evapotranspiration, water transport in the non-saturated zone (NSZ) and in the saturated zone (SZ).

Scientific research should at first contemplate a global analysis of a region and adapt to different spatial and temporary scales. Such research and an integrated treatment of the cycle (surface water, groundwater, hydrometeorological variables) are essential to take actions towards a balance between maintained socioeconomic development, water needs and the environmental protection of plains. The topics covered in this thesis tend to satisfy precisely these requirements according to three working focal points:

- Regional characterisation of hydrological processes
- Quantification and modelling of the above-mentioned processes at basin level
- Detailed description of methodologies or technologies for measuring the characteristics of these processes

Different methodologies and techniques, some regarded as traditional and some as innovative, have been used to study the region. Geophysical exploration, hydrogeochemical characterisation, environmental isotope identification and drilling construction have been included. Synergic results, contributing to an integrated model for the area of study, have been obtained from the combination of these techniques.

The area of study comprises the coastal plain of Río de La Plata (Argentina). The urban process began 100 years ago in this area. Urbanisation modified natural conditions: elevation of natural terrain and changes in natural drainage, industries and city establishment. Such coastal plain, with still almost the same natural conditions, was investigated in the north of this area by Pera (2004).

In the region under study the current conditions include intensive land use, groundwater overexploitation, solid waste disposal and industrial issues. These conditions have produced different effects, which will be analysed later on:

- Reduction of pluviometric infiltration
- Reduction of evaporation and transpiration phenomena
- Increase in surface water streams
- Groundwater chemistry quality alteration

Finally, it should be noted that Integrated Coastal Zone Management (ICZM) has been designed to 'join up' all the policies that have an effect on coastal regions. It deals with both planning and management of coastal resources and coastal space. ICZM is not just an environmental policy. Although the need to protect natural ecosystem functioning is one of its key aims, ICZM also seeks to improve the economic and social well-being of coastal zones and help them develop their full potential as modern, vibrant communities. In the coastal zone, these environmental and socioeconomic goals are intrinsically interconnected.

All the management activities related to subsurface resources require the understanding of its features, characteristics and properties.

Objectives

The overall objective of this thesis is to describe groundwater behaviour in the area of study. This behaviour is essential for defining environmental management criteria for regional sustainable development.

The specific objectives are:

- To use geophysical methods to determine groundwater characteristics, especially to recognise soil composition.
- To perform boreholes to verify hydrogeological conditions.
- To install and operate a groundwater monitoring network.
- To describe the main features of groundwater level variations.
- To analyse hydrochemical features of aquifer units.
- To isotopically characterise groundwater.
- To deepen our knowledge of the behaviour of infiltration, flux, and contamination in natural conditions or in areas with human activities.
- To use several techniques to obtain an accurate model.
- To formulate a conceptual model of groundwater behaviour.

Organisation of the thesis

This thesis is divided into seven chapters that approach each thematic unit.

Chapter 1 is an introduction.

Chapter 2 introduces the area of study. First, the geographical location is included. Second, social and economic characteristics are discussed. Third, the physical features of the region are described: weather, soils and surface water resources. This chapter has been based on a compilation of background information.

Chapter 3 deals with regional geological and hydrogeological characteristics in terms of an analysis of the compiled precedents.

Chapter 4 describes all the tasks undertaken here for each of the topics mentioned above. Two types of objectives are distinguished in the geophysical survey: one exploring the lithological section of interest in all its depth and the other dealing with high-definition shallow exploration that enables a detailed characterisation of shallow

subsurface. The techniques used for analytical determination, limit of quantification, sampling standards and display of graphical results are included with chemical data. Origin and estimation of groundwater age is recognised with the application of isotopes.

Chapter 5 discusses the results as a whole and introduces a model.

Chapter 6 displays the conclusions and recommendations.

Chapter 7 concerns the theoretical background and methodologies used throughout this thesis. First, the geophysical methods employed here are included. Second, the hydrogeochemical concepts are described. And finally, the application of environmental isotopes to study groundwater evolution is summarised.

2. GENERAL CHARACTERISTICS OF THE AREA

2.1 Location

The area of study is located in the República Argentina in South America (Figure 2.1.1)



Figure 2.1.1 República Argentina in South America

in the northeastern region of the Province of Buenos Aires (Figure 2.1.2)

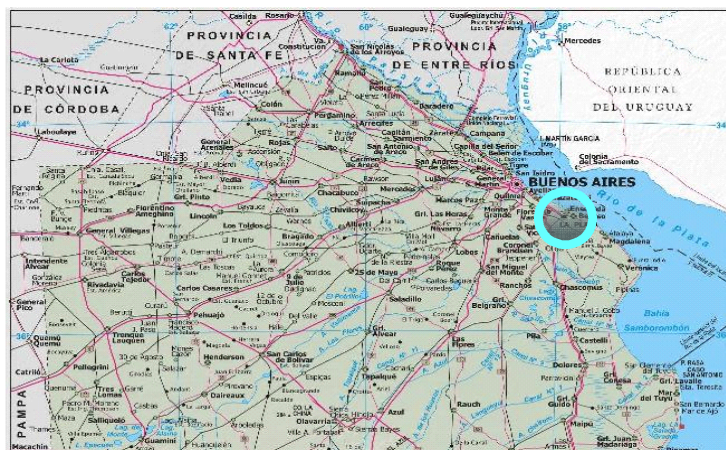


Figure 2.1.2 N.E. of Buenos Aires province

in the cities of Berisso and Ensenada, close to La Plata city (Figure 2.1.3)



Figure 2.1.3 Cities of Berisso and Ensenada

2.2 Social and economic aspects

The moderate weather and the particular location of the region are ideal for business settling because of its proximity to the largest Argentine population and industrial conglomerate, called Conurbano Bonaerense (the suburbs of Buenos Aires) and to Ciudad Autónoma de Buenos Aires (Buenos Aires city). This city has excellent road and rail links as well as seaways and airways. La Plata - Buenos Aires motorway and Autovía 2 (dual carriageway) is very important roadworks. Ferrocarril General Roca (railway line), Puerto La Plata (port) and an airport are also important links.

The area of study has an intermediate population density (66.1 people per km²), lower than the average of Conurbano Bonaerense but higher than the provincial average (46.7 people per km²). The spatial configuration of the region is well-balanced. La Plata (620.3 people per km²) like any capital city of a province, is located among intermediate cities with neighbouring rural areas and has plenty of artistic, cultural and scientific events to offer.

A high proportion of population at a potentially active age is concentrated in La Plata, Berisso and Ensenada districts. This is probably due to migratory phenomena, the attraction exerted by universities or demand for both industry and public sector jobs.

Partido	Población		
	Total	Varones	Mujeres
Berisso	80.092	38.950	41.142
Ensenada	51.448	25.135	26.313
La Plata	574.369	277.587	296.782

Access to the area

Road access. The primary routes that run through the region are the national routes 2, 3 and 11 and the provincial ones, 6 and 205. It is also important to mention La Plata - Buenos Aires motorway, which connects both cities as well as Berazategui, Avellaneda and Quilmes districts. In addition to connecting those two cities, route 2 links the region under study with Mar del Plata city going through important localities.

Fluvial and maritime access. The area of study includes Puerto La Plata. Inaugurated in 1890, this port was built pursuant to the political decision to found a city with the same name as the new capital of the Province of Buenos Aires in 1882. Although the port is provincial, the area of main influence coincides with the region under study. Over many decades, the port has been the epicentre of intense economic activity in the region and boosted the development of the cities of La Plata, Ensenada and Berisso. The port has had numerous uses: liquid and general cargos, with a great deal of movement of meat exports. The advantage of Puerto La Plata over other ports in the region is its connection and ferry services.

Free Trade Zone. La Plata Free Trade Zone is located in a piece of land bounded by Puerto La Plata and Astillero Río Santiago, covers a surface area of 70 hectares and has good road and maritime access. This strategic location has turned the Free Trade Zone into an international distribution and logistics centre with about 180 currently settled direct users.

Railway access. Ferrosur Roca S.A. is the cargo operator that connects the main production centres in the south and east of Buenos Aires Province. Most non-metallic minerals and building materials are transported by the national railway system through Ferrosur Roca from the cement plants in Olavarría. In fact, in 2005, 65% of the total freight of such branch line comprised this type of product.

Educational level

Overall, the region shows very good educational indicators compared to the rest of the Province of Buenos Aires and the country. The percentage of students attending educational institutions is higher than the average of the province and country, especially in basic education, that is, education for three- to fourteen-year-olds.

A high attendance percentage is also observed in the group encompassing fifteen- to seventeen-year-olds. This percentage equals or surpasses the average of the whole country.

The age group receiving higher education reveals very good indicators, too. La Plata should be highlighted since it easily surpasses the percentages of the country and the whole Province of Buenos Aires.

Regional industry. General Characteristics

Analysing the gross value of industrial output (GVIO) per district in 1993, a high concentration is observed in Ensenada district (66%),

followed by La Plata districts. The sector of chemical products, by-products of oil, carbon, rubber and plastics accounts for 67.3% of GVIO of the region. Most of the activity involved in this sector takes place in Ensenada district, the main petrochemical complexes in Argentina. Moreover, this activity is the most important one in La Plata district.

The basic metal manufacturing industry represents 11% of the region and is especially concentrated in Ensenada district. On the other hand, food, beverage and tobacco production represents 10.9% of the region and La Plata district is the most representative of this activity.

To sum up, the processes of urbanisation and industrialisation in the analysed region have taken place over a period of more than 100 years.

2.3 Climatic characterisation

The region is subject to mild and wet climate, with average annual rainfall that is slightly higher than 1000 mm and an average annual temperature of 15.7° C. The data obtained within the period 1991-2000 from the reference meteorological station that is closest to the project's area (No. 87593 of the World Meteorological Organization, WMO) was used to describe the area in terms of climate. These data belong to La Plata Aero (National Weather Service) and have the following geographical coordinates: Latitude: - 34.58° S. Longitude: - 57.54° W. Altitude: 19 metres a.m.s.l.

Precipitation

Figure 2.3.1 shows the average monthly precipitation from 1991 to 2000.

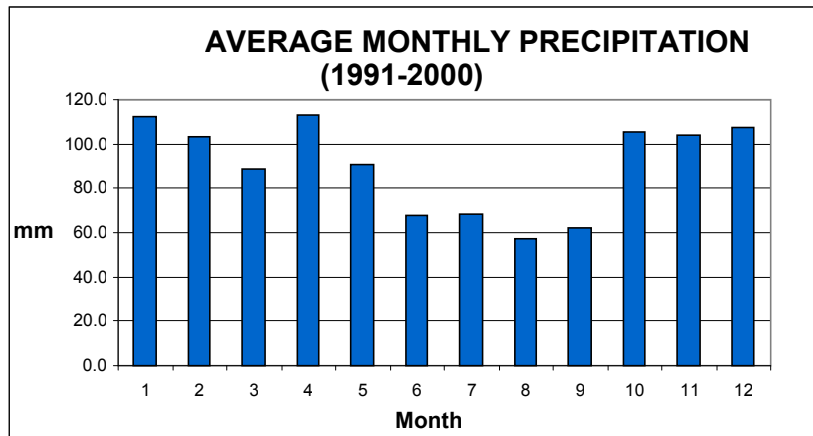


Figure 2.3.1. Average monthly precipitation

Although rainfall is irregularly distributed throughout the year, its intensity is higher between October and April. The total average reaches 1079.3 mm/yr. Summer and autumn are the most humid seasons and winter is the driest one in the rainfall pattern. Mean seasonal precipitation (1991-2000) is distributed according to the values shown in Figure 2.3.1, with its maximum in April (113.1 mm) and its minimum in August (57.5 mm).

Temperature

The average annual temperature from 1991 to 2000 is 15.7° C. Figure 2.3.2 shows the maximum, minimum and mean temperatures of La Plata. In summer, the highest mean temperature value is registered in January: 21.2° C. The maximum mean monthly value is 24.4° C and is registered in January whereas the minimum mean monthly temperature is 6.3° C and is registered in July.

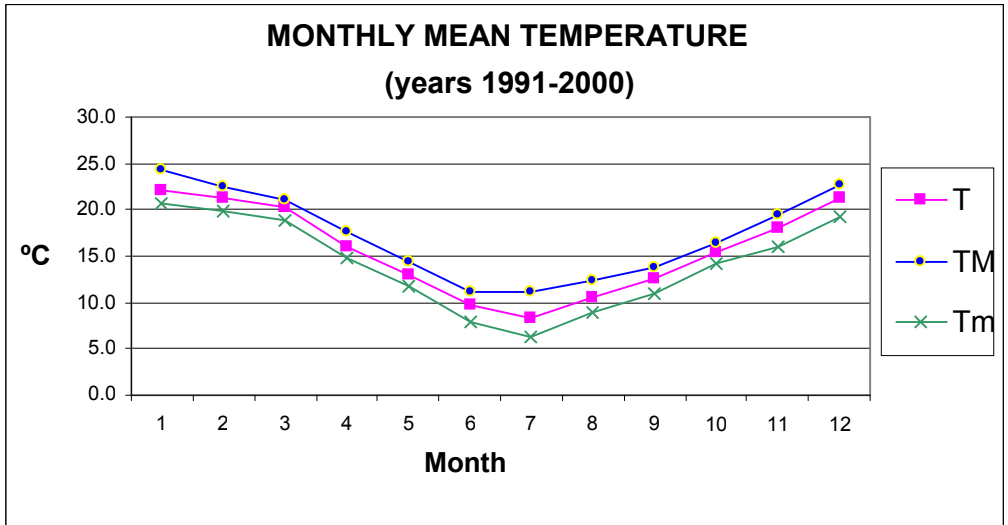


Figure 2.3.2 Maximum, minimum and mean monthly temperatures (La Plata Aero Reference Station).

Winds

Figures 2.3.3, 2.3.4 and 2.3.5 show the mean monthly wind speed and the mean wind speed and frequency in terms of direction.

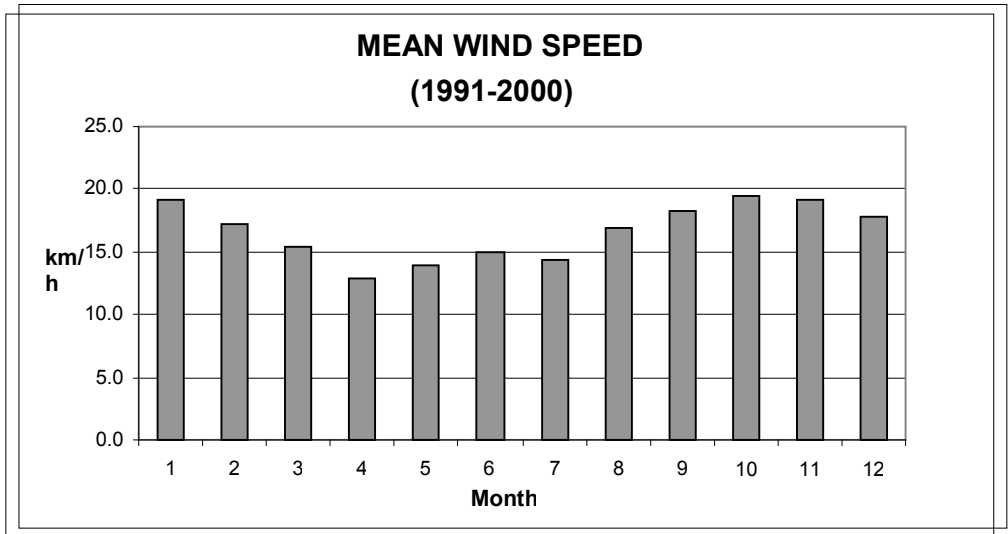


Figure 2.3.3. Mean wind velocity (La Plata Aero Reference Station)

The mean annual wind speed is 18.9 km/h. The maximum velocity has been recorded in August, with 25.9 km/h, followed by that of February,

with 24.1 km/h. The highest frequency of winds comes from the east and northeast directions.

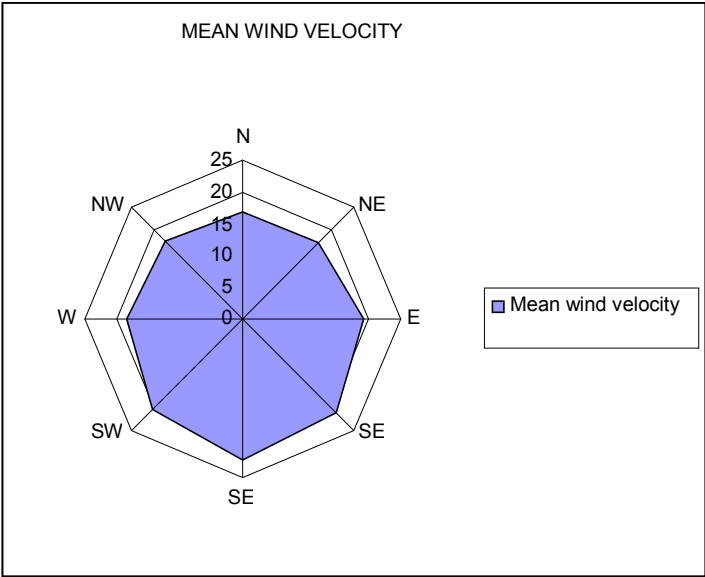


Figure 2.3.4. Mean wind velocity in terms of direction (La Plata Aero Reference Station)

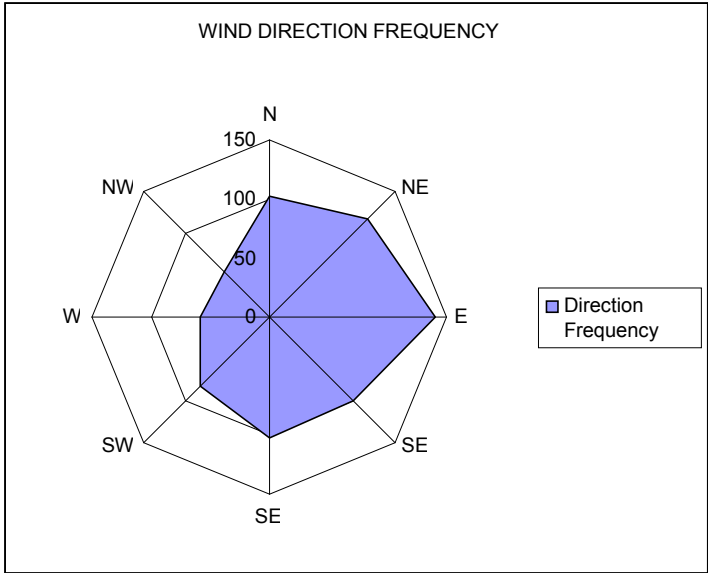


Figure 2.3.5. Wind direction frequency in terms of direction (La Plata Aero Reference Station)

Atmospheric pressure

The atmospheric pressure data shown in Table 2.3.1 belong to La Plata Aero Reference Station. In other words, these data are the pressure values at the station level in hectopascals (hPa). Mean atmospheric pressure ranges from 1008.5 hPa in December to 1017 hPa in July.

Table 2.3.1: Atmospheric pressure

AP	JAN	FEB	MAR	APR	MAY	JUN
(hPa)	1009.1	1011.0	1011.9	1012.8	1014.9	1014.2
AP	JUL	AUG	SEP	OCT	NOV	DEC
(hPa)	1017.0	1016.6	1015.7	1013.7	1011.2	1008.5

Relative humidity

Figure 2.3.6 shows the mean monthly relative humidity variations. The figures obtained here indicate an average of 76.73% throughout the year, with seasonal variations that do not differ from the aforementioned value in more than 10%.

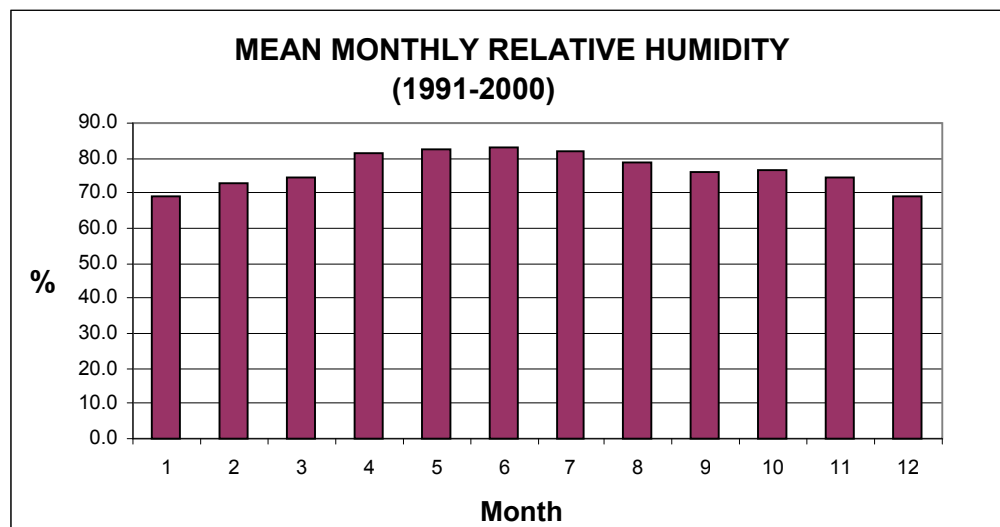


Figure 2.3.6. Mean monthly relative humidity from La Plata Aero Station.

Water budget

In order to estimate real evapotranspiration, Thornthwaite method was used (Thornthwaite y Mather, 1955). The values obtained are shown in Table 2.3.2.

Table 2.3.2. Water balance following Thornthwaite method (EVT: evapotranspiration)

	SEP	OCT	NOV	DEC	JAN	FEB	MAR	APR	MAY	JUN	JUL	AUG	Total
temperature	12.5	15.5	18	21.2	22.1	21.2	20.2	16.1	12.9	9.8	8.3	10.6	
Heat Index	4.00	5.55	6.95	8.91	9.49	8.91	8.28	5.87	4.20	2.77	2.15	3.12	70.21
Potential EVT	40.4	57.0	72.4	94.2	100.7	94.2	87.2	60.6	42.5	27.3	20.9	31.0	
No. days month	30	31	30	31	31	28.3	31	30	31	30	31	31	
No. daylight hours	12.5	11.2	10	9.4	9.7	10.6	12	13.3	14.4	15	14.7	13.7	
Actual EVT	42.0	55.0	60.4	76.2	84.1	78.3	90.1	67.1	52.6	34.1	26.5	36.6	703.1
Precipitation	62.1	105.1	104.3	107.1	112.2	103.0	88.4	113.1	90.9	67.4	68.2	57.5	1079.3
EVT	42.0	55.0	60.4	76.2	84.1	78.3	90.1	67.1	52.6	34.1	26.5	36.6	703.1
Deficit	0.0	0.0	0.0	0.0	0.0	0.0	0.0	0.0	0.0	0.0	0.0	0.0	0.0
Storage	0	20.1	50.0	50.0	50.0	50.0	50.0	48.3	50.0	50.0	50.0	50.0	
Surplus	0.0	20.2	43.9	30.9	28.1	24.7	0.0	44.3	38.3	33.3	41.7	20.9	326.2

Figure 2.3.7 shows the monthly evolution of soil moisture storage and water surplus.

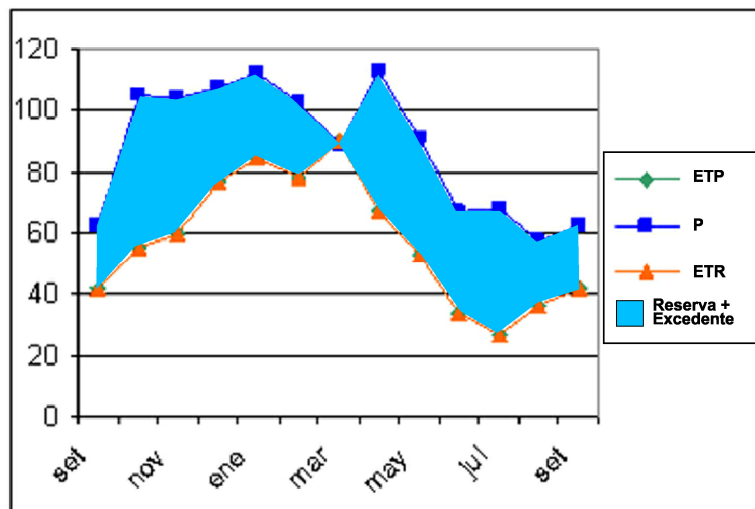


Figure 2.3.7. Evolution of soil moisture storage and surplus

It is possible to carry out a climate classification that reflects a global characterisation of the relevant period with the results yielded from the mean monthly water budgets. According to these indexes, the climate of the region can be classified as B2C'2“r”a', where B2 stands for humid climate and C'2 for microthermal climate (Thorntwaite, op. cit.). This indicates that the regional climate has PE values higher than 570 mm, with nil or little water deficiency (“r”) and a summer concentration percentage of thermal efficiency that is lower than 33.9% (a'). The region can be affected by variations within certain limits that will depend on the particular surplus and/or deficit occurrence of each year.

Normally the climatic characteristics indicate that there is water excess that can cause infiltration, runoff and depress storage.

2.4 Soil. General conditions

Three overlapping materials of different origin can be distinguished in the natural ground of the region:

a) In the surface, approximately from 0.80 to 1.50 m deep, there is highly clayey material, possibly of mixed origin (fluvial and marine), with distinctive contraction-expansion features revealed by abundant landslides and crevices. Traces of clay illuviation (coatings) can be identified, despite being slightly hidden due to contraction - expansion features (Cappannini y Mauriño, 1966).

b) Below is marine origin material of about 1.00 m thick and sandy to sandy loam texture. A series of thick and thin layers mixed with pieces of small shells in different degrees of fragmentation are sometimes observed .

c) Beneath this material, there is intensely-crushed, dun-coloured massive loessial material, with calcium carbonate accumulation that looks like thick concretion, of loamy to silt loamy texture (Pampeano).

All grounds usually have drainage deficiencies due to surface flooding, frequently accompanied by phreatic level close to the surface. That is revealed by hydromorphic features (mottled, iron-manganese concretions) (Giménez et al. 1992). In most cases, the first two materials have high interchangeable sodium content and they sometimes have soluble salts, too.

Because of its drainage deficiency, the highly clayey texture of the soil and its high content of interchangeable sodium and sometimes soluble salts, the ground is suitable only for cattle raising and afforestation with adapted species.

2.5 Surface water resources

In the coastal plain, where the project is being developed, river beds stray, disappearing into Bañado Maldonado and Bañado de Ensenada (marsh). Watersheds practically disappear because of the flat relief and in most cases discharge into Río de La Plata can only be achieved through canalizations.

Most streams are perennial or permanent in the lower stretches of their basins due to underground contribution (Varela et al, 2002). However, in their medium and high stretches, streams become intermittent since their basins are located above phreatic surface. Data from existing measurements (Auge, 1995) show a runoff rate of 6% compared to the rain, with mean water level ranging from 30 to 70 L/s. In the coastal plain, water is most frequently driven into Río de La Plata through canalizations, which have a regional discharge direction towards the northeast.

Due to the topography and drainage net mentioned above, these bodies do not have significant water levels. They constitute bodies of slow flow that can considerably augment in periods of pouring and increasing rain, which are affected by variations in tide and “sudestada”. When river levels rose sharply, most of the natural area is affected by flooding.

The area belonging to Ensenada marshlands naturally represents an area of groundwater discharge. The natural expansion and retraction of flooded surfaces, apart from rising surface water and “sudestadas”, is related to phreatic level rise and depression. Nevertheless, the temporary influence of heavy rain should be highlighted since marshlands additionally receive direct precipitation in the area and influx of courses located in the highest places.

In conclusion, phreatic variations are mainly related to weather conditions. There are both short fluctuations caused by rain and longer fluctuations caused by the alternation of dry and humid periods.

3. GEOLOGICAL SETTING

3.1 Regional and structural geology

The area is located in the Chaco-Pampeano basin on the passive margin of South America (Ramos, 1999), characterised by low tectonic and seismic activity since Mesozoic era (Russo et al, 1979). The basement outcropping on the northern coast readily submerges in a southward direction under the plains, located at -486 meters in La Plata, reaching the deepest point in Salado basin.

Salado basin is a depression that is perpendicular to the coast, genetically linked to the rift valley opened between Africa and South America giving rise to the Atlantic Ocean and being under subsidence for most of its history (Figure 3.1.1) (Rolleri, 1975). Over metamorphic basement and late-Jurassic lower-Cretaceous volcanic rocks, its sedimentary register goes from Middle-Cretaceous to Quaternary, with up to 6000 meters thick, disposed in an overlapping sequence. Deposits are continental and marine changing to exclusively marine origin in the continental shelf (Braccacini, 1980; Tavella and Wright, 1996).

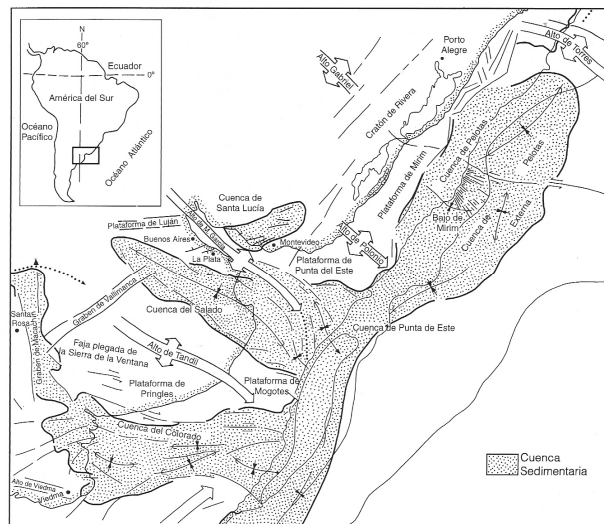


Figure 3.1.1 Structural elements

The upper sequence of the basin is composed of younger than Miocene sediments, which can be divided into three major units (Yrigoyen, 1975). The lowermost is composed of marine origin green clays, the intermediate is composed of fluvial origin sands on the continent changing to marine equivalent facies on the shelf, and the upper terms are represented by loess-like sediments on the continent changing to marine in an arrangement representing at least four different transgressive events (Parker et al, 1999; Violante and Parker, 1999).

Quaternary sea level variations due to glacial periods and eustatic movements deeply affected the geomorphology of the whole area, whose evolution towards the actual state started 2.4 million years ago, when a fluvial environment was installed (Parker et al, 1994). That was followed by successive transgressions and regressions during the Plio-Pleistocene before the post-last glacial maximum transgression (Violante and Parker, 1999).

Guilderson et al (2000) reconstructed a eustatic relative sea-level curve based on AMS ^{14}C dated shells by resampling sediment cores previously analysed by Fray and Ewing (1963) and Parker and Violante (1982). The curve so obtained shows a minimum sea-level ca 16,690 years BP at 157 meters below present sea level, although those data are not conclusive about the position of the last glacial maximum (Violante and Parker, 2003). After subtracting tectonic effects, Guilderson et al (2000) concluded that eustatic component of the sea-level rise during the transgression following the last glacial maximum was 105 meters.

After the last glacial maximum, sea level began to rise. No evidence about changes in rise rate was found before 8,600 years BP. However, certain erosive features exposing Plio-Pleistocene marine sequences and interrupting the deposition of post-LGM sediments were found in the outer step of Río de La Plata terrace. This suggests an interruption on

the sea level rise (Violante and Parker, 2003). According to Cavalotto et al (1995), Violante and Parker, (2000), and Cavalotto (2003), between 8,600 and 6,000 years BP there was change in rise rate, slowing until it reached the altitude of +6 meters above present sea level, followed by a fall at different rates towards its current position.

3.2 Geomorphology

The area analysed in this work is located within the geomorphologic region known as Undulate Plain (Frenguelli, 1950), in the north of Buenos Aires Province (Figure 3.2.1). The boundaries of the region are:

- NE and E: Río Paraná alluvial plain and Río de la Plata estuary.
- N: Arroyo del Medio and High Plain (Province of Santa Fe).
- W and SW: Dune Plain.
- The southern boundary consists of the watershed with Río Salado basin (Depressed Plain).

The general area is characterised by having a dominant gradient towards NE and extreme altitudes of 30 meters a.m.s.l. in the watershed coincident with the SW boundary and of 0 meters on the banks of Río de La Plata. Extreme topographic gradients range from 1.3 to 0.7 meters/km.

Three main morphological components can be distinguished in the flat region mentioned above, namely, Coastal Plain, Low Plain and High Plain (Cappanini y Domínguez, 1961). Another component encompassing these can also be recognised: Coastal Cliff or Step. The area analysed in this project is located in the flat area of the coastal plain and at the foot of the cliff or step.

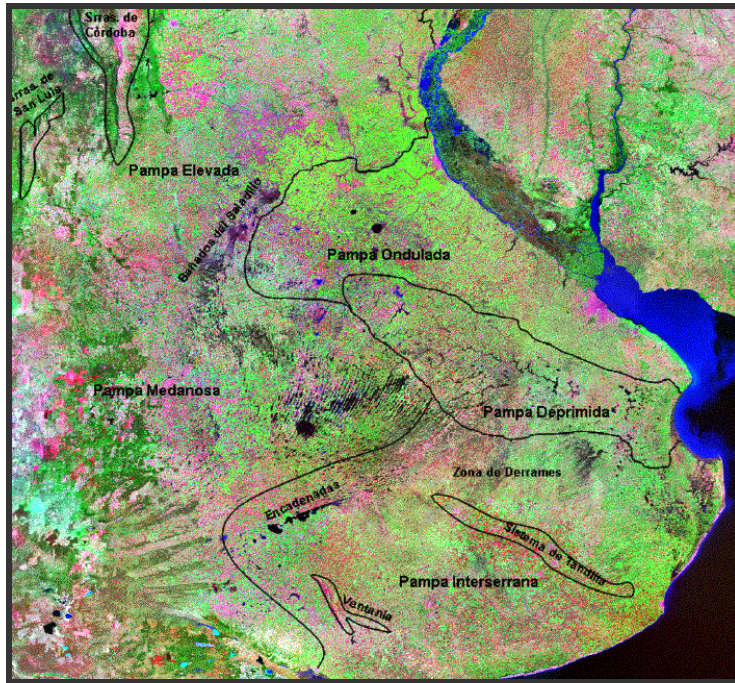


Figure 3.2.1: Geomorphologic regions. The area of study is located within the Undulate Plain

Coastal dynamics of Río de La Plata

The river regime is influenced by discharge of its two main tributaries: Paraná and Uruguay. Their annual discharge is 16,000 m³/s and 6,000 m³/s respectively (C.A.R.P., 1989) and has no significant effect on Río de La Plata level. This river opens out into a wide estuary of approximately 35,000 km², where its levels are regulated by tides and the typical weather conditions: “sudestadas” and cold south winds push its water respectively towards the Argentine coast or the Uruguayan coast.

Tides: A usual tide has very little amplitude (0.46/0.52 m), belonging to a microtidal range. Syzygial mean heights range from 0.67 to -0.08 meters and the quadrature ones range from 0.55 to 0.01 m, decreasing inward (Servicio de Hidrografia Naval, 1993). Tide amplitude also decreases towards the Uruguayan coast, which is accounted for by the

Coriolis effect. The currents generated by these tides play an important role in modelling the riverbed.

Waves: The registered mean wave height is 0.31 meters (Halcrow, 1969). The highest waves occur in the outer sector and the lowest waves occur in the inner one. The wind direction caused by the greatest swells decreasingly blows ESE and E in the external stations whereas in the internal ones it blows E and ESE (C.A.R.P. 1992).

Littoral currents: Littoral currents are induced by waves and generate a flow parallel to the coast, with a resultant on the southern bank of Río de La Plata towards the northeast and southeast of Punta Piedras. These currents cause sediment transport (littoral drift) in opposite direction to that caused by river inflows circulating slightly further away from the shore (Fig.3.2.2.). The effect of the littoral currents is evident due to the definite northeast orientation of the fluvial valleys crossing Buenos Aires coastal plain and of inflowing suspended sediment plumes (Cavalotto, 2005).



Figure 3.2.2.: Satellite image showing the littoral drift in the coastal zone of Río de La Plata

The resulting effect of the factors mentioned above can be shown in current images of the coastal area at low tide, where megaripples are visible on bottom sediments and creeks that are subparallel to the coast. Figure 3.2.2 shows the drift current transport direction.

The coastal plain in the southern bank of Río de La Plata evolved on a modelled substratum during the Holocene transgression. Its current configuration resulted from the process of progradation that took place together with the last relative sea level drop (Parker et al, 1999).

The evolution of the coastal plain was controlled by the interaction of hydrometeorological conditions (wind-wave interaction, currents and tides), muddy depocentre migration, relative sea level fluctuations, and pre-Holocene surface geometry. Sea level geometry and fluctuations determined the distribution, extension and development of sedimentary sequences whereas hydrometeorological conditions established the measurement of sediment inflow and transport (Violante and Parker, 1999).

The most important feature of pre-Holocene surface is the old Río de La Plata fluvial valley. When the last sea level rise reached the top edge of the valley, Punta Piedras (a point located on the southern edge of the coastal plain) acted as the focus of southeastern waves. This triggered the formation of two littoral currents with opposite directions: one northwestward (towards Río de La Plata) and the other southwestward (towards Samborombón bay). Such conditions still exist today.

Coastal evolution is summarised in three moments: estuarine, coastal plain and fluvioestuarine delta, representing the processes of paleovalley fill, coastal progradation and installation of a deltaic system respectively (Cavalotto, 2005).

The coastal plain under study can be divided into the following units (Cavallotto, 2005):

Mud flat. A mud flat appears as a poorly drained flat and concave surface with development of unintegrated wetlands or marshes constituting, in some areas, a true hygrotape covered with scrubs. It consists of a sequence of coastal paleolines whose orientation implies a prograding sequence towards the northeast. It is interpreted as a sequence of wetlands originated in an environment associated with common conditions of the freshwater-saltwater interface.

Coastal levee: “It is a gentle small hill extended along the outer edge of the coastal plain, from the northern end of the area of study to Punta Blanca, except for the area interrupted by an erosive coastal. It consists of a sequence of parallel beach ridges that have grown in the same direction as the littoral drift (towards the NW), and hence enclose a low floodable area behind.

Local characterisation

This research work is done in the geomorphologic unit known as Coastal Plain (Figure 3.2.4). This unit spreads in a strip of 5 to 8 km wide, arranged parallel to Río de La Plata coastline (Fidalgo y Martínez, 1983).



Figure 3.2.3 Landsat image of the area of study

It is a flat relief located between an altitude of 5 meters a.m.s.l. and sea level. It has monotonous features and bad drainage with mean topographic gradients of 0.5 m/km (Laurencena et al, 2002). Surface watersheds do not practically occur here. There are depressed areas, where wetlands and poorly defined watercourses originate. This zone sometimes shows an anarchic drainage design. It contains a sequence of shapes that arose during the Holocene transgressive-regressive cycle.

The Coastal Plain shows several subunits, the largest being called mud flat (Cavallotto, 2005). It is such a scarcely drained flat and concave surface that unintegrated wetlands or marshes develop there. Sedimentary sequences include: a) sandy and clayey silts, b) greenish brown and green to yellowish/greyish green clays which are about 0.80 to 2.50 m thick, and c) a few mollusc valves. Massive brownish-grey loessic material and abundant calcareous concretions appear below, between 2 and 10 m deep (Ensenada Formation). The present wetland soil develops on sediments that are 1.00 to 1.50 m thick. From the surface, it is comprised of fine sequences of dark-brown-to-black plastic and adhesive clays, abounding in iron oxide concretions. Sedimentation conditions are related to clay flocculation in an estuarine environment with distinct signs of continentalization at the end of its evolution.

3. 3 Stratigraphy

The stratigraphic units of the area are well known due to several exploratory boreholes carried out by Secretaría de Minería de la Nación and the former water supply state company Obras Sanitarias de la Nación. In particular, Plaza de Armas well reaches the crystalline basement and contains a detailed log. All depths refer to the topographic 0 IGM.

CRYSTALLINE BASEMENT (Precambrian). Composed of granites and gneiss belonging to the Brazilian Shield, the crystalline basement outcrops on Isla Martín García (50 km north of Buenos Aires) and is located in La Plata (60 km south of Buenos Aires) at -486 m deep.

OLIVOS FORMATION (Lower Miocene) (Groeber, 1945). Over 200 m thick and -486 to -271 m deep, Olivos Formation is comprised of an alternation of red sands and clays with gypsum and calcium carbonate becoming conglomeratic towards the base. Two sections can be distinguished: a) the base, composed of sand and gravel with abundant gypsum intercalations and b) the top, made up of reddish clays with carbonate and gypsum. Under arid climate conditions, the origin of this formation is continental (Aeolian-Lacustrine).

PARANÁ FORMATION (Upper Miocene) (Groeber, 1945). Up to 200 meters thick and -271 to -63 meters deep, Paraná Formation is composed of sequences of red greenish sands and marine origin clays towards the top of the formation (-154 to -63 meters). A psammitic level is found at the base (-271 to -154 meters). It is composed of medium to coarse quartz sands with marine fossils and it is 12 to 20 meters thick. The upper level is constituted by greenish bluish clays, with abundant marine fossils.

PUELCHE FORMATION (Plio-Pleistocene) (Santa Cruz, 1972). Puelche Formation is located in the well at -63 to -44 m, has unconsolidated medium to fine quartz fluvial sand, and is 15 to 25 m thick. The basal section is constituted by fine- and coarse-grained pale yellow sands. Over them there is a section of fine-grained sand with scarce magnetite.

PAMPEANO FORMATION (Upper Pleistocene) (Fidalgo et al, 1975). Up to 50 meters thick and -44 to 0 meters deep, Pampeano Formation is composed of silt and silty sand with volcanic glass and concretion of secondary calcium carbonates of aeolian and fluvial origin. These sediments outcrop in the upper parts of the area, are the components of the high plain (upper terrace) and underlie the Post-Pampeano Formation in the coastal plain.

POST-PAMPEANO FORMATION (Pleistocene-Holocene). Post-Pampeano Formation is comprised of clayey silt and sandy sediments of lacustrine fluvial and marine origin forming the coastal plain. Its occurrence is limited to fluvial valleys linked to the estuary, and its thickness grows and becomes sandier coastward.

3.4 Hydrogeology

The relationship between the geologic units and groundwater flux in the area makes it possible to individuate a three-layer aquifer system where each component of the system has well-defined characteristics.

Regarding Paraná Formation as a point of reference, the characteristics of the hydrogeologic units of the area of study can be summarised as follows.

Hydrogeologic Basement

The Crystalline Basement is the basal aquifuge unit of the aquifer systems that develop above it. It is composed of igneous and metamorphic rocks. It has been reached at different points by several organisations, for instance, at -130.8 meters a.m.s.l. in Paraná Delta and at -466.6 meters in La Plata, tilting steeply towards Río Salado basin. It acts as an impervious base of the aquifer system (Sala, 1975).

Hypo-Paraná Section

On top of Hypo-Paraná Section a continental sedimentary sequence is divided into three subsections. The best known of these subsections is the upper one, Olivos Formation, with approximately 250 meters of red sandstone and clay. This formation has various aquitard levels and some aquifers of variable salinity, which are still little known today.

The sandiest levels of Hypo-Paraná Section have aquifer potential. Although the high dissolved solids preclude its use for the most demanded application: drinking water and irrigation, it is suitable for some industrial applications. Olivos Formation carries high sulphate water with salinity contents from 6 to 60 g/l (Hernández et al, 1975).

Paraná Section

Paraná Section is located above the previous section and is of marine origin. It consists of bluish grey and green clay with sandy intercalations and abundant marine fossils. It abounds in aquiclude sediments and there are some high performance aquifer intercalations. Its thickness increases towards the south of the region and can exceed 500 meters. Moreover, discharges of up to 180 m³/h have been obtained through industrial drilling.

The central problems of exploiting Paraná Section are the aquifer depth and high water salinity, water salinity ranging from 10 to 30 g/l (Hernández et al, 1975). A pumping test performed in aquifer levels of this formation gave a transmissivity value of $5.8 \cdot 10^{-3} \text{ m}^2 \text{ s}^{-1}$ with a storage capacity of $1.1 \cdot 10^{-4}$, values within the range of Puelche unit.

Epi-Paraná Section

Epi-Paraná Section is composed of Puelche, Pampeano and Post-Pampeano sediments.

Although its basal sections have some confining behaviour, Pampeano aquifer acts as a free aquifer. It is recharged by direct rainfall infiltration in the interfluvium, being influent in terms of creeks in undisturbed areas. Besides, it constitutes the only means for receiving recharge and discharge water by vertical movement in the Puelche aquifer.

Puelche aquifer, constituted by the homonymous formation, is the main hydrogeologic unit in the area because of its surface distribution: more than $8.3 \cdot 10^4 \text{ km}^2$ in Buenos Aires Province (Auge y Hernández, 1983). Due to its relative shallow position, good water quality and dense population in the area, it is the most exploited aquifer in Argentina. It is used for public and industrial supply in locations that are not served by treated river water.

The water from Puelche aquifer is good quality, with less than 1 g l⁻¹ calcium bicarbonate type, readily turning to sodium bicarbonate type by flow. Its hydraulic conductivity is about $1.5 \cdot 10^{-5}$ to 5.8 m s^{-1} (Auge, 1990) and its storage capacity is about 0.1 to 0.05. Its regional flow moves towards Río de La Plata, with low regional hydraulic gradient.

High Plain

From a hydrogeologic perspective, the sequence above the Hydrogeologic Basement in the High Plain includes the described sections: Epi-Paraná, Paraná and Hypo-Paraná (Auge, 1995). The first one is the most superficial and encompasses Pampeano sediments and Puelche sands. These units are the most widely known and the most significant ones in hydrologic budgets.

Pampeano sediments include the phreatic table and are located most closely to the terrain surface. It is mainly composed of silt and subordinately composed of reddish brown sand and clay, frequently containing calcium carbonate concretions or banks. It is about 50 m thick. Based on previous experiments, its infiltration capacity ranges from 5 to 10 m/day and its transmissivity coefficient is approximately 200 m²/day.

Puelche sands underlie Pampeano loess and represent the most important aquifer in the northeast of Buenos Aires Province. They can be described as fine- to medium-grained quartz sands, their grains becoming bigger with depth and varying in thickness between about 20 m to 30 m in the analysed area. Average transmissivity is 500 m²/day (Auge, 1995) and water has low salinity (less than 1000 mg/l) and is therefore suitable for human consumption.

Coastal Plain

Parallel to Río de La Plata, the Coastal Plain is the last sector of a series of small streams cleaving La Plata city and its periphery. Some illustrative streams are: El Gato, Maldonado and El Pescado and their affluents (Fidalgo y Martínez, 1983). This plain is a flat environment developed between altitudes of 5 to 0 metres a.m.s.l., with mean topographic gradients of 0.5 m/km.

This monotonous, badly-drained relief, where surface watersheds do not practically occur, is locally interrupted by swells (sand levees and shell ridges) displayed parallel to the coast.

There is poor hydrogeologic information available about the Coastal Plain. Due to its high groundwater salinity, only a few perforations have gained relevant information about its hydrogeologic behaviour and environmental significance. Hence, with the aim of identifying the hydrogeologic conditions of the area of study, three boreholes were drilled. Such fieldwork will be described below.

4. MATERIALS AND METHODS. RESULTS.

Data and information directly obtained in the area of study are described below.

Tasks performed throughout this study can be classified into two large groups:

- a) Those performed only once.
 - b) Those performed periodically.
-
- a) The first group of tasks encompasses:
 - i) Geophysical survey campaigns. During these campaigns, VES and electrical imaging registers were obtained. By means of a geophysical survey it is possible to gain indirect information about the thicknesses of the formations identified in the bibliography.
 - ii) Construction of three deep boreholes. These boreholes reached Paraná Formation, crossing all the Puelche Formation. Contracting a private borehole drilling company was necessary for drilling them since Universidad Nacional de La Plata does not have suitable equipment for doing so.
 - iii) Description of cutting. It was provided during drilling operations to describe the lithological sequence.
 - iv) Geophysical logging in each borehole. It was performed so as to gain the required information for a correct completion of the wells.
 - v) Hydraulic tests. They were conducted in order to determine the hydraulic parameters of the aquifer system.
 - vi) A phreatimeter network. It was set up by staff from the Applied Geophysics Department of Universidad Nacional de La Plata, with the use of equipment belonging to it. These boreholes

were also logged, and a relevant hydraulic trial was carried out.

vii) Sample collection. Samples were collected for isotope determination. The isotopes determined here were ^{18}O , ^2H and Tritium.

b) The second group of tasks, those performed periodically, consists of:

i) Level measurement. It was taken monthly during the three years of fieldwork, starting in October 2006 and finishing in June 2009.

ii) Sample collection. Samples were collected for the determination of physical and chemical parameters. Over a period of three years, from October 2006 to April 2009, semestral samplings of every phreatimeter constructed in the area of study were carried out to determine main ions and some minor elements, as well as other parameters required for a correct hydrochemical interpretation.

All these tasks involved financial support, which was provided by Universidad Nacional de La Plata and the Government of the Province of Buenos Aires.

4.1. GEOPHYSICAL SURVEY

Two of the methods described in chapter 4 have been used to characterise the area of study. Vertical Electric Sounding (VES) has been applied with the aim of characterising the relevant stratigraphic section up to Paraná formation.

A technique that combines sounding and profiling, also known as 2D tomography or imaging survey, has also been used. Surface and shallow

subsurface profiles, both natural and in sites containing anthropic fill of diverse composition, have been obtained with this technique.

4.1.1 Vertical Electric Sounding

Field methodology

In the area of study, three Schlumberger VES surveys were conducted with a maximum current circuit (AB) spacing of 1,000 metres. In this type of techniques a linear tetrapolar and symmetrical device is placed at a specific observation point in the ground. The field work consists of obtaining an apparent resistivity curve by making a current I (commuted) flow through the current circuit and by measuring the potential V difference generated between the potential electrodes (MN).

On this basis, each value of apparent resistivity has been yielded (in ohm.m) as follows:

$$\rho_{ap} = K \frac{\Delta V}{I}$$

where K is the geometric constant of a device that takes into account the four-electrode array in the ground.

The field datum (curve of apparent resistivities) must be inverted in order to obtain a resistivity distribution with depth that mathematically satisfies the observed curve (i.e. in less than an experimental error band). Hence, as the aim of the method is to attain this resistivity distribution with depth, varied mathematical techniques are used. These techniques will be mentioned below.

Equipment

RESPC01 was the measuring equipment used here. This instrument has an automatic reading system whose results are automatically averaged. Its readings can continue until the operator is satisfied with the stability of reading. In addition, these averages are more reliable than those obtained with single reading systems.

In electric sounding mode, this instrument directly calculates ρ_{ap} , showing it in $\Omega.m$ on a digital display and providing an error estimate, as well. In long sounding surveys, like the measurements taken here, the instrument measures low signals, ensures optimal penetration and has low energy consumption. It also has a microprocessor that controls and monitors measurements guaranteeing optimal sensitivity. As the microprocessor performs each measurement, it checks the circuits and the positions of switches. It verifies the condition of the battery, too. And if necessary, it can have warning systems or error codes.

Furthermore, 500m cable reels, stainless steel current electrodes and $Cu-SO_4Cu$ non-polarisable electrodes were used to measure ΔV .

Processing sequence

The processing of curves was carried out with a programme for horizontal stratified media (one dimension) and following a basic sequence available in it. This software consists in the following steps:

- Obtaining an initial model following Zohdy (1989).
- Reducing the number of model parameters (Orellana, 1982).
- Assessing the model equivalence and inversion with a priori information (Pous et al, 1987).

The software works using an interactive computer system (Johansen, 1975). The model's response in all these cases was given in a

convolutional manner using Johansen’s linear operator (op. cit.). This operator deals with a sampling of a resistivity transform of 10 points per log decade and has a length of 141 coefficients. It was considered adequate to evaluate resistive contrast curves like those occurring in the area.

Location of sounding surveys

Table 4.1.1 indicates the location of sounding surveys.

Table 4.1.1 Location of VES

VES1	S	34	54	0.6		W	57	55	42.2
VES2	S	34	53	7.8		W	57	54	20.1
VES3	S	34	51	57.7		W	57	53	12.0

The table shows the geographical coordinates of plotted points, expressed in degrees, minutes and seconds (WGS 84). A plan of the location of these sounding surveys is shown below (Figure 4.1.1).



Figure 4.1.1 Location of VES

Analysis of measurements

The field device design was produced according to the expected thicknesses, considering the previous information. The measured curves are gentle curves of good quality and do not show important interferences or noise. Apparent resistivities are alternated in their morphology, making it possible to classify these curves as made up of 3/4 layers. As the series appears in different abscissa values every time, there is a variation in layer depth and thickness.

As mentioned above, the curves were first processed through an automatic fit routine following Zohdy. The result was a first model of as many layers as measuring points the curve had. The model for VES1 is shown in Figure 4.1.2.



Figure 4.1.2 VES 1

Although this is an excellent mathematical adjustment model, it lacks physical meaning so as to provide a geological designation. Therefore, a

reduced model with the lowest possible number of layers is generated in order to create a model that takes significant variations into account.

The reduced VES1 is described below (Figure 4.1.3).

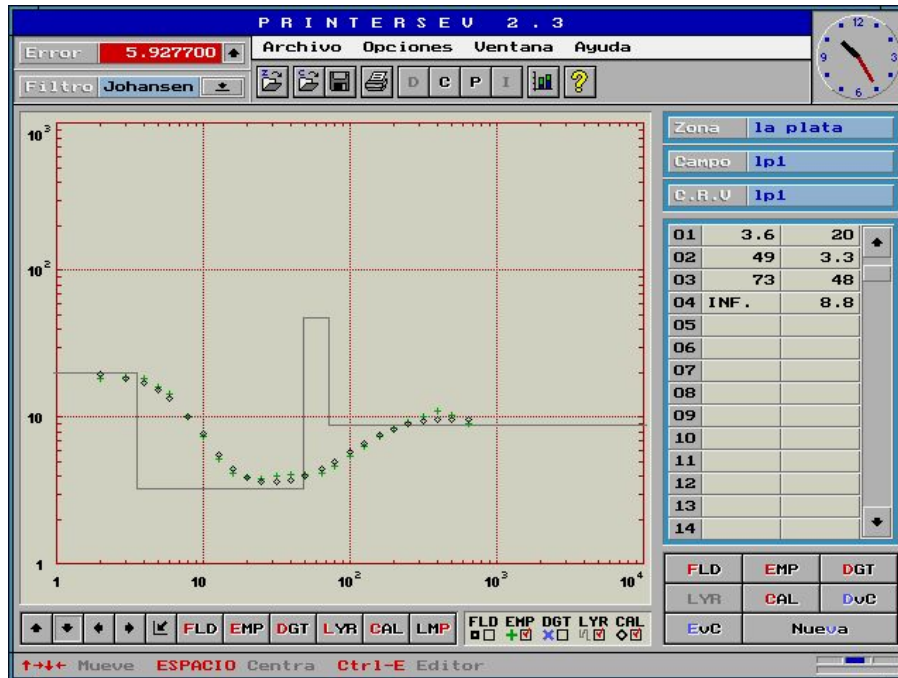


Figure 4.1.3 Reduced VES 1 model.

1. The first value, up to 4 metres deep, shows surface values.
2. Between 4 and 49, there is a conductive layer corresponding to Pampeano level.
3. Between 49 and 73, there is a resistive layer ascribable to Puelche sands.
4. Finally, there is a conductive substratum attributable to Paraná formation.

The Figure 4.1.4, VES2 displays lower thicknesses and usually lower resistivity values.

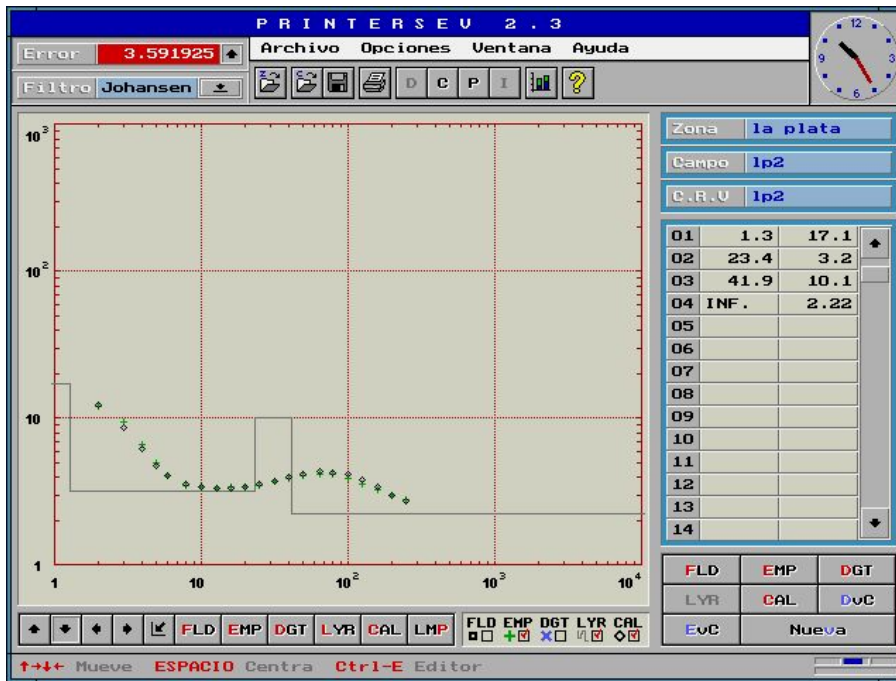


Figure 4.1.4 VES 2

The Puelche layer appears at 23 metres (much higher than VES1) and resistivity reaches 10 ohm.m. That is, a higher content of salts in the formation's interstitial water is expected.

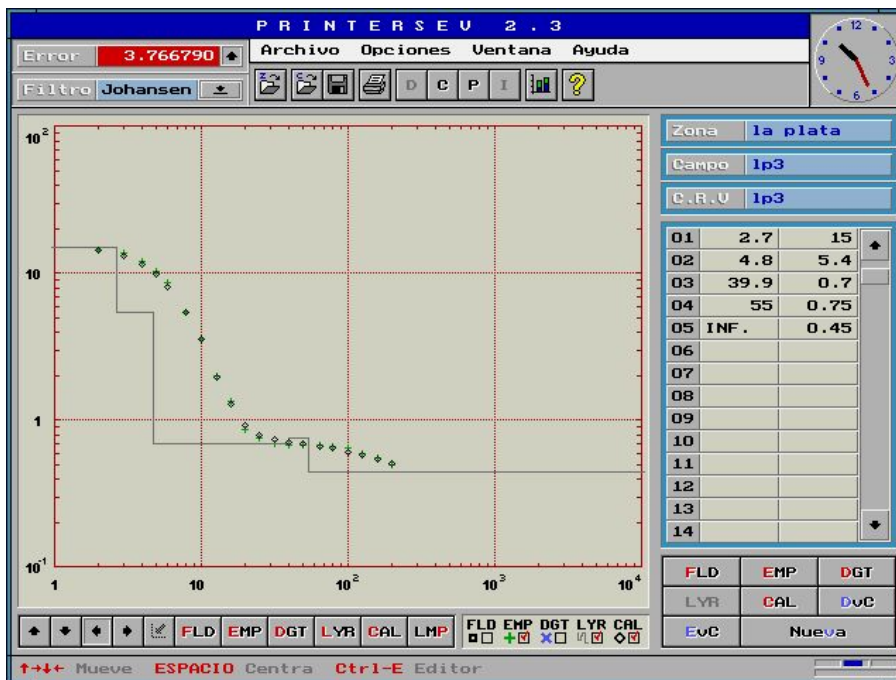


Figure 4.1.5 VES 3

VES3 was measured closer to the bank of Río de la Plata (Figure 4.1.5).

This curve shows an average surface value, attributable to Post Pampeano level. Then values decrease rapidly, which means the environment is much more conductive. In other words, for the same lithological formations, interstitial water has high saline contents. This interspersions between 40 and 55m is probably due to the presence of sands (equally saturated in salt water).

In short, the sections adopted are shown in Table 4.1.2.

Table 4.1.2 True resistivity sections

VES1		VES2		VES3	
Depth	ρ	Depth	ρ	Depth	ρ
3.6	20	1.3	17.1	2.7	15
49	3.3	23.4	3.2	4.8	5.4
73	48	41.9	10.1	39.9	0.7
∞	8.8	∞	2.22	55	0.75
				∞	0.45
RMS	5.9%	RMS	3.6%	RMS	3.7%

Based on these true resistivity sections, a longitudinal geoelectrical profile is shown below (Figure 4.1.6).

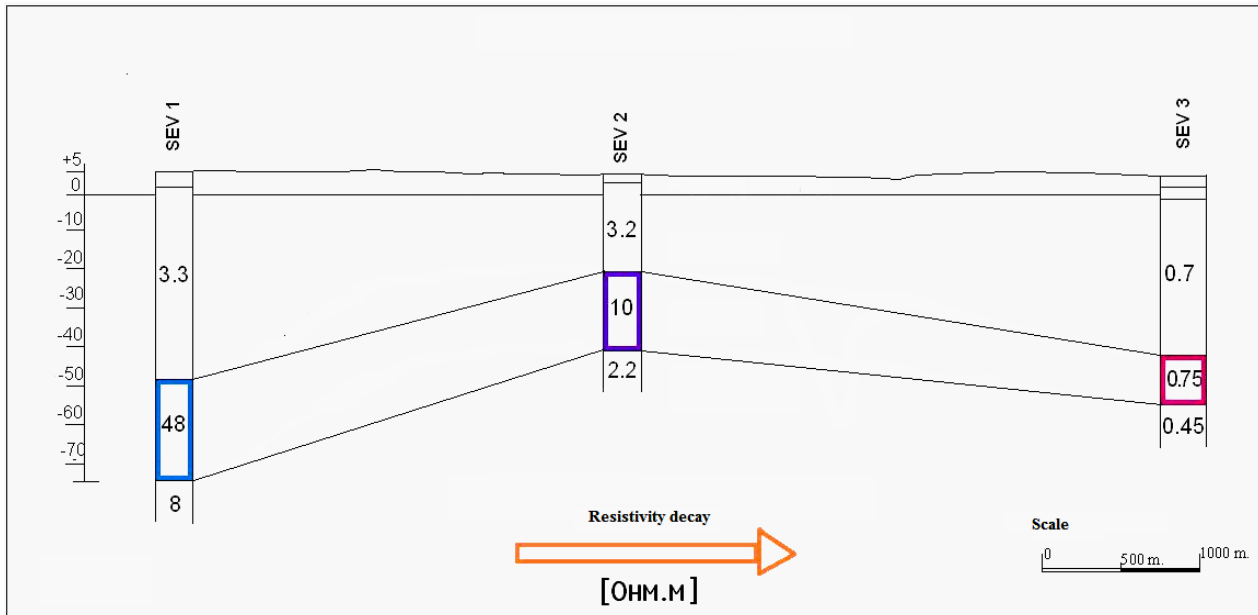


Figure 4.1.6 Resistivity profile

Through these sounding surveys, it is possible to identify the thickness variations of the lithological formations of a multilayer aquifer. Such soundings also indicate the evolution towards an increasingly conductive environment as the coast is reached, which can be associated with a greater content of salts in interstitial water.

4.1.2 Electric imaging survey

Field methodology

Electric profiling, in dipole-dipole array, was the technique used for constructing a subsurface imaging survey (also called tomographic image). It consists of a linear device through which resistivity variation in forward direction, at depths that can be regarded as constant, is recorded.

Apparent resistivity was calculated as follows:

$$\rho_{ap} = K \frac{\Delta V}{I}$$

where K is the geometric constant of the relevant device. Values are expressed in ohm/m.

An array with the following parameters was especially used in the survey: spacing “a” between 1m electrodes. For each station, measurements for n=1 to n=8 values were made, “n” being the different levels (with depth) of data coverage. Apparent resistivity pseudoprofiles were built up with the values thus obtained. These values provided qualitative knowledge of resistivity variations throughout the profile.

Equipment

A Scintrex IPR-12 Time Domain IP/Resistivity Receiver was used. Energization was conducted with a Scintrex IPC-9/200W source.

The IPR-12 Time Domain IP/Resistivity Receiver has an automatic reading system. The results from each reading are processed in real time and enable the operator to work on as many samples as they consider appropriate, in a number of cycles adjustable by reading. This software controls and monitors all measurements guaranteeing optimal sensitivity and good use of the instrument. While taking each measurement, the instrument checks the power supply, circuits and natural conditions.

It should be highlighted that the IPR-12 Time Domain IP/Resistivity Receiver allows simultaneous reading of up to eight potential dipoles, thus enabling interesting production times. It stores measured resistivity and chargeability values, calculates constant K values for each position and displays statistical values that indicate how reliable the stored values are.

Synchronisation between the source and the receiver is automatic and controlled by the first potential dipole. The source generates a DC signal

commuted in cycles of selectable duration. Therefore, spontaneous potential compensations can be avoided because they are statistically performed.

Processing sequence and interpretation

A two-dimensional model was made from the data already mentioned by using RES2DINV software. The 2D model used for the inversion programme consists of representing the subsurface in rectangular blocks. The block distribution fits the pseudoprofile data distribution. A forward modelling routine calculates the apparent resistivity values and an inversion routine makes use of a nonlinear least-squares optimisation technique. As the programme includes several options related to various geological features, it is possible to change its parameters in the various stages of the process. Hence, its use can be optimised in different circumstances.

The final result of the process is a model of true resistivity. An error is expressed as RMS (root mean square), a measurement of the differences between the apparent resistivity values calculated by the proposed model and those measured in the field. Once the preliminary model is found, consecutive iterations are carried out. That is, the immediate solution to the problem is achieved by minimising the RMS between the observed resistivity and the calculated apparent resistivity.

Analysis of measurements

To characterise the response of natural ground and that of anthropic fill, some sections of the area of study have been selected. The location of these sections is shown in Figure 4.1.7.



Figure 4.1.7 Profiling survey areas. Natural ground (blue) and anthropic fill (red)

The data and model obtained in natural ground is shown in Figure 4.1.8.

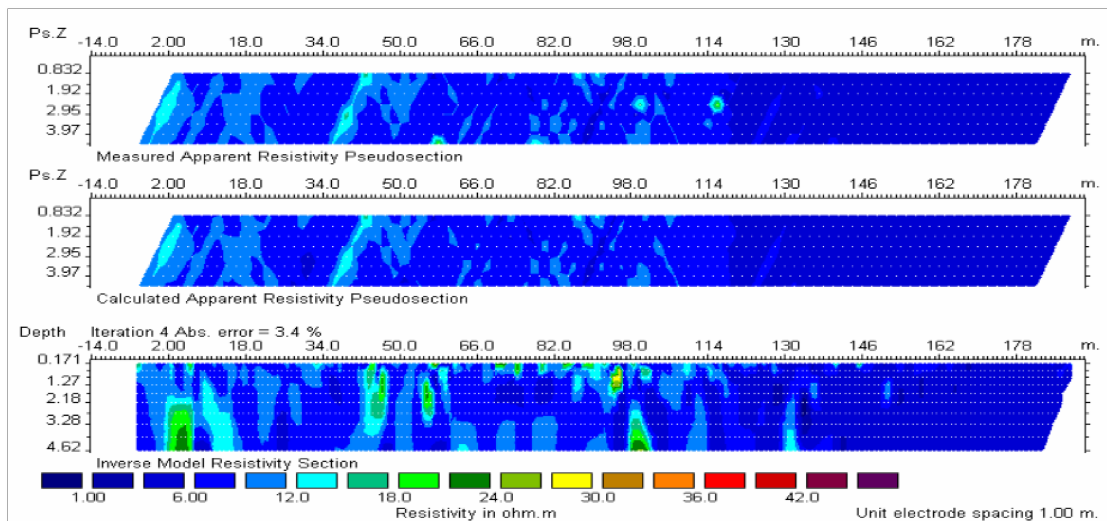


Figure 4.1.8 Natural soil data and model

This response has characteristic values in 6 ohm.m, and coincided with the registered values of Pampeano level in VES surveys.

The data and model obtained from anthropic inclusions is shown in Figure 4.1.9.

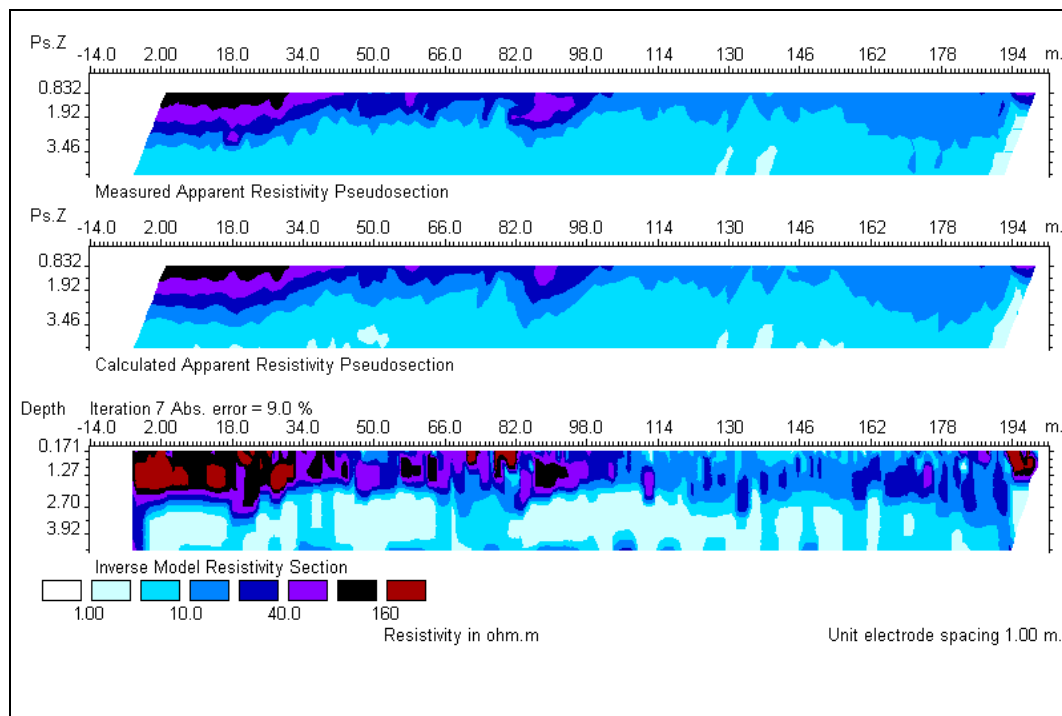


Figure 4.1.9 Data and model with anthropic inclusions

where resistive inclusions can be identified.

When attempting to determine this type of inclusions, for instance because they can be regarded as contaminants, several profiles are plotted in a section.

In coincidence with the electrical profiles, geologic profiles were drawn (Figure 4.1.10). These geologic profiles were used to attribute resistivity ranges to the different materials. This area is an industrial area, where it was not possible to drill perforations. The company only authorised the use of indirect techniques Figure (4.1.11).

Linea 6

- Cobertura
- Camino
- escombros contaminados
Con petroleo
- Arboleda con escombros
contaminados
- Arboleda

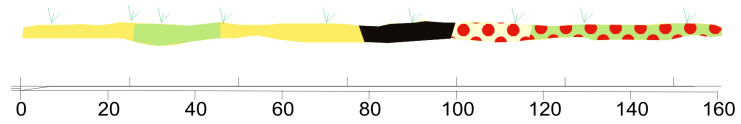


Figure 4.1.10 Geological Profile

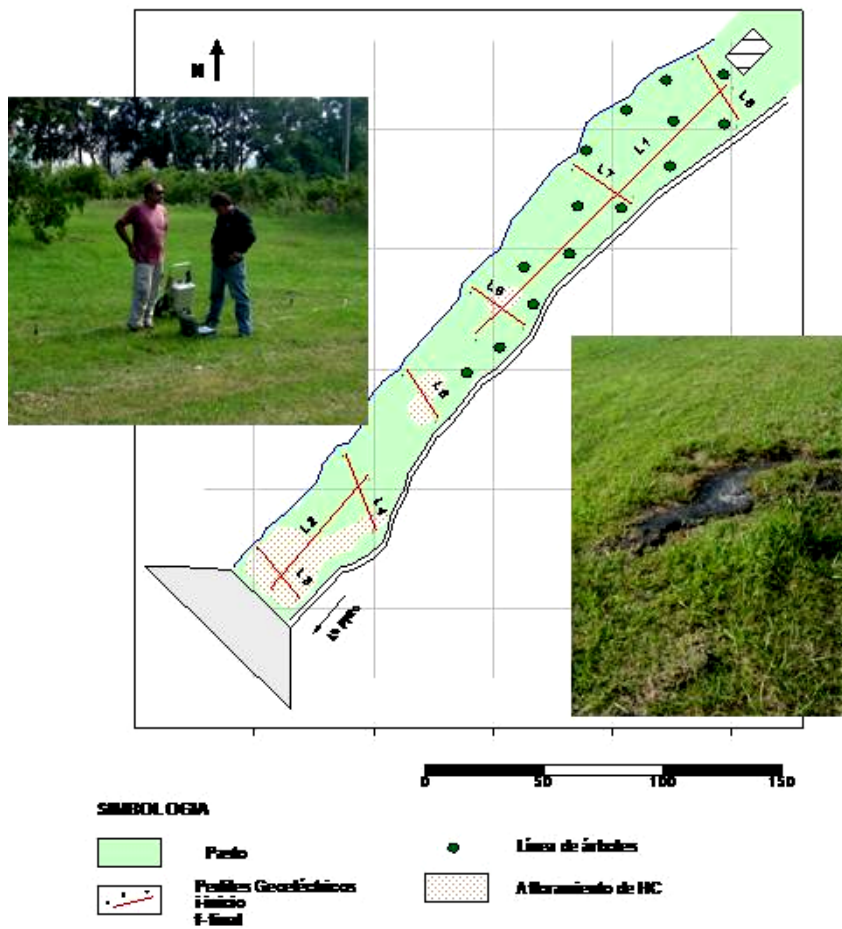
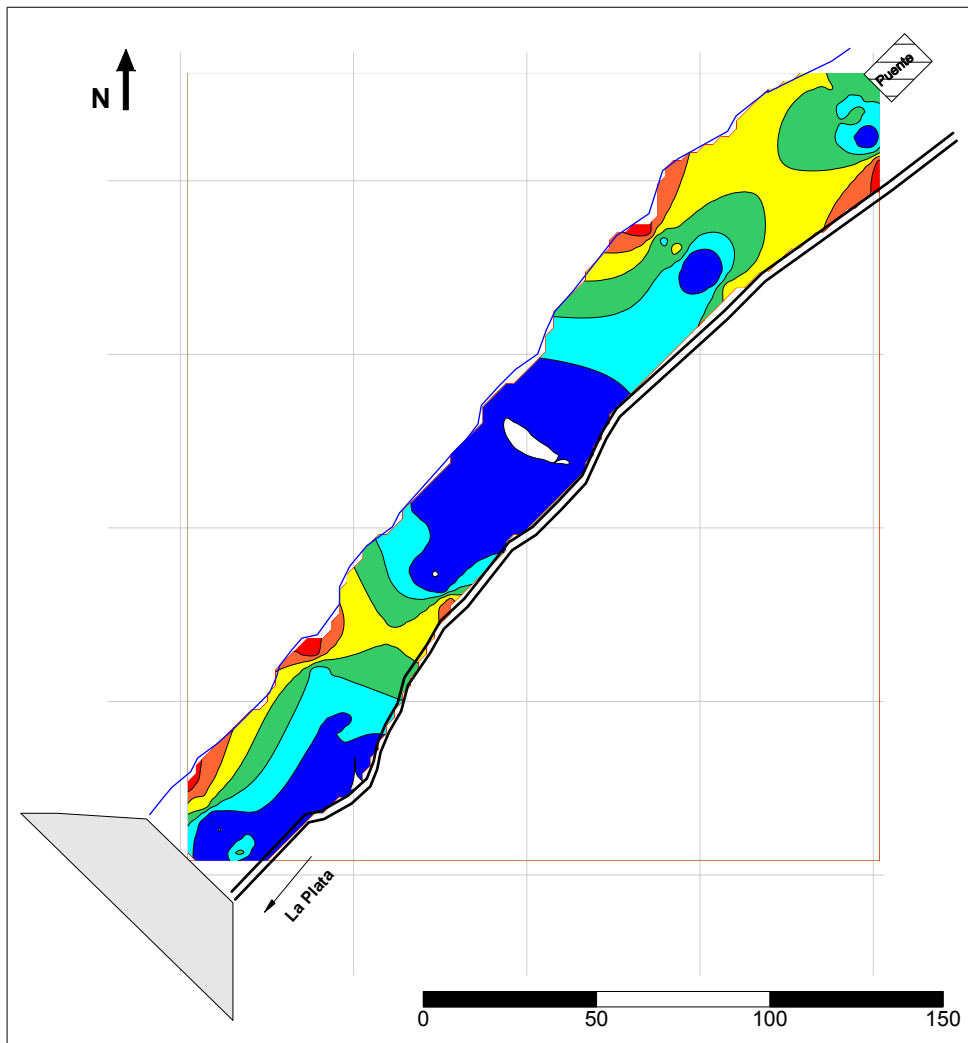


Figure 4.1.11 Survey area

With the information gathered maps were drawn for each level (Figure 4.1.12).



Reference

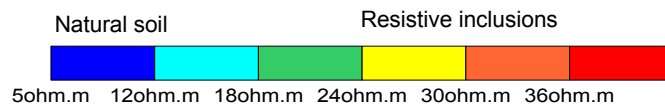


Figure 4.1.12 Resistivity map at -2.5 meters

Interpretation contributed to characterise the distribution of various materials in a matrix equivalent to natural ground.

Two different electrical methods with different resolution capacity were used. An approximation to the problem under study was made with each of them. By means of vertical electric sounding, it was possible to

create an electrical model throughout the analysed lithological profile and also to know a priori that the interstitial water of those formations is salt-enriched towards Rio de La Plata. On the other hand, with the use of imaging surveys it was possible to construct models on such a scale that resistive inclusions in an environment similar to the natural one could be identified.

4.2 GEOLOGICAL PROFILE

In order to verify the geological conditions in situ, 3 boreholes reaching Paraná Formation were drilled. They were then cased to be used in physical and chemical monitoring of water.

The vicinity of El Dique (PU01), Tiro Federal (PU02) and prefecture premises in Puerto La Plata (PU3) were defined as appropriate sites for drilling these boreholes.



Figure 4.2.1 Location of Puelche wells

Drilling tasks began with a stratigraphic reconnaissance survey. In a two-inch diameter, cutting (lithological) sampling was done (metre to metre) until the base of Puelche aquifer was determined.

According to the results drawn from the borehole, two definitive boreholes, corresponding to each of the monitored aquifers, were designed in each site.

The borehole was widened to a six-inch diameter, up to the least permeable layer located above the roof of Puelche aquifer. Casing was run in to this level with PVC pipes of 110 mm in diameter. Cementation in the annular space and bottom of the borehole was, in turn, carried out.

Cement was set adequately, in 24 hours. After the cement plug was drilled out until it reached the final depth defined in the design, drilling continued with a four-inch diameter. Such depth was the upper section of the aquifer in all three cases.

Subsequently, a stainless steel Johnson's screen with an opening of 0.25 mm was placed with its extension pipe and pipe organisers, as well as a gravel annular fill. Gravel (2–4 mm) was introduced in the annular space between the formation and the external side of pipes.

Variable-rate pumping was used for borehole development and cleaning. Once the water withdrawn showed crystalline features, this process was over.

In order to construct the definitive monitoring wells in the Pampeano aquifer, drilling took place between a six-inch diameter and the established final depth.

PVC casing was subsequently run. The PVC pipelines were 110 mm in diameter and slotted in their lowest section. Gravel was inserted up to a top layer of low permeability and a rubber pack was then placed with the aim of isolating this material from the phreatic layer.

Finally, the borehole was cleaned through variable-rate pumping.

The Figures 4.2.2, 4.2.3 and 4.2.4 show a basic design of the boreholes and the lithology crossed by each.

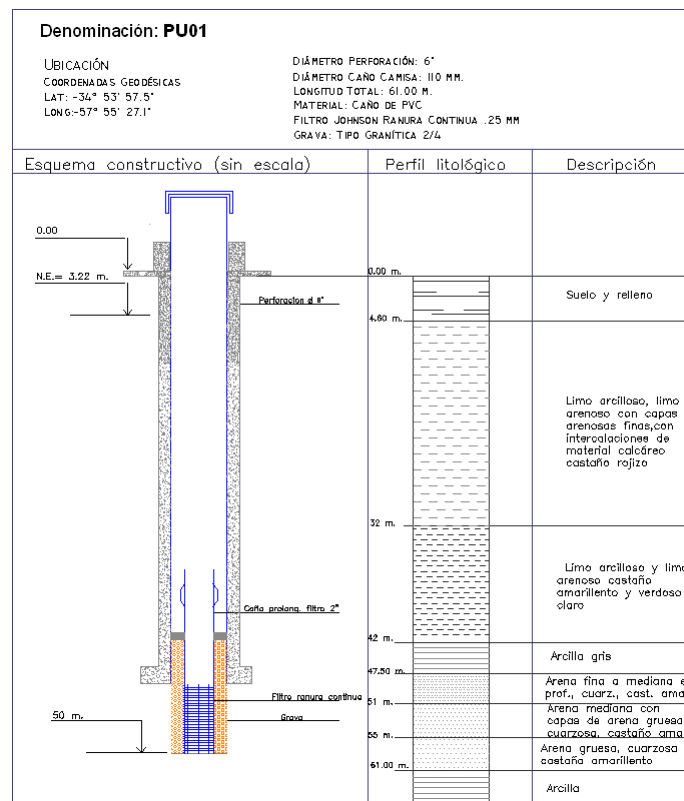


Figure 4.2.2 Description of borehole PU01

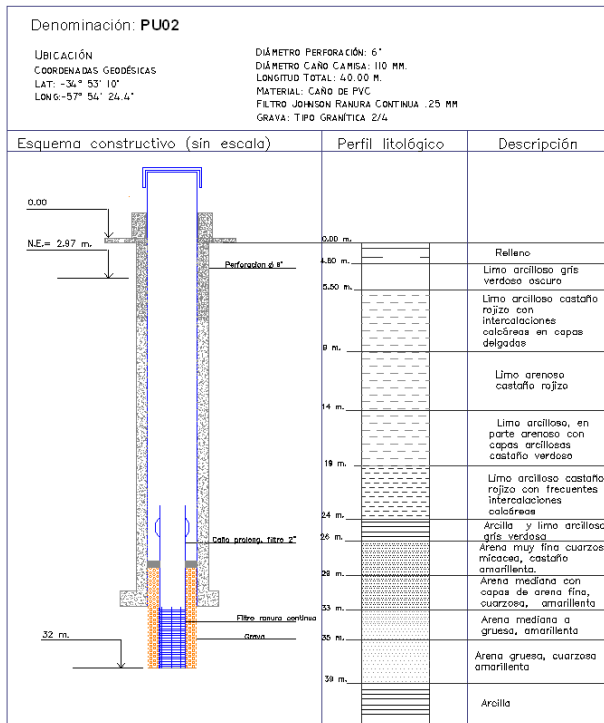


Figure 4.2.3 Description of borehole PU02

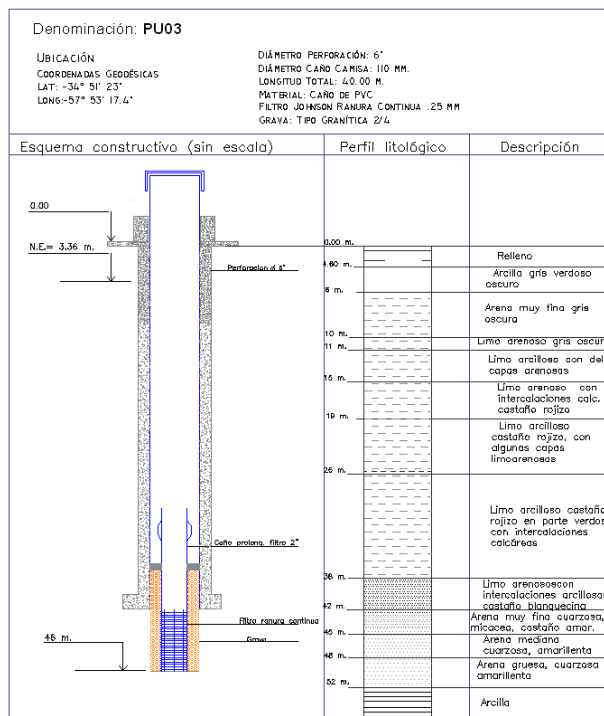


Figure 4.2.4 Description of borehole PU03

Figure 4.2.5 shows a well log measured in PU01 borehole. The record values are typical for the formations:

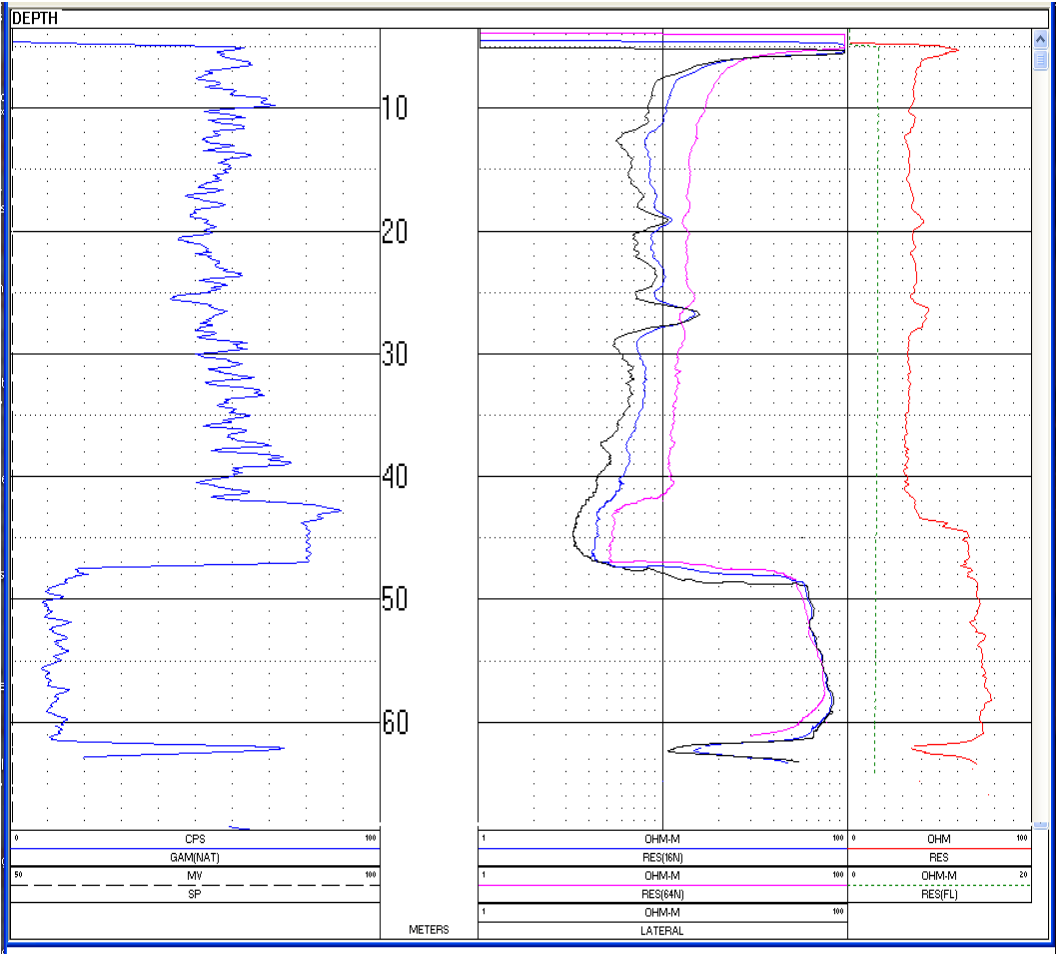


Figure 4.2.5 El Dique well log record

For Pampeano sediments around 50 cps in natural gamma record, and 10 ohm.m for resistivity tools; for clay 80 cps in gamma record and 6 ohm.m for resistivity tools; 20 cps in gamma record and 50 ohm.m in resistivity tools for Puelche sands (Ainchil et al, 2007)

Figure 4.2.6 shows a hydrogeological profile that links the boreholes mentioned above, displaying the position of the hydrogeological units and their thickness variations in the area.

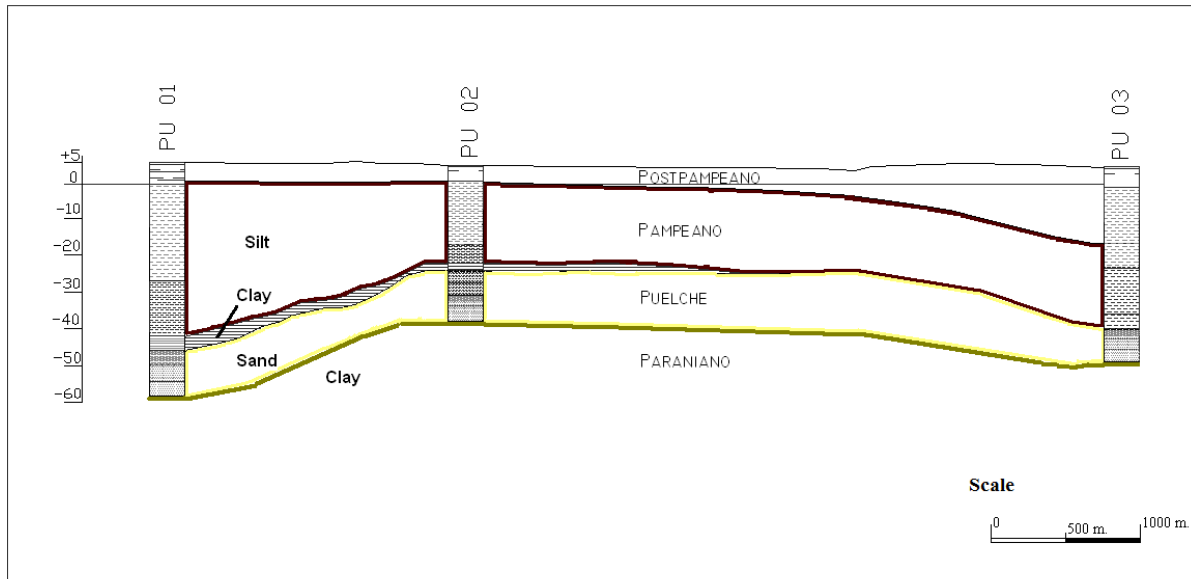


Figure 4.2.6 Geological profile

Puelche sands, which represent the most important aquifer in the northeast of Buenos Aires Province, include a sequence of usually well-selected yellowish brown quartz sands. They overlie bluish green clays of Paraná Formation. This aquifer roof consists of fine-grained silty sands (grain size increasing with depth) that become coarser towards the base. Thickness slightly decreases from the continent to the coast because it is 14 meters in El Dique, 13 meters in Tiro Federal and 10 meters in Puerto La Plata.

The contact between Pampeano sediments and Puelche sands is clear in El Dique and Tiro Federal boreholes: in the former, through about 5 meters thick grey clay, and in the latter, through about 2 meters grey clay. However, in Puerto La Plata, once the typical sand is defined, there is no more gradual variation in grain size.

Pampeano sediments are the base of Post-Pampeano ones. The latter are composed of grey or greenish clayey and sandy silts of marine estuarine origin. They usually form a low-permeability unit, with some fine-grained sandy silt intercalations of higher permeability values that are more frequent from Berisso and Ensenada to the coast.

Disappearing around La Plata and Berisso boundary (122 Avenue), these sediments increase their thickness towards the bank of Río de La Plata, reaching 15 meters in Puerto La Plata.

The characteristics of the materials that are close to the terrain surface, including their hydraulic properties and geomorphologic location, have direct influence on runoff, precipitated water infiltration and transport of possible contaminants towards phreatic water.

According to the surveys, Post-Pampeano sediments can be covered with filling material of variable thickness, sometimes exceeding 3 m. On the whole, it is predominantly clayey-silty material with calcareous intercalations, mixed with building material in some areas, but which do not fundamentally change the general condition of relative low permeability.

Hydraulic parameters of Pampeano and Puelche Formations are expected to have similar values in the coastal plain as no lithological variations occur. Nevertheless, as hydraulic conductivity is a property that is not exclusive of the medium but is also affected by fluid characteristics (it is density and viscosity dependent), different values should be taken into account as the result of increasing water salinity in the low plain. Silty clay facies of Post-Pampeano Formation have an average hydraulic conductivity ranging from $1 \cdot 10^{-9}$ m s⁻¹ when determined on a small scale by single wells and odometer tests to $1 \cdot 10^{-8}$ m s⁻¹ when estimated on a larger scale with Tritium profiles and seepage meters (Logan and Rudolph, 1997).

4.3 MONITORING NETWORK

A network with 17 piezometers, distributed in the area of study so that they cover all of it, was designed for the purpose of this work. Figure 4.3.1 shows their distribution.

With the aim of selecting the appropriate sites for these wells, field surveys were conducted. Part of this task involved consultations with the owners of the preliminarily selected places and analyses of the operating conditions for the installation of measurement stations. From an operating viewpoint, places that are easily accessible during any time of the year and where monitoring wells are not damaged by acts of vandalism were identified.

The combination of hydrologic characteristics and operating conditions led to distinguish two types of sites: one related to institutions (Hospital Naval, Vivero Municipal de Berisso, Astillero Río Santiago, Prefectura Naval, etc) and the other one related to public places (squares, pavements, etc).

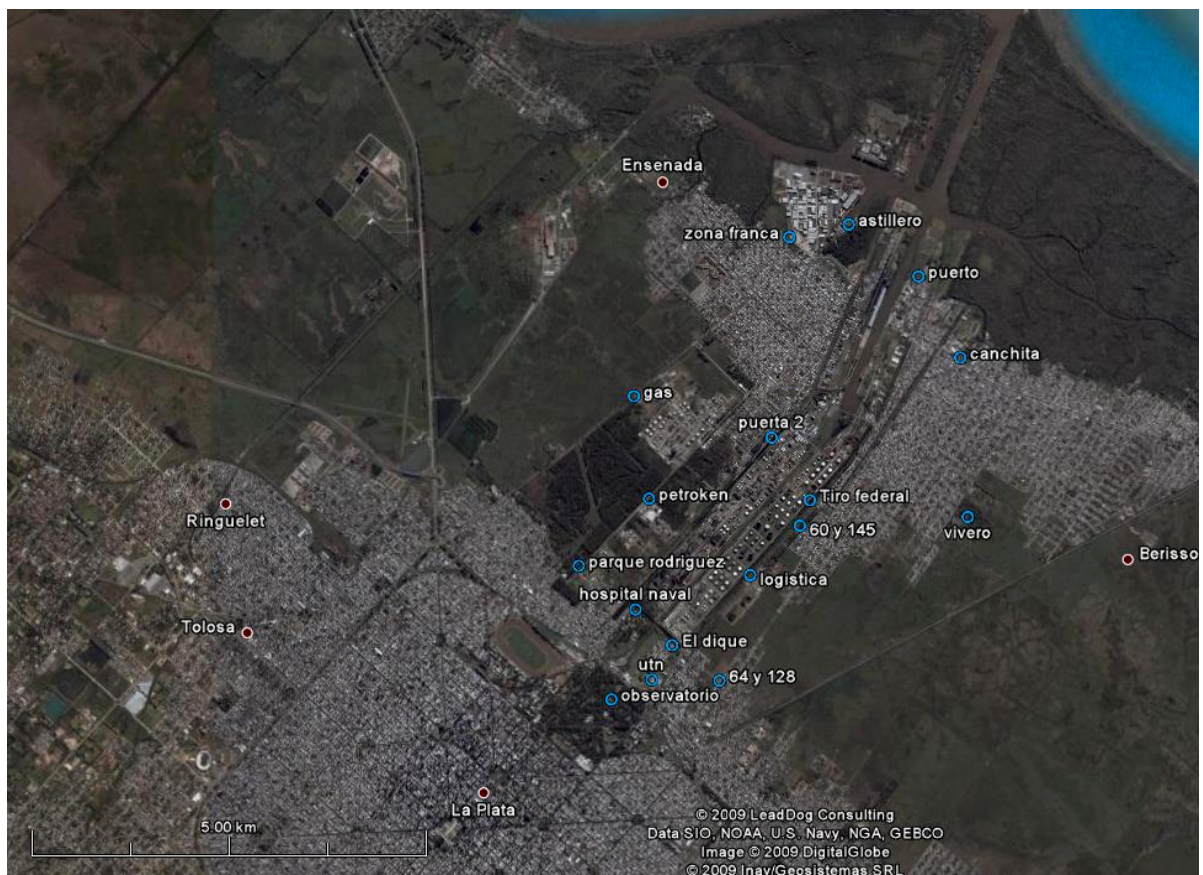


Fig. 4.3.1 Distribution of sampling points in the area of study

Their geographical coordinates, altitudes and location references are summarised in Table 4.3.1.

Table 4.3.1 Location of monitoring points

<i>Phreatimeter</i>	Geodesic Coordinates POSGAR 94		Altitude [a.m.s.l.]
<i>Puerto</i>	S 34°51'22,8"	W 57°53'20,4"	3.34
<i>Canchita</i>	S 34°52'00,4"	W 57°53'34,3'	3.02
<i>Zona Franca</i>	S 34°51'20,3"	W 57°54'22,4'	2.82
<i>Vivero</i>	S 34°53'07,4"	W 57°52'57,8"	2.37
<i>60 y 154</i>	S 34°53'13,9"	W 57°54'23,3"	2.89
<i>Logística</i>	S 34°53'31,5"	W 57°54'45,3"	3.3
<i>Tiro federal</i>	S 34°53'10,2"	W 57°54'24,8"	4.02
<i>El Dique</i>	S 34°53'57,5"	W 57°55'27,6"	5.1
<i>128 y 64</i>	S 34°54'16,5"	W 57°55'02,5"	2.69
<i>UTN</i>	S 34°54'16,2"	W 57°55'37,0"	4.92
<i>Hospital Naval</i>	S 34°53'47,9'	W 57°55'44,9"	3.76
<i>Petroken</i>	S 34°53'03,0"	W 57°55'38,3"	2.11
<i>Puerta 2</i>	S 34°52'38,8"	W 57°54'43,2"	3
<i>Astillero</i>	S 34°51'11,0"	W57°54'00,1"	3.09

Gas Ensenada	S 34°52'22,0"	W 57°55'45,7"	2.04
Parque Gral Rodriguez	S 34°53'33,4"	W 57°56'17,3"	3.6
Observatorio	S 34°54'24,6"	W 57°55'57,8	12.61

The fulfilled tasks involved preparation of the site, lithological sampling, design, casing, borehole cleaning and termination as well as a protection structure.

Boreholes were installed in a diameter of 4". A manual drill (auger) was used by two operators, with 1m rods. The total depth, ranging from 3 to 5 m, was determined by considering that it had to identify water in the phreatic layer, by foreseeing extreme oscillations at phreatic levels and with the aim of obtaining an adequate water column for the relevant sampling.

A lithological description of the samples was made in the well opening, and after reaching the final depth, a natural gamma and conductivity logging was measured. Subsequently, casing was run with especially obliquely slotted 63-mm PVC pipes and a 1 mm thick saw.

The annular space between the borehole wall and the pipe was filled with selected gravel of 2 to 4 mm in order to avoid slot obturation. Graveling was performed up to 30 cm above the upper part of slots and it was later cemented up to the surface.

Once this task was fulfilled, borehole cleaning through low-rate pumping was carried out so as to remove existing sedimentary particles.

The well and protection structure were completed in terms of two modalities. In institutions or premises with restricted access, the upper

end of the pipeline, overhanging between 20 and 50 cm from ground level, was emplaced with a round cement base and its opening was sealed with a cap. In those locations with public access, the well was located at ground level, its opening was closed like in the previous case but it was protected with a small chamber beneath the surface, covered with a special cap.

The design of wells and the recognised lithology are shown schematically in Figure 4.3.2. The description of each of them is included in the Annex 1 (Well description, page 195).

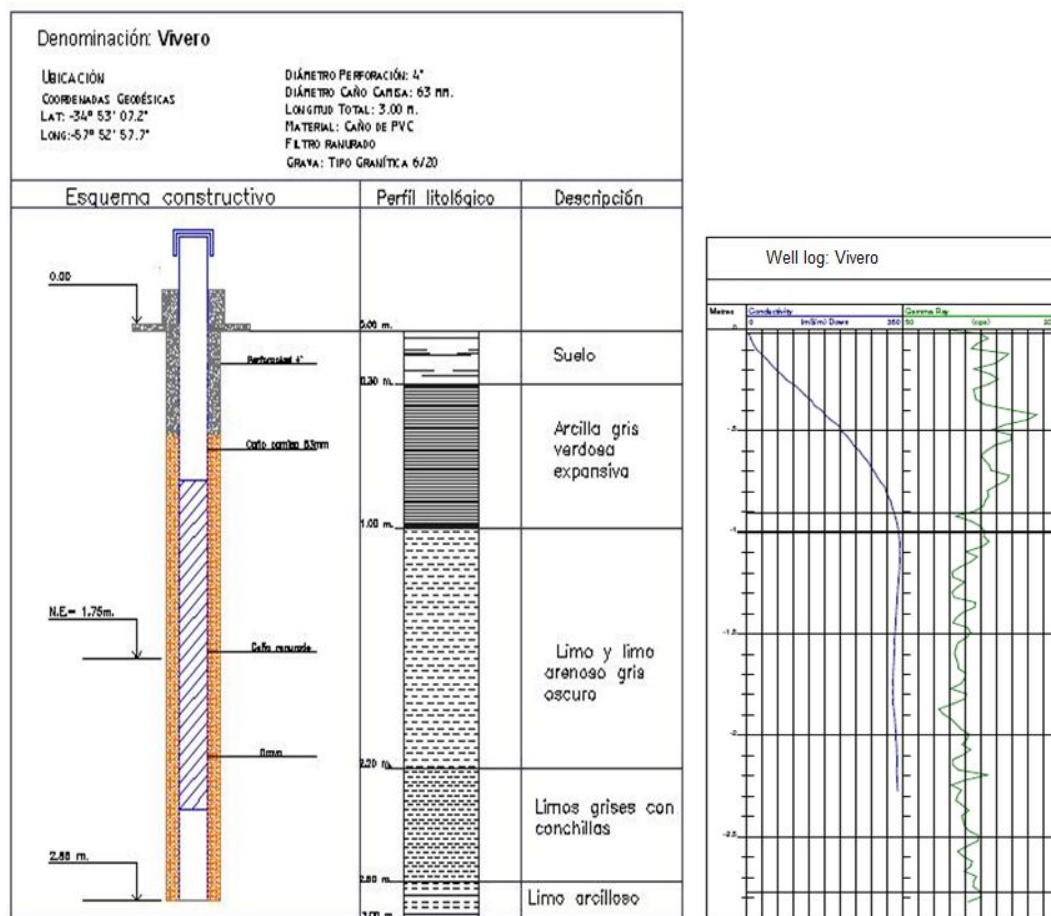


Figure 4.3.2 Example of well construction and well log

The network was completed with three sets of boreholes reaching the two lower aquifer levels: Pampeano and Puelche. These sets coincide with the locations called El Dique, Tiro Federal and Puerto. These boreholes are described in Figures 4.2.2, 4.2.3 and 4.2.4.

Hydraulic conductivity

The hydraulic conductivity was determined by means of a pump test and the slug test performed in the wells. The typical values are: a) phreatic: 0.2 to 0.5 m.d⁻¹, b) Pampeano: 1 to 4 m.d⁻¹ and c) Puelche: 18 to 24 m.d⁻¹. Figures 4.3.3 and 4.3.4 show output of slug test and pump test.

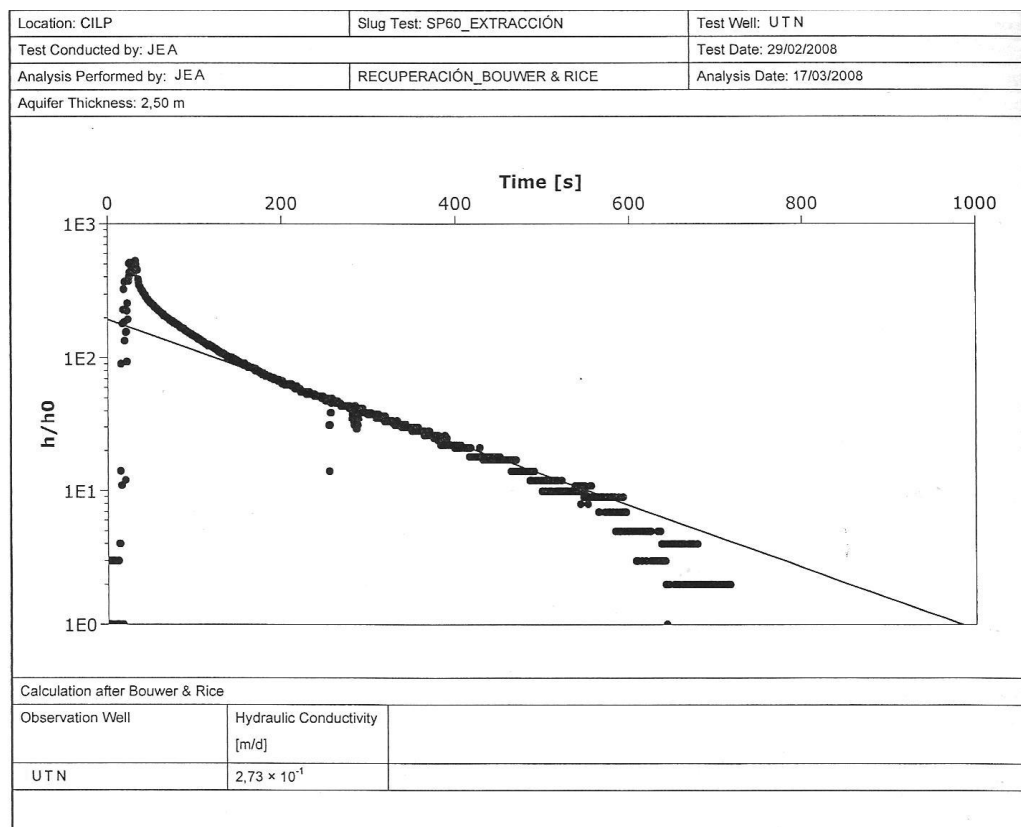


Figure 4.3.3 Typical slug test output



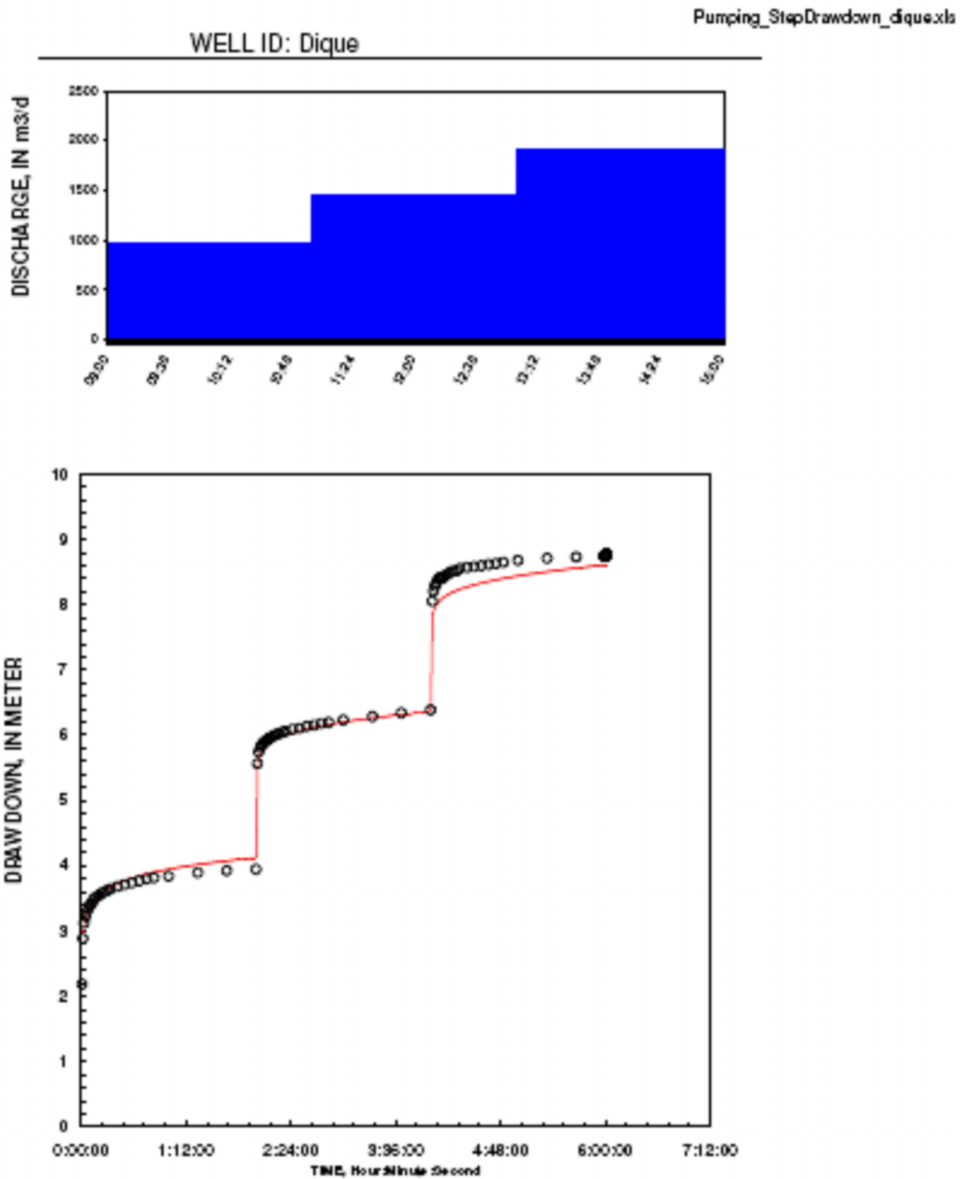


Figure 4.3.4 Typical pump test output

An aquifer test (or a pumping test) is conducted to evaluate an aquifer by stimulating the aquifer through constant pumping, and observing the aquifer's response (drawdown) in observation wells. Aquifer testing is a common tool that hydrogeologists use to characterize a system of aquifers, aquitards and flow system boundaries.

A slug test is a variation on the typical aquifer test where an instantaneous change (increase or decrease) is made, and the effects are observed in the same well. This is often used in geotechnical or engineering settings to get a quick estimate (minutes instead of days) of the aquifer properties immediately around the well.

Aquifer tests are typically interpreted by using an analytical model of aquifer flow (the most fundamental being the Theis solution) to match the data observed in the real world, then assuming that the parameters from the idealized model apply to the real-world aquifer. There are several software or spreadsheets for the analysis of aquifer-test and slug-test data (USGS, 2002).

4.4 LEVEL VARIATION

As mentioned before, a monitoring network provides two types of data: physical, related to the register of level variation, and chemical, concerned with the chemical composition of water.

In order to begin analysing the level data registered throughout this thesis, it is convenient to observe the behaviour of precipitations throughout the same period. The Figure 4.4.1 shows the values of monthly precipitation from December 2006 to June 2009.

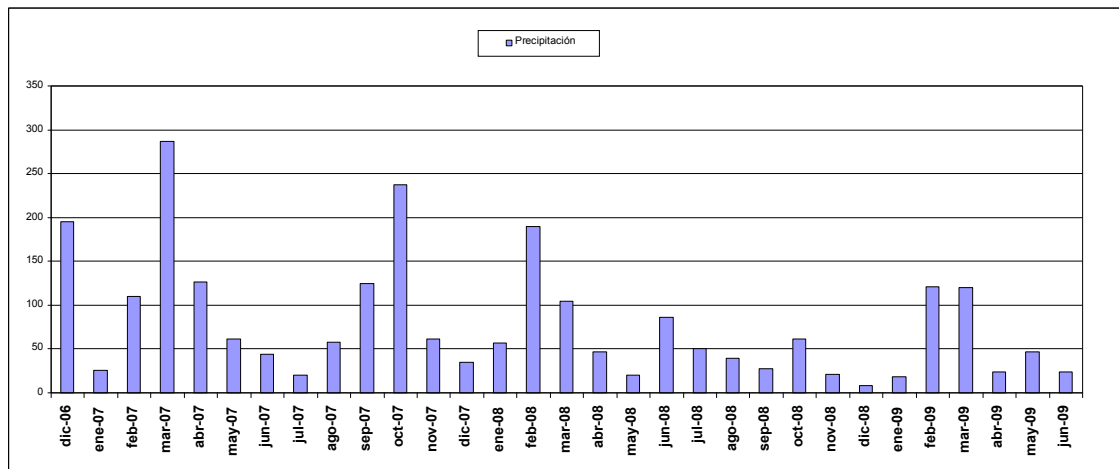


Figure 4.4.1 Precipitation sequence

Precipitation values were lower during 2008. This is the transcription of a report from Servicio Meteorológico Nacional: During 2008, the amount of totalised precipitation showed a negative standard, with strong impact on various activities. If the accumulated rainfall in such period of time is compared with the mean value in 1961-1990, it can be seen that precipitations were lower than the normal ones in most of the region. In some of its localities the accumulated values have been the lowest in the last 47 years. The accumulated rainfall in the centre of the region represented 40-60 % of the normal value or, in other words, there was a deficit of 60-40 %.

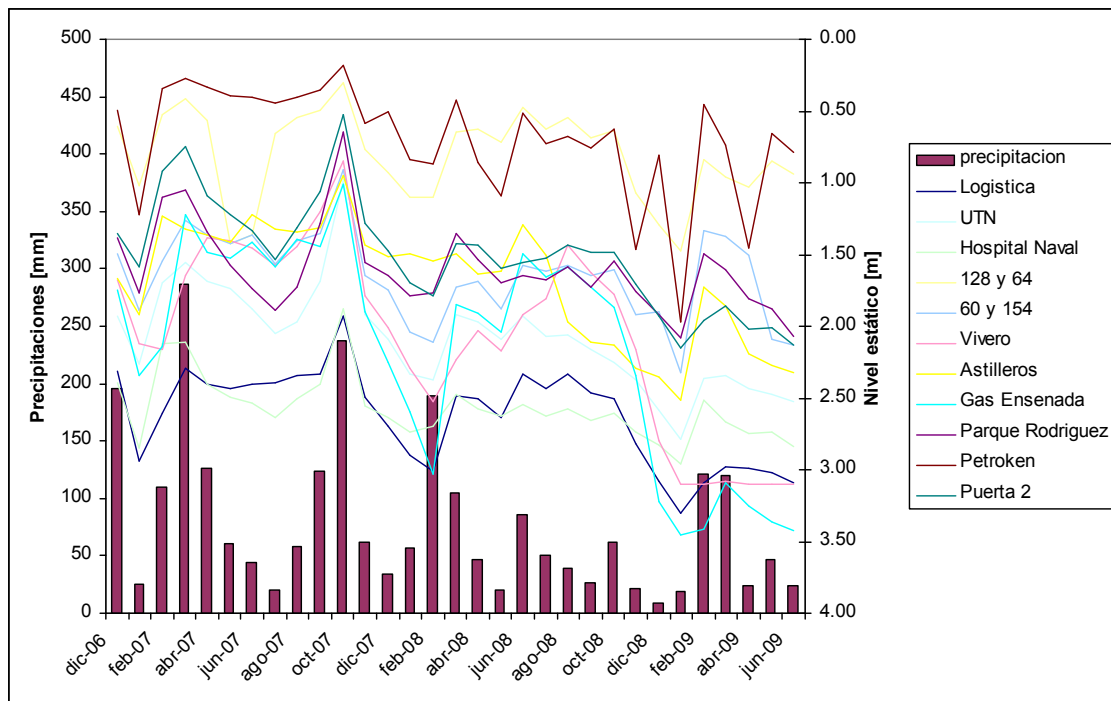
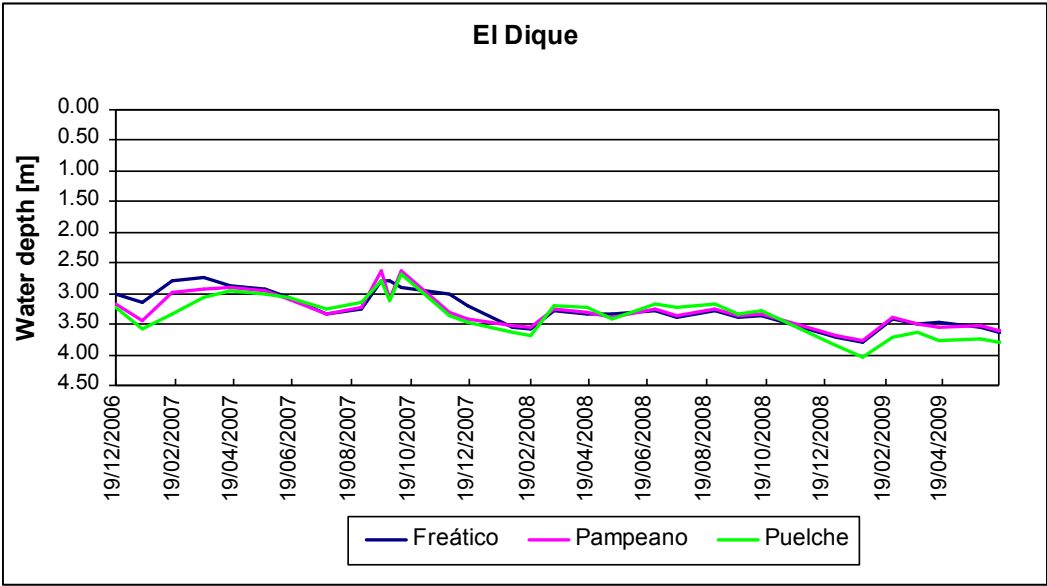


Figure 4.4.2 Phreatic level variation

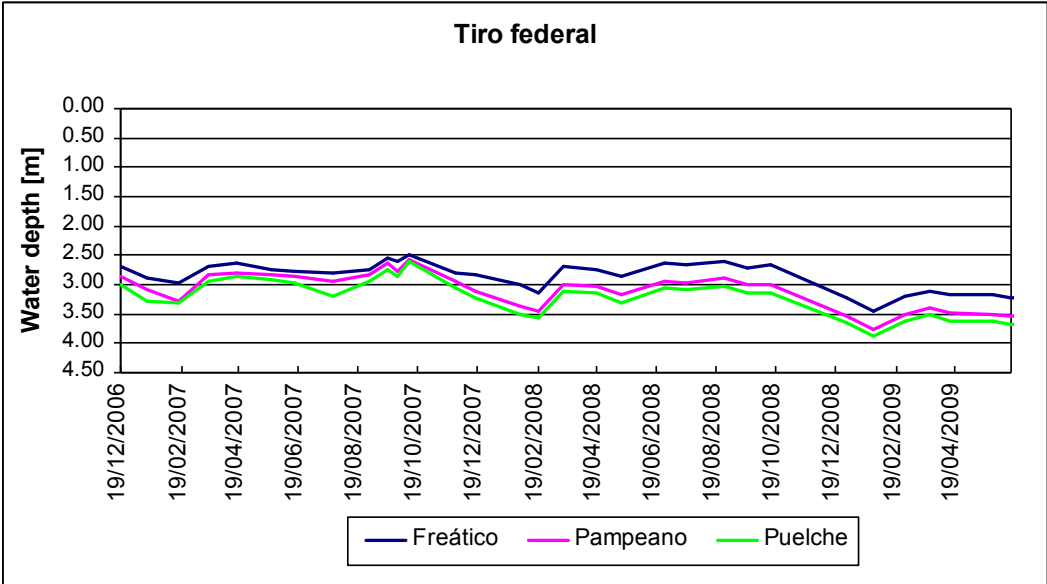
This Figure 4.4.2 illustrates variation in phreatic level depth. The precipitation register is also illustrated here. It clearly shows temporary sensitivity in respect of oscillations of precipitation and evapotranspiration. Moreover, a relative homogeneity in the oscillations

of most points should be noted, as well as the rapid phreatic level variation on account of precipitations of some significance.

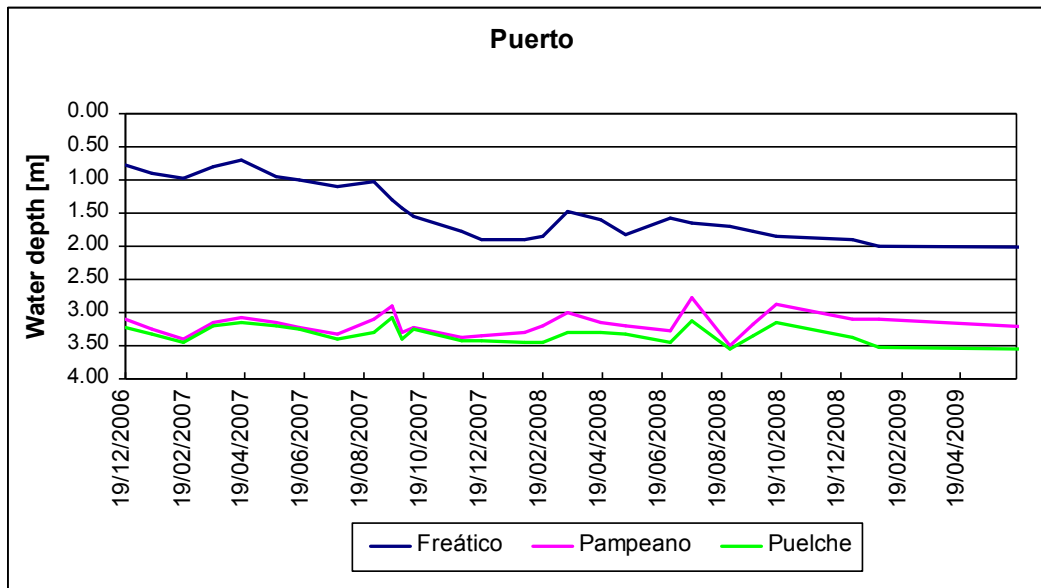
Potentiometric level variation in the three sets of boreholes that reach phreatic, Pampeano and Puelche post-levels was also registered. This variation is displayed in the following Figures 4.4.3 a,b and c.



a)



b)



c)

Figure 4.4.3 a), b) and c): Variation in phreatic, Pampeano and Puelche level

The Figure 4.4.3 shows the observed oscillations according to the monthly measurements taken in the three monitoring sites (El Dique, Tiro Federal and Puerto) between December 2006 and June 2009. These variations reflect both the hydraulic connections between levels in a single system and some delay in their fluctuations follow the processes of the hydrological cycle.

4.5 GROUNDWATER FLUX

Based on the hydrogeologic features recognised by drilling, associated with knowledge of regional behaviour, it is possible to establish the existence of a unique groundwater system, of a multi-unit nature, that encompassing the phreatic, Pampeano and Puelche aquifers. It could be stated that, although there are vertical differences of permeability, they have a hydraulic continuity.

Such characteristic linked to the flat relief of the area can provisionally provide a differentiation between a local runoff system and a regional one. Local runoff, characterised by the phreatic layer configuration, is

the active element of the system, since it is here where the system recharge directly takes place. On the other hand, regional flow does so indirectly through overlying units.

Two flux maps drawn with data from different settings are shown below. The first one (April 2007, Figure 4.3.6) shows levels at the end of a summer with normal precipitations and the second one (December 2008, Figure 4.3.7) shows levels after a year of substantial rainfall deficit.

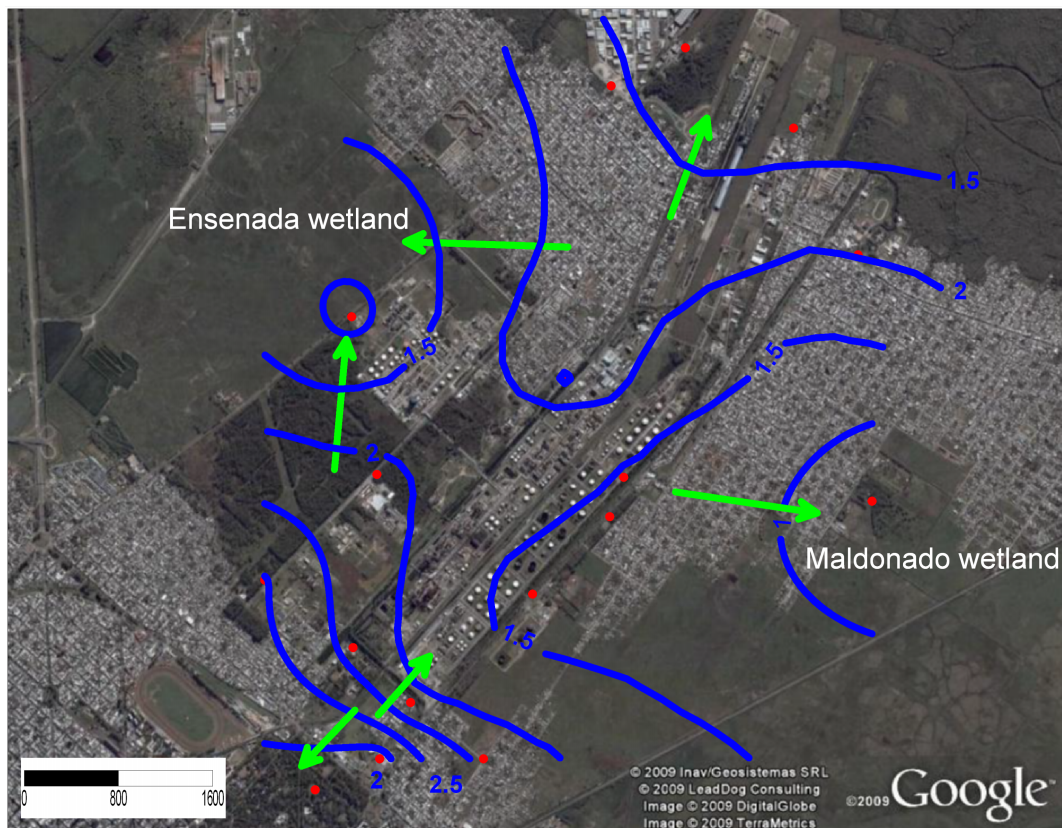


Figure 4.3.6 Flux map in April 2007



Figure 4.3.7 Flux map in December 2008

Although in each situation the levels have diverse values, the shape of curves, and hence the phreatic morphology, remains the same.

Several sectors, from La Plata to Río de La Plata, can be distinguished in terms of the general morphology of the phreatic layer. These sectors are:

a- area of recharge predominance close to La Plata: There is a local diverging flow from the border zone between La Plata and Berisso. The depth of the phreatic levels shows a marked contrast between those located towards the north of 122 Street, where they appear between 2 and 3 m, and those towards the south, where they can surpass 10 m.

b- area of partial discharge predominance: There is local convergent runoff towards the lowest parts, represented by Maldonado wetland and

Ensenada wetland. Phreatic levels are located at shallow depth (1meter) or outcroppings, which proves that the area is partially flooded according to the time of year. Discharge is essentially accounted for by evapotranspiration and efflux towards some courses that diverge and drain this area.

c- area of local recharge predominance: In this area, a local diverging flow arises from a strip that is topographically slightly higher and that belongs to the environment where the urbanised areas of Berisso and Ensenada are located. Runoff occurs towards the low parts mentioned above (south) and towards the bank of Río de La Plata.

d- partial and final discharge area: Runoff moves locally towards Río Santiago and other existing courses, and regionally towards Río de La Plata. It is an area directly affected by river level oscillations.

In general, industrial sectors constitute a high sector in the phreatic surface. When this positive morphology of the phreatic layer, which remotely surpasses 3 meters a.m.s.l., is analysed in detail, it shows secondary peculiarities stemming from the activities done in the area. Thus, there appear domes that could represent areas of recharge predominance, coinciding with the largest stretches of green spaces and local depressions (discharge zones).

Regional groundwater flow is related to groundwater flow in Pampeano and Puelche units. The general runoff in the analysed area flows southwesterly - northeasterly, tending to discharge into Río de La Plata.

The possible behaviour of regional groundwater dynamics can be analysed in terms of the precise relationship between the recognised piezometric levels (Figure 4.4.3). It must be borne in mind that as the hydraulic potential differences between the collected levels are subtle (lower than 5 cm), there is very slow water transfer between levels.

In El Dique borehole, according to its hydraulic potential, Pampeano aquifer could be supplying water to both the phreatic and Puelche aquifers.

In Tiro Federal, the piezometric levels of both Pampeano and Puelche aquifers are lower than phreatic levels but have level variations between them. Hence, the direction of possible supplies is vertical but variable in sense at the same time.

In Puerto, Pampeano and Puelche aquifers are progressively lower compared to the phreatic one. They show a typical setting of vertical recharge from the phreatic layer as a result of low flow influence.

4.6 CHEMICAL CHARACTERISTICS OF GROUNDWATER

The hydrogeochemical characterisation that will be dealt with in this chapter contributes to differentiate between local and regional underground flows.

Sampling representativeness

Sampling was performed according to a procedure based on ASTM D5903-96 (2006) Planning and Preparing for Groundwater Sampling Event, ASTM D4448-01 (2007) Sampling Groundwater Closet Wells, ASTM D6634-01 (2006) Selection of Purging and Sampling Devices for Monitoring Wells, and ASTM D6452-99 (2005) Purging Methods for Wells Used for Groundwater Investigations.

Prior to the extraction or collection of a sample, purge was performed in order to remove the water suspended in the well by means of a bailer. Before initiating this process, the static levels were measured up. The criterion of fixed volume was used to define the quantity of water to be extracted with a bailer. This criterion had to guarantee the eviction of

stagnant water volume. The volume of water contained in the well had to be extracted at least 3 times.

Once the purge was concluded, the recovery of the original prepurging water level was possible and only then was the sample collected for its analysis.

4.6.1 Chemical characteristics of the phreatic layer

In this hydrogeochemical characterisation of groundwater 14 sampling sites were considered. All of them showed the phreatic aquifer, and 3 clusters of piezometers also showed Pampeano and Puelche aquifers. These wells were called Dique, Tiro Federal and Puerto and respectively located in the zones defined as recharge, medium zone and discharge of the area of study, according to the hydrodynamic model used.

The list of parameters used during the samplings taken in October 2006, April 2007, October 2007, April 2008 and October 2008, as well as the analytical methodology used and its respective limit of quantification, is displayed in Table 4.6.1

Table 4.6.1 Analytical methodology and LOQ

Parameters	Analytical methodology	Unit	LOQ
Arsenic	SM 3500/3114-C	mg/L	0,01
Benzene	EPA 8260	µg/L	10
Bicarbonate	SM 2320-B	mg/L	0,5
Cadmium	SM 3500/3111-B	mg/L	0,01
Calcium	SM 3500 Ca-B	mg/L	0,5
Carbonate	SM 2320-B	mg/L	0,5
Zinc	SM 3500/3111-B	mg/L	0,01
Chloride	SM 4500 CI-B	mg/L	1
Cobalt	SM 3500/3111-B	mg/L	0,02

Copper	SM 3500/3111-B	mg/L	0,02
Electric conductivity	SM 2510-B	µs/cm	0,1
Chromium	SM 3500/3111-B	mg/L	0,02
Ethylbenzene	EPA 8260	µg/L	10
Total phenols	SM 5530-C	mg/L	0,05
Fluoride	SM 4110-B	mg/L	0,1
Total hydrocarbons	EPA 8015	mg/L	0,2
Magnesium	SM 3500/3111-B	mg/L	5
Mercury	SM 3500/3112-B	mg/L	0,001
Nickel	SM 3500/3111-B	mg/L	0,01
Nitrate	SM 4110-B	mg/L	5
Nitrite	SM 4110-B	mg/L	0,05
pH	SM 4500H*-B	pHu	0,01
Lead	SM 3500/3111-B	mg/L	0,02
Potassium	SM 3500/3111-B	mg/L	1
Dry residue	SM 2540-B	mg/L	1
Sodium	SM 3500/3111-B	µg/L	10
Sulphate	SM 4500 SO4-E	mg/L	1
Sulphur	SM 4500 S D	mg/L	0,1
Toluene	EPA 8260	µg/L	10
Xylene	EPA 8260	µg/L	10

Method 3111 uses an atomic absorption spectrometer in the flame absorption mode.

Method 3500 uses either a flame photometer or an atomic absorption spectrometer in the flame emission mode.

Method 2320 for determining alkalinity uses the titration method.

Method 5530C describes chloroform extraction.

Method 4110 Provides methods for the determination of a number of non-metallic analytes by the use of ion chromatography (IC), which eliminates the need to use hazardous reagents. These analytes include: bromide; chloride; fluoride; nitrate; nitrite; phosphate; and sulfate. This section includes methods for IC with chemical suppression of eluent

conductivity (4110B) and single-column IC with electronic suppression of eluent conductivity and conductimetric detection.

Method 4500 is equivalent to Method 4110 for Cl, SO₄ y sulphur.

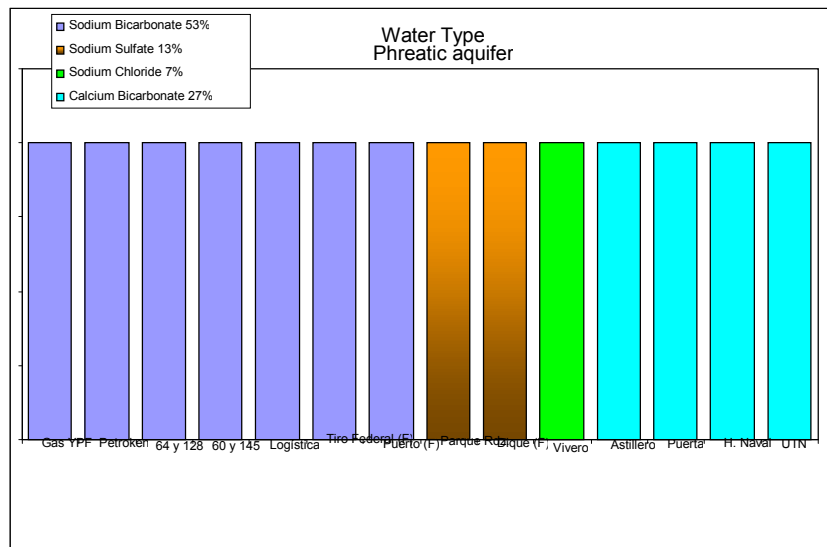
Method 2540B gives the method for total solids dried at 103-105°C.

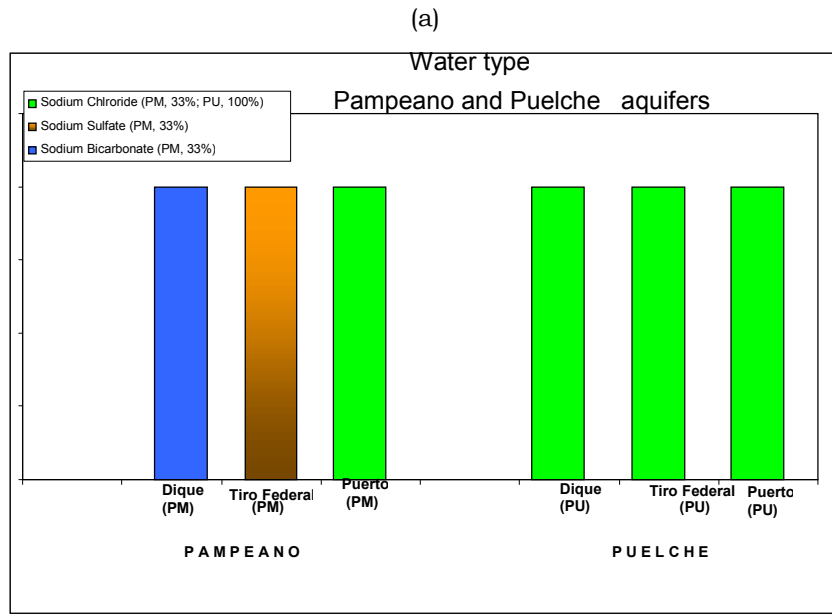
EPA 8260 for VOCs uses GC/MS capillary column technique.

EPA 8015 for nonhalogenated organics uses GC/FID technique.

Usual parameters within major and minor ions were taken into consideration for the hydrogeochemical characterisation. That is, for cations, calcium, magnesium and potassium were considered, and for anions, bicarbonate, chloride, sulphate and nitrate. Those data were treated adequately for their subsequent interpretation through common methods such as temporary evolution graphs, hydrogeochemical maps, Stiff diagrams and Piper diagrams. The remaining analytes were treated individually.

Samples were taken following the standards for this type of work. The volume of piezometers was removed at least three times immediately before collecting a sample, obtained with a 1.3-cm polythene bailer with a shutoff valve. All the ionic relations were calculated from the concentrations in mg/L.





(b)

Fig. 4.6.1 a) and b). Percentage distribution of the different types of water found in phreatic, Pampeano and Puelche aquifers

Figures 4.6.1 a) and b) show the types of water found in the various points of observation, based on the mean values of the data sets obtained during the 5 samplings collected throughout 2 years. Results from phreatic, Pampeano and Puelche aquifers are displayed here. The reported analytical results of each of them are shown in the respective Annex 2 (Chemical data table, page 202). Due to space limitations and reading easiness, this chapter only includes the data and figures regarded as representative of the topic.

A predominance of sodium-bicarbonate water (53%), followed by calcium-bicarbonate water (27%), sodium-sulphate water (13%) and only one point with sodium-chloride water (7%), was found in the phreatic layer. The point with sodium-chloride water is Vivero, located in the lowest extreme of the area of study. The predominance of chloride ion in this particular case can possibly be associated with maintenance tasks of the nursery where the well was drilled, that is, treatment, soil

fertilisation, irrigation, etc., with the subsequent process of ion evaporation and concentration.

Analytical data were processed and the information obtained was dumped onto the relevant plane through modified Stiff diagrams. The distribution of the different types of water found in the area of study is graphically represented on the horizontal plane in the Figure 4.6.2.

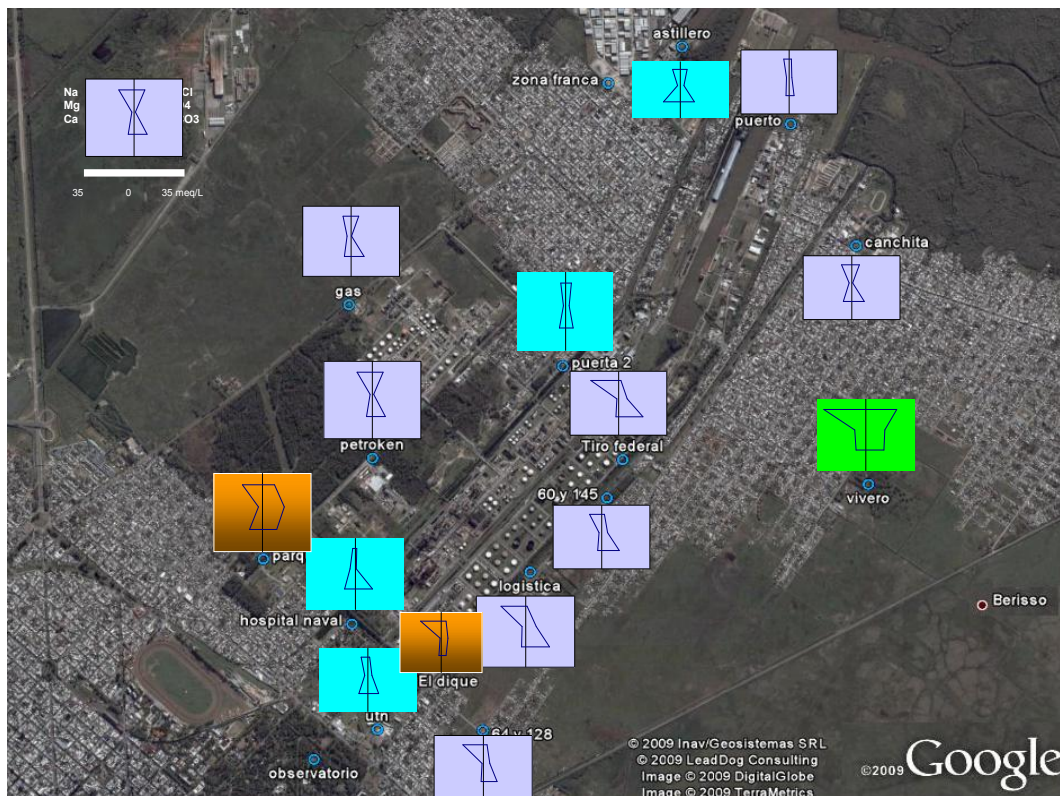


Fig. 4.6.2 Graphical representation by modified Stiff diagrams (Custodio, 1965) of the different types of water found in the phreatic aquifer

Local flow, represented by phreatic water, show marked chemical variations in the horizontal plane (Figure 4.6.2). Values lower than 1,000 mg/L (CE) coincided with the local recharge area (central strip). There was less mineralisation and water was rich in calcium bicarbonate. In the direction of flow, water varied in concentration and type, enriching in sodium ions in the area linked to the local discharge of the phreatic layer (Maldonado and Ensenada wetlands). The highest

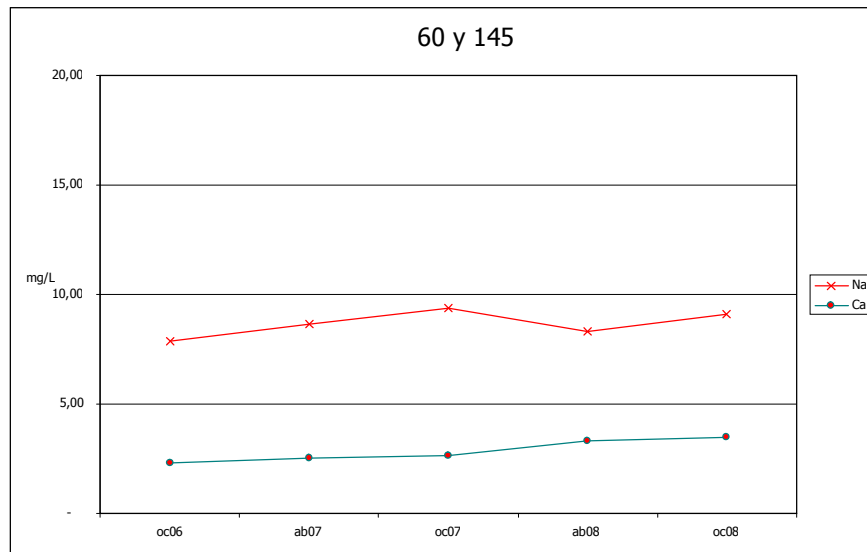
values of salinity were registered there, exceeding 2,000 mg/L (CE) and reaching a maximum of 3,850 mg/L (CE). In the southeast, water evolved into the sodium-chloride type, with extreme chloride values ranging from 630 to 1,160 mg/L, alkalinity from 650 to 1,300 mg/L, sulphates from 480 to 840 mg/L and sodium from 630 to 870 mg/L, whereas in the southwest there was water of a sodium-sulphate type, with sulphate values between 600 and 880 mg/L and sodium values between 250 and 460 mg/L.

In regard to cations, practically all the samples were sodic, except for four of them that had a slight predominance of calcium and magnesium but at the same time significant content of sodium. The most important variations in terms of value occurred in a seasonal manner: an increase in ion concentration was observed in the month of April every year, coincident with the period of low water. Although most of the concentrations were very similar over time, there was a slight rise in October 2008.

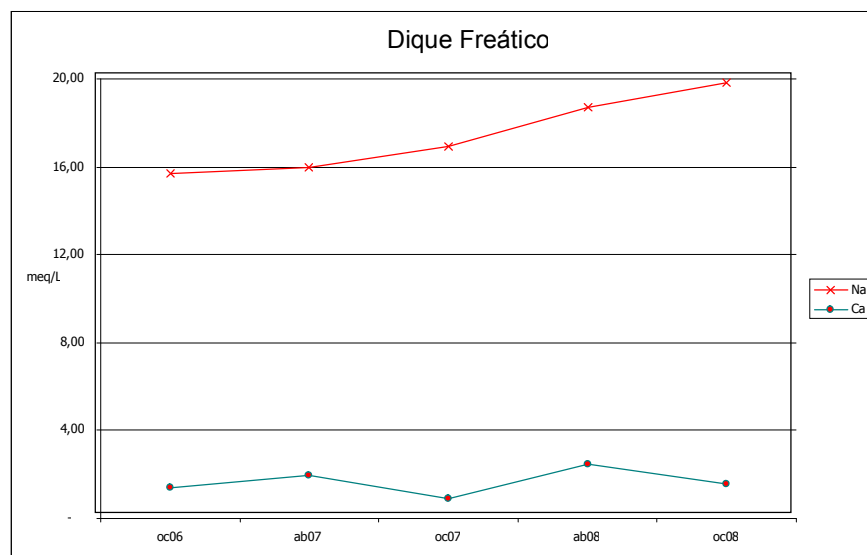
The concentration of sodium ion in fresh water varied between 0.05 and 20 meq/L (between 1 and 460 mg/L). However, higher values were usually found. The concentration of sodium ion in seawater hardly ever exceeded 500 meq/L (11,500 mg/L). It had very high solubility and was difficult to precipitate. It was easily affected by changes in base and usually associated with ion Cl. In this case, the origin of sodium could be related to the dissolution of sedimentary rock of marine origin, though mainly as supply by rainwater infiltration and rise in concentration by slow flow rate.

Like the classification of fresh water, almost all the samples had contents lower than 20 meq/L (Na), except for Vivero, Logística and Tiro Federal (phreatic) wells, slightly surpassing this value.

Some representative diagrams of major ion evolution are shown in Figure 4.6.3 a) and b). The diagrams for each point are included in the Annex 3 (Chemical variations plot, page 213).



a)



b)

Fig. 4.6.3 a) and b). Graphical representation of time variations in sodium content (meq/L) in the phreatic aquifer

The point called Vivero had the highest content of sodium, reaching 37 meq/L (850 mg/L). It is the most extreme point in the area of study and the high content of this ion can be due both to the nursery's own

maintenance processes (irrigation-evaporation-concentration), as mentioned before, and to the increase by water residence time.

Overall, a slight trend of increase in concentration of both sodium and calcium over time can be observed. This is almost certainly related to the periods of drought that were registered in the last few months.

Astillero, Puerta 2, Hospital Naval and UTN points had a predominance of calcium. An example is shown in Figure 4.6.4.

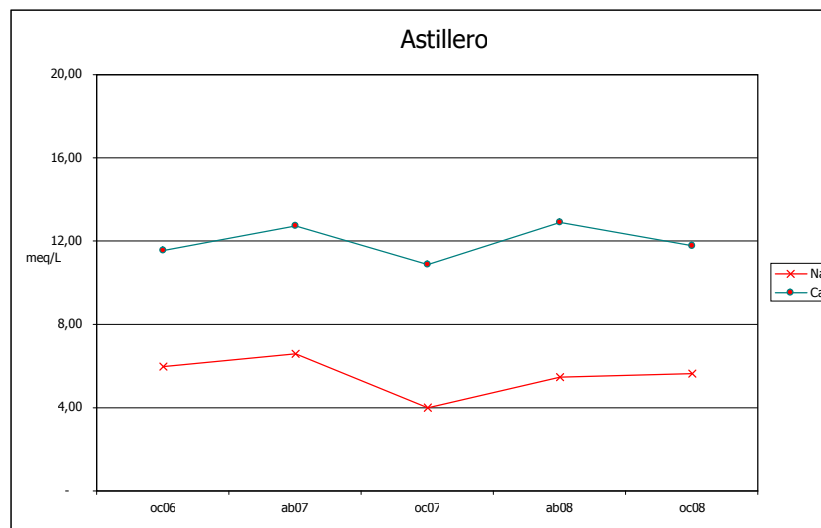
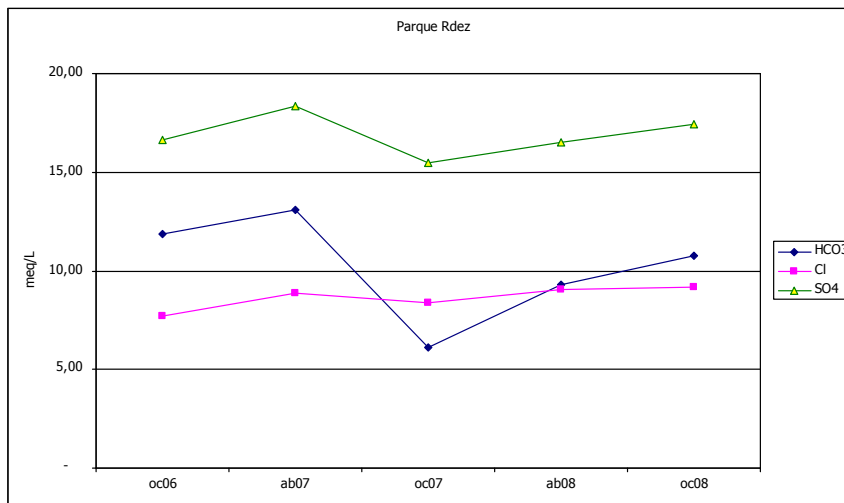
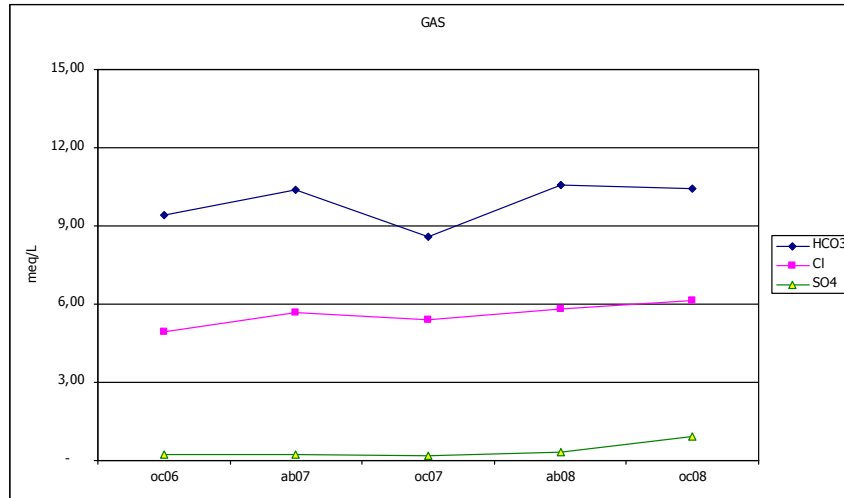


Fig. 4.6.4 Graphical representation of time variations in calcium content (meq/L) in the phreatic aquifer

In regard to anionic predominance, most of the samples proved to be bicarbonate, with extreme values ranging from 2 meq/L (130 mg/L) in Puerto (F) to 24 meq/L (1,460 mg/L) in Tiro Federal (F); followed by sulphate and chloride samples. Examples of each case are displayed in Figure 4.6.5. Although most of the samples were bicarbonate, those that were sulphate had higher mineralisation than the bicarbonate ones, the content of sulphate ions being markedly high (> 800 mg/L). The high content of sulphate ions in some of the samples, being the predominant anion, could be related to the existence of intercalations of gypsum

lenses in the area of study. The samples with the highest content of chloride were located in urbanised areas of Berisso.



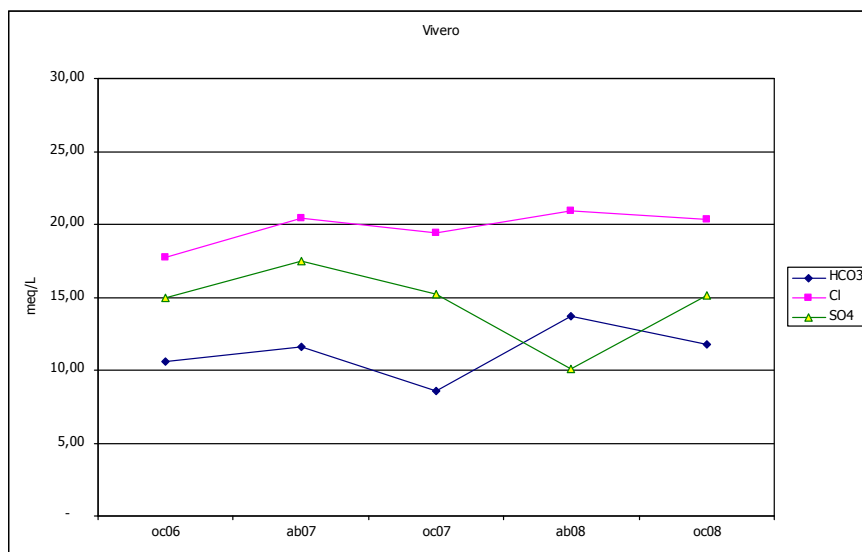


Fig. 4.6.5 Graphical representation of time variations in major anion content (meq/L) in the phreatic aquifer

Like cations, concentrations of anions varied in a seasonal manner and over time, with a slight rise in October 2008 sampling. This rise could reflect the period of drought that was registered in Figure 4.4.1 of precipitation. The remaining Figures are included in the Annex 3 (Chemical variations plot, page 213).

In connection with total solid values, the bicarbonate samples had low content, between about 550 and 1,500 mg/L; the sulphate samples had values between 1550 and 2,500 mg/L; and the chloride ones had values between 2,600 and 4,400 mg/L, surpassing the content of other samples. The Figure 4.6.6 shows both seasonal trend and increase over time, October 2008 contents being the highest.

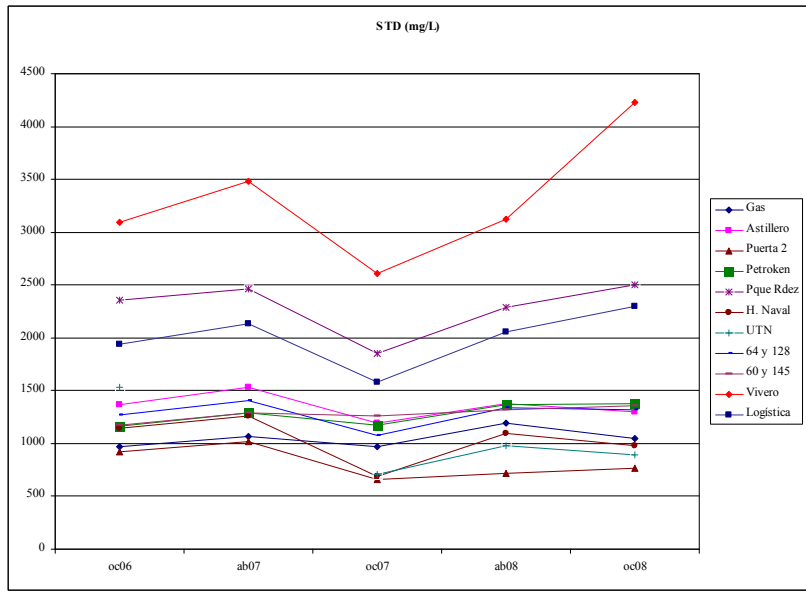


Fig. 4.6.6 Graphical representation of STD content (mg/L) reported in various samplings in the phreatic aquifer

Data analysis was also performed with Piper diagrams because they can represent anions and cations simultaneously. These diagrams are useful since many analyses can be displayed in a single diagram without creating confusion. Waters that are chemically similar are divided into groups and can be classified according to their location in the diagram.

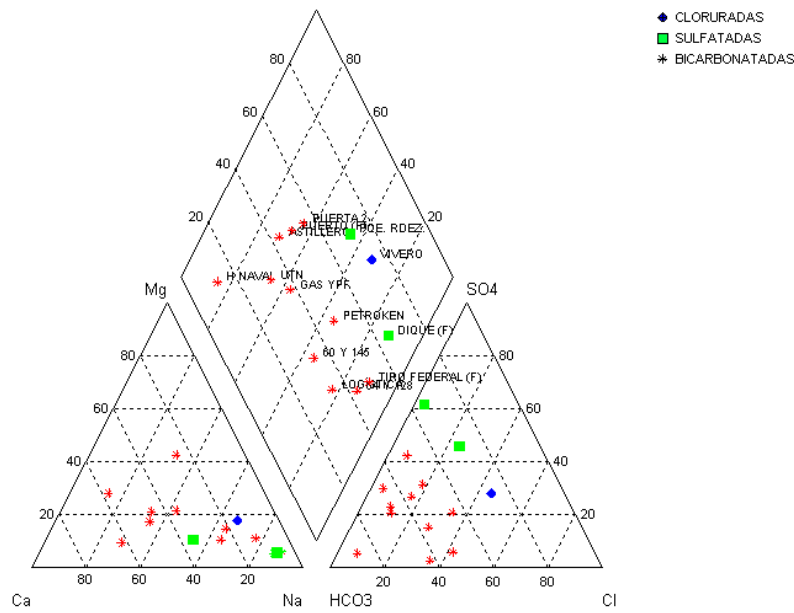


Fig. 4.6.7 Graphical representation of the phreatic aquifer in a Piper diagram

Figure 4.6.7 shows the mean values of the samples at phreatic level. It also shows the distribution of these samples, mainly grouping the bicarbonate and sodium-calcium ones. In addition, sulphate and chloride water types found in the area of study are displayed and separated from the rest.

4.6.2 Chemical characteristics of Pampeano and Puelche aquifers

Unlike those found in the phreatic aquifer, the conditions found in Pampeano and Puelche aquifers were different. In both aquifers and during the same sampling campaigns, samples were collected in the following points: Dique, Tiro Federal and Puerto. Results from the analyses yielded different types of water than those found in the phreatic aquifer.

The variations in water type found in Pampeano aquifer are important because each of the samples showed a different water type. Dique showed sodium-bicarbonate water whereas Tiro Federal had sodium-sulphate water and Puerto had sodium-chloride water.

Graphical representations of water found in these three points, both in Pampeano and Puelche aquifers, are included in Figure 4.6.8 and 4.6.9 by means of modified Stiff diagrams (Custodio, 1965).

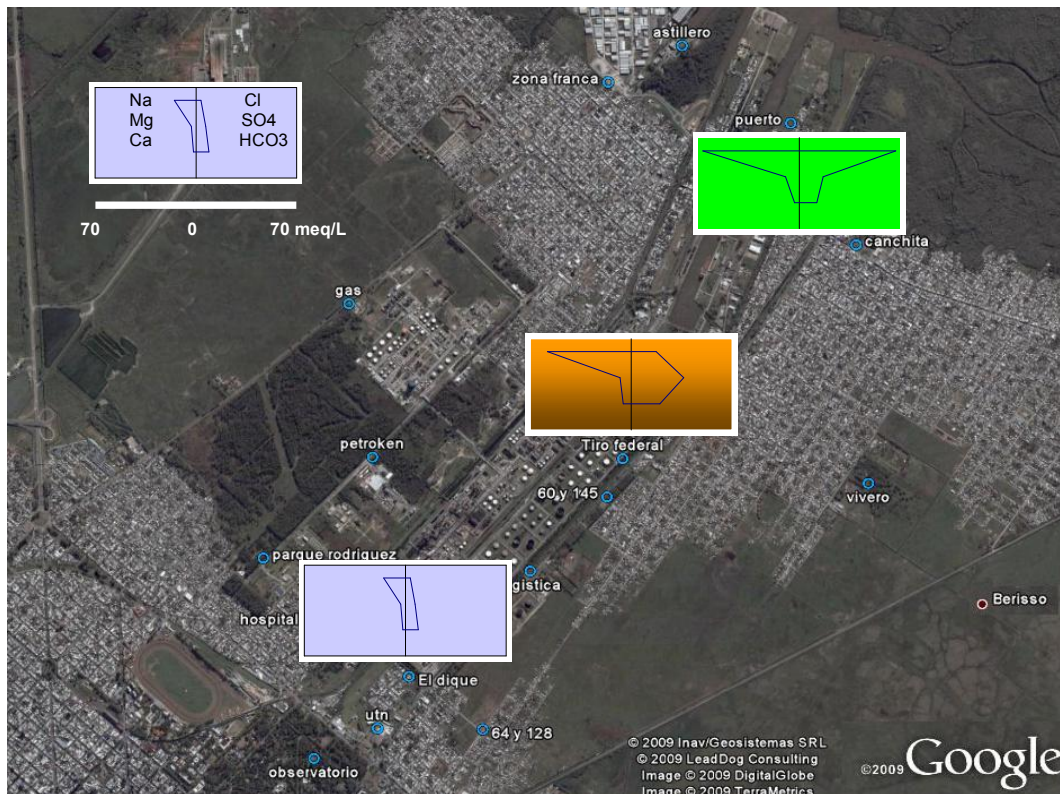


Fig. 4.6.8 Graphical representation by modified Stiff diagrams (Custodio, 1965) of the different types of water found in Pampeano aquifer

Concentrations found in Pampeano aquifer were higher than those in the phreatic, practically doubling the values of the different ions. In connection with cations, sodium was likewise the predominant one, with extreme values between 13 meq/L (300 mg/L) in Dique and 77 meq/L (1,765 mg/L) in Puerto.

The evolution observed in Dique was water changing from a sodium-sulphate type, possibly due to the occurrence of gypsum formations in such a point in the phreatic aquifer, to a sodium-bicarbonate type in Pampeano aquifer and a sodium-chloride type in Puelche aquifer. This evolution showed a slight decrease in sodium ion content (from 17 to 15 meq/L [from 400 to 350 mg/L]) between the phreatic and Pampeano aquifers. However, there was a significant increase towards Puelche aquifer, with a mean value of slightly more than 30 meq/L (700 mg/L), showing features of affected water due to possible mixture with seawater

or as rise in concentration caused by flow slowness in the area. It should be remembered that the mean value of sodium reported for seawater was about 400 meq/L (9,500 mg/L) whereas for fresh water it did not exceed 20 meq/L.

Although there was no variation in calcium ions between the phreatic and Pampeano aquifers, with contents of approximately 1.7 meq/L (35 mg/L), there was variation in Puelche aquifer, with values of up to 6 meq/L (123 mg/L). A content of 19 meq/L (400 mg/L) in seawater has been reported in literature.

On the other hand, a marked increase in magnesium ions, from 0.8 to 3 meq/L (from 10 to 37 mg/L) was observed between the phreatic and Pampeano aquifers. It reached 7.4 meq/L (90 mg/L) in Puelche aquifer. However, in practical terms, it did not have major impact in water type. The content of this ion ranges from 1 to 100 mg/L (8 meq/L) in fresh water and can reach 1,200 mg/L (100 meq/L) in seawater.

In short, water in Dique point changed with depth from a sodium-sulphate type of low mineralisation in the phreatic aquifer, through a slightly more mineralised sodium-bicarbonate type, to a clearly sodium-chloride type with an important increase in mineralisation.

In the point called Tiro Federal the behaviour was different. The phreatic aquifer had sodium-bicarbonate water, with low mineralisation, in keeping with the water found in its neighbouring points. In the Pampeano aquifer, this point had sodium-sulphate water with a clear increase in mineralization and with a vast increase in sodium ion content. This content ranged from 20 to 58 meq/L (460 to 1,340 mg/L) between the phreatic and Pampeano aquifers and reached 112 meq/L (2,580 mg/L) in the Puelche one, where water was of a sodium-chloride type.

Similarly, calcium and magnesium ions largely increased with depth. However, sodium ion still predominated.

In regard to anions, bicarbonate predominated in the phreatic aquifer. It had a mean value of 17 meq/L (1,080 mg/L) and reached 20 and 21 meq/L in Pampeano and Puelche aquifers respectively. Sulphate was the predominant anion in Pampeano aquifer, reaching mean concentrations of 37 meq/L (1,760 mg/L) and slightly decreasing towards Puelche aquifer, with mean values of 27 meq/L (1,325 mg/L). Chloride was the predominant anion in Puelche aquifer, with mean values of 93 meq/L (3,275 mg/L), contrasting with those encountered in the phreatic and Pampeano: 1.9 and 17 meq/L (67 and 614 mg/L) respectively.

There was thus a clear trend of ionic enrichment with depth, with significant increase in sodium and chloride ions, characteristic of seawater. Their values ranged from about 420 meq/L to 495 meq/L respectively. Hence, it could be assumed that it was concerned with the effects of a possible mixture of old seawater from the lower formation with supply of meteoric water from the phreatic aquifer. As this mixture had relatively high flow rates too, it could also be assumed that there was certain enrichment (mainly) in sodium ions.

Finally, in the case of Puerto, there was sodium-bicarbonate water in the phreatic aquifer, in keeping with the surrounding area, with very low mineralisation and clearly meteoric water. Water was sodium-chloride in Pampeano aquifer. Thus, ionic content largely increased. This type of water was also present in Puelche aquifer, with a substantial increase in ionic content.

In regard to cations, an important evolution took place because it ranged from sodium contents of 3.7 to 66.5 meq/L (86 a 1,530 mg/L) between the phreatic and Pampeano aquifers to extreme mean values of 146

meq/L (3,355 mg/L) in Puelche. Although calcium and magnesium also showed a marked increase in their concentration, ranging from 2 to 65 meq/L and from 2 to 54 meq/L respectively from the phreatic level to Puelche level, the predominance of sodium was clear at the three levels. Besides, the increase in magnesium ion content could be related to the mixture with seawater proposed above.

In regard to anions, bicarbonate increased the mean values of 3.5 to 12 meq/L (215 to 740 mg/L) but this value decreased again in the Puelche aquifer, going back to about 4 meq/L. On the other hand, chloride increased its mean value considerably between the different strata. It ranged from 1.5 to 67 meq/L (54 to 2,380 mg/L) between the phreatic and Pampeano aquifers to 285 meq/L (10,100 mg/L) in the Puelche aquifer. The maximum punctual value found exceeded 12,000 mg/L. According to literature, seawater has contents of chloride ion of 493 meq/L (17,500 mg/L).

Sulphate also increased with depth, from 2 to 17 meq/L (98 to 800 mg/L) between the phreatic and Pampeano aquifers to a mean value of 37 meq/L (1,753 mg/L) in Puelche aquifer.

Like calcium and magnesium cations, sulphate clearly increased with depth, also matching the existing increase in mineralisation that could be associated with supply of long-standing seawater, likely to occur in the lowest aquifer. The values found for seawater reached 50 meq/L (2435 mg/L).

Figure 4.6.10 represents all these changes in water quality, between the aquifers.



Fig. 4.6.9 Graphical representation by modified Stiff diagrams (Custodio, 1965) of the different types of water found in Puelche aquifer

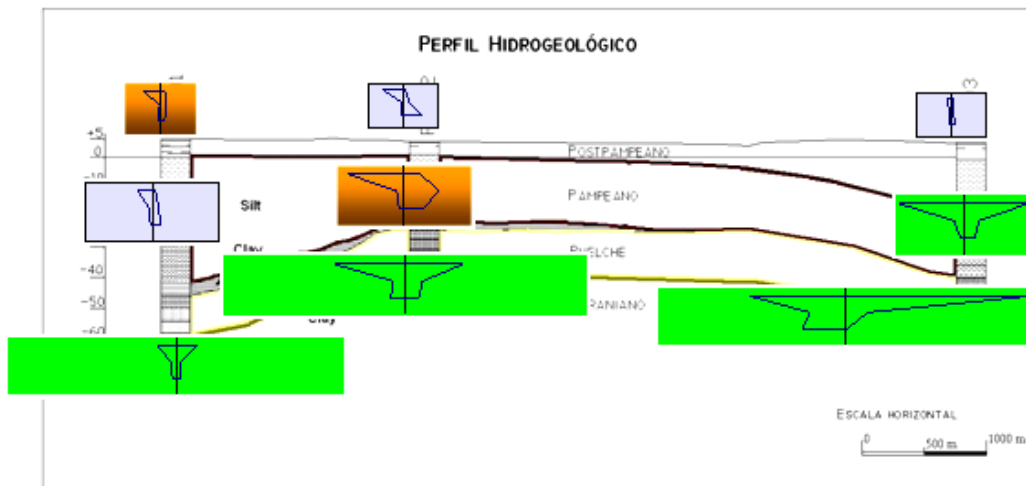
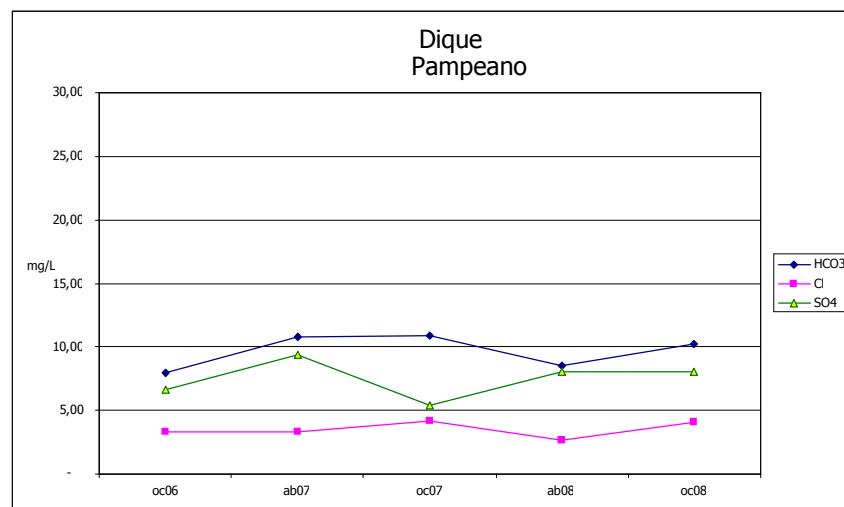
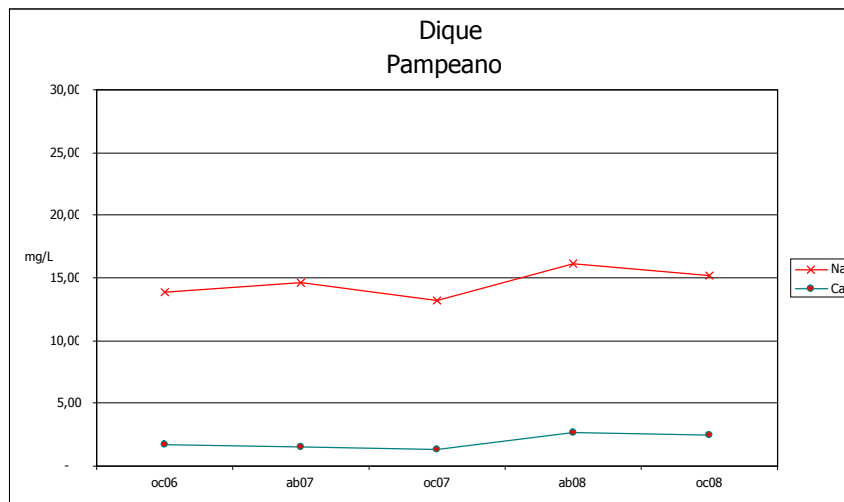


Fig. 4.6.10 Graphical representation by modified Stiff diagrams (Custodio, 1965) of the profiles of different types of water found in the phreatic, Pampeano and Puelche aquifers

The contents of major ions and variations over time for Dique point in Pampeano and Puelche aquifers are illustrated in Figure 4.6.11. The rest of the Figures are included in the respective Annex 3 (Chemical variations plot, page 213) Figure 4.6.11 shows the predominance of sodium cation as well as the variations in terms of anions that have been mentioned for each particular case. Although there appears to be some variation, ionic content does not vary significantly over time and there is not any great influence in terms of increase in concentration for the last sampling. This could be attributed to precipitation decrease, as seen in the phreatic aquifer.



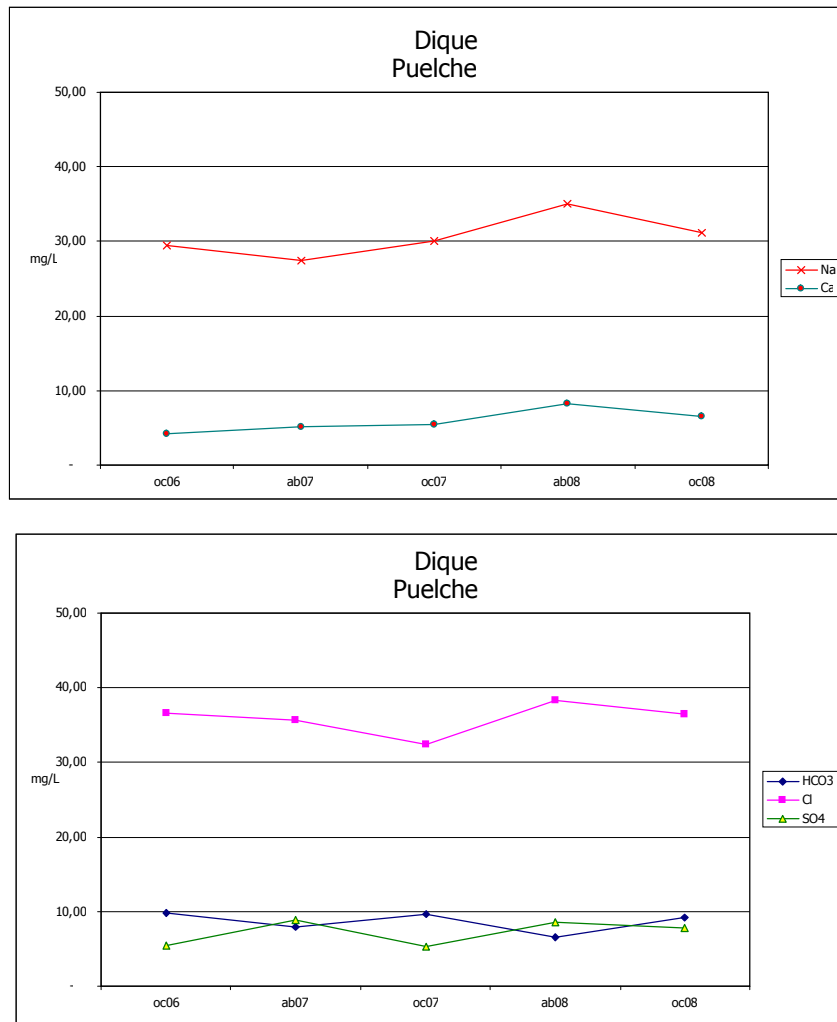


Fig. 4.6.11 Graphical representation of time variations in major ion content (meq/L) in Pampeano and Puelche aquifers

4.6.3 Minor ions and trace elements

In addition to the parameters described above, some analyses of minor ions and trace elements were performed. The relation between them is included in this chapter's list of parameters and the analytical results are included in the Annex 2 (Chemical data table, page 202). The results of such parameters are described below. Argentina has a Código Alimentario Nacional (National Food Code). In Chapter 12 that Code describes admitted maximum values of certain parameters for drinking water. Table 4.6.2 shows those values.

Table 4.6.2 Water quality parameters

Código Alimentario Argentino Artículo 982 - (Res Conj. SPRyRS y SAGPyA N° 68/2007 y N° 196/2007)	
Parámetro Físico	Máximo
Turbiedad	3 N T U
Color	5 Pt-Co scale
Olor	Sin olor
pH	6.5 – 8.5
Sustancias Inorgánicas	Máximo [mg/l]
Amoníaco NH ₄ ⁺	0.20
Antimonio	0.02
Aluminio (Al)	0.20
Arsenico (As)	0.01
Boro (B)	0.5
Bromato	0.01
Cadmio (Cd)	0.005
Cianuro (CN ⁻)	0.10
Zinc (Zn)	5.0
Cloruro (Cl ⁻)	350
Cobre (Cu)	1.00
Cromo (Cr)	0.05
Dureza Total (CaCO ₃)	400
Fluor (F)	1.7
Hierro Total (Fe)	0.30
Manganeso (Mn)	0.10
Mercurio (Hg)	0.001
Niquel (Ni)	0.02
Nitrato (NO ₃)	45
Nitrito (NO ₂)	0.10
Plata (Ag)	0.05
Plomo (Pb)	0.05
Selenio Se)	0.01
TDS	1500
Sulfatos (SO ₄)	400
Cloro activo residual	0.2

In the phreatic aquifer, contents of arsenic, cadmium, zinc, cobalt, fluoride, mercury, nitrate, nickel and lead were found in some samples (Table 4.6.3). Most of them exceed the maximum in Table 4.6.2.

Table 4.6.3 As, Cd, Zn, Co, F, NO₃, Ni, Ld contents

Parameter (LOQ mg/L)	Maximum value (mg/L)	Site	Date	Sites with analyte
Arsenic (0.01)	0.32	Dique (F)	Apr 07	64 y 128, Dique (F), Gas, H. Naval, Logística, Pque. Rdz., Petroken, Puerta 2 and Vivero
Cadmium (0.01)	0.03	Vivero	Apr 08	Vivero
Zinc (0.01)	0.2	H. Naval	Apr and Oct 08	60 y 145, Astillero, Gas, H. Naval, Logística, Pque. Rdz., Petroken, Puerta 2 and UTN
Cobalt (0.02)	0.048	Pque Rdz	Oct 06 and Apr 07	Astillero, Pque. Rdz., Vivero
Nitrate (5)	31	Vivero	Oct 08	64 y 128, Astillero, H. Naval, Logística, Pque. Rdz., Petroken, Puerta 2, Puerto (F) and Vivero
Lead (0.02)	0.09	Astillero and Vivero	Apr and Oct 08	60 y 145, Astillero, Gas, H. Naval, Logística, Pque. Rdz., Petroken, UTN and Vivero
Nickel (0.01)	0.03	Vivero	Apr and Oct 08	64 y 128, H. Naval, Pque. Rdz., Petroken, UTN and Vivero
Fluoride (0.1)	2.1	Dique (F)	Apr 07	60 y 145, 64 y 128, Astillero, Dique (F), Gas, H. Naval, Logística, Pque. Rdz., Petroken, Puerta 2, Puerto (F), Tiro Federal (F), UTN, and Vivero

Mercury (0.001)	0.007	Pque Rdz	Apr 07	64 y 128, Astillero, Gas, H. Naval, Logística, Pque. Rdz., Petroken, UTN and Vivero
--------------------	-------	----------	--------	---

In some cases, the values reported by the laboratory match the limit of quantification of the analytical technique. Hence, it is not possible to determine with precision whether the element is present or whether the values are within the analytical error. Nevertheless, for the purpose of this work, the reported values have not been modified. The Tables of analytical results included in the Annex 2 (Chemical data table, page 202) show the values reported by the laboratory for all parameters.

The presence of arsenic and fluoride is related to the natural existence of these elements within the area of study. However, the presence of all the other parameters can be associated with industrial and/or urban activity in the zone surrounding this area. Their existence in the aquifer is thus anthropogenic.

Although the reported values are not excessively high, their existence demands closer long-term monitoring of these elements with the aim of diagnosing the real state of such water and its evolution. Moreover, it demands a correct association among the diverse activities, both urban and industrial, in order to appropriately avoid their entry into the aquifer, as well as identifying their correct arrangement.

There was no benzene, copper, chromium, ethylbenzene, total phenols, total hydrocarbons, sulphur, toluene and xylene reported in any sample.

Arsenic and fluoride were the sole parameters reported as present in the water samples from Pampeano and Puelche aquifers. No other analysed parameter was revealed in these aquifer strata.

Table 4.6.4 As and F contents

Well	Parameters (mg/L)	As	F
LOQ (mg/L)		0.01	0.1
DIQUE (PU)	Apr 08	0.01	0.5
DIQUE (PU)	Oct 08	0.01	0.5
DIQUE (PU)	Apr 07	0.01	0.6
DIQUE (PM)	Apr 08	0.02	0.4
PUERTO (PM)	Apr 08	0.02	0.6
TIRO FEDERAL (PM)	Apr 08	0.02	0.9
DIQUE (PM)	Oct 07	0.02	
TIRO FEDERAL (PM)	Oct 08	0.03	0.9
PUERTO (PM)	Apr 07	0.03	0.6
TIRO FEDERAL (PM)	Apr 07	0.04	1.0
DIQUE (PU)	Oct 06	0.04	0.8
TIRO FEDERAL (PM)	Oct 07	0.04	0.6
DIQUE (PU)	Oct 06	0.04	0.5
DIQUE (PM)	Oct 06	0.09	0.8
TIRO FEDERAL (PM)	Oct 06	0.17	1.4
PUERTO (PM)	Oct 06	0.21	0.9
TIRO FEDERAL (PU)	Oct 06	0.21	1.3

The points with reported contents of arsenic, arranged from minimum to maximum, are illustrated in Table 4.6.4 . The first reported values can be considered within the expected analytical error because they are precisely on the limit of quantification of the analytical technique. It is therefore not possible to accurately determine whether there is As or not. These points belong to Dique (PU) in April 2007, April 2008 and October 2008. Likewise, the points with content of As have been correlated to the values of F and NO₃.

The highest values reported for As were 0.23 and 0.32 mg/L in Dique (F) point in October 2006 and April 2007 samplings respectively. In subsequent samplings in such a point, values higher than 0.1 mg/L

were reported in October 2007, April 2008 and October 2008 samplings. Concentrations of As were also reported in October 2006 in Dique (PM) and (PU), reaching 0.04 and 0.09 mg/L respectively.

Fluoride was detected in practically all the samples.

The values found for both arsenic and fluoride are associate with background values that appear naturally in the area of study, without being it possible to attribute them to any kind of anthropogenic input.

Table 4.6.5 F and As contents

Well	Parameters (mg/L)	F	As
LOQ (mg/L)		0.1	0.01
DIQUE (PM)	Apr 08	0.4	0.02
DIQUE (PU)	Oct 07	0.4	
PUERTO (PU)	Oct 07	0.4	
DIQUE (PU)	Oct 06	0.5	0.04
DIQUE (PU)	Apr 08	0.5	0.01
DIQUE (PU)	Oct 08	0.5	0.01
PUERTO (PM)	Apr 07	0.6	0.03
PUERTO (PM)	Apr 08	0.6	0.02
PUERTO (PU)	Apr 08	0.6	
TIRO FEDERAL (PM)	Oct 07	0.6	0.04
DIQUE (PU)	Apr 07	0.6	0.01
PUERTO (PU)	Oct 08	0.6	
PUERTO (PM)	Oct 08	0.7	
PUERTO (PU)	Apr 07	0.8	
DIQUE (PM)	Oct 06	0.8	0.09
PUERTO (PU)	Oct 06	0.8	0.04
TIRO FEDERAL (PM)	Apr 08	0.9	0.02
TIRO FEDERAL (PM)	Oct 08	0.9	0.03
TIRO FEDERAL (PU)	Apr 08	0.9	

PUERTO (PM)	Oct 06	0.9	0.21
TIRO FEDERAL (PU)	Oct 07	0.9	
DIQUE (PM)	Apr 07	0.9	
TIRO FEDERAL (PM)	Apr 07	1.0	0.04
PUERTO (PM)	Oct 07	1.0	
TIRO FEDERAL (PU)	Oct 08	1.1	
TIRO FEDERAL (PU)	Apr 07	1.2	
TIRO FEDERAL (PU)	Oct 06	1.3	0.21
TIRO FEDERAL (PM)	Oct 06	1.4	0.17

4.7 Environmental isotope results

In April 2008, 23 samples corresponding to the three analysed aquifer levels (phreatic, Pampeano and Puelche) were obtained. Isotopic analyses were performed by isotope ratio mass spectrometry at “Instituto de Geología y Geocronología Isotópica” (INGEIS). Hydrogen gas for ^2H analysis was obtained by water reduction using zinc, following the procedure developed by Coleman et al. (1982). CO_2 for ^{18}O analysis was done by water- CO_2 isotopic equilibration and Tritium by electrolytic enrichment followed by liquid scintillation counting.

The isotopic composition of rainwater was assessed with results drawn from the precipitation station of Ciudad Universitaria (Buenos Aires). The stable isotope averages until 2003 matched $\delta^{18}\text{O} = -5.3\text{‰}$ and $\delta^2\text{H} = -30\text{‰}$. An input concentration of about 8-9 TU was estimated for Tritium levels.

The definition of recharge in hydrological systems is essential to conduct a water balance and propose a conceptual model of aquifers. The use of isotopic techniques in the field of study, together with other techniques, intends to provide more information about recharge dynamics and salinisation mechanisms.

Results of $\delta^{18}\text{O}$ and $\delta^2\text{H}$ are shown below (Table 4.7.1):

Table 4.7.1 Isotope results

IAEA	Drilling	$\delta^{18}\text{O}$ ‰	$\delta^2\text{H}$ ‰
No	ID	± 0.2	± 1
20128	Hospital Naval	-5.9	-34
20129	Puerto- Pampeano	-4.2	-31
20130	Puerto- Freático	-5.0	-31
20131	vivero	-5.8	-35
20132	puerta2-YPF	-6.3	-43
20133	Astillero	-3.0	-23
20134	Logistica	-4.9	-30
20135	Shell Calle Cortada	-6.2	-37
20136	Parque M. Rodríguez	-7.1	-43
20137	Puerto-Puelche	-2.8	-19
20138	Petroken	-4.4	-30
20139	Facultad Afuera	-4.8	-30
20140	Facultad Adentro	-5.2	-32
20141	Gas Ensenada	-4.0	-29
20142	UTN	-4.9	-32
20143	Puelche El Dique	-4.5	-30
20144	Pampero El Dique	-5.1	-31
20145	Freático El Dique	-5.3	-31
20146	Tiro Federal Puelche	-3.1	-20
20147	Tiro Federal Freático	-5.1	-29
20148	Tiro Federal Pampeano	-4.1	-27
20149	128 y 64	-5.1	-31
20150	145 y 60	-5.4	-31

Isotopic analyses are shown in the conventional plot of $\delta^2\text{H}$ vs. $\delta^{18}\text{O}$ (Figure 4.7.1)

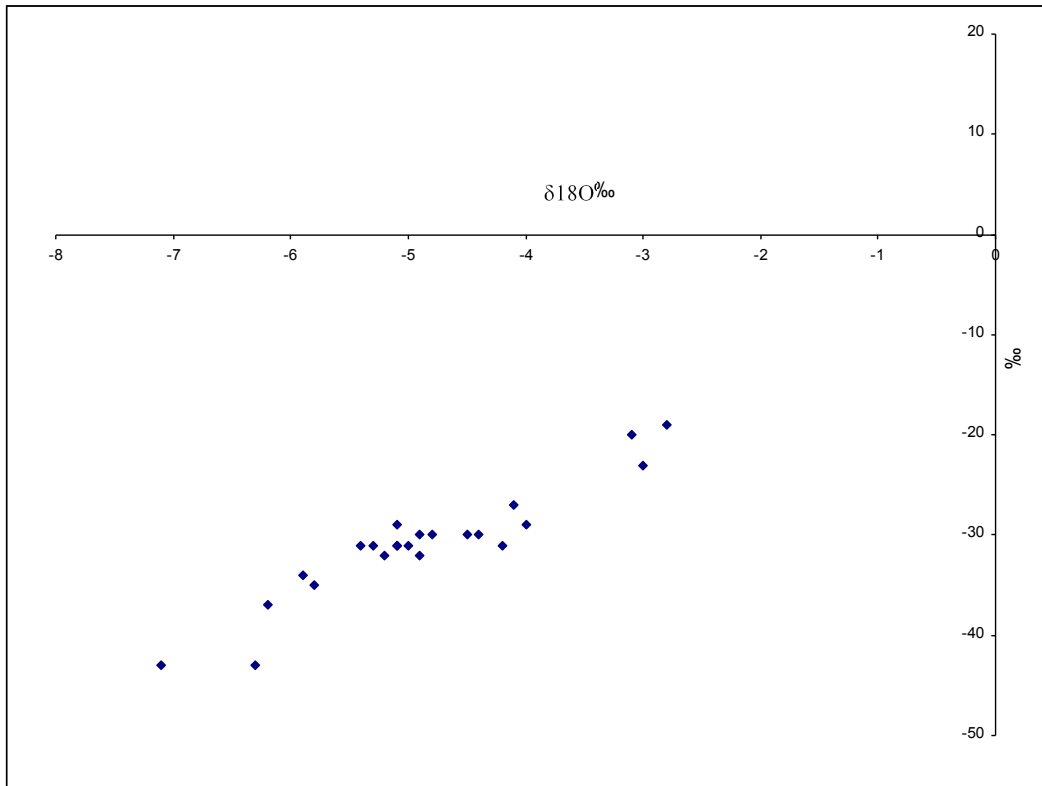


Figure 4.7.1 Plot $\delta^2\text{H}$ vs. $\delta^{18}\text{O}$ of the total number of samples

4.7.1 Isotopic composition. Stable isotopes

Groundwater composition in mild climates accurately reflects the isotopic composition of the locality's average rainfall. However, there could be processes that modify it during recharge mechanisms, such as evaporation prior to infiltration or seasonal variations. The comparison between $\delta^{18}\text{O}$ groundwater values and precipitation on a regional scale shows the connection between them. Nevertheless, as mentioned before, they can differ under certain circumstances, for instance, evaporation in the upper soil layers may result in enrichment of heavy isotopes.

Groundwater isotopic composition a priori shows values included in those measured in Ciudad Universitaria collection station, thus indicating their probable meteoric origin. The values measured range

from -2.8 to -7.1 for $\delta^{18}\text{O}$ and from -19 to -43 for $\delta^2\text{H}$. However, the dispersion of values as well as the high salinity in some wells suggests there is a combination of several processes.

Table 4.7.2 b calculus

IAEA No.	Sender No.	$\delta^{18}\text{O} \text{ ‰}$ ± 0.2	$\delta^2\text{H} \text{ ‰}$ ± 1	$\delta^2\text{H} \text{ ‰} - 8 \delta^{18}\text{O} \text{ ‰}$
20128	Hospital Naval	-5.9	-34	13
20129	Puerto- Pampeano	-4.2	-31	3
20130	Puerto- Freático	-5.0	-31	9
20131	vivero	-5.8	-35	11
20132	Puerta 2	-6.3	-43	7
20133	Astillero	-3.0	-23	1
20134	Logistica	-4.9	-30	9
20135	Shell Calle Cortada	-6.2	-37	13
20136	Parque M. Rodríguez	-7.1	-43	14
20137	Puerto-Puelche	-2.8	-19	3
20138	Petroken	-4.4	-30	5
20139	Facultad Afuera	-4.8	-30	8
20140	Facultad Adentro	-5.2	-32	10
20141	Gas Ensenada	-4.0	-29	3
20142	UTN	-4.9	-32	7
20143	Puelche El Dique	-4.5	-30	6
20144	Pampero El Dique	-5.1	-31	10
20145	Freático El Dique	-5.3	-31	11
20146	Tiro Federal Puelche	-3.1	-20	5
20147	Tiro Federal Freático	-5.1	-29	12
20148	Tiro Federal Pampeano	-4.1	-27	6
20149	128 y 64	-5.1	-31	10
20150	145 y 60	-5.4	-31	12

The following plot shows the distribution of results from aquifers.

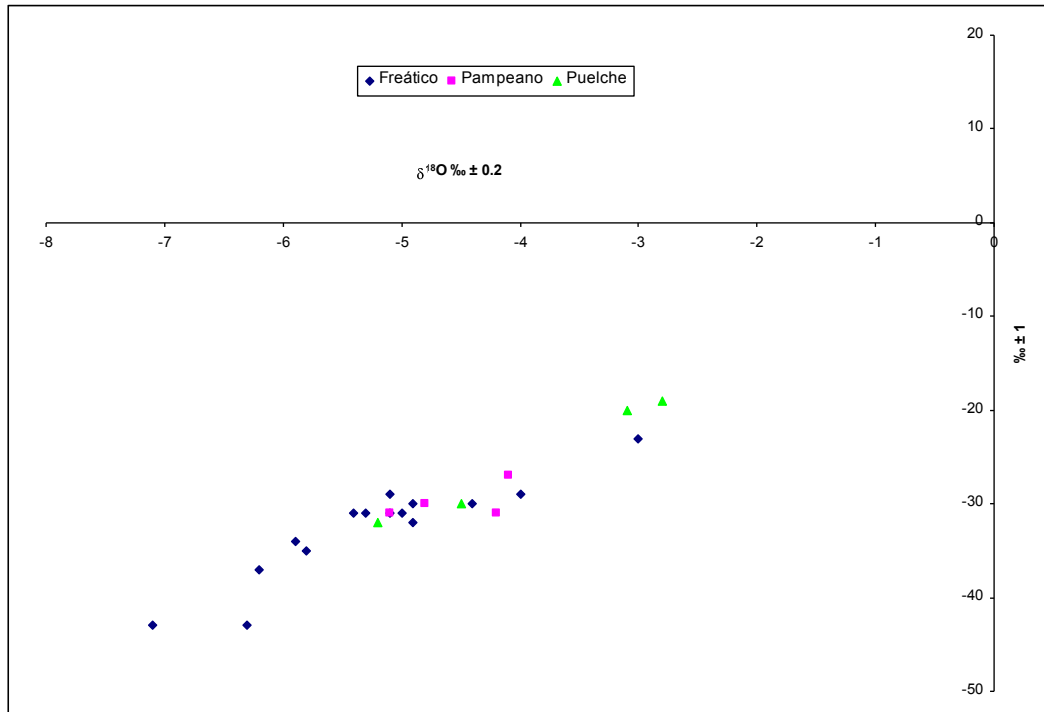
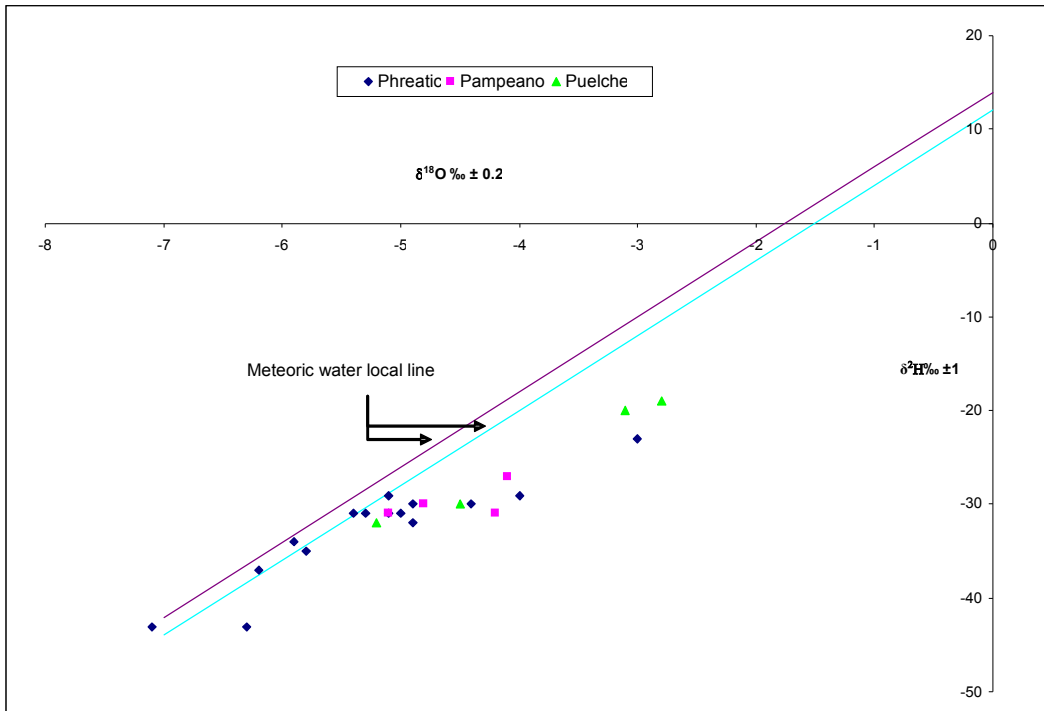


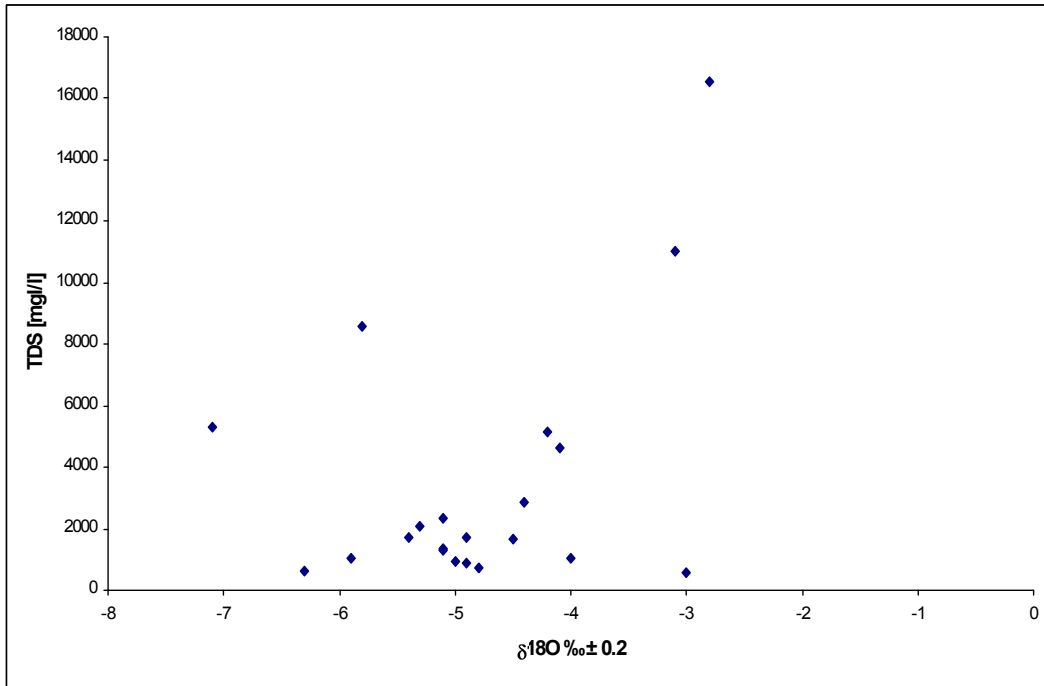
Figure 4.7.2 Plot $\delta^2\text{H}$ vs. $\delta^{18}\text{O}$ of the total number of samples of each aquifer

In the following plot (Figure 4.7.3) the local meteoric water line has been added, given by the equation $\delta^2\text{H} = 8 \delta^{18}\text{O} + 12/14 \text{‰}$ (Dapeña and Panarello, 2004)



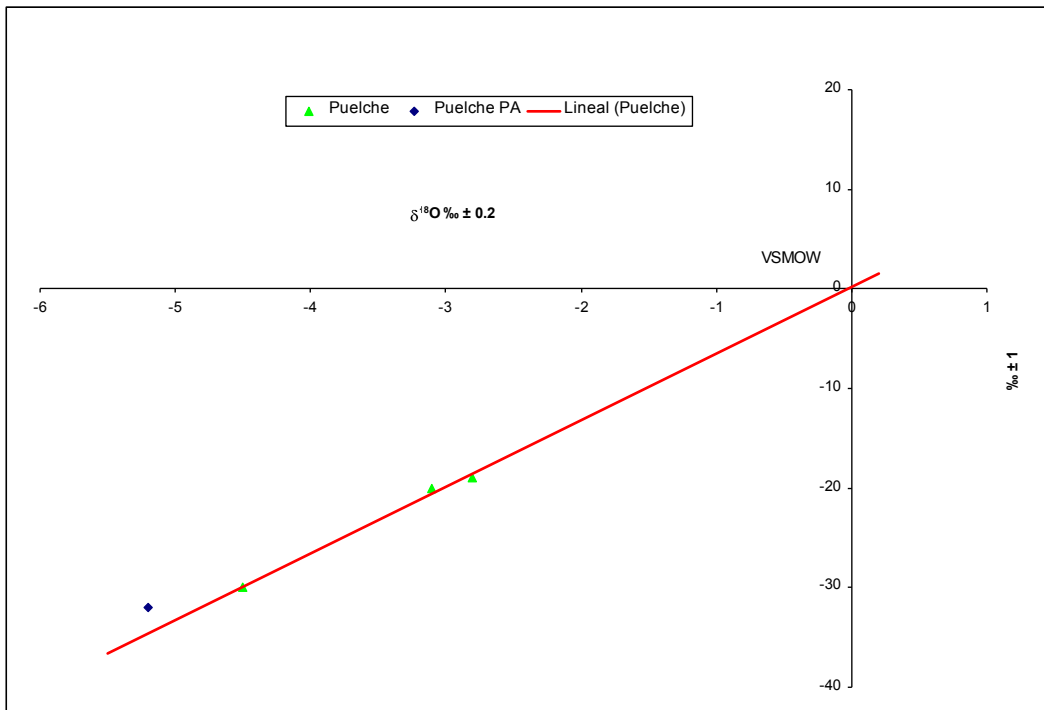
4.7.3. Plot $\delta^2\text{H}$ vs. $\delta^{18}\text{O}$ of the total number of samples with LMWL

A remarkable coincidence in the isotopic composition of aquifers can be observed. Therefore, its interrelation and linkage with the current hydrological cycle is confirmed. Fluctuations in isotopic values are due to processes such as evaporation prior to infiltration. The high values of salinity also suggest the involvement of these processes. Moreover, they indicate the occurrence of salt enrichment along the path. A plot of Total Dissolved Solids vs. $\delta^{18}\text{O}$ is included below (Figure 4.7.4).



4.7.4 Plot TDS vs. $\delta^{18}\text{O}$ of the total number of samples

It is interesting to note that the samples corresponding to Puelche aquifer, extracted from the coastal region, are arranged in a straight line projected over the SMOW value (Figure 4.7.5).



4.7.5 Plot $\delta^2\text{H}$ vs. $\delta^{18}\text{O}$ of samples from Puelche aquifer

This situation, together with the high saline content of such samples, shows there is mixture of Puelche aquifer with seawater of a composition similar to SMOW. Furthermore, the point measured outside the coastal plain does not align. Thus, the possible mixture does not extend up to the high plain.

The isotopic composition of fresh water and saline water mixtures describes a straight line of mixture in a plot of $\delta^{18}O$ vs. δ^2H . Each point is placed according to the percentage of saline water of the sample. Identifying the saline component of brine water in similar cases is thus possible through the isotopic method.

As an alignment trend similar to the Puelche samples with the VSMOW value is observed in the plot TDS vs. $\delta^{18}O$ (Figure 4.7.6), the hypothesis of mixture with seawater is reinforced.

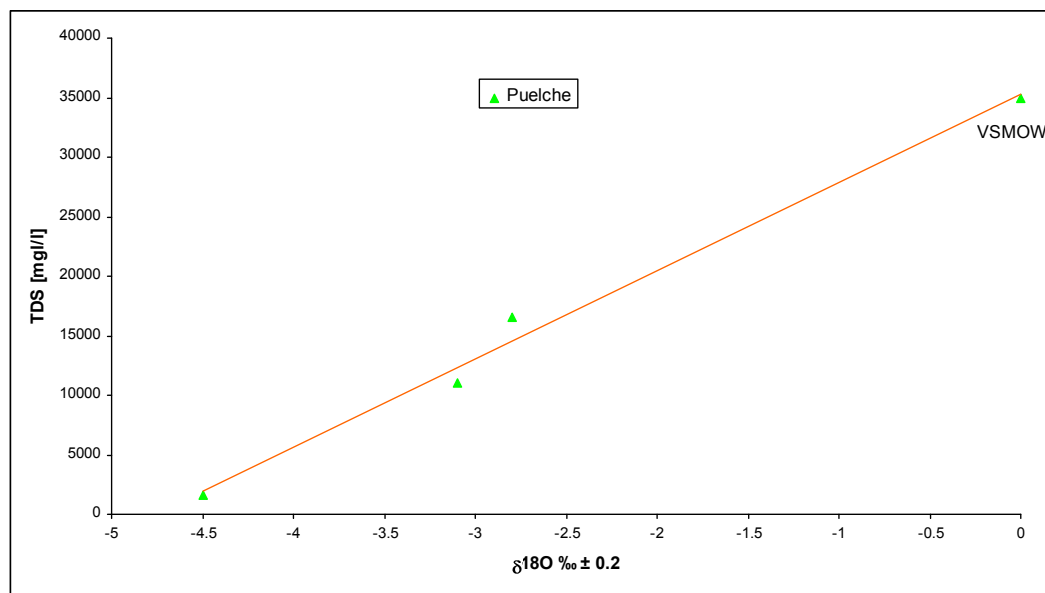


Figure 4.7.6 Plot TDS vs. $\delta^{18}O$ and VSMOW in Puelche samples

On the other hand, the phreatic and Pampeano samples, with higher dispersion, show the presence of other enrichment processes, associated with evaporation and flow (Figure 4.7.7).

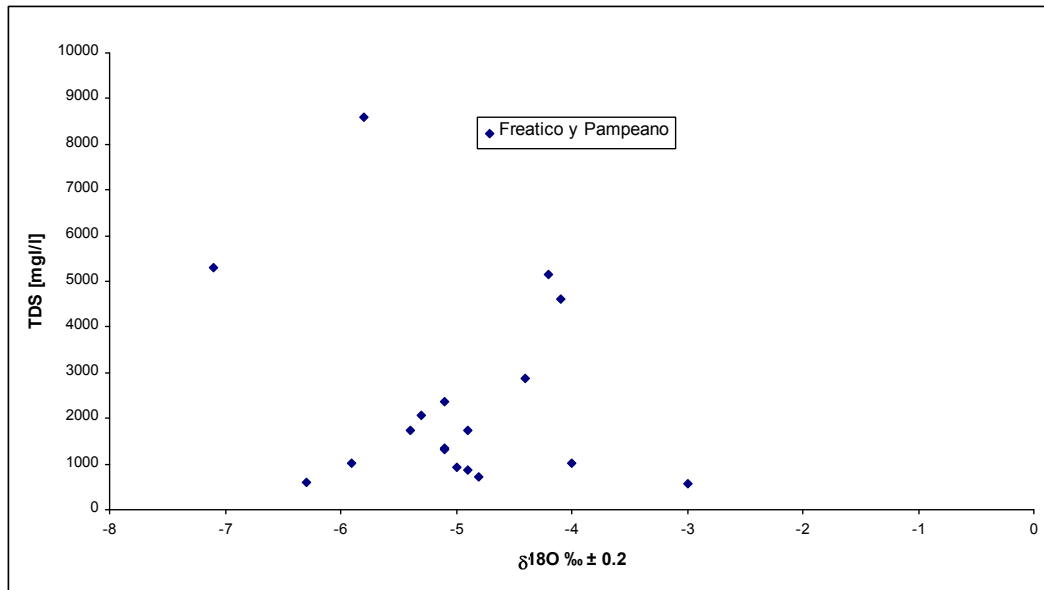


Figure 4.7.7 Plot TDS vs. $\delta^{18}\text{O}$ in Phreatic and Pampeano samples

From the analysis of isotopic composition, it could be drawn that aquifer system recharges concern meteoric water, with some evaporation prior to infiltration. In their evolution, the processes of enrichment by flow prevail at Pampeano level, whereas the mixture with seawater is predominant in the coastal zone of Puelche aquifer.

4.7.2 Tritium

In April 2008, 23 samples corresponding to the three analysed aquifer levels (phreatic, Pampeano and Puelche) were obtained. The isotopic analyses were conducted at INGEIS laboratories (Buenos Aires).

The results obtained are indicated in Table 4.7.3.

Table 4.7.3 Tritium values

IAEA No.	Drilling ID	Tritium Concentration TU
20128	Hospital Naval	5.3 \pm 0.5
20129	Puerto- Pampeano	\leq 0.3
20130	Puerto- Freático	5.2 \pm 0.5
20131	Vivero	3.5 \pm 0.4
20132	Puerta 2	3.9 \pm 0.3
20133	Astillero	53 \pm 2.0
20134	Logística	3.6 \pm 0.3
20135	Shell Calle Cortada	7.0 \pm 0.4
20136	Parque M. Rodríguez	4.4 \pm 0.3
20137	Puerto-Puelche	\leq 0.2
20138	Petroken	14.3 \pm 0.6
20139	Facultad Afuera	1.8 \pm 0.3
20140	Facultad Adentro	3.1 \pm 0.3
20141	Gas Ensenada	40.1 \pm 1.6
20142	UTN	15.7 \pm 0.8
20143	Puelche El Dique	1 \pm 0.3
20144	Pampeano El Dique	1.3 \pm 0.4
20145	Freático El Dique	1.7 \pm 0.4
20146	Tiro Federal Puelche	\leq 0.3
20147	Tiro Federal Freático	2.7 \pm 0.4
20148	Tiro Federal Pampeano	0.5 \pm 0.4
20149	128 y 64	5.3 \pm 0.4
20150	145 y 60	5.4 \pm 0.4

Since the hydrological regime from Río de la Plata is influenced by rain, Tritium levels should be in the range of that of precipitation on the basin. South American monitoring stations from IAEA's GNIP Programme show the 1962 peak and then progressive decay leading to

current values coherent with cosmogenic production from 5 - 7 TU. Tritium concentrations in precipitation are shown (Figure 4.7.8)

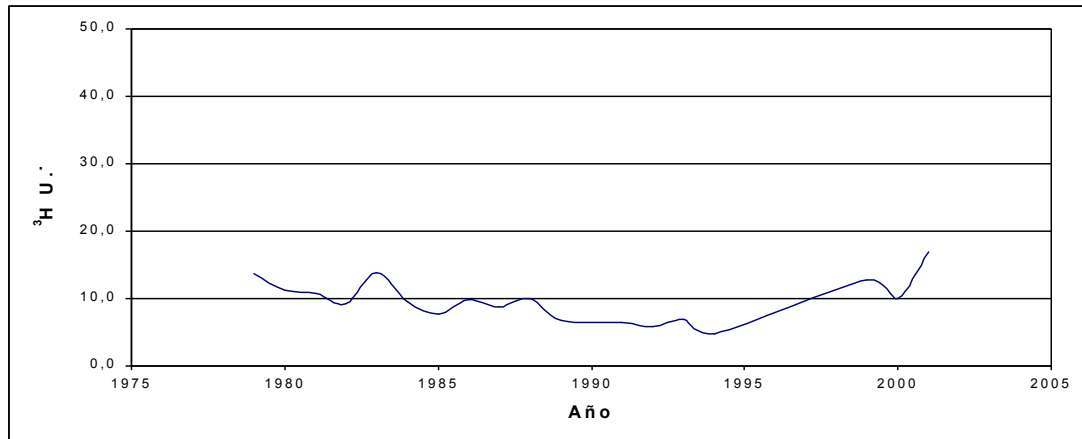


Figure 4.7.8 Tritium values in precipitation. Source: INGEIS. Red Nacional de Colectores de Argentina. Data base. Internal draft. Inédito. (2009)

However, because Atucha nuclear power station is located upstream, the Tritium level is at least one order of magnitude greater than average precipitation, up to 30 TU in samples taken from the river in front of the study area. Thus, Tritium is used to trace the existence of river contribution to groundwater. Although the coastal plain is a small area, groundwater geochemistry is variable as a result of the processes involved in it. Mixing, focussed recharge, evaporation and redox reactions strongly modify groundwater composition.

Obtained results are different for hydrogeologic units. Values found in the phreatic aquifer, from 3.9 to 7 TU, are within the expected range according to precipitation averages. The value of Astillero of 53 ± 2.0 TU, the highest ever registered, is located very near Río de La Plata, built on sands of that river and is almost certainly caused by its influence. The same origin cannot be attributed to the value found in Gas de Ensenada, of 40.1 ± 1.6 TU.

Very low Tritium values have been found in Puelche aquifer, which confirms the presence of water of marine origin (Tritium free). A slight increase is observed from the coast inwards. Once again, vertical recharge can be determined from the values obtained in the sample outside the coastal plain.

5. DISCUSSION

Results obtained with each method or technique will be analysed altogether in this section in order to see how each of them contributes to the construction of a conceptual model that explains groundwater behaviour in the coastal plain.

In principle, the results from the geoelectrical survey show variations in thickness among the different lithologies, later verified in the boreholes. They also display a significant decrease in resistivity values in northeastern direction, that is, towards Río de La Plata. This condition is exclusively attributable to an increase in salinity of the contained water, because the lithology is the same. Again, the results obtained indirectly are verified with chemical data.

This major salinity increase found in contained water from the Puelche sands of the borehole located in Puerto, which is proved with chemical analyses, is probably the most interesting result of this research work. The results from chemical analyses already indicate characteristic contents of seawater. If deuterium and ^{18}O isotopes are added to the results obtained, the presence of seawater is corroborated, since samples match VSMOW samples. Finally, water is found to be Tritium free and hence it is not related to the recent hydrological cycle.

These results represent a relevant contribution to the discussion about the origin of water in Puelche aquifer in the coastal zone because this zone is the discharge area of the aquifer. This is verified because as samples are collected closer to the high plain, mixture with more recent water can be recognised. In other words, the high plain constitutes the discharge area for Puelche water, although its flow is very slow and vertical movements begin to predominate. Discharged fresh water cannot push seawater in the proximity of the river. Water with low saline content occurs only in Puelche aquifer in El Dique position.

Geoelectrical, hydrochemical and isotopic profiles are consistent with this model (Figure 5.1).

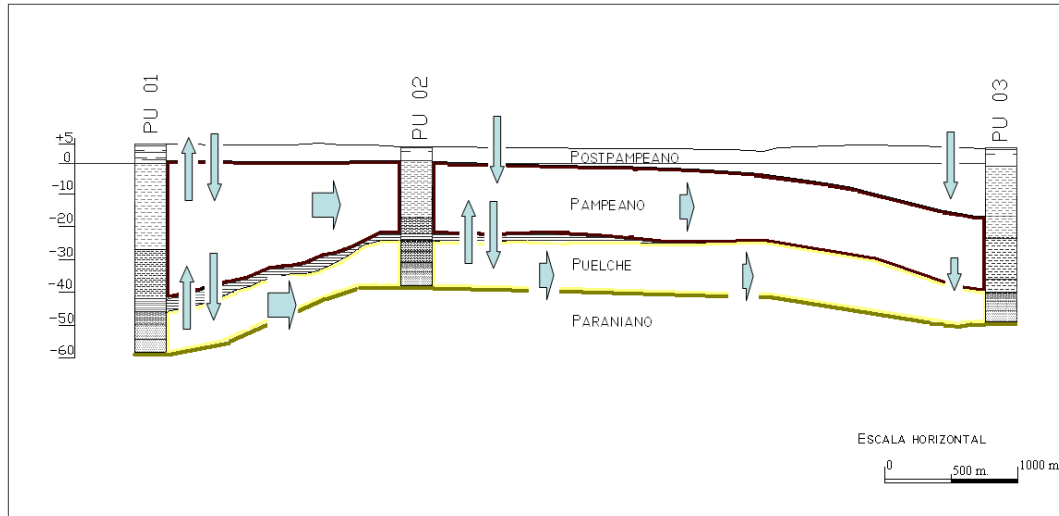


Figure 5.1 Conceptual model

The general direction of regional runoff could be defined with the analysis performed here. Previously, this information was deduced by extrapolation of data from boreholes of neighbouring areas. The hydraulic behaviour of groundwater in the analysed region rose in importance due to its proximity to the area of potable water supply to La Plata.

Exploitation of groundwater from Puelche sands, due to its high productivity and excellent quality, has fulfilled the population's requirements since 1885. This intense exploitation imposed a regime characterised by depression cones in constant expansion, causing an inversion of natural hydric gradients. Thus, groundwater originally draining from La Plata to Río de La Plata changed the direction of its flux, giving rise to saline intrusion from Puelche aquifer, located in the coastal plain (Figure 5.2). As a result, the exploitation wells located in

El Bosque, La Plata, have had signs of salinisation since 1945, which led to close them down.

As pumping ceased, the aquifer levels were recovered. However, due to the lack of monitoring boreholes, particularly in the coastal plain area (area of study), it was not possible to establish whether current pumping, further away inland than the initial one, affected the flux towards natural discharge zones.

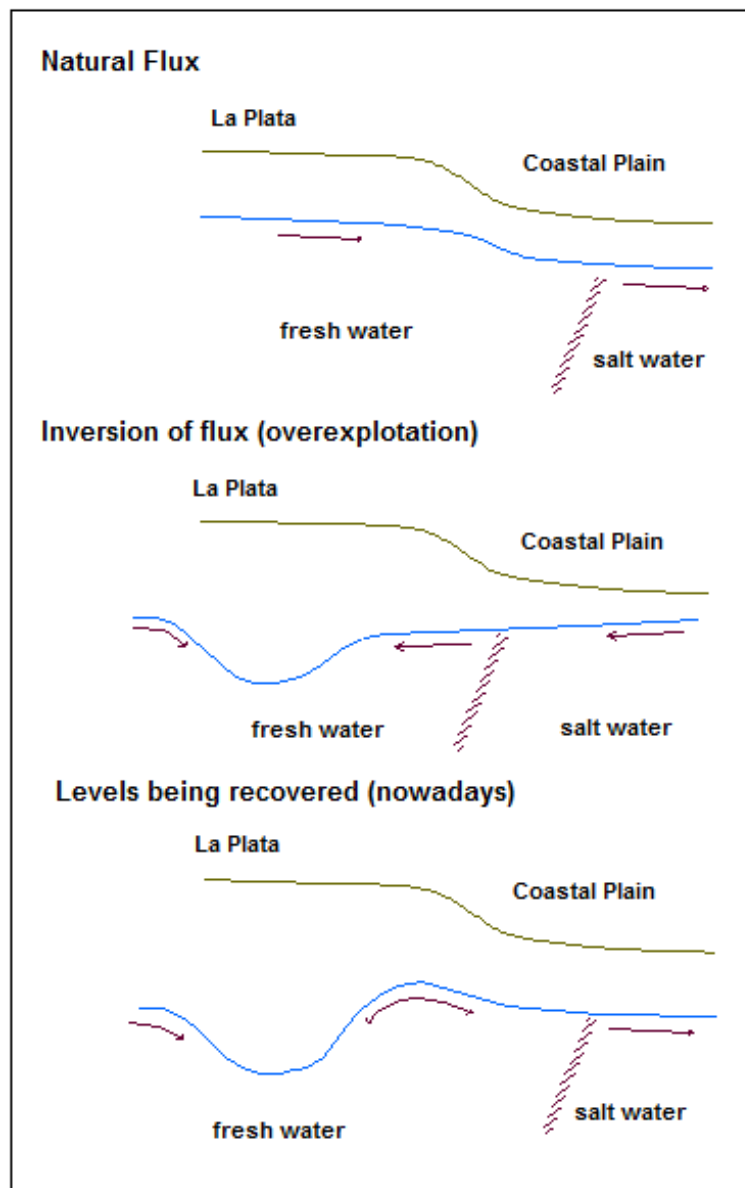


Figure 5.2 Flux evolution

Nowadays the saline intrusion in Puelche aquifer does not reach the position of El Dique borehole, which has water with low saline content.

The existence of a watershed in Pampeano and Puelche aquifer runoff, like that of the phreatic layer, approximately on the border of La Plata and Berisso, could be inferred from the verifications carried out here. Hence, the flow in both aquifers (Pampeano and Puelche) would be generated towards the coast.

6. CONCLUSIONS

1. Geophysical methods represent a first approach to studying the area, providing a successful characterisation of its main aspects. They are low-cost techniques. Resistivity levels that may be associated with lithology and saline content of saturation water have been established. Sands bearing fresh water have values of approximately 40 ohm.m and at the other extreme, since they are saturated with saltwater, they decrease until 0.7 ohm.m. Planning drilling tasks is possible by means of geoelectrical surveying.

2. Deep boreholes are useful to gain knowledge of the complete stratigraphic section. Once integrated into a monitoring network, they can contribute to understanding the temporal variation of the parameters analysed here.

3. The monitoring network, including both shallow and deep boreholes, makes it possible to describe the relationships between precipitations and levels. The hydraulic supply ratio among analysed aquifer levels can be described as well.

4. In the phreatic aquifer, calcium-bicarbonate water has been found in 27% of the samples concerned with points in the so-called recharge zone. In addition, sodium-bicarbonate water has been found in 53% of the sampled points, covering the area of wetlands, or lower areas, in the direction of flow. And finally, sodium-chloride water has been found in 7% of the samples in the outermost zones of the area of study.

In Puelche aquifer, the deepest one, sodium-chloride water with high contents of both ions has been the only type found. The maximum value of chloride found exceeded 12,000 mg/L, like the value reported for seawater in literature. Sodium reached values higher than 3,300

mg/L. In Pampeano aquifer, the three types of water have been found, their values ranging from those reported in the phreatic aquifer to those reported in Puelche. This would imply a mixture zone between both extreme aquifers.

Based on the maximum permissible values for drinkable use of the local regulation (Table 4.6.2), water from the phreatic aquifer has a classification of drinkable water, with the exception of the zone of the point named Vivero, since the values of some ions exceed the mentioned regulation. For the Pampeano aquifer, the area near to the river presents characteristics of drinkable water, on not having exceeded the maximum permissible values of the norm. The Puelche aquifer presents this condition at El Dique point.

Despite shallow aquifer water could be considered as potable, not exceeding the maximum values allowed according whit local regulations, it has to be considered that this aquifer has a high vulnerability to anthropogenic pollution, because of its shallow level and also industrial activities in the study area.

None of the samples in the Pampeano or Puelche system has shown presence of the different trace elements or minor ions that have been analysed here.

5. From the analysis of the environmental isotopes, groundwater origin has been defined, distinguishing water of meteoric origin from that of marine origin. Phreatic levels show their meteoric origin and some of them show the river water influence, enriched in Tritium. Samples from Puelche aquifer are aligned with VSMOW straight line in the coastal plain and are Tritium-free, too. This is one of the central points of this research work. Furthermore, the difference in the results from the borehole located in the high plain should be highlighted here. Samples belonging to the Pampeano aquifer are transitional.

6. Each of the techniques used contributes to a better understanding of an aspect of the problem analysed here. It is possible to design a reliable model by integrating all these techniques.

So far, the coastal zone has been considered an area without any presence of potable groundwater supply due to its high saline content. This has led to regard the coastal plain as an inert area. Therefore, landfill or industries with dangerous effluents have been located in this coastal zone.

The results in this thesis indicate that the zone must be considered an active element in the hydrological cycle. Actions taken in the coastal plain will have effects on the whole system. In other words, decisions that will be made for the economic development of the area should be based on a precaution principle. This principle states that actions must be taken to prevent any possible damage to the coastal plain. One should not wait to be certain that some damage has been caused in order to solve it.

Recommendations

Both the experiences involved in this thesis and the results obtained can be taken as a starting point for adopting criteria for the use and protection of resources in the area of study. Integrated management of the area is necessary in order to reach a balance between water and environmental requirements.

This management of water resources should be associated with the area neighbouring La Plata city, where groundwater is the most significant source of water supply.

The monitoring network installed for the purpose of this study should continue running, facilitating, thus, the control and monitoring of phreatic and piezometric levels of groundwater and of its chemical features.

In terms of vulnerability and risks of groundwater resources, it is necessary to minimise the use of industrial contaminants and restrict the use of herbicides, pesticides and fertilizers in rural areas.

Actions taken to strike a balance between water demand and protection of the environment in the analysed area are indispensable and constitute a basis for the socioeconomic development of the region.

The tasks fulfilled here have shown the complexity of the hydrogeological problem and the fragility of the system against external agents. These problems demand more detailed assessment. Immediate action aimed at no less than avoiding deterioration of the current situation is required.

It should be borne in mind that the area of study is subject to constant pressure, with high industrial and population density. This situation, characteristic of different coastal regions, can worsen the quality of water, reduce its availability and cause problems of pollution and erosion, sometimes having serious social and economic consequences.

Coastal regions like that studied here require special attention from the politicians in charge of them. Hence, it is necessary to adopt a coordinated policy for the littoral of Rio de La Plata, by devising strategies concerning the integrated management of coastal zones. With this in mind, it will be important to spread the results obtained in this research work among public organisations and institutions that have competence on this subject matter at a national, provincial and municipal level.

The strategy will involve planning and management of natural resources and their association with regional activities. Nevertheless, this is not the solution to all the problems. It is a dynamic process evolving over time.

The fundamental aspect of this integrated strategy is to bring the following agents closer together: a) the relevant politicians from the city councils of Ensenada, Berisso and La Plata, b) those from the environment agency of the Province of Buenos Aires, c) national departments with authority on this subject matter (Environment, Energy, Transport, etc.), and d) private agents, especially industries whose activities affect the region.

The hydrogeological characterisation carried out here is a first step towards an integrated management of the area and not just an environmental measure. While the need to protect the functioning of natural ecosystems is a core aim of the strategy, the integrated management also seeks to improve the economic and social well-being of coastal zones and help them develop the community's potential.

All in all, according to the assessment of water resources undertaken here, it is necessary to continue characterising this natural and anthropic environment. Therefore, the employment of strategies towards an integrated management of the area is required. This management entails a relatively low cost. However, the economic and social benefits can be substantial.

7. THEORETICAL BACKGROUND

In this section are discussed the theoretical background and methodologies used throughout this thesis. First, the geophysical methods employed here are included. Second, the hydrogeochemical concepts are described. And finally, the application of environmental isotopes to study groundwater evolution is summarised.

7.1 APPLIED GEOPHYSICS TO THE EARTH'S ENVIRONMENT

Geophysics is the study of the Earth using methods of Physics. Solid Earth Geophysics is traditionally divided in two main fields of study: Global Geophysics and Exploration Geophysics. The former involves studies of large scale problems related to the Earth's gross structure and dynamic behaviour, whereas the latter deals specifically with applications of geophysical techniques to problems of oil/gas, water and mineral exploration.

In recent years many geophysical techniques have been used for conducting environmental investigations. The existing methods of Exploration Geophysics can be adapted to meet these targets. Most targets of environmental interest are at shallow depths.

The suitability of a particular technique depends on the physical property contrasts involved between the target structure and its surroundings, depth of investigation, and the nature and thickness of the overburden.

The cost factor is also an important criterion for choosing which geophysical method to use for a given problem. The cost estimate of a selected technique in a survey area depends on local terrain conditions, size of the area, grid spacing and number of survey points, instruments

to be employed, required precision, depth of investigation and details of interpretation.

Groundwater is an important part of the Earth's environment. Many of the environmental problems are directly or indirectly related to the location of groundwater and its protection from contamination sources of various kinds. Physical properties of many rocks are significantly altered by water in pores and fissures, and the degree of alteration varies with water quality. This makes it possible to locate water bearing structures and to investigate the quality of water by using appropriate geophysical techniques.

7.1.1. Electrical methods

Resistivity

Methods from Applied Geophysics can be classified according to whether they measure variations in a "natural" or artificial "induced" field. In the first case, by measuring a force field on the Earth's surface, anomalies or variations are individuated and interpreted as heterogeneities or geological structures in the subsurface. In the second case, variations in response to an artificial field are studied, which may also be influenced by buried structures or geologic bodies. The electrical prospecting method belongs to the second type.

Probably the most widely used geophysical technique is electrical measurement. Many types of these measurements are made on the ground surface to investigate subsurface conditions in an area. In the most commonly used method, an electric current is driven through the ground and the resulting potential differences are measured in the surface.

This chapter describes the theoretical principles, field procedures and interpretation techniques of electrical methods, also called resistivity methods.

A physical contrast, electrical resistivity, is necessary to use electrical methods. The electrical resistance of a material is usually expressed in terms of its resistivity. If the resistance between opposite faces of a conducting body of length l and uniform cross sectional area A is R , the resistivity, ρ , is expressed as:

$$\rho = RA/l$$

The SI unit of resistivity is ohm.meter (Ωm). The conductivity $\sigma = 1/\rho$ of a material is defined as the reciprocal of its resistivity and measured in siemens per metre (S/m).

In most rocks electrical conduction is essentially electrolytic since most mineral grains (except metallic ores and clays) are insulators. Electrical conduction takes place through interstitial water in pores and fissures. Groundwater filling the pore space of a rock is a natural electrolyte with a considerable amount of ions contributing to conductivity.

Hard rocks are bad conductors of electricity, so they have high resistivity. However, many geological processes can alter a rock and significantly lower its resistivity. For instance, dissolution, faulting, shearing, weathering and hydrothermal alteration usually increase porosity and fluid permeability, and hence lower resistivity. By contrast, precipitation of calcium carbonate or silica reduces porosity and hence increases resistivity. Hardening of rocks by compaction and/or metamorphism will reduce porosity and permeability and hence increase resistivity.

The resistivity of porous sedimentary formations is highly variable, depending on the degree of saturation and the nature of pore electrolytes. The resistivity ρ of these rocks, when containing interstitial water of resistivity ρ_w , is proportional to ρ_w and can be expressed as:

$$\rho = F \rho_w$$

where the proportional factor F is called formation factor. F depends largely on the pore geometry and the degree of saturation.

If clay minerals are present in water bearing rocks, a relatively large number of ions may be released from such minerals through ion exchange processes. The ions provided by these processes add to the normal ion concentration in pore water and the net result is increased conductivity. Therefore, all rocks containing clay minerals (in wet state) exhibit abnormally high conductivity.

Resistivity is, thus, an extremely variable parameter, not only from formation to formation but even within a particular formation. There is no general correlation of lithology with resistivity. Nevertheless, a broad classification is possible according to which clays and shales, sands and gravel, compact sandstones and limestones, and unaltered crystalline rocks are considered. Figure 7.1.1 shows the approximate ranges of earth materials. Note that salt water is highly conductive, sea ice is more resistive than sea water and groundwater, and water saturated frozen ground is highly resistive.

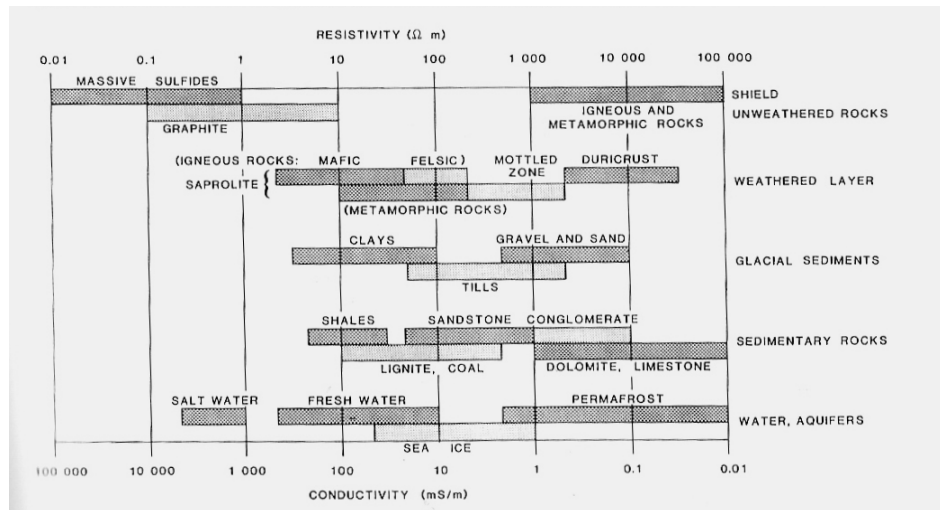


Figure 7.1.1 Typical ranges of electrical resistivity of earth materials (Palacky, 1987)

Theory of current flow - Potential distribution in homogeneous ground

The simplest approach to the theoretical study of current flow in the earth is to consider a completely homogeneous isotropic earth layer of uniform resistivity. Let us consider a homogeneous layer of length l and resistance R through which a current I is flowing. The potential difference ΔV across the ends of the resistance is given by Ohm's law:

$$\Delta V = RI \quad (7.1.1)$$

Using the relationship between $R = \rho l / A$ the above equation can be rewritten as:

$$\Delta V / l = \rho I / A \quad (7.1.2)$$

If we let the length of the conducting layer in the equation tend to zero and regard it as an element of uniform resistivity ρ , then it can be rewritten in gradient form:

$$-\text{grad } V = \rho i \text{ or } E = \rho i \quad (7.1.3)$$

where i is the current density per unit of cross sectional area and E (the electric field) is the negative gradient of the scalar potential V in the direction of l .

The next step in the development of the theory is to derive the potential in a homogeneous medium due to a point source of current. Now consider a semi-infinite conducting layer of uniform resistivity bounded by the ground surface and let a current of strength $+I$ enter at point C_1 on the ground surface (Figure 7.1.2). This current will flow away radially from the point of entry and at any instant its distribution will be uniform over a hemispherical shell of an underground region of resistivity ρ .

At a distance r , away from the current source, the hemispherical shell has a surface area of $2\pi r^2$, so the current density I would be:

$$i = I / 2\pi r^2 \quad (7.1.4)$$

The potential gradient $-\partial V / \partial r$ associated with the current is given by Equation 4.1.3 which, when using Equation 7.1.4, can be written as:

$$-\frac{\partial V}{\partial r} = \rho i = \rho I / 2\pi r^2 \quad (7.1.5)$$

The potential at a distance r is obtained by integrating Equation 7.1.5 and is:

$$V_r = I\rho / 2\pi r \quad (7.1.6)$$

This is the basic equation which enables the calculation of potential distribution in a homogeneous conducting semi-infinite medium.

From Equation 7.1.6 it is easy to see that the potential difference between two points P₁ and P₂ caused by current +I at the source is:

$$\Delta V = \frac{I\rho}{2\pi} \left(\frac{1}{C_1P_1} - \frac{1}{C_1P_2} \right) \quad (7.1.7)$$

Likewise, the potential difference between P₁ and P₂ caused by current - I at the sink is:

$$\Delta V = -\frac{I\rho}{2\pi} \left(\frac{1}{C_2P_1} - \frac{1}{C_2P_2} \right) \quad (7.1.8)$$

The total potential difference is given by the sum of the right-hand side of Equations 7.1.7 and 7.1.8:

$$\Delta V = \frac{I\rho}{2\pi} \left(\frac{1}{C_1P_1} - \frac{1}{C_1P_2} - \frac{1}{C_2P_1} + \frac{1}{C_2P_2} \right) \quad (7.1.9)$$

On rearranging Equation 7.1.9, the following is obtained:

$$\rho = 2\pi \frac{\Delta V}{I} \frac{1}{(G)} \quad (7.1.10)$$

where (G) is an abbreviation of the expression in brackets in Equation 7.1.9. The factor 2π / (G) is the geometric factor of an electrode array.

Apparent resistivity and electrode configuration

Equation 7.1.10 can be used to compute the true resistivity of the underground provided that the underground is completely homogeneous. The resulting resistivity should be constant and independent of both electrode array and surface location. For inhomogeneous earth, resistivity ρ (as computed in Equation 7.1.10)

will vary between a) altering the geometrical arrangement of electrodes and b) moving them on the ground surface without altering their geometry. The resistivity obtained from Equation 7.1.10 for an inhomogeneous underground is, therefore, designated as apparent resistivity, ρ_a .

Apparent resistivity is a formal concept and should not be regarded as some kind of resistivity average encountered in a heterogeneous underground formation. This concept is very useful in applying the resistivity method to subsurface investigation. In order to interpret apparent resistivity properly, the array with which it has been determined must be taken into account.

A number of different electrode arrays have been designed for field surveys. For each array, apparent resistivity ρ_a can be obtained by using the appropriate geometric factor in Equation 7.1.10. The array used here is described below (Figure 7.1.2).

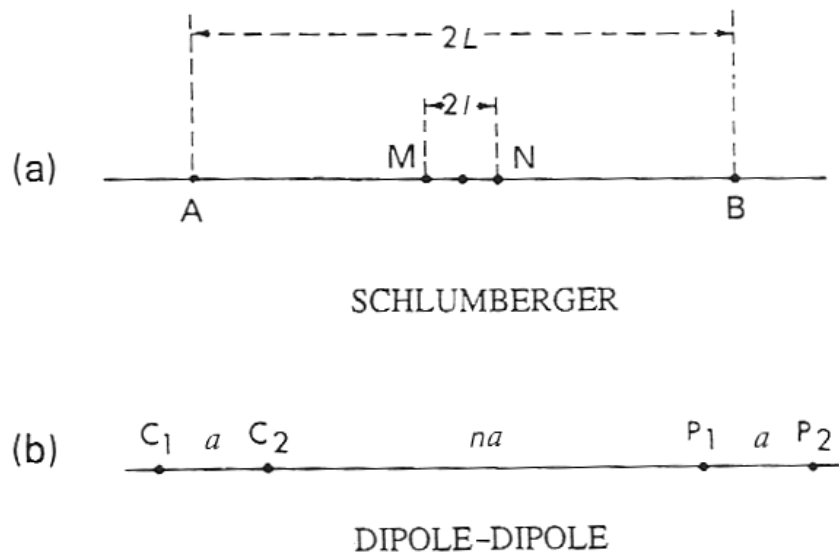


Figure 7.1.2 Typical electrode arrays

In the Schlumberger array (symmetrical $L > 5l$), resistivity is determined by:

$$\rho_a = \frac{\pi L^2}{2l} \frac{\Delta V}{I} \quad (7.1.11)$$

In this method, the centre point of the electrode array remains fixed, but the spacing between the electrodes is increased to obtain more information about the deeper sections of the subsurface. The Schlumberger array is widely used in sounding surveys to study the variation of resistivity with depth.

In the dipole-dipole array the spacing between the current electrodes pair, $C_2 - C_1$, is given as “a” which is the same as the distance between the potential electrodes pair $P_1 - P_2$. If the spacing between the two pairs is relatively large ($na > a$), each pair may be treated as an electrical dipole. The equation of resistivity then is:

$$\rho_a = \pi a n(n+1)(n+2) \frac{\Delta V}{I} \quad (7.1.12)$$

The advantage of the dipole-dipole array is that noise is effectively due to the low EM coupling between the current and potential circuits.

The forward problem solution: Stefanescu’s integral

The forward problem in electrical prospecting is the determination of the potential produced at the surface of a multilayered media by a punctual source, located at the same surface.

The problem for two layers must be solved first so that the general formula can be worked out. All over the points, except the source, the potential must follow Laplace's equation

$$\nabla^2 U = 0 \quad (7.1.13)$$

which is expressed in cylindrical coordinates

$$\frac{\partial^2 U}{\partial r^2} + \frac{1}{r} \frac{\partial U}{\partial r} + \frac{\partial^2 U}{\partial z^2} = 0 \quad (7.1.14)$$

because of the symmetry of the problem. Laplace's equation is not zero at the source, so it is a non-homogeneous problem. The solution will then be to add a particular integral to the general solution. Such general solution is obtained by means of variable separation:

$$U = R(r)Z(z) \quad (7.1.15)$$

Equation 7.1.14 can be rewritten as:

$$\frac{1}{R(r)} \left(\frac{d^2 R}{dr^2} + \frac{1}{r} \frac{dR}{dr} \right) + \frac{1}{Z(z)} \frac{d^2 Z}{dz^2} = 0 \quad (7.1.16)$$

To verify Equation 7.1.16, both terms must be equal to the same parameter with the opposite sign. Let λ^2 be the parameter. Then

$$\frac{1}{Z(z)} \frac{d^2 Z}{dz^2} = \lambda^2$$

$$\frac{1}{R(r)} \left(\frac{d^2 R}{dr^2} + \frac{1}{r} \frac{dR}{dr} \right) = -\lambda^2$$

and their solutions are:

$$Z(z) = e^{\pm \lambda z}$$

$$R(r) = J_0(\lambda r)$$

where $J_0(\lambda r)$ is the Bessel function of order zero whose behaviour is well known. Any linear combination will be a solution to the homogeneous equation:

$$(A'e^{-\lambda z} + B'e^{+\lambda z})J_0(\lambda r)$$

Provided that the coefficients are functions of λ parameter, the more general combination is obtained by integrating it as:

$$U = \int_0^{\infty} [A'(\lambda)e^{-\lambda z} + B'(\lambda)e^{+\lambda z}] J_0(\lambda r) d\lambda \quad (7.1.17)$$

To obtain the general solution to the non-homogeneous problem, a particular solution must be introduced. For instance, the solution of a uniform semi space of resistivity ρ_1 (Equation 7.1.6):

$$U = \frac{I\rho_1}{2\pi} \frac{1}{(r^2 + z^2)^{1/2}}$$

At this point, Weber Lipschitz's integral can be used.

$$\frac{1}{(r^2 + z^2)^{1/2}} = \int_0^{\infty} e^{-\lambda z} J_0(\lambda r) d\lambda$$

Then

$$U_1 = \frac{I\rho_1}{2\pi} \int_0^{\infty} [e^{-\lambda z} + A(\lambda)e^{-\lambda z} + B(\lambda)e^{+\lambda z}] J_0(\lambda r) d\lambda$$

and

$$U_2 = \frac{I\rho_1}{2\pi} \int_0^{\infty} [C(\lambda)e^{-\lambda z} + D(\lambda)e^{\lambda z}] J_0(\lambda r) d\lambda$$

The solution to the equation is reached by applying the boundary conditions:

$$U = \frac{I\rho_1}{2\pi} \int_0^{\infty} K(\lambda) J_0(\lambda r) d\lambda \quad (7.1.18)$$

where $K(\lambda)$ is the 'kernel function' which is controlled by the layer resistivities and thicknesses. Equation 7.1.18 is known as Stefanescu's integral.

Computation of apparent resistivity by linear filters

Nowadays, potential as well as apparent resistivity is calculated with recurrence formulas and linear filtering techniques. These techniques follow the idea presented by Koefoed (1979). The general expression for potential V at the surface over a series of horizontal layers is:

$$U = \Delta V = \frac{I\rho_1}{2\pi} \int_0^{\infty} K(\lambda) J_0(\lambda r) d\lambda \quad (7.1.19)$$

where I is the current source strength, ρ_1 is the resistivity of the first layer, l is the integration variable, r is the distance from the current source to the surface point where the potential is measured, $J_0(lr)$ is the Bessel function of order zero whose behaviour is completely known, and finally $K(l)$ is the 'kernel function', a function of the given layer resistivities and thicknesses.

Today, recurrent computations of the effects of successive layers are made using a 'resistivity transform' function, T , which is related to the

kernel function, K . The resistivity transform function (Koefoed, 1979) is defined by:

$$T_i(\lambda) = \rho_i K(\lambda) \quad (7.1.20)$$

The resistivity transform $T(\lambda)$ has the physical dimension of resistivity (Ωm) and the variable λ has the dimension of inverse length ($1/\text{m}$). It has been shown by Koefoed that, if $T(\lambda)$ is plotted as $1/\lambda$, the relationship is similar to the variation of apparent resistivity with electrode spacing for the same sequence of horizontal layer. Function $T(\lambda)$ can be very efficiently computed recursively for a stack of $n-1$ layers, each with resistivity ρ_i and thickness h_i over a resistivity substratum. According to Sunde, the recursive relationship is:

$$\begin{aligned} L_1 &= \frac{\rho_n - \rho_{n-1}}{\rho_n + \rho_{n-1}} = K_{n-1} \\ M_1 &= \frac{1 + L_1 e^{-2\lambda E_{n-1}}}{1 - L_1 e^{-2\lambda E_{n-1}}} \\ L_i &= \frac{\rho_{n-i+1} M_{i-1} - \rho_{n-i}}{\rho_{n-i+1} M_{i-1} + \rho_{n-i}} \\ M_i &= \frac{1 + L_i e^{-2\lambda E_{n-i}}}{1 - L_i e^{-2\lambda E_{n-i}}} \\ L_{n-1} &= \frac{\rho_2 M_{n-2} - \rho_1}{\rho_2 M_{n-2} + \rho_1} \\ M_{n-1} &= \frac{1 + L_{n-1} e^{-2\lambda E_1}}{1 - L_{n-1} e^{-2\lambda E_1}} \end{aligned} \quad (7.1.21)$$

$$\text{where } M_{n-1} = T(\lambda) \quad (4.1.22)$$

A relationship between apparent resistivity (ρ_a , measured by a four-electrode configuration) and the resistivity transform can be derived by making use of equations. For example, the relationship for the Schlumberger array with current electrode separation $2L$ is:

$$\rho_a = L^2 \int_0^{\infty} T(\lambda) J_1(\lambda L) \lambda d\lambda \quad (7.1.23)$$

where $J_1(l)$ is the Bessel function of order one.

Exploiting the linear relationship between the resistivity transform and the apparent resistivity functions, Ghosh (1971) showed that only one simple filtering operation is required to transform $T(l)$ values for a layered sequence into ρ_a values. By using a small number of fixed coefficients it is possible to make very rapid computations of theoretical curves for a multilayered resistivity distribution. The problem is recast in the form:

$$\rho_a = \sum_{k=k_{\min}}^{k_{\max}} T(\lambda) f_k \quad (7.1.24)$$

where the coefficients of a moving average filter are represented by f_k . The linear filtering approach can be effectively applied to transform the resistivity sounding data yielded with one type of electrode array into another.

Thus, the apparent resistivity calculated from the distribution of resistivities and thicknesses of a given electrode array can be determined. This is known as the solution to the forward problem. The inversion of measured data will be discussed later.

7.1.2 Field procedures and selection of electrode array

Electric sounding and profiling procedures

The aim of a resistivity survey is to delineate boundaries (both horizontal and vertical) in a heterogeneous ground. In practice this is accomplished by two distinct procedures often called, by analogy, vertical electric sounding and electric profiling (or trenching).

Vertical electric sounding (VES)

When the ground consists of a number of fairly horizontal layers, it is necessary to determine the vertical variation in resistivity. Vertical electric sounding (VES) is based on the fact that the depth of penetration of the current increases with rising current electrode spacing.

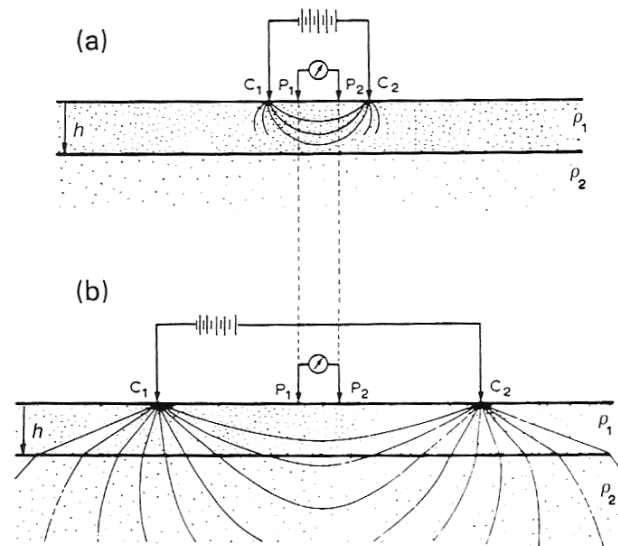


Figure 7.1.3 Principle of vertical electric sounding. When current electrode separation increases, a greater fraction of current penetrates deeper.

Figure 7.1.3 illustrates the VES concept applied to a two-layer problem. When the current electrode spacing C_1-C_2 is small compared with the upper layer thickness h , the apparent resistivity determined by measuring ΔV between the potential electrodes P_1 and P_2 is virtually the same as the upper layer resistivity ρ_1 . This is because a very small fraction of the current penetrates into the substratum below the boundary.

As the electrode separation is increased, a greater fraction of current penetrates deeper. The actual depth of penetration of the current in a two-layer underground region depends on several factors. Some of them are current source power, sensitivity to near-surface inhomogeneities,

resistivity contrast between the surface layer and the substratum, and the degree of electrical anisotropy of the layer media.

The previous Figure shows two and three typical layer curves for the variation in apparent resistivity in a Schlumberger electric sounding survey. Here the potential probes are fixed and the current electrodes are systematically moved outwards in steps. In practice, the current electrode distance L is increased from the midpoint of the array, from 6 to 10 times per log decade.

The current trend in resistivity sounding surveys favours the Schlumberger array. Since only two electrodes are moved, it is much more convenient to use this array for field routine instead of the Wenner array. Furthermore, as the potential electrodes remain fixed, the effect of near-surface inhomogeneities in their vicinity (due soil conditions, weathering, etc) is always constant.

Electric profiling

If the layers or boundaries are vertical planes, rather than horizontal, another procedure is adopted. The object of electric profiling is to detect lateral variations in ground resistivity. For example, in the Schlumberger (gradient) method of electric profiling, the current electrodes (A,B) remain fixed at a very large distance and the potential electrodes (M,N) with a small constant separation are moved between A and B. The following equation is used to calculate ρ_a :

$$\rho_a = \frac{\pi}{2l} \frac{(L^2 - x^2)}{L^2 + x^2} \frac{\Delta V}{I} \quad (7.1.25)$$

for each position the mobile pair of potential electrode takes. At the end of the profile line, the gradient setup is transferred to the adjacent line

and so on, until the area under study has been covered. The curve shows the apparent resistivity curve obtained by Schlumberger gradient profiling across a vertical contact between two rock formations.

7.1.3 Interpretation of resistivity data

For the purpose of geological interpretation, the data of resistivity surveys can be presented in two forms: profiles and maps. In the case of electric sounding with an expanding electrode configuration, the results are usually presented as a series of graphs (curves) expressing the variation of ρ_a with increasing electrode separation. These curves represent, at least qualitatively, the variation in resistivity with depth. In relatively simple cases, involving only two or three horizontal layers, interface depth estimation can be made by comparing the field data with the theoretical apparent resistivity curves. In the light of the available geological data, a fairly satisfactory picture of the stratification can often be deduced.

In a profiling survey with constant electrode spacing, data may be presented as: a) graphs showing the resistivity variation along the traverses or b) a contour map displaying the lines of equal resistivity. Such a map shows the ground lateral resistivity variation in terms of the depth of penetration for a given electrode spacing. Contour map plotting may not always be essential. Two-dimensional vertical structures such as faults, dikes, contact zones, etc, are often easily detectable on the resistivity profiles measured across the strikes of these features.

The quantitative interpretation of resistivity data for a multilayered structure is not a straightforward process and the user should constantly guard against the confidence of arriving at a unique solution.

Problems of electrical equivalence introduce an ambiguity in the interpretation of intermediate layer resistivities and thicknesses.

Some of the commonly used interpretation techniques will be mentioned below.

Interpretation by master curves and auxiliary graphs

Probably the most widely known master curves are the two-, three- and four-layer master curves for the Schlumberger array calculated by Orellana and Mooney (1966).

Curve matching methods are now becoming obsolete because of the general availability of more sophisticated computerised techniques.

Inversion of vertical electric sounding data using Zohdy's technique

Zohdy's (1989) technique is essentially a least-squares optimization technique in which a starting model is successively adjusted until the difference between the observed data and the model data of apparent resistivity, ρ_a , is reduced to a minimum. The novel feature of the technique is that it does not require an initial guess of the number of layers and layer parameters. Zohdy starts by assuming that the number of layers in the initial model equals the number of digitised points on the observed curve ρ_a . The resistivity of the first layer takes the value ρ_a of the first point of the curve, the second layer takes the value of the second point, and so on. Firstly, the depth of each layer is taken as the electrode spacing. Secondly, these values are multiplied by a constant to obtain a match between the observed values and calculated values at

the data points. Finally, the adjustment of depths by this procedure lasts until the rms% deviation is reduced to a minimum (Figure 7.1.4).

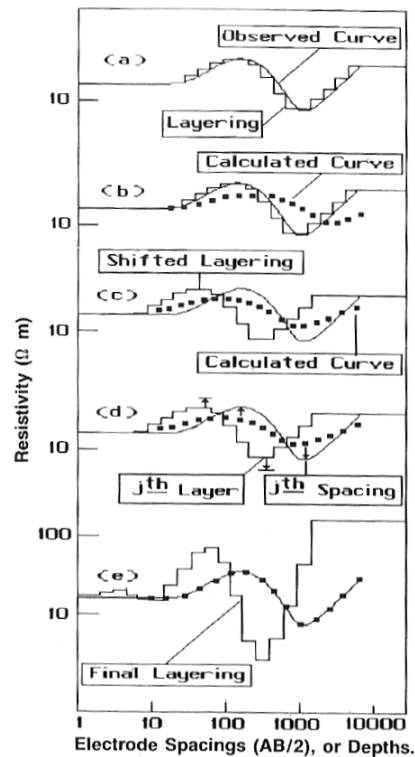


Figure 7.1.4 Zohdy's iterative process

This process of depth adjustment should, in effect, bring the calculated curve in phase with the observed curve. The adjustment of amplitudes of ρ_a is done iteratively by varying the resistivity of the model layers while keeping the boundaries fixed. Each layer resistivity is adjusted by a factor equal to the ratio of the observed values and the calculated values in the following way:

$$\rho_{i+1}(j) = \rho_i(j) * \rho_0(j) / \rho_{ci}(j) \quad (7.1.26)$$

where i is the number of iterations carried out, j is the number of layers, $\rho_i(j)$ is layer resistivity j th at iteration i , $\rho_0(j)$ is the observed value of ρ_a at spacing j th on the sounding curve, and $\rho_{ci}(j)$ is the calculated ρ_a at spacing j th for i th iteration.

As mentioned above, this process of amplitude adjustment is repeated until the rms% difference between the observed values and calculated values reaches a minimum, typically 5%. Figure 4.1.4 shows the stages of the iterative process. The calculated values are obtained by using the linear filter method described above. Zohdy's method provides a well behaved convergence.

Interpretation of combined electric profiling and sounding

When searching for both lateral and vertical variations in resistivity, the dipole-dipole configuration is often used. Figure 7.1.5 presents a commonly used display for plotting apparent resistivity data. In the collinear dipole-dipole array the current electrodes are first placed at station 1 and 2 and the potential electrodes at 3 and 4 so that $n=1$. The values of I , ΔV , n and a are introduced in Equation 7.1.12 to compute apparent resistivity. The plotting point is placed at the intersection of two lines starting from the mid-point of the C1-C2 and P1-P2 dipole pairs, with a 45° angle to the horizontal. The dipole-dipole array is then moved at step of spacing a . The measurements along the profile are repeated for $n=2,3,4\dots$ and plotted in a similar way.

The picture of apparent resistivity so obtained is called a vertical 'pseudosection' of the ground because, while measurements along the profile are indicative of lateral resistivity variations, measurements with a large value of "n" are supposed to contain more information about deeper inhomogeneities than those with a smaller "n".

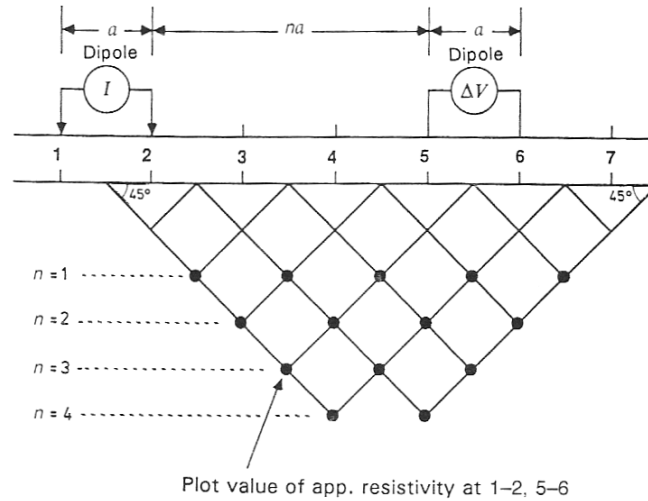


Figure 7.1.5 Construction of a 'pseudosection'

However, the pseudosection is not a true representation of subsurface resistivity distribution. A more exacting procedure of interpretation consists of iteratively computing the resistivity response of a two-dimensional model until the calculated section is found. This section should reasonably match the observed one.

Two-dimensional inversion methods

All inversion methods essentially aim at finding a model for the subsurface whose response agrees with the measured data. In the cell-based method used by RES2DINV software, the model parameters are the model block resistivity values, while the data are the measured apparent resistivity values. It is well known that for the same data set there is a wide range of models whose calculated apparent resistivity values match the measured values to the same degree. Besides trying to minimise the difference between the measured and calculated apparent resistivity values, the inversion method also attempts to reduce other quantities that will produce certain desired characteristics in the resulting model. The additional constraints also help to stabilise the inversion process. The RES2DINV programme uses an iterative method

whereby, starting from an initial model, the programme tries to find an improved model in which the calculated apparent resistivity values are closer to the measured ones. One well-known iterative inversion method is the smoothness constrained method (deGroot-Hedlin and Constable, 1990). It has the following mathematical form:

$$(JTJ + \mathbf{u}F)d = JTg - \mathbf{u}Fr \quad (7.1.27)$$

where

F = smoothing matrix

J = Jacobian matrix of partial derivatives

r = vector containing the logarithm of the model resistivity values

\mathbf{u} = damping factor

d = model perturbation vector

g = discrepancy vector

The discrepancy vector, g, contains the difference between the calculated and measured apparent resistivity values. The magnitude of this vector is frequently given as an RMS (root-mean-squared) value. This is the quantity that the inversion method seeks to reduce in an attempt to find a better model after each iteration. The model perturbation vector, d, is the change in the model resistivity values calculated using the above equation. It normally results in an “improved” model. The above equation tries to minimise a combination of two quantities: the difference between the calculated and measured apparent resistivity values as well as the roughness (i.e. the reciprocal of the model smoothness) of the model resistivity values. The damping factor, \mathbf{u} , controls the weight given to the model smoothness in the inversion process. The larger the damping factor, the smoother the model. However, the apparent resistivity RMS error will probably be larger.

The basic smoothness-constrained method as given in Equation 7.1.27 can be modified in several ways so that it might yield better results. In

order to emphasise the vertical (or horizontal) changes in the model resistivity values in the resulting model, the elements of smoothing matrix F can be modified. In the above equation, all data points are given the same weight. In some cases, the effect of bad points on the inversion results can be reduced by using a data weighting matrix. Very noisy data with a small number of bad datum points with unusually high or low apparent resistivity values can be taken as an illustration. Equation 7.1.27 also intends to minimise the **square** of the spatial changes, or roughness, of the model resistivity values. This tends to produce a model with a smooth variation of resistivity values. This approach is acceptable if the actual subsurface resistivity varies in a smooth and gradational manner. The subsurface geology sometimes consists of a number of regions that are internally almost homogeneous but with sharp boundaries between different regions. In this case, an inversion formulation that minimises **absolute** changes in the model resistivity values can sometimes give significantly better results.

7.2 HYDROGEOCHEMISTRY

7.2.1 MAJOR CONSTITUENTS IN GROUNDWATER

In natural groundwater most dissolved substances are in ionic state. Many of these ions are usually present and their sum represents almost the totality of the dissolved ions. These are the fundamental ions or major constituents, and most of the chemical and hydrogeochemical aspects rest upon them.

The fundamental ions are:

ANIONS: Chloride (Cl), Sulphate (SO_4^-), Bicarbonate (HCO_3^-)

CATIONS: Sodium (Na^+), Calcium (Ca^{++}), Magnesium (Mg^{++})

Nitrate (NO_3^-), carbonate (CO_3^{2-}) and potassium (K^+) ions are frequently considered within the group of major ions, though their ratio is generally low.

The rest of the ions and dissolved substances usually occur in outstandingly smaller amounts and are therefore called minor ions. They habitually constitute less than 1% of the total ionic content. Trace elements also occur but in amounts that are difficult to measure.

Anions

Chloride ion

If evaporites and rocks of marine origin are excepted, rocks usually have a poor ratio of chloride. However, given the high solubility of their salts, they rapidly change into aqueous phase and can reach very high concentrations.

Rainwater can be an important source of chloride ion, especially in areas close to the coast, quickly decreasing inland. As a chloride ion is almost an ideal tracer because it does not form low solubility salts, or oxidise or reduce itself in natural water, or is significantly adsorbed or involved in biochemical processes.

The concentration of chloride in groundwater is highly variable, from less than 10 mg/L to more than 3,000. In natural brines, close to saturation of NaCl, it can reach nearly 200,000 mg/L. Seawater contains approximately 20,000 mg/L.

Sulphate ion

Sulphate ions derive from terrains formed in marine ambient, from oxidation of sulphurs that are widely distributed in igneous and sedimentary rocks, from organic substance decay, etc.

Nevertheless, the dissolution of sulphate salts (fundamentally gypsum and anhydrite) is the most quantitatively important supply of this ion to groundwater.

In fresh waters, the normal concentration of sulphates can vary between 2 and 150 mg/L. In seawaters and bonded to Ca, it can reach 5,000 mg/L. In brines and bonded to Mg and Na, it can reach 200,000 mg/L.

Bicarbonate, carbonate and CO₂ ions

Carbon dioxide dissolved in water and the diverse compounds it forms in water play an important role in water chemistry. It dissolves in water according to its partial pressure (pCO₂). Whereas a part of it remains in dissolution as gas, another part reacts with water and forms carbonic acid, which is in turn partially dissociated to form carbonate and bicarbonate ions.

Carbon dioxide dissolved in water comes mainly from the edaphic zone. The dissolution of limestones and dolomites, fostered by input of CO₂ and/or organic or inorganic acids, is another main source of carbonates and bicarbonates.

Bicarbonate ions are the dominant carbonated species in water with pH lower than 8.3, that is, in most natural groundwater. Concentrations usually vary between 50 and 400 mg/L in this water, although they can reach values of up to 800 mg/L. Concentrations of up to 1,000 mg/L

can occur in water that is poor in Ca and Mg or where there are phenomena of CO₂ release within the aquifer (e.g. sulphate reduction).

Nitrate, nitrite and ammonium ions

Nitrogenous compounds occurring in natural water are intimately related to the nitrogen cycle. Most nitrogen appears in gaseous form in the atmosphere (78% in volume). In oxidised form, it constitutes a relatively important fraction in soils and organic substances (animal or plant tissues that extract it from the atmosphere for their metabolism). However, nitrogen is only present in rocks as a minor element.

Nitrogen can occur as NH₃, NH₄ and, by oxidation, these reduced forms can change into NO₂, and finally into NO₃, the most common and stable form. In general, NH₄, or free ammonia, occurs only as trace in groundwater. This compound is the final product of the reduction of organic or inorganic nitrogenous substances that naturally incorporate themselves into groundwater. Since the presence of ammonia contributes to microbial multiplication, its detection in water in large quantities is considered indicative of probable recent contamination.

Nitrite ions occur in water either as a consequence of NH₃ oxidation or of nitrate (microbial or not) reduction. Its presence in water should be regarded as a well founded sign of possible recent contamination. Nevertheless, the mere presence of nitrite and ammonia in groundwater cannot be considered a result of contamination without analysing the possible causes of its presence.

Nitrates can occur in groundwater either from the dissolution of rocks containing them, which is rare, or due to bacterial oxidation of organic matter. Nitrate concentration in uncontaminated groundwater seldom exceeds 10 mg/L. The origin of nitrate in groundwater is not always clear. Nitrates are relatively stable but they can be fixed by soil or

reduced to nitrogen or ammonia in reducing environments. They are often indicative of contamination.

The type of contamination that rises the presence of nitrate in groundwater is related to urban, industrial and cattle raising activities and, quite frequently, to inadequate intensive fertiliser practices with nitrogenous compounds.

Cations

Calcium ion

Calcium ion is usually the main cation in most natural waters due to its wide diffusion in igneous, sedimentary and metamorphic rocks. In sedimentary rocks it most commonly occurs in the form of carbonates (calcite, aragonite and dolomite) or sulphates (gypsum and anhydrite).

Controls of calcium concentration in groundwater can be summarised as follows: 1) carbonate equilibrium, 2) input of H^+ , and 3) ionic exchange.

Ionic exchange between calcium and other cations (mainly sodium), retained in the surface of the minerals that water comes into contact with, increases substantially in clayey soils with low permeability.

The concentration of Ca varies substantially in groundwater. Concentrations between 10 and 250 mg/L are frequent in fresh waters whereas in gypsum soil waters they can reach 600 mg/L, and in brines they can reach 50,000 mg/L.

Magnesium ion

Less abundant than calcium in natural water, magnesium ion derives from the dissolution of carbonate rocks (magnesian dolomites and limestones), evaporites and ferromagnesian silicate alteration, as well as from seawater.

As solubility of magnesite (MgCO_3) in natural groundwater is higher than that of calcite, MgCO_3 does not precipitate directly from dissolution under normal conditions.

The processes of ionic exchange also influence magnesium concentrations in groundwater. Here, magnesium, in preference to calcium, is retained in soils and rocks.

In natural water, the content of magnesium ion does not usually exceed 40 mg/L. In calcareous soils, it can surpass 100 mg/L. In evaporitic soils, it can reach values of 1,000 mg/L.

Sodium ion

Sodium is released by weathering of albite silicates and by dissolution of sedimentary rocks of marine origin and evaporitic deposits, where it mainly occurs as NaCl. An important source of sodium is seawater supply in coastal regions, both by marine intrusion or by rainwater infiltration to which sodium is added from the sea.

Sodium salts are highly soluble and tend to remain in solution because, unlike calcium, no reactions of precipitation are produced among them. However, sodium can be adsorbed in clays that can easily undergo cationic change and it can be exchanged with calcium, decreasing water hardness.

The presence of sodium in natural waters is highly variable, reaching up to 120,000 mg/L in evaporitic zones. However, it seldom exceeds 100 or 150 mg/L in normal fresh waters.

Potassium ion

Potassium ions are caused by weathering of feldspars and occasionally by solubilization of evaporite deposits, especially of sylvite salts (KCl) or carnalite salts (KCl MgCl₂).

Potassium tends to be irreversibly fixed in processes of clay formation and of adsorption in the surface of minerals that can easily undergo ionic exchange.

In groundwater, it does not usually exceed 10 mg/L, except for some brines. Sometimes, higher concentrations can be indicative of contamination by sewage dumping.

7.2.2 PHYSICAL AND CHEMICAL CHARACTERISTICS

Temperature

For practical purposes, it could be stated that there exists a "neutral zone" with constant temperature in aquifers. Above it, the most significant thermal influence is that of daily or seasonal variations in ambient temperature. Beneath this zone, the predominant factor is the geothermal gradient or temperature variation with depth, usually being 3°C/100 m in continental areas.

Conductivity, dry residue and total dissolved solids

As a result of its ionic content, water conducts electricity. As ionic concentration increases, conductivity also increases to a certain extent.

The unit of measurement is $\mu\text{S}/\text{cm}$ or $\text{mmho}\cdot\text{cm}$. Temperature variation greatly modifies conductivity.

Normal values of conductivity range from 100 to 2,000 $\mu\text{S}/\text{cm}$ in fresh water, are about 45,000 $\mu\text{S}/\text{cm}$ in seawater and can reach 100,000 $\mu\text{S}/\text{cm}$ in brines.

Dry residue (DR) refers to the substances that remain after the evaporation of certain water volume, generally a litre, once those in suspension have been removed.

Total dissolved solids (TDS) measure the weight of all substances dissolved in water, irrespective of whether they are volatile or not. TDS are not exactly the same as DR due to dehydration processes, loss of CO_2 , etc, which take place when water is heated at 110 °C to obtain dry residue.

Several factors (type of ion, dissociation rate, ionic mobility, etc) determine that there is not any close relation between conductivity and DR or TDS.

pH

As a general rule, the pH of natural waters ranges only from 6.5 to 8.5. However, it can exceptionally vary between 3 and 11. It plays an important role in many chemical and biological processes of natural groundwater (carbonatic equilibrium, redox processes, etc). And since it is easily volatile, it must be determined while the sample is being collected.

Total alkalinity (TAC) and alkalinity (TA)

The alkalinity of water determines its ability to neutralize acids. Thus, TAC measures this ability up to pH=4.5 and TA measures it up to pH=8.3.

In most natural waters alkalinity is produced by carbonate and bicarbonate ions. However, other weak acids like silicic, phosphoric, boric, and organic acids can sometimes contribute in a substantial manner.

Anions	Rainwater	Seawater	Groundwater
Chloride	0-20 mg/L	2000 mg/L	10-250 mg/L
Sulphate	0-10 mg/L	3000 mg/L	10-300 mg/L
Bicarbonate	0-20 mg/L	120 mg/L	50-350 mg/L
Nitrate	0 - 5 mg/L	1 mg/L	0-300 mg/L

Cations

Sodium		10,000 mg/L	5-150 mg/L
Calcium		400 mg/L	10-250 mg/L
Magnesium		1,200 mg/L	1 - 75 mg/L
Potassium		400 mg/L	1 - 10 mg/L

Other characteristics

Conductivity	45000 $\mu\text{S}/\text{cm}$	100-200 $\mu\text{S}/\text{cm}$
--------------	-------------------------------	---------------------------------

Units of measurement of concentration

Ionic contents are normally expressed in milligrams/litre (mg/L). This unit (mg/L) is used for minor ions.

It is often important to use milliequivalents/litre (meq/L), usually referred to as "r". For instance, r Ca means meq/L of Ca.

Conductivity is expressed as $\mu\text{S}/\text{cm}$, equivalent to micromhos/cm.

Water in equilibrium must have an equal amount of anions and cations (concentrations expressed in meq/L) so that the difference between them can be used as a measure of errors included in analytical determinations as:

$$\text{Error (\%)} = 100 * \{ (E_{\text{an}} - E_{\text{cat}}) / (E_{\text{an}} + E_{\text{cat}}) \}$$

7.2.3 MONITORING NETWORKS

A monitoring or observation network can be defined as a group of points (wells, soundings and springs) that provide information about hydraulic, hydrochemical and physical characteristics of an aquifer.

Network design and optimisation

The establishment of an observation network, whatever its purpose, must be based on sound knowledge of an aquifer, at least in terms of its boundaries and essential hydrodynamic characteristics. Although it is true that an observation network is often used precisely to gain knowledge of an aquifer, it is also true that a badly designed network can lead to serious interpretation errors. Hence, it should be borne in mind that an observation network must always be supervised and optimised.

A good network must meet the following basic requirements:

- Accessibility to points of observation
- Exhaustive and uniform spatial distribution
- Sufficient density
- Knowledge of the characteristics of points
- Representativeness

It is seldom possible to establish a network that satisfies all these requirements, and it will be necessary to resort to the available points.

Whenever it is possible, a network can be optimised on the basis of intuitive, methodological and economic criteria, but also by using estimation methods based on statistical techniques.

7.2.4 GROUNDWATER SAMPLING

General precautions in samplings

Sample containers were made of polythene, both for major ions and for trace and minor elements. One of the most important operations is to clean containers. As a general rule, plastic containers were cleaned by previously rinsing them twice or three times and afterwards filling them with a solution of 1M hydrochloric acid (10% in volume). The containers were later rinsed with distilled water, until there was no acid left in it.

When sampling, bottles were rinsed several times with sampling water in order to remove possible residues in them. Also it is necessary to avoid the formation of air bubbles in samples since they can modify diverse parameters, such as bicarbonates and calcium. To avoid air bubbles, once the bottle had been filled and a meniscus obtained, a cap was screwed on tightly.

In many cases it is convenient to collect proportional samples for different determinations. Each proportional sample should be treated in terms of the parameters to be determined. Thus, for metal determination, nitric acid (0.5 ml/L) was added. Furthermore, samples should be stored at 4°C before analysing them. Its analysis should be performed as swiftly as possible and within the period recommended in manuals (Standard Methods, Field Manual for Water Quality Sampling Arizona Water Resources Research Center (1995), Custodio and Llamas (1983)).

Once the samples were in the laboratory, basic preservation and analysis requirements were met.

Measurement of unstable constituents

In order to determine the physical and chemical characteristics of water samples, it is necessary to remember that some groundwater properties or constituents can vary with sample storage even a few minutes after sample collection. Temperature can be a good example, but it is not the only one: parameters like conductivity, pH and bicarbonate can also be subject to important changes over time. These parameters should be analysed in situ with simple but reliable methods, even though this is not always possible.

Representation of hydrochemical data

When dealing with a hydrological problem in terms of its temporal and spatial scope, a large volume of analytical data is generated and only by using diverse methodology is possible to use them all.

Although it is always difficult to achieve a proper balance, it is advisable to manipulate only really necessary data and, above all, to endeavour to

obtain the minimum information required to make an interpretation. In any case, data should always be as reliable as possible.

There are no general methodological approximations that can be routinely used. However, there are some representation techniques that are almost inevitable. Their aim is not only to turn data into graphs but also to use such graphs to obtain all the possible information from these data.

Some of the most common graphical approaches are:

- Temporal evolution
- Spatial distribution
- Stiff pattern diagrams
- Triangular diagrams

Temporal evolution graphs

Temporal evolution graphs represent variations in any parameter over time in a specific point. They can display trends and reveal seasonal variations, for instance. If evolution and other parameters (for example, rain) are compared, dependence relations can be observed.

Temporal evolution is studied with what is known as isocontent maps, composed of isolines or lines of equal concentration in the case of ions. Maps for other parameters, like temperature, conductivity, ionic relations, can also be drawn.

Isolines always require refinement with hydrogeologic or hydrochemical criteria.

Spatial distribution

A spatial distribution map deals with a concrete variable and helps visualise the distribution of parameters and gain information about their spatial evolution.

Stiff pattern diagrams

Stiff pattern diagrams (Figure 7.2.1) depict the major ion composition of a water sample. A polygonal shape is created from three parallel horizontal axes extending on either side of a vertical zero axis. Cations are plotted on the left side of the zero axis, one to each horizontal axis, and anions are plotted on the right side. The resulting shape provides information about water type, can be used for comparisons and is illustrative when inserted in hydrochemical maps. Concentration values are expressed in milliequivalents per litre (meq/L).

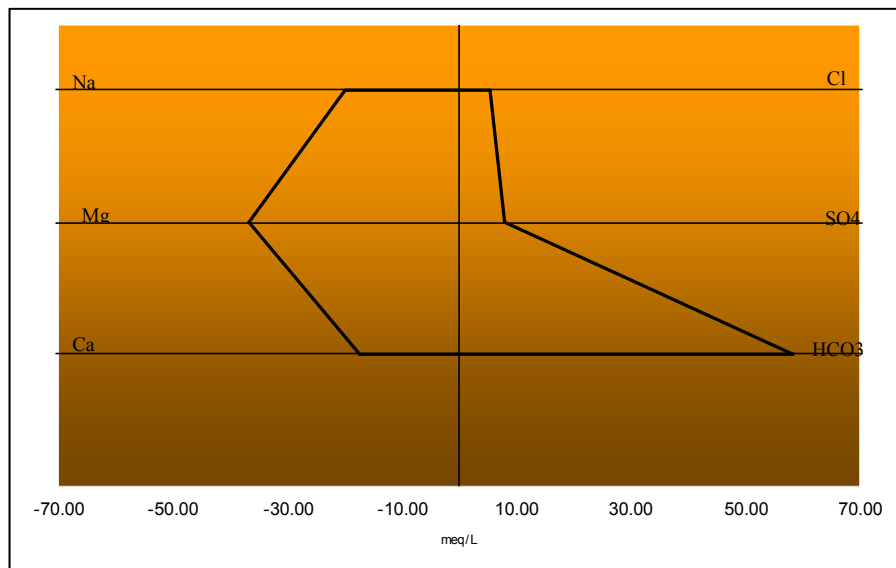


Figure 7.2.1 Stiff pattern model

Triangular diagrams

Three variables of a single observation are represented with a point in a triangular diagram. Each apex corresponds to 100% of each variable, expressed in meq/L. The most widely used triangular diagram is the Piper diagram (Figure 7.2.2), which separates cations and anions in two triangles and in a central rhomboidal field for both of them.

A triangular diagram displays the major chemical composition of many waters on a single graph, facilitating water comparison and classification. With the use of Piper diagrams, waters can be divided into groups according to their hydrochemical family, and genetic relations can be established. For example, if points are aligned between two extreme waters, they represent a mixture between those extreme waters. Deflections of a mixture line can be due to modifying processes occurring after the mixture.

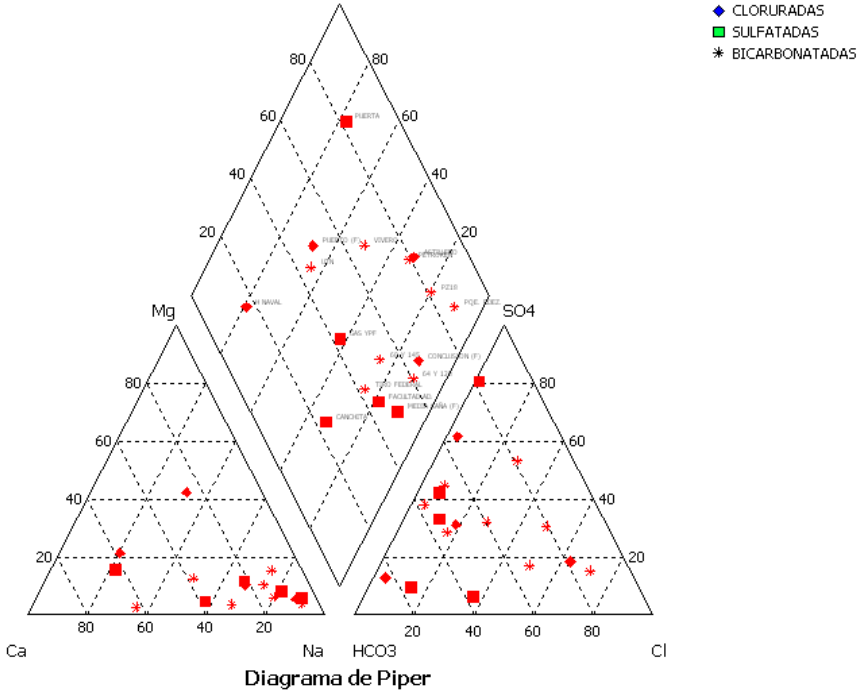


Figure 7.2.2. Piper diagram model

7.3. ENVIRONMENTAL ISOTOPES

The environmental isotopes are those that appear in the environment, which are widely distributed and participate in the natural cycles. Particularly hydrogen and oxygen isotopes are very important, because they are components of the water molecule. They offer a wide range of possibilities to study the processes within the hydrologic cycle (Dapeña, 2007).

7.3.1 Definitions and nomenclature

A nuclide is a species of atom characterised by the constitution of its nucleus, especially the number of protons (Z) and the number of neutrons (N) it contains. The mass number (A) of a given nuclide is the sum of its number of protons and neutrons. Nuclides are located in the periodic table of elements according to their increasing Z . Number Z gives the name to an element. Nuclides with equal Z but different N , and hence different A , occupy the same position in the table and are called isotopes (Figure 7.3.1).

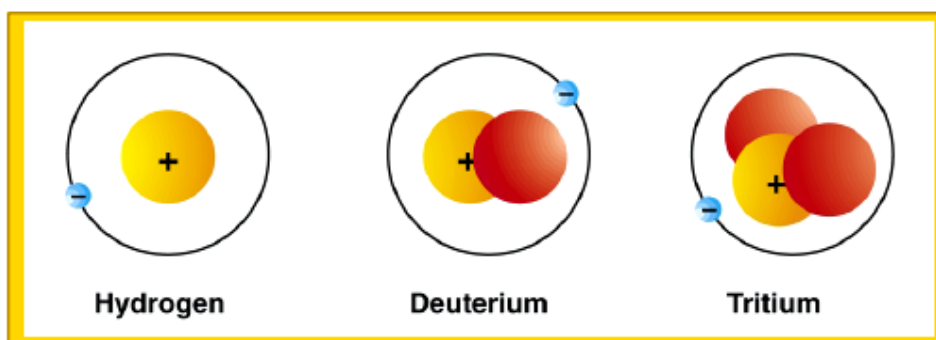


Figure 7.3.1 Hydrogen isotopes. Genesis JPL-Nasa
http://genesismission.jpl.nasa.gov/science/mod2_aei/index.html

Chemical elements are present in nature as a mixture of their isotopes in different ratios (abundances).

Isotopes are denoted in the form of A_ZX , in which the superscript indicates the mass number and the subscript indicates the atomic number. In practice only the superscript (AX) is used. For example, 2H , ${}^{18}O$, ${}^{13}C$.

Nuclides can be stable or unstable. For light elements ($Z \leq 20$) the greatest nuclear stability is achieved when Z:N ratio is close to 1 and for heavy elements it increases to 1.5.

Stable isotopes

Stable isotopes are those which do not change their nuclear properties over time. Some of the most important ones in isotopic geochemistry are:

H, He, Li, Be, C, N, O, F, Ne

Unstable or radioactive isotopes

Unstable or radioactive isotopes may convert into other nuclides over time. This change is described by means of a law of decay. In a given period of time, known as the half-life of a radioisotope, half the original number of isotopes disintegrates (Figure 7.3.2). This period can vary considerably, from fractions of seconds to millions of years. The Tritium (3H), radioactive isotope of hydrogen, and ${}^{14}C$, radioactive isotope of carbon, are commonly used in hydrogeology.

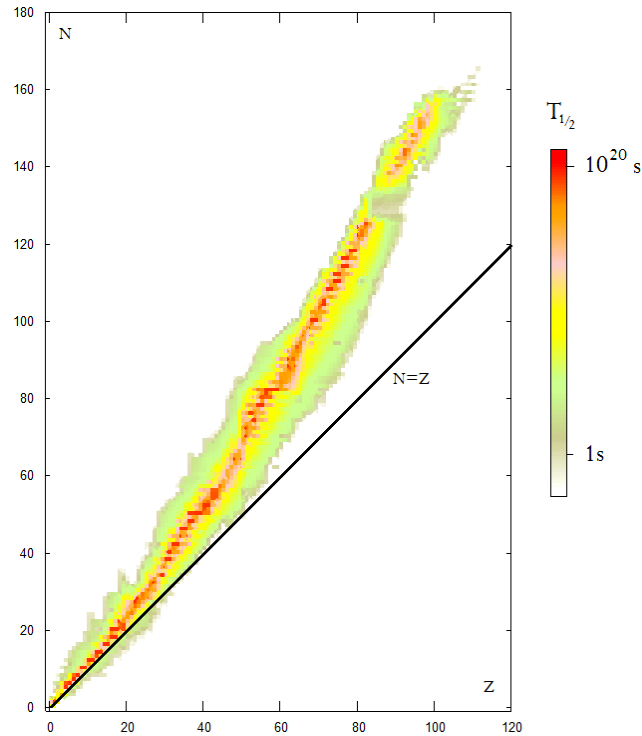


Figure 7.3.2 Isotope half lives. Note that the darker, more stable isotope region departs from the line of protons $Z =$ neutrons N , as the element number Z becomes larger.
 Wikimedia Commons. Public domain.

Environmental isotopes

Environmental isotopes are defined as those that occur in nature, have a broad distribution and participate in natural cycles. Hydrogen and oxygen environmental isotopes are of interest as constituents of groundwater molecules. These isotopes offer a wide range of possibilities to study processes in the hydrological cycle.

Stable isotopes

Hydrogen isotopes

Natural hydrogen is a mixture of two stable isotopes: protium (1H) and deuterium (2H or D), whose average abundance is presented below:

Table 7.3.1 Average abundance of stable isotopes of hydrogen (Way et al, 1950)

Isotope	Mass number	Isotopic abundance
1H	1	99.9844%
2H	2	0.0156%

Oxygen isotopes

Natural oxygen is a mixture of three isotopes: ^{16}O , ^{17}O and ^{18}O , whose average abundance is:

Table 7.3.2 Average abundance of stable isotopes of oxygen (Nier, 1950)

Isotope	Mass number	Isotopic abundance
^{16}O	16	99.7590%
^{17}O	17	0.0374%
^{18}O	18	0.2039%

Isotopes in species of water molecules

The most abundant molecular species of water is made up of two atoms of hydrogen isotope of mass number 1 (protium) and an oxygen atom of mass number 16 ($^1H\ ^1H\ ^{16}O$). In addition to this molecular species, those heavier species including an atom of deuterium (2H) or of oxygen 18 (^{18}O) are of interest.

If stable isotopes of oxygen (^{16}O , ^{17}O and ^{18}O) and hydrogen (1H and 2H) are considered, there are five types of water with different molecular weight and nine possible isotopic compositions.

Table 7.3.3 Possible isotopic compositions of H₂O

Molecule	Molecular weight
$^1H\ ^1H\ ^{16}O$	18
$^1H\ ^1H\ ^{17}O$	18
$^1H\ ^2H\ ^{16}O$	19
$^1H\ ^2H\ ^{17}O$	20
$^1H\ ^1H\ ^{18}O$	20
$^2H\ ^2H\ ^{16}O$	20
$^1H\ ^2H\ ^{18}O$	21
$^2H\ ^2H\ ^{17}O$	21
$^2H\ ^2H\ ^{18}O$	22

Due to their abundance, the most frequently used combinations in hydrogeology are $^1H\ ^1H\ ^{16}O$, $^1H\ ^1H\ ^{18}O$ and $^1H\ ^2H\ ^{16}O$. These three species occur in seawater in the following estimated ratios:

Table 7.3.4 Main ratios (Dansgaard, 1964)

997,680 per million	Mass 18	$^1H\ ^1H\ ^{16}O$
320 per million	Mass 19	$^1H\ ^2H\ ^{16}O$
2,000 per million	Mass 20	$^1H\ ^1H\ ^{18}O$

According to their history in the hydrological cycle, these ratios vary from one type of water to another. Isotopic description can be very useful in studying the origin and behaviour of water.

7.3.2 Isotopic fractionation

As isotopes contain the same number and arrangement of electrons, the chemical behaviour of all the isotopes of a given element is similar. However, isotopes have differences in their masses and in the physicochemical properties of the molecules containing them. These

differences bring about redistributions of isotopes, in nature as well as in the laboratory, between phases or chemical compounds in the system. This accommodation towards a state of stable or unstable equilibrium is known as isotopic fractionation (Panarello, 1987).

In nature, fractionation occurs in most light elements, (Z to 20) made up of more than one isotope. That is, isotopic fractionation can be defined as the difference in the concentration of isotopes of a given element between two or more phases or chemical compounds in mutual isotopic exchange. Such a difference quantifies by means of a fractionation factor. Fractionation mechanisms allow us to interpret geological, hydrogeological, atmospheric, climatic processes, among others.

Isotopic ratio (R): the relation between the number of molecules containing the rarest species (in general the heaviest one) and the number of molecules of the most common species.

$$R_{X^*} = \frac{\text{No_of_molecules_}X^*}{\text{No_of_molecules_}X} = \frac{(X^*)}{(X)}$$

where X* and X are isotopes of a given element.

The isotopic ratio R for oxygen and hydrogen isotopes in water is equal to:

$$R_{^{18}\text{O}} = \frac{\text{No_of_molecules_}H_2\text{ }^{18}\text{O}}{\text{No_of_molecules_}H_2\text{ }^{16}\text{O}} = \frac{(^{18}\text{O})}{(^{16}\text{O})}$$

$$R_{^2\text{H}} = \frac{\text{No_of_molecules_}^1\text{H}^2\text{HO}}{\text{No_of_molecules_}^1\text{H}^1\text{HO}} = \frac{(^2\text{H})}{(^1\text{H})}$$

Fractionation factor (α): the relation between the isotopic ratios of two phases or species in equilibrium. It is usually expressed as:

$$\alpha = \frac{(X^*/X)_{in_molecule_A}}{(X^*/X)_{in_molecule_B}}$$

where X and X* are isotopes of an element contained in molecules A and B.

The change of state or phase is a special type of isotopic fractionation process and the separation coefficient can be defined as:

$$\alpha = \frac{(X^*/X)_{phase1}}{(X^*/X)_{phase2}}$$

The factor has the value of a thermodynamic equilibrium constant and depends on temperature. In equilibrium and isotopic exchange reactions, the fractionation factor is related to the equilibrium constant (K):

$$\alpha = K^{1/N}$$

where N stands for the number of exchanged atoms.

Enrichment factor (ϵ) is defined as:

$$\epsilon = \alpha - 1 \text{ or } \epsilon (0/00) = 1000 \epsilon$$

Isotopic deviation (δ): the absolute abundance of stable isotopes is not usually measured in water or other natural compounds. What is only determined is the relative difference in ratio between the heavy isotope and the light one (generally the most abundant) of the sample according to a reference. The Greek letter δ is used to designate that difference

and, as the differences between the samples and the reference are very small, it is expressed in δ (‰) and defined as follows:

$$\delta (\text{‰}) = ((R_s - R_R) / R_R) * 1000$$

where δ is isotopic deviation in parts per thousand

R: isotopic ratio

s: sample

R: international reference

A positive ^{18}O or ^2H value means that the ^{18}O or ^2H content of the sample is greater than the standard content (enriched sample, i.e. greater concentration of heavy isotopes). A negative value indicates the opposite (depleted sample).

References and standards

According to what has been mentioned, it is necessary to have reference materials because isotopic ratio measurements are compared with those values. The reference or standard used for water is V-SMOW (Vienna Standard Mean Ocean Water) defined by Craig (1961).

The first standard universally adopted as reference for oxygen and hydrogen isotopic variations was known as SMOW (Standard Mean Ocean Water), but it rapidly exhausted. This brought about the definition of reference used nowadays. It is a sample prepared with an isotopic composition similar to that of seawater. Due to the precision reached in water isotope measurement, new standards of reference meeting all the needs of a study that involves isotopic analysis are now being prepared.

To improve the uniformity of analyses performed by various laboratories, a second standard, with a content of heavy isotopes that is

as close as possible to the lowest boundaries observed in natural water, was created. This sample is known as SLAP (Standard Light Antarctic Precipitation). Afterwards, an intermediate standard called GISP (Greenland Ice Sheet Precipitation) was incorporated. International reference values are shown below.

Table 7.3.5 International references

	$\delta^{18}O$	δ^2H
V-SMOW	0	0
SLAP	-55.5	-428
GISP	-24.8	-189.5

The preparation of these references is difficult and expensive. Each laboratory needs to define their own secondary references, which must be calibrated following V-SMOW and SLAP.

The laboratory that conducted the determinations for this study (INGEIS, Universidad de Buenos Aires) has the following secondary references:

Table 7.3.6 Secondary references from INGEIS Laboratory of Stable Isotopes

Name	Standard name	Collection date	$\delta^{18}O$	δ^2H
H ₂ O-INGEIS-07	ATLANTICO Agua Océano Atlántico	1980	-0.45	-5.9
H ₂ O-INGEIS-08	PLAN: Base Marambio Antártida	1980	-16.21	-123.0
H ₂ O-INGEIS-09	BATW-6: Agua Corriente Buenos Aires	1991	-2.90	-17.8
H ₂ O-INGEIS-10	BELGRANO Base Belgrano Antártida	1999	-22.52	-175.2
H ₂ O-INGEIS-11	SM Base San Martín Antártida	1999	-12.54	-117.6
H ₂ O-INGEIS-12	BATW Agua Corriente Buenos Aires	2002	-4.41	-27.4

References were measured in the International Atomic Energy Agency.

Main processes of isotopic fractionation

The processes that cause the phenomenon of isotopic fractionation take place in different types of chemical reactions and physical phenomena. The main processes are: Isotopic exchange reactions and Kinetic processes.

Isotopic exchange

Isotopic exchange involves processes with several different mechanisms. This term defines the exchange of atoms between chemical compounds or phases when equilibrium is achieved. The phenomena of interest in the hydrological cycle will be dealt with later on.

Kinetic processes

In kinetic processes fractionation is caused by the difference in reaction velocity of the different isotopic species bearing molecules of a given element.

There is usually a preferential enrichment in the light species in reaction products since bonds between light isotopes break more easily than those in heavy isotopes. If the molecules of water that contain ^{18}O or ^2H are considered, the preferential enrichment is often associated with fast or unidirectional processes such as reactions involving biological processes, evaporation, diffusion, etc.

Rayleigh equation

It is necessary to refer to Rayleigh distillation in order to understand the processes of isotopic separation related to mechanisms of evaporation-condensation in the hydrological cycle. This distillation defines

fractionated distillation processes and supposes quasi-static conditions and constant removal of vapour. It assumes ideal distillation, a homogeneously mixed infinite reservoir, where there is no reaction with the product (vapour) and the following is fulfilled:

- The material is continuously removed from a mixed system containing molecules of two or more isotopic species.
- The fractionation accompanying the removal process at any time is described by the fractionation factor.
- It cannot change during the process.

Under these conditions, the evolution of the isotopic composition of the residual material is given by:

$$\frac{R_f}{R_0} = f^{(\alpha-1)}$$

where R_f and R_0 is the isotopic ratio at time f and 0, F is the liquid's residual fraction, and α is the fractionation factor.

7.3.3 Isotopic fractionation in the hydrological cycle

General principles

The main cause of isotopic fractionation in the hydrological cycle is due to the difference in molecular mass of the constituent isotopic species of a water molecule. When this relative difference is appreciable, as in oxygen isotopes and especially in hydrogen ones, there are slight differences in physical properties. This can be observed in the table below, which shows properties of normal water, deuterated water and pure water with ^{18}O . These species do not occur in nature.

Table 7.3.7 Physical properties of three isotopic species of water

PHYSICAL PROPERTY	H ₂ O	H ₂ ¹⁸ O	² H ₂ O
Density at 20°C (g/cm ³)	0.9982	1.1078	1.1032
Highest density temperature (°C)	4.000	4.305	11.240
Molar volume at 20°C (cm ³ /mol)	18.049	18.072	18.129
Fusion point at 1 atm (°C)	0.00	0.28	3.81
Boiling point at 1 atm (°C)	100	100.14	101.42
Vapour pressure at 100°C	760		721.6

Due to differences in mass, the heaviest molecules have more inertia or less motion. This leads to a redistribution of the species when they are subjected to physical processes. Vapour pressures of different molecular isotopic species are inversely proportional to their masses. As regards water, the pressure vapour of isotopic species determines the relation between the heavy species and the light ones in the liquid and vapour phases. Therefore, the species containing light molecules, which have higher vapour pressure, evaporate more rapidly and condense more slowly than the heavy ones. In other words, they have a tendency to remain in vapour phase during the change of state.

It is stated that in water containing ¹H ¹H ¹⁸O, ¹H ²H ¹⁶O and ¹H ¹H ¹⁶O molecules of mass 20, 19 and 18 respectively, vapour enriches in the ¹H ¹H ¹⁶O molecule, while residual liquid does so in ¹H ²H ¹⁶O and ¹H ¹H ¹⁸O. During the evaporation process, ¹H ¹H ¹⁶O species has vapour pressure that is significantly greater than the other two. For this reason, vapour formed by liquid water evaporation is enriched in ¹⁶O and ¹H. However, ¹⁸O and ²H are concentrated in the liquid phase.

In the hydrological cycle, the water that evaporates from the ocean surface is enriched in ^{16}O and ^1H in the vapour phase because the species containing H_2^{16}O has higher vapour pressure than those containing H_2^{18}O or $^2\text{H}_2^{16}\text{O}$. Consequently, $\delta^{18}\text{O}$ and $\delta^2\text{H}$ of water vapour in the atmosphere over oceans are negative.

In short, the processes of evaporation and condensation are the main determining factors in isotopic fractionation in the water cycle.

Evaporation

Isotopic fractionation during evaporation depends upon the conditions in which the change of state is produced. If an initial volume of water V_0 with isotopic ratio R_0 undergoes evaporation, reducing itself to a V_e value, the isotopic ratio of that residual volume (R_f) is expressed by the equation:

$$R_f = R_0 \cdot f^{\left(\frac{1}{\alpha} - 1\right)}$$

where f is the residual fraction given by V_e/V_0 ratio.

During evaporation from surface water bodies, hydrogen and oxygen isotope fractionation depends upon surface temperature, wind velocity, salinity, and fundamentally humidity. With low humidity, water-vapour exchange is minimal. In nature, evaporation behaves like a progressive process of non-equilibrium. Water is enriched in both isotopes (^2H and ^{18}O). This enrichment depends on the content of humidity: the more content of humidity there is, the less the fractionation. Therefore, evaporation effects are significant when calculating water balances and salt concentration in lakes or similar bodies.

Condensation

Since it is produced very slowly, water vapour condensation always occurs in nature under equilibrium conditions. If R_0 and R_f are the isotopic ratios in the initial and final vapour masses, then

$$R_f = R_0 \cdot f^{(\alpha-1)}$$

Fractionation among oxygen isotopes in the water vapour of a cloud and the raindrops it produces is a natural example in the hydrological cycle. The resulting depletion of $^{18}\text{O}/^{16}\text{O}$ ratio in residual vapour and the instantaneous isotopic composition of water drops is given according to the fractionation of residual vapour in the cloud.

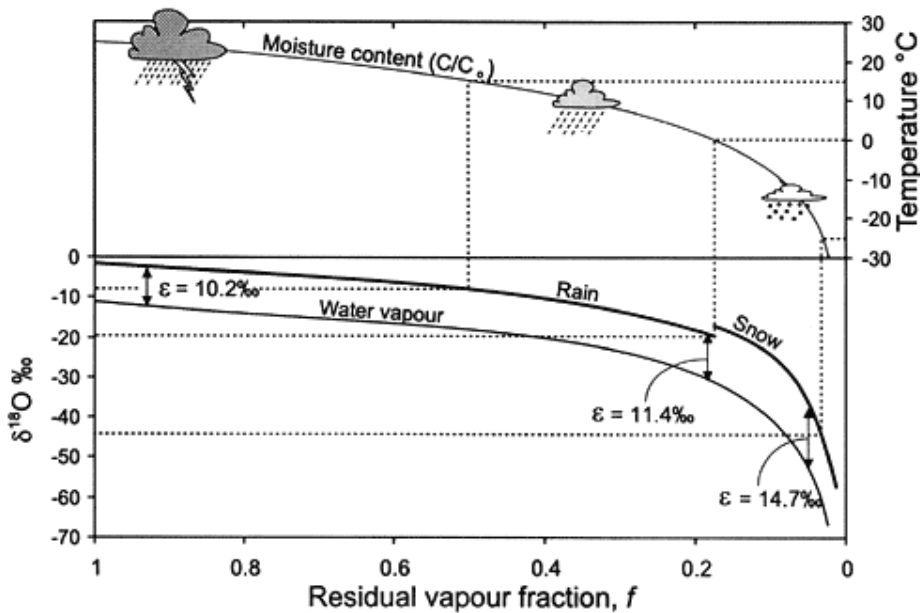


Figure 7.3.3 Change in the ^{18}O content of rainfall according to a Rayleigh distillation, starting with $\delta^{18}\text{O}_{\text{vapor}} = -11\text{‰}$, temp. = 25°C , and final temp. of -30°C . Note that at 0°C , fractionation between snow and water vapour replaces rain-vapour fractionation. The fraction remaining has been calculated from the decrease in moisture carrying capacity of air at lower temperatures, starting at 25°C . Dashed lines link $\delta^{18}\text{O}$ of precipitation with temperature of condensation. (Clark and Fritz, 1997)

Solidification

The coefficients of water freezing are much lower than in processes of evaporation and condensation. Logically, the ice produced is isotopically heavier than the water originating it. If the water mass is large and well-mixed, the process takes place under equilibrium conditions. If there is not a good mixture, the successive ice layers are increasingly lighter. Both phenomena occur in nature.

Isotopic composition of water in the hydrological cycle

Water in the hydrosphere occurs in its three physical states: solid, liquid and vapour. In liquid state it constitutes the rain, rivers, lakes and groundwater. In solid state it occurs in the form of ice, snow and hail. Finally, water vapour is very abundant in the low layers of the atmosphere and in the surface layers of the Earth's crust.

The concept of water cycle describes the movement or transport of water masses from one place to another, involving changes of state. This "perpetual" movement has two main causes: a) energy provided by the sun for the process of evaporation and b) gravity, which causes precipitation of condensed water.

The ocean is the starting point to describe the processes involved in the hydrological cycle. The ocean contains 97% of the planet's water and has a homogeneous chemical composition, too.

The hydrological cycle (Figure 7.3.4) is a continuous process through which a particle of evaporated water from the ocean returns to the surface as precipitation and surface and underground runoff. In every stage of the process, changes of phase are produced: not all the precipitated water returns to the surface, some evaporates again and

some is blocked by plant cover or impermeable surfaces, bringing about runoff and infiltration. Some forms the bodies of surface water, streams, lakes, rivers, which are finally carried back to the oceans. Some is released back into the atmosphere through biological processes of evapotranspiration. Some seeps into the soil and becomes groundwater, whose flux is also driven into the oceans.



Figure 7.3.4 Hydrological cycle (Custodio et al, 2002)

Isotope separation in the hydrological cycle

The traditional hypothesis to explain the distribution of hydrogen and oxygen stable isotopes is the atmospheric vapour resulting from ocean evaporation (cloud formation) and vapour condensation (precipitation). Figure 7.3.5 shows the standard diagram of isotope fractionation in the hydrological cycle.

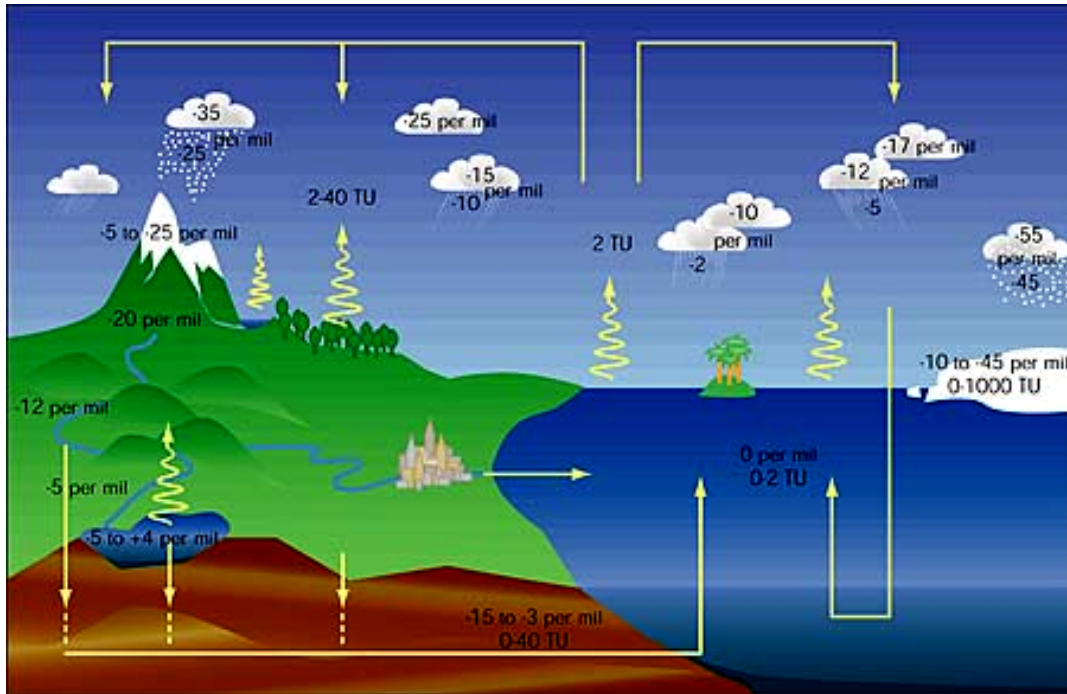


Figure 7.3.5. The isotopes of the water molecule: tritium and $\delta^{18}\text{O}$, label the global water cycle (IAEA, www.isohis.iaea.org)

Isotopic composition of oceans

The isotopic composition of oceans is uniform, except in certain areas of reduced size (estuaries of plentiful rivers, inland seas, and enclosed bays). The isotopic variations within oceans are relatively lower. There are variations of 1‰ for $^{18}\text{O}/^{16}\text{O}$ and of 10 ‰ for $^2\text{H}/^1\text{H}$.

Atmosphere and vapour formation

The mean surface temperature of oceans varies from about 0° C in the Polar Regions to over 29° C in the East Equatorial Pacific. The main source of vapour (70%) in the troposphere comes from the evaporation of subtropical warm seas. Vapour is enriched in ^{16}O and ^1H because H_2^{16}O has higher vapour pressure than H_2^{18}O or $^2\text{H}_2^{16}\text{O}$. Consequently, $\delta^{18}\text{O}$ and $\delta^2\text{H}$ of water vapour in the atmosphere over oceans are negative.

Precipitation

Precipitation is caused by cloud vapour mass cooling. When atmospheric vapour undergoes consecutive processes of cooling and condensation with formation of clouds and precipitation, the heaviest and least volatile molecules condense, leaving more depleted residual vapour in 2H and ^{18}O . As a result, successive precipitations derived from the same initial vapour mass may progressively deplete. Due to the fact that precipitation is mainly a consequence of cooling, the following condensation phases always occur at lower temperatures. That is, condensation rate depends on temperature. Hence, one might expect an isotopic ratio between the isotopic composition and its temperature of formation. Consequently, oxygen and hydrogen isotope fractionation increases as temperature lowers. In other words, as temperature drops because of altitude, δ value becomes increasingly more negative for precipitating rainwater.

It is well known that concentrations of 2H and ^{18}O in precipitation are linearly related. The equation, empirical, is very useful in hydrogeology. This relation regarding meteoric water unaffected by evaporation was stated by Craig (1961b) and is called global meteoric water line (GMWL)

$$\delta \ ^2H = 8 \ \delta \ ^{18}O + 10 \text{ ‰}$$

When vapour is generated from sea surface at 100% of humidity, there cannot be movement away from equilibrium and the y-intercept must be 0. However, global atmospheric vapour is developed with humidity values of 85% and that phenomenon increases the y-intercept value of this straight line in a factor of +10‰.

Another process affecting the isotopic composition of rain is evaporation both from bodies of surface water and droplets below the cloud base. As

a result, δ^2H and $\delta^{18}O$ are placed along a lower-slope straight line, called evaporation line. In most cases, it varies between 4 and 6, depending on relative humidity.

Finally, the most general expression is:

$$\delta^2H = a \delta^{18}O + b$$

where a varies from 6.5 to 8 and b from 0 to 30 according to the origin and previous history of air mass, season, latitude, altitude, etc.

Thus, local meteoric lines that help characterise input function in hydrological systems in different regions can be defined. For this purpose, a network of precipitation sampling called Global Network for Isotopes in Precipitation (GNIP) has been created.

Factor b , which can be written as $b = \delta^2H - \delta^{18}O$, is called deuterium excess and is a parameter inherent in the original value. In most continental precipitations it is +10. A higher value is associated with low humidity content and low-to-high humidity content at the time of vapour formation. This characteristic can be associated with oceanic regions.

In areas where evaporation and/or evapotranspiration are high, recondensations of that vapour are produced. These rains are referred to as recycled and have high values of deuterium excess (areas of big lakes, jungles).

On a global scale, it can be observed that the contents of 2H and ^{18}O in precipitation are linked to the mean air temperature in the sampling site. Basically, the temperature-isotope relation results from the conditions prevailing in a cloud at the time of precipitation. These relations are described by Dansgaard's equation:

$$\delta^{18}\text{O} = 0.69t - 13.6 \text{ with } t \text{ in } ^\circ\text{C}$$

Dansgaard stated that the critical factors in the isotopic composition of precipitation are the origin of vapour mass and the temperature at which condensation occurs. From these GNIP data, he observed that variations measured in precipitations are related to: a) geographical and climatic factors and b) parameters influencing them, such as latitude and altitude. He also found a relation to rainfall and movement of humidity-laden fronts into the continent. He referred to these variations as effects (Figure 4.3.6) and defined the altitude effect, the latitude effect, the seasonal effect, the continental effect and the amount effect.

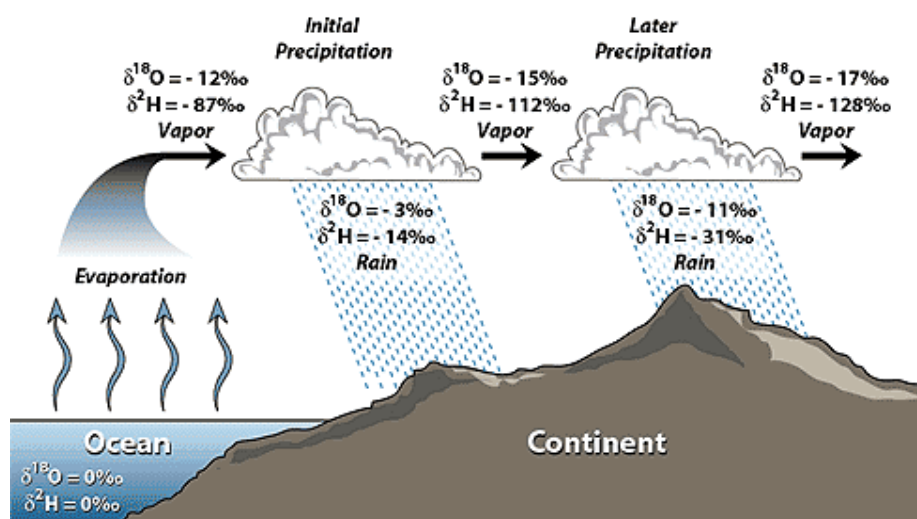


Figure 7.3.6 . Rainout effect on $\delta^2\text{H}$ and $\delta^{18}\text{O}$ values (based on Hoefs 1997 and Coplen et al. 2000).

Albero and Panarello (1981) analysed the relation with monthly mean content of stable isotopes in the southern hemisphere. They describe a good correlation with temperature in high and mid latitudes and with rainfall in low latitudes.

7.3.4 Considerations for interpretation

Dansgaard's effects are a characteristic of air masses and the basis upon which isotopic methods are used in hydrogeological studies. In addition, because of this dependence on climatic and geographical factors, isotopic composition is used to validate atmosphere general circulation models.

Surface water bodies

If evaporation processes occur from the ocean, the composition of the precipitated phase is not affected. On the other hand, if they occur from a lake, reservoir or inland sea, the precipitated phase is enriched in heavier isotopes.

Surface runoff

Water circulating over the surface (runoff) is the hydrological system's response to precipitation and involves pre-storm water and directly precipitated water. These components could be isotopically distinguished. Therefore, the variation in time and space of environmental isotopes can contribute to the understanding of runoff mechanisms.

Groundwater

Research on the origin and features of groundwater has been one of the most successful areas of application of natural stable isotope abundance variation studies. Such research is possible due to the conservative nature of stable isotope composition in water from an aquifer. The origin of water can thus be unequivocally characterised because, provided that it is not exposed to temperatures higher than

80° C, groundwater “remembers” the isotopic composition of its origin, even after long periods.

According to its origin, groundwater can be divided in two categories:

a) Meteoric water

Meteoric water derives from precipitation or surface freshwater, usually recharging through the soil in the non-saturated zone. The isotopic composition of groundwater is generally equal to that of local precipitation, at least in wet areas. In arid regions, there is commonly an enrichment of heavy isotopes in groundwater compared to rainwater, due to rapid and strong evaporation even when droplets are moving.

b) Paleowater

Paleowater is meteoric water originated in a distant past, especially during periods in which the prevailing weather conditions were different from the current ones.

When an aquifer reaches 80° C, a change in the isotopic conditions of water takes place and the composition does not correspond to the original. This is typical of geothermal conditions.

At great depths, in stratigraphic sections, there is salt water, which can be the remnant of original seawater. Due to its low movement, chemistry is dominated by the interaction with rocks. This water has been studied because of the possible relation with oil and gas. Its isotopic composition can also be analysed in order to study its origin and evolution.

Precipitation - groundwater

As mentioned above, water of meteoric origin has an isotopic composition similar to the mean composition of precipitation falling

onto the recharge area. This similarity is not exact since it can enrich or deplete in some cases, especially in arid regions. In these areas, there is enrichment of heavy isotopes as a result of processes of evaporation.

Changes in isotopic composition are usually caused by processes of recharge. It is important, therefore, to take into account whether there is mixture with deep fossil water.

Not all the precipitated water reaches aquifers. Part of it diverges like surface runoff and undergoes reevaporation on the ground. However, this is a fortuitous fact, non-correlated with variations in isotopic composition. It does not distort average values. But when the lost water is characterised by a different isotopic composition, for example in summer rain with higher evaporation, the recharged water differs from the mean. This process has been referred to as selection in order to distinguish it from the fractionation accompanying the loss of evaporated water in open systems.

The process of infiltration begins with accumulation in non-saturated zones. Surpassing some capacity, there is recharge to an aquifer. In arid areas, there is enrichment of heavy isotopes caused by evaporation.

In areas covered by vegetation the main loss of water is by transpiration, but this process is not fractionating with water isotopes. Isotopic composition variability between areas is known as geographical variability in the isotopic content of precipitation. The altitude effect has been the most common factor. The magnitude of this effect depends upon the weather and topography.

Another geographical factor normally used in hydrological research is the presence of bordering zones between regions with various climates. The air masses of each region cause precipitation with different properties.

For any quantitative application of water labelling, the isotopic composition of groundwater source should be homogeneous in the geographical area under study. With this in mind, variations in time and space must be taken into account.

Although no area is completely uniform, the stratigraphic section may behave as a homogeniser of recharge water throughout the recharge surface. Mixing in aquifers is a slow process, so it could be stated that there is an assembly of parcels of water moving along well-defined flow lines.

The mixing slowness produces intermediate positions between completely mixed systems (streams) and those which do not mix (such as tree rings and layers of snow). The mixture probably speeds up during discharge or pumping.

Groundwater salinisation

Groundwater salinity and its origin and prevention are serious problems. Some sources of salinisation, such as marine intrusion or surface saltwater, are associated with distinctive isotopic features of meteoric water. Here the isotopic technique is based on the identification of the water mixture that gives rise to groundwater salinisation.

The isotopic signature is usually better preserved in an aquifer than the components of salinity, since these are subject to processes of ion exchange, precipitation, etc.

Precipitation and groundwater. Relation between their isotopic compositions

It is generally assumed that, in most cases, groundwater of meteoric origin has isotopic compositions similar to those of local mean precipitations. This is due to the integrating feature of aquifers. However, there are phenomena which lead to differentiation between both compositions, among them:

1. Partial evaporation of water on the surface, caused when an aquifer recharges from rivers, lakes or dams.
2. Recharges through rivers or dams with water from areas far from aquifers.
3. Mixing in aquifers with water from different origins.
4. Insufficient residence time in aquifers so as to reach the annual average of isotopic composition.
5. Partial evaporation in non-saturated areas.
6. Isotopic exchange of oxygen with carbonates or silicates at medium to high temperatures.

7.3.5 Groundwater dating

The term “age” came into common usage in hydrogeology but it could be misleading because hydrodynamic mixing and flow path convergence integrate a variety of groundwater with different recharge origin and ages. The age gradients along the flow path will be preserved only under particular conditions, like regional artesian aquifers. The correct expression to be used instead of “age” is “Groundwater Mean Residence Time”. Knowing the mean residence time of groundwater is crucial for sustainable management, since exploitation of groundwater with no active recharge is mining (Clark and Fritz, 1997).

Only Tritium as part of a water molecule can date water, since other dating methods developed using dissolved solids like ^{14}C or gases may be affected by physicochemical and biological reactions, and therefore require model assumptions to correctly interpret values. Furthermore, in order to correctly date groundwater it is essential to know the input function, the time dependent amount of infiltrated radioactive tracer.

Assessments of mean residence times can be performed by a number of isotope techniques, including the use of seasonal stable isotopic variations, preserved in aquifers with short mean residence times (Chlorofluorocarbons). However, the most applied techniques are based on radionuclide decay. Long half-life radioisotopes (^{14}C , ^{36}Cl) can be used to date paleogroundwater, whereas short life ones (^3H , ^{222}Rn) indicate modern recharge. In this section the dating of water with Tritium will be discussed.

According to Clark and Fritz (1997), dating groundwater with Tritium can be carried out with the following qualitative and quantitative approaches:

Velocity of the 1963 peak: identification of the 1963 peak in groundwater establishes its “age”. Tritium pattern in precipitation can be preserved in systems with little or no advective mixing, where new recharged water moves downward the profile displacing the older one. The peak was actually washed out and is preserved only in low infiltration rate zones or areas with thick non-saturated zones. Below the water table, hydrodynamic dispersion and mixing attenuates the Tritium input function. Nevertheless, in some cases it is possible to identify the peak in groundwater, enabling the calculation of flow velocities and mean circulation times.

Radioactive Tritium decay dating method is based on the assumption that the input function is known and that residual Tritium is only the result of a decay process:

$$a_t H = a_0 {}^3H \times e^{-\lambda t}$$

where $a_0 {}^3H$ is the initial Tritium activity, $a_t {}^3H$ is the residual activity (measured sample). Considering that λ is equal to $\ln 2$ /half-life and half-life of Tritium is 12.43 years, the above equation may be written:

$$t = -17.93 \ln \left(\frac{a_t {}^3H}{a_0 {}^3H} \right)$$

By using this equation, starting from a known initial Tritium activity at the time of recharge, mean residence time can be determined. Due to the natural low levels of Tritium, the useful range for dating is less than 50 years and suitable for “young” groundwater.

Tritium in water is expressed in Tritium units (TU), where

$$1TU = \frac{1 \text{ atom } {}^3H}{10^{18} \text{ atom } H}$$

The large content of Tritium injected into the atmosphere by nuclear tests conducted between 1945 and 1963 gave rise to a concentration peak of this isotope in precipitation (10000 TU in 1963). Later, as the artificial production of Tritium has decreased, levels have diminished due to decay as well as dilution.

Input function for Tritium in groundwater: Tritium in precipitation presents seasonal and annual variations resulting in a complex input function (Figure 7.3.7)

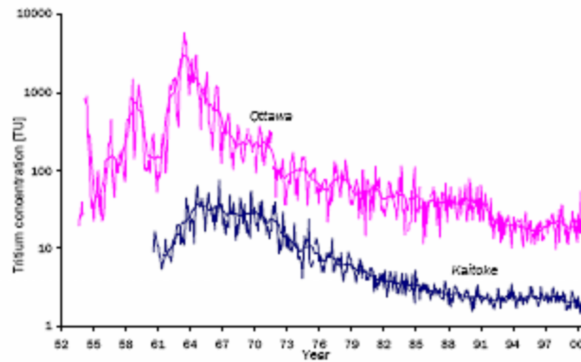


Figure 7.3.7 Tritium input function for N and S hemisphere (IAEA, Isotope Hydrology Section)

Nowadays, the artificial production of Tritium is the result of nuclear power stations, home refuse and some industries.

As mentioned above, the use of Tritium for water dating implies knowing the input function of hydrological systems, that is, the concentration of ^3H in precipitation, rivers and influent water bodies. Tritium values similar to those of precipitation from which an aquifer recharges indicate short time of infiltration. Lower values could indicate intermediate time or a mixture between recent water and Tritium-free water. Tritium-free water is that which does not contain Tritium due to its long residence time in aquifers. If Tritium values related to precipitations are too low, interpretation will be hampered. The use of Tritium with stable isotopes as well as groundwater chemistry makes it possible to determine processes of mixture and salinisation.

Tritium concentrations in precipitation are registered by networks such as GNIP.

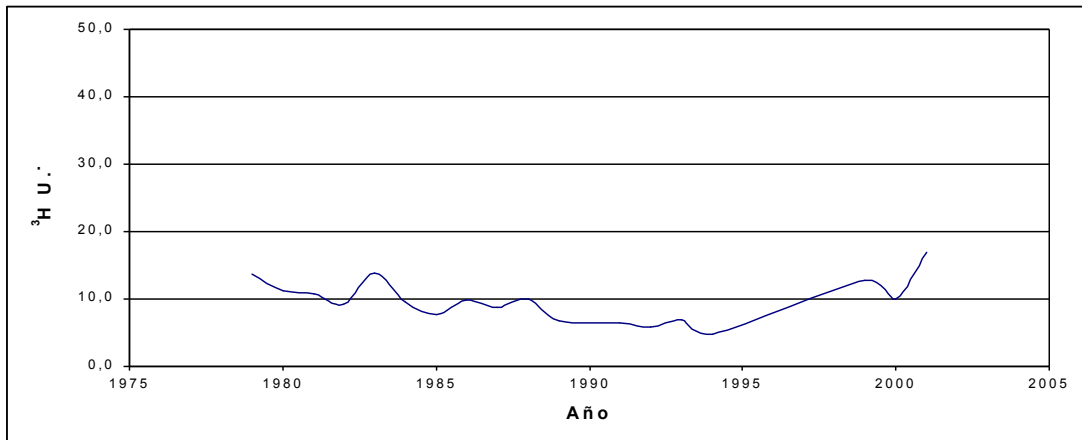


Figure 7.3.8 Tritium values in precipitation. Source: INGEIS. Red Nacional de Colectores de Argentina. Base de datos. Internal draft. Inédito. (2009)

8. Bibliography

Aguas Argentinas. 1997. Calidad de las aguas de la Franja Costera Sur del Rio de la Plata (San Fernando - Magdalena).

AGOSBA, OSN, SIHN. 1994. Calidad de las aguas de la Franja Costera Sur del Rio de la Plata (San Fernando - Magdalena).

Ainchil, J.; Kruse E.; Calahorra F., Ruiz, Soledad. 2007. Interpretación de perfilaje de pozos en la estimación de características hidrológicas. V Congreso de Hidrogeología. ISBN:978-987-23936-1

Ainchil, J., Kruse, E., Mazzoldi, A. 2008. Caracterización hidrogeológica de un área industrial en el NE de Buenos Aires Actas IX Congreso ALSHUD. Trabajo completo, Quito, Ecuador.

Albero M.C. y Panarello H. O. 1981. Tritio e isotopos estables en aguas de precipitaciones en América del Sur. Interamerican Symposium on Isotope Hydrology. Bogotá. Colombia: 91-109.

Allison, G. B., Barnes, C. J., Hughes, M. W., Leaney, F. W. J., 1983. Effect of climate and vegetation on Oxygen-18 and Deuterium profiles in soils. Isotope Hydrology 1983, IAEA Symposium 270, September 1983 Austria Vienna, 105 – 123.

Aravena, R., Evans, M. L., Cherry, J. A. 1996. Stable isotopes of oxygen and nitrogen in source identification of nitrate from septic systems. Groundwater 31, 180 – 186.

Archie, G.E..1942. The electrical resistivity log as an aid in determining some reservoir characteristics. Trans. Am. Inst. Min., Metall. Pet. Eng. 146, 54–62.

ASTM International. Standards worldwide. www.astm.org

Auge, M. Hernandez M. A.1983. Características geohidrológicas de un acuífero semiconfinado (Puelche) en la Llanura Bonaerense. Su implicancia en el ciclo hidrológico de llanuras dilatadas. Proc. International Colloquium on the Hydrology of Extensive Plains, Buenos Aires, Argentina, Vol. 2, pp. 1021–1042.

- Auge, M.: 1986, Hydrodynamic behaviour of the Puelche Acuífero in Matanza River Basin. *Groundwater*, Vol. 25, No. 5, Dublin, Ohio, pp. 636–642.
- Auge, M., 1990. Aptitud del agua subterránea en La Plata, Argentina. Seminario Latino-Americano de Medio Ambiente y Desarrollo. Bariloche, Argentina. pp191-201.
- Auge, M., 1991. Sobreexplotación del acuífero Puelche en La Plata, Argentina. XXXIII International Congress International Association of Hydrogeologists. Vol 1, 411 – 415.
- Auge, M.P., 1995. Manejo del agua subterránea en La Plata- Argentina. Informe Convenio Univ. Nac. de Buenos Aires- International Development Research Centre.
- Auge M. P., M. I. Nagy. 1996. Origen y evolución de los nitratos en el suelo y el agua subterránea de La Plata. Provincia de Buenos Aires - Argentina. 3er Congreso Latinoamericano de Hidrología Subterránea. Actas: 1-12. San Luis Potosí. México. 111
- Auge, M., Nagy, M. I.1999. Estado del agua subterránea respecto a la contaminación con agroquímicos en La Plata – Provincia de Buenos Aires. In Proc : II Congreso Argentino de Hidrogeología- IV Seminario Hispano-Argentino sobre temas actuales de la Hidrología Subterránea.
- Baylac, P.1985. Ondas de Tormenta en el Río de la Plata. Consejo Nacional de Investigaciones Científicas y Técnicas (CONICET), report.
- Bracaccini, O. L.1980. Cuenca de Salado. Segundo Simposio de Geología Regional Argentina, Academia Nacional de Ciencias, Córdoba, Argentina, 2 pp.879 –918.
- Bracaccini, O.L. 1972. Cuenca del Salado, Geología Regional Argentina. Academia Nacional de Ciencias.
- Böttcher, J. Strebel, O., Voerkelius, S., Schmidt H. L. 1990. Using isotope fractionation of nitrate nitrogen and nitrate oxygen for evaluation of nitrate in a sandy aquifer. *Journal of Hydrology* 114, 413 – 424.
- Burgos, J., Vidal A. 1951. Los climas de la República Argentina según la clasificación de Thornthwaite. *Meteoros* 1, 3 – 23.

- Cappannini, D. y Domínguez, O., 1961. Los principales ambientes geodafológicos de la Provincia de Buenos Aires. IDIA, 163, 33-39
- Cappannini, D. y Mauriño, V., 1966. Suelos de la zona litoral estuárica comprendida entre las ciudades de Buenos Aires al norte y La Plata al sur. INTA, Buenos Aires.
- Cavalotto José Luis, Roberto A. Violante y Ferrán Colombo.2005. Evolución y cambios ambientales de la llanura costera de la cabecera del río de la Plata. Revista de la Asociación Geológica Argentina, 60 (2): 353-367
- Clark, I. D. Fritz, P. 1997. Environmental Isotopes in Hydrogeology. CRC press LLC.112 ISBN 1-56670-249-6. 328p.
- Clayton R. N., Friedman, I., Graff, D. L., Mayeda, T. K., Meents, W. F., Shimp, N. F. 1966. The origin of saline formation waters, Isotopic Composition. Journal of Geophysical Research 71, 3869 – 3882.
- Coleman M.L., Sheperd T.J., Durham J.J., Rouse J.E. and Moore F.R. 1982. A rapid and precise technique for reduction of water with Zinc for Hydrogen isotope analysis. Anal Chem 54: 993-995
- Comisión Administradora del Rio de la Plata. 1989. Estudio de la Contaminación en el Rio de La Plata. Informe de avance.
- Comisión Nacional de Normas. 1973. Normas de calidad y control para aguas de bebida –suministros públicos.
- Coplen, T.B. 1988. Normalization of oxygen and hydrogen isotope data. Chemical Geology 72: 467-473.
- Coplen, T.B., 2000, Laboratory Information Management System (LIMS) for Light Stable Isotopes: U.S. Geological Survey Open-File Report 00-345, 121 p
- Craig, H. 1961a. Standard for reporting concentrations in deuterium and oxygen-18 in natural Waters. Science, 133:1833-1834.
- Craig, H. 1961b. Isotope variations in meteoric waters. Science, 133: 1702-1703.
- Craig, H. and Gordon, L. I. 1965. Deuterium and oxygen-18 variations in the ocean and the marine atmosphere. Stable isotopes in

Oceanographic studies and Paleotemperatures. E. Tongiorgi Editors, Lab Geol Nucl. Pisa: 1-122

Custodio, E. Llamas M. R. Editors. 1983. Hidrologia Subterranea. Ediciones Omega S. A. Barcelona, Spain. ISBN 84-282-0446-2.

Dansgaard, W. 1964. Stable isotopes in precipitation. Tellus. N° 16, 436-468.

Dansgaard, W. 1969. Oxygen-18 analysis of water. Medd. Gronland 177:33.

Dapeña, C. and Panarello H.O. 2004. Composición isotópica de la lluvia de Buenos Aires. Su importancia para el estudio de los sistemas hidrológicos pampeanos. Revista Alsuhd 4:17-25.

Dapeña, Cristina. 2007. Isotopos ambientales livianos. Su aplicación en hidrología e hidrogeología. Tesis doctoral. UBA.

Dapeña, C. and Panarello H.O. 2007. Application of environmental isotopes techniques to selected hydrological Pampean System. Argentina. International Symposium on Advances in Isotope Hydrology and its role in Sustainable Water Resources. HIS. Vienna, Austria.

Douglas, M., Clark, I. D., Raven, K., Bottomley, D. 2000. Groundwater mixing dynamics at a Canadian Shield mine. Journal of Hydrology 235, 88 – 103.

Duclout, J. 1901. Informe del inspector general Ing. Jorge Duclout sobre los pasos Martin Garcia. Inspeccion general de Navegacion y Puertos. Servicio de Hidrografia Naval, Archivo Técnico.

Eagleason P. 1991. Opportunities in the Hydrologic Sciences. Commission on Geosciences, Environment and Resources. National Research Council. USA

EASNE. 1972. Estudio Aguas Subterraneeas del N.E. de la Provincia de Buenos Aires. CFI serie tecnica. N°24. La Plata.

Fidalgo, F., y O.R. Martinez. 1983. Algunas características geomorfológicas dentro del Partido de La Plata, Provincia de Buenos Aires. Revista Asociación Geológica Argentina, XXXVIII (2), 263 - 279. Buenos Aires

- Fidalgo, F., de Francesco, F., Pascual, R., 1975. Geología Superficial de la Llanura Bonaerense. Relatorio VI Congreso Geológico Argentino. Pág. 103 – 138. Bahía Blanca. Censo Hortiflorícola de la Provincia de Buenos Aires. 2005. Buenos Aires
- Figgini, A., Hernandez, M. A., Levin, M., Sala, J. M., Salati, E. 1975. Genesis and Mechanism of intrusion by brakish waters in the littoral of the River Plata, Argentina. Upub. Report. Franklyn, M. T., McNutt, R. H., Fray, Ch., Ewing, M., 1963. Pleistocene sedimentation and fauna of the Argentine Shelf. Proceedings of the Academy of Natural Sciences of Philadelphia 115 (6), 113 – 152.
- Freeze, R. A. and Cherry J. A. 1979. Groundwater. Prentice Hall, INC. ISBN 0-13-365312-9. 113
- Frenguelli, J. 1950. Rasgos generales de la morfología y la geología de la Provincia de Buenos Aires. LEMIT, Serie II n° 33, La Plata.
- Fritz, B., Richard, L., McNutt, R.H. 1992. Geochemical modelling of Sr isotopic signatures in the interaction between granitic rocks and natural solutions. In: Kharaka, Y. K., Maest, A. S. Editors, Water–Rock Interaction WRI7, vol. 2, pp. 927 – 930.
- Fritz, P., Frappe, S. K. 1982. Saline groundwaters in the Canadian Shield – a first overview. Chemical Geology 36, 179 – 190.
- Fritz, S. J., Drimmie, R. J., Fritz, P. 1991. Characterizing shallow aquifers using Tritium and ^{14}C : Periodic sampling based on Tritium Half- Life. Applied Geochemistry 6, 13 – 33.
- Förstel, H. 1982. $^{18}\text{O}/^{16}\text{O}$ ratio of water in plants and their environment. H. L. Schmidt, H. Förstel and K. Heinzinger Editors, Stable Isotopes. Elsevier, Amsterdam, The Netherlands. 503-516.
- Gazis, C., Feng, X. 2003. A stable isotope study of soil water: evidence for mixing and preferential flow paths. Geoderma, 15 pages.
- Environmental Isotopes in the Hydrological Cycle. Principles and applications. UNESCO International Hydrological Program V. Technical Documents in Hydrology. N 39, Vol. IV.
- Gonfiantini, R. 1978. Standards for stable isotope measurements in natural compounds. Nature, 271, 534-536.

- Gonfiantini, R., Zuppi, G. M. 2003. Carbon isotope exchange of DIC in karst groundwater. *Chemical Geology* 197, 319 – 336.
- Gimenez J.; Hurtado M.; Cabral M. y Da Silva M. (1992). Estudio de suelos del Partido de La Plata. Consejo Federal de Inversiones – Universidad Nacional de La Plata. Informe Final. La Plata.
- Groeber, P., 1945. Las aguas surgentes y semisurgentes del Norte de la Provincia de BsAs. *Rev, La Ingeniería* 6: 371-387.
- Guerrero, R. A., Acha, E. M., Framiñan, M. B., Lasta, C. A. 1997. Physical oceanography of the Rio de la Plata Estuari, Argentina. *Continental shelf research*. Vol 17 n 7, 727 – 742.
- Hernandez M, Fili M, Auge M, Ceci J (1975) Geohidrología de los acuíferos profundos de la Provincia de Buenos Aires. Sexto Congreso Geológico Argentino, Buenos Aires, Acta 2: 479-500. Septiembre de 1975
- Hernandez M. A. and Sala J. M. 1972. Un metodo simple para analisis y el pronóstico de avance del frente salino. *Semin. Avanz. sobre Des. y Manejo de Recursos Hidricos Subterranos*. Gob.Argentino Israel OEA. Tomo II Buenos Aires.
- Hernandez M. A. 1975. Efectos de la sobreexplotacion de aguas subterranas en el Gran Buenos Aires y alrededores Republica Argentina. II Congreso Ibero Americano de Geologia Economica.
- Hernandez M.A. 1978. Reconocimiento hidrodinamico e hidroquimico de la interface agua dulce agua salada en las aguas subterranas del Estuario del Plata. Partidos de Quilmes y Berazategui. *Proc XII Cong. Geol. Arg.* Vol. 2. AGA, Buenos Aires pp 273-285.
- Hoefs, J. 1997. *Stable Isotope Geochemistry*. Springer-Verlag. 4th edition. Berlin.
- Horth G., Cattoggio, J. A. 1990. Distribution of chlorinated pesticides and individual polychlorinated biphenils in biotic and abiotic compartments of the Rio de la Plata, Argentina. *Environmental Science and Technology* 24, 498 – 505.
- IAEA. 2001. Isotope Hydrology Information System The ISOHIS. Accessible at: <http://isohis.iaea.org>

IAEA, 1999. Origins of salinity an impact of fresh groundwater resources: optimisation of isotopic techniques. Consultant meeting for formulation of a future CRP.

IAEA/WMO, 2002. "Global Network for Isotopes in Precipitation. The GNIP Database". <http://isohis.iaea.org>

INGEIS, 2009. Red Nacional de Colectores de Argentina. Base de datos. Informe Interno. Inédito.

Johansen, H.K. 1975. An interactive computer graphic display terminal system for interpretation of resistivity sounding. *Geophysical Prospecting*, 23 449-458.

Johnson D. W. 1984. Sulphur cycling in forests. *Biogeochemistry* 1, 29 - 43.

Kruse E. y E. Zimmermann. 2002. Hidrogeología de Grandes Llanuras. Particularidades en la Llanura Pampeana (Argentina). *Groundwater and Human Development (IAH Congress)*. ISBN 987-544-063-9. Publicación Workshop. Mar del Plata (Argentina).

Kirchner J. W. 1992. Heterogeneous geochemistry of catchment acidification. *Geochimica et Cosmochimica Acta* 56, 2311 - 2327.

Koefoed, O, 1979. *Geosounding principles. Resistivity Soundings Measurements*. Elsevier. Amsterdam 276pp.

Laurencena, P.; Varela, L.; Kruse, E; Rojo, A. y Deluchi, M. 2002. Características de las variaciones freáticas en un área del Noreste de la Provincia de Buenos Aires. *Groundwater and Human Development*. Bocanegra, E., Martínez, D, Massone, H. (Eds). ISBN 987-544-063-9. Pág: 547- 552. Mar del Plata.

Levin, M., Cortelezzi C. R., Figgini, A. J. 1973. Uso de isotopos estables (Deuterio y Oxigeno-18) para determinacion del origen de la salinizacion del Puelchense en la ciudad de La Plata y alrededores. *Proc. V Congreso Geologico Argentino, Vol. 1. Asociacion Geologica Argentina*. Buenos Aires. 373-393

Logan W. S., Rudolph, D. 1997. Microdepression-focused recharge in a coastal wetland, La Plata, Argentina. *Journal of Hydrology*. 194 221-238.

- Logan W. S., Nicholson, R. V. 1998. Origin of dissolved groundwater sulphate in the coastal plain sediments of the Rio de la Plata, eastern Argentina. *Aquatic Geochemistry* 3, 305-328.
- Lucas L. L., Unterwever M. P. 2000. Comprehensive review and critical evaluation of the half- life of Tritium. *Journal of Research of National Institute of Standards and Technology*. Volume 105
- Min. de Economia de la Nacion, Instituto Nacional de Estadisticas y Censos (INDEC). 2001. Censo Nacional de Poblacion y Vivienda.
- Mook W. 2000. Introduction Theory Methods Review. In W. E. Mook, Editor, 2001. *Environmental Isotopes in the Hydrological Cycle. Principles and applications*. UNESCO International Hydrological Program V. Technical Documents in Hydrology. N 39, Vol. I.
- Nace, R. L. 1969. World water inventory and control. R. J. Chorley Editor, *Water Earth and Man*. Methuen, London.
- Nier, A.O. 1950. A redetermination of the relative abundance of the isotopes of carbon, nitrogen, oxygen, argon and potassium. *Phys. rev.* 77:789.
- Orellana E. 1982. "Prospección geoelectrica en corriente continua". Ed. Paraninfo. Madrid.
- Panarello H., Dapeña C. 2003. Stable isotopic composition of the Rio de la Plata Estuary: a consequence of ITCZ movement and ENSO related phenomena, *Proceedings International Symposium on Isotope Hydrology and Integrated Water Resources Management*, Austria.
- Panarello, H.O. 1987. Relaciones entre cocentraciones de isotopos livianos utilizados como indicadores ambientales y de paleotemperaturas. Tesis doctoral. UBA.
- Panarello, H., Dapeña, C., Auge, M. 1992. Mecanismos de salinizacion del aqua subterranea de la zona de La Plata, Buenos Aires Argentina: su interpretacion por medio de los isotopos ambientales.
- Panarello, H.O. and Dapeña, C. 2001. Stable isotope composition of the Rio de la Plata estuary: an attempt to relate to meteorological variables. *III South American Symposium on Isotope Geologia*. Pucón, Chile. Actas CD. ROM.

Panarello, H.O., Dapeña C., Auge, M. 1993. Estudio isotópico de la salinización del agua subterránea en la ciudad de La Plata y sus zonas vecinas, Buenos Aires Argentina. Proc XII Cong. Geol. Arg. Vol. 6. AGA, Buenos Aires pp 146-152.

Parker, G., Violante, R.A. 1982. Geología del frente de costa y plataforma interior entre Pinamar y Mar de Ajo. Acta Oceanographica Argentina 3 (1),57 -91.

Parker, G., Paterlini, C. M.,Violante, R. A. 1994. Edad y Genesis del Rio de la Plata. Revista Asociación Geológica Argentina 49 (1 -2),11 -18.

Parker,G., Paterlini, C.M., Violante, R. A., Costa, I. P., Marcolini, S., Cavallotto, J.L. 1999. Descripción geológica de la Terraza Rioplatense (Plataforma interior norbonaerense). Servicio Geologico Minero Argentino (SEGEMAR), Boletin N°. 273, Buenos Aires, Argentina.

Pera Iburguren, S, H. Panarello, J. Ainchil, G.M. Zuppi. 2003. Isotope hydrology of the multilayer aquifer in N.E. Buenos Aires Province, Argentina, International Symposium on Isotope Hydrology and Integrated Water Resources Management Proceedings IAEA Scientific Meetings, Viena

Pera Iburguren, S. 2003. Surface water- groundwater interactions in transition environments: the Rio de La Plata coastal plain. Tesis doctoral. Università Ca' Foscari Venezia

Pous, J.; Marcuello, A. and Queralt P. 1987. Resistivity inversion with apriori information. Geophysical Prospecting 35. p/590-603.

Ramos, V., 1999. Las provincias geológicas argentinas. En: R. Caminos (ed.) Geología Argentina. SEGEMAR, Anales 29, 41-97, Buenos Aires.

Rolleri, E., 1975. Provincias Geológicas Bonaerenses . VI Congreso Geológico Argentino, Relatorio , Bahía Blanca, 29-54

Ronco, A., Camilion, C., Manassero, M. 2001. Geochemistry of Heavy Metals in bottom sediments from streams of the western coast of the Rio de la Plata estuary, Argentina. Environmental Geochemistry and Health, 23 89-103.

Rozanski, K., Froehlich, K., Mook W., Surface Water. In W. E. Mook, Editor. 2001. Environmental Isotopes in the Hydrological Cycle. Principles and applications. UNESCO International

Russo, A., Ferello, R. y Chebli, G., 1979. Llanura Chaco Pampeana. Actas del Segundo Simposio de Geología Regional Argentina , Córdoba, 1, 139-183

Sala, J.M. 1975. Recursos hídricos (Especial mención de las aguas subterráneas). Relatorio Geología de la Provincia de Buenos Aires. VI° Congreso Geológico Argentino: Actas: p. 169-193

Santa Cruz, J.N.,1972. Estudio sedimentológico de la Formación Puelches. Provincia de Buenos Aires. Revista de la Asociación Geológica Argentina. Tomo XXVII. N° 1.

Spalding, R.F., Exner, M.E. 1993. Occurrence of nitrate in groundwater a review. Journal of Environmental Quality 22 3. 392 - 402.

Sharma, P.V. 1997.Environmental and engineering geophysics. Cambridge University Press. ISBN 0-521-57632-6

Tavella,G. F.,Wright, C. G. 1996. Cuenca del Salado. In Ramos, V.A.,Turic,M.A.(Eds.),Geologia y Recursos Naturales de la Plataforma Continental Argentina. Relatorio 13th Congreso Geologico Argentino y 3th Congreso de Exploracion de Hidrocarburos, Buenos Aires, Argentina, pp.95 –116.

Tavella, G. 2005. “Cuenca del Salado” Relatorio del XVI Congreso Geológico Argentino

Tarantola, A. and Valette B. 1982. Generalized non linear inverse problem solved using least squares criterion. Geophysics, 20, 219-232.

Thornthwaite, C. W., An approach toward a rational classification of climate. 1948. **Geographical Review**, 38:55-94.

Thornthwaite, C. W., Mather J. R., Carter D. B. 1957. Instructions and tables for computing potential evapotranspiration and the water balance. Publ. in Climatology, 10:181-311.

Thornthwaite, C. W., Mather J. R. 1955. "Instruction and tables for computing the potential evapotranspiration and the water balance". Climate Crewel Inst. of Technology. 10(3).

- Torgersen, T., Clark, W. B., Jenkins, W. J. 1979. The Tritium/Helium-3 method in hydrology. *Isotope Hydrology 1978*. Vol II. IAEA Symposium 228.
- Urien, C. M. 1972. Rio de la Plata Estuary environments. *Geological Society of America Memoir 133*. 213 - 234
- U.S. Geological Survey. 2002. Documentation of the spreadsheets for the analysis of Aquifer test and Slug test data. Open file Report 02-197.
- Vara, C., 1974. Ondas de Plataforma del Mar Argentino. *Servicio de Hidrografia Naval Bulletin*, 9 (3) 191-196.
- Varela, L.; Laurencena, P.; Kruse, E.; Deluchi, M y Rojo A. 2002. Reconocimiento de la relación aguas superficiales - aguas subterráneas en la cuenca del arroyo del Gato. Buenos Aires. *Groundwater and Human Development*. Bocanegra, E., Martínez, D, Massone, H. (Eds) 2002. ISBN 987-544-063-9. Pág: 1334-1341. Mar del Plata.
- Violante, R. A., Parker, G. 1999. Historia evolutiva del Rio de la Plata durante el Cenozoico superior, Vol.1. 14° Congreso Geologico Argentino, Salta, Argentina, pp.504 - 507.
- Violante, R. A., Parker, G. 2003. The post-glacial maximum transgression in the de la Plata river and adjacent inner continental shelf, Argentina. *Quaternary International*.
- Way, K., Fano, L., Scott, M.R., and Thew, K. 1950. Nuclear data. A collection of experimental values of halflives, radiation energies, relative isotopes abundance, nuclear moments and cross sections. *Natural Bureau of Standards. US Circ 499*.
- Yrigoyen, M.R. 1975. "Geología del subsuelo y plataforma continental" Relatorio. *Geología de la Provincia de Buenos Aires*. 6° Congreso Geológico Argentino, Actas pp. 139-168
- Yrigoyen, M.R. 1999. Los depósitos cretácicos y terciarios de las Cuencas del Salado y del Colorado. *Geología Argentina*. Segemar.
- Zambrano, J.J. 1974. Cuencas sedimentarias en el subsuelo de la provincia de Buenos Aires. *RAGA Tomo XXIX*
- Zimmerman, U., Münnich, K. O. and Roether, W., 1967. Downward movement of soil moisture traced by means of hydrogen isotopes.

Isotopes techniques in the hydrological cycle. Geophysical monograph Series 11, American Geophysical Union.

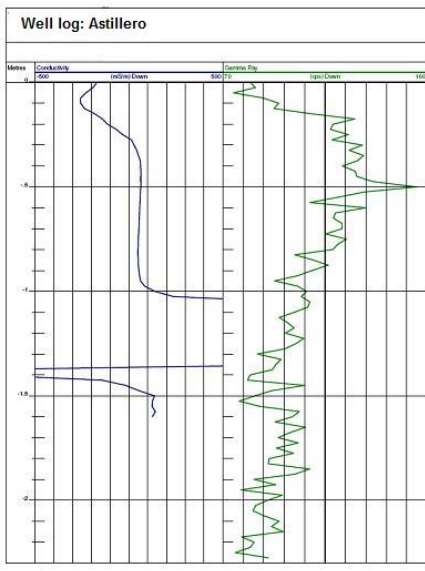
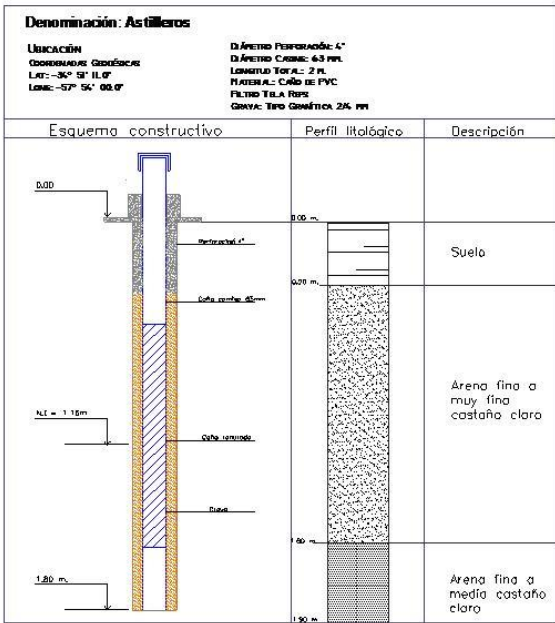
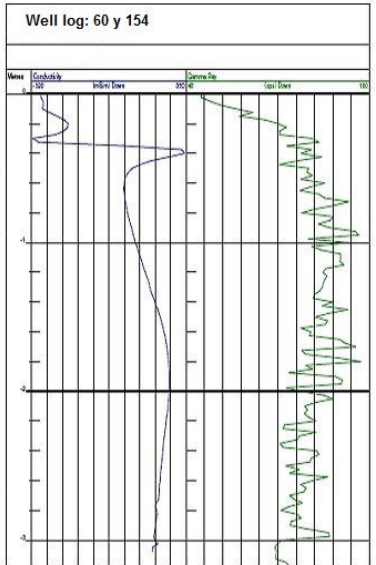
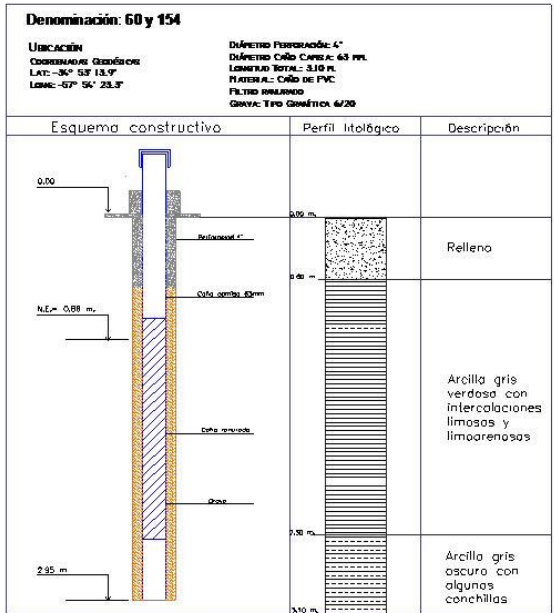
Zohdy A. R. 1989. A new method for the automatic interpretation of Schlumberger and Wenner soundings curves. Geophysics Vol. 54 Nro 2 p/245-253.

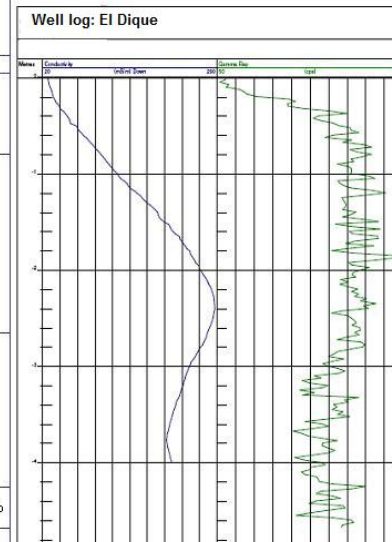
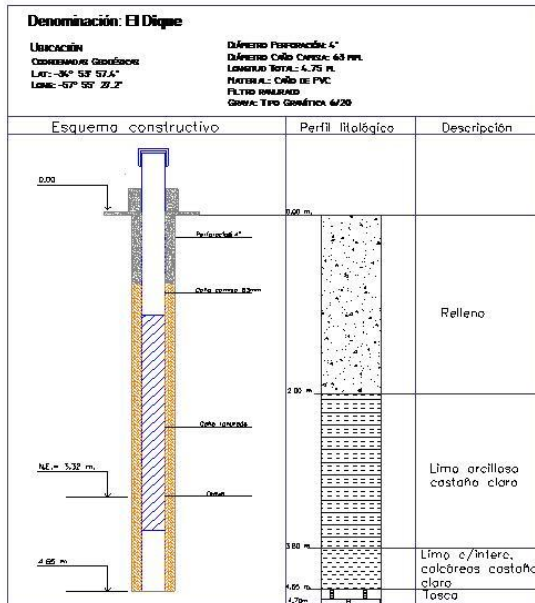
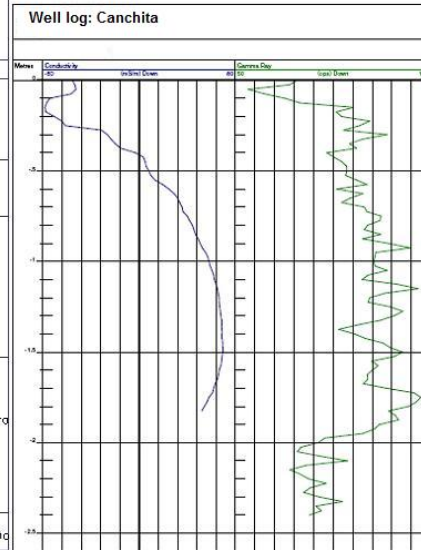
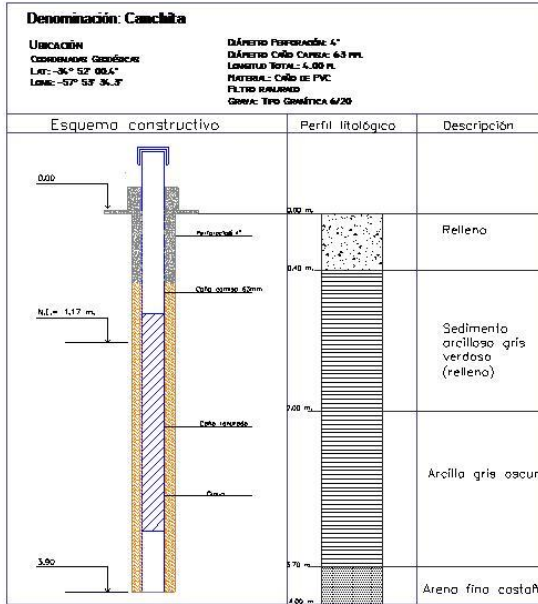
Zuppi G.M. 2008. The groundwater challenge, In CORRADO CLINI; IGNZIO MUSU; MARIA LODOVICA GULLINO EDITORS, Sustainable development and environmental management Experience and case studies, DORDRECHT, Ed. Springer, pp. 49-64. (ISBN 978-1-4020-6597-2)

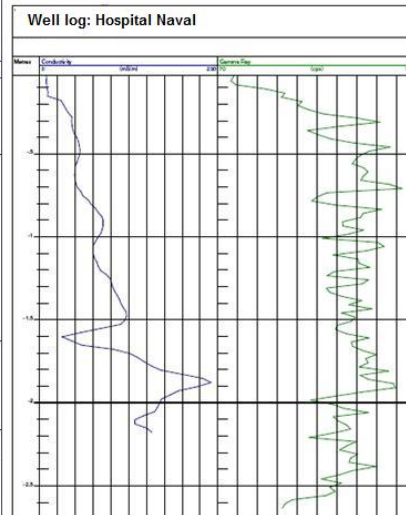
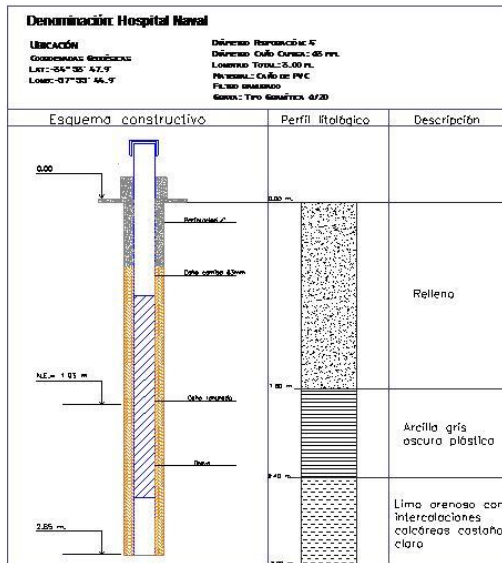
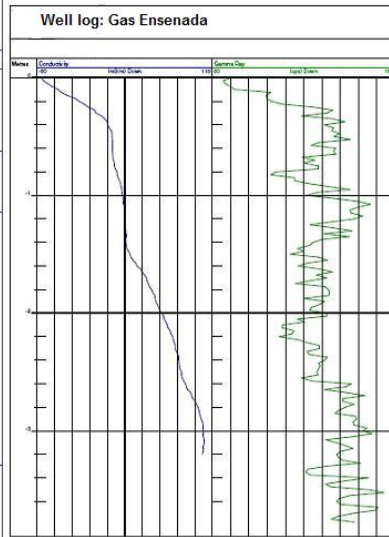
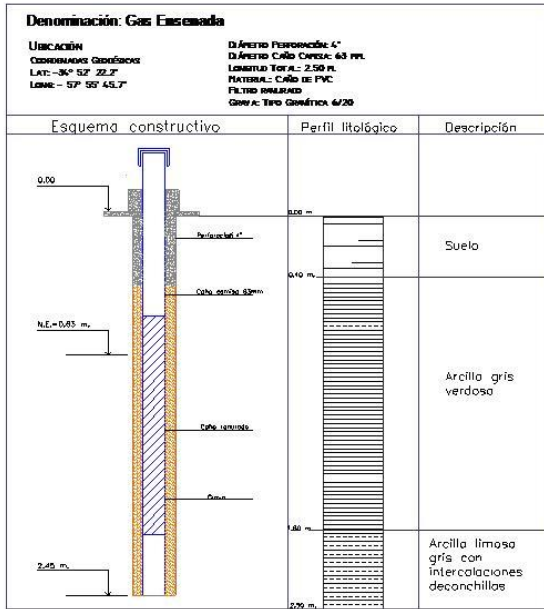
Zuppi G.M. 2002. Isotopic content of rainfall as climatic indicators, Comptes Rendus Acad. Scie. Paris, Geosciences, 334, 7, 519-520, Rivista COMPTES RENDUS. GÉOSCIENCE, ECLOGAE GEOL. HELV., volume 334 (7), pp. 519-520. (ISSN 1631-0713)

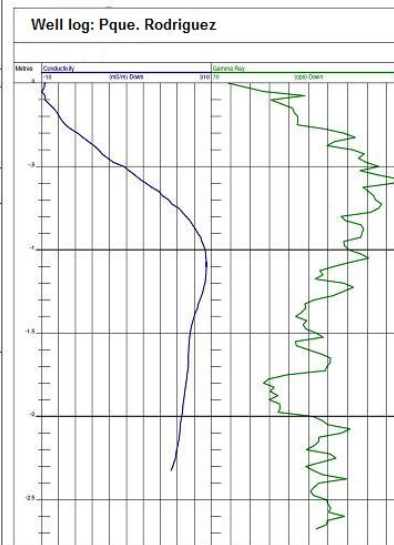
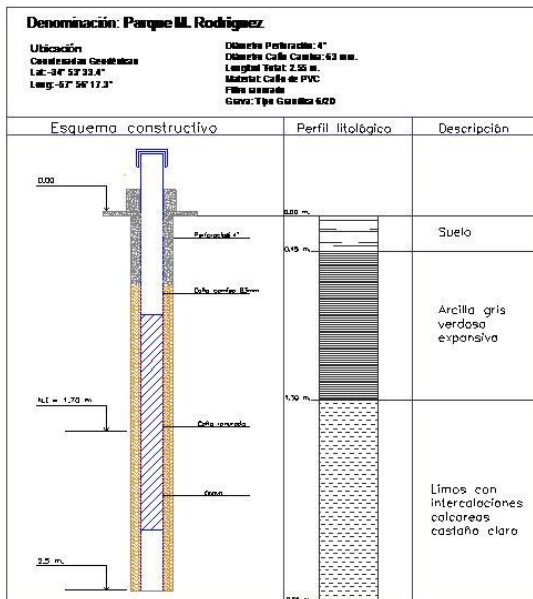
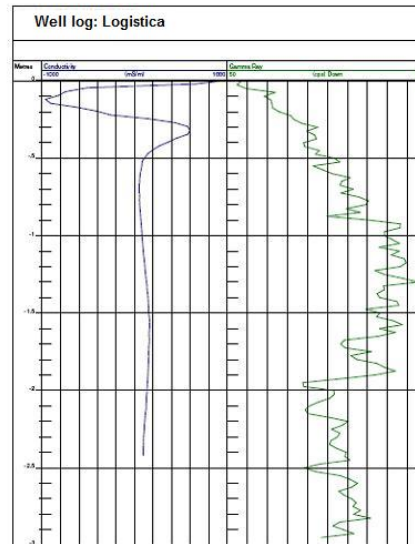
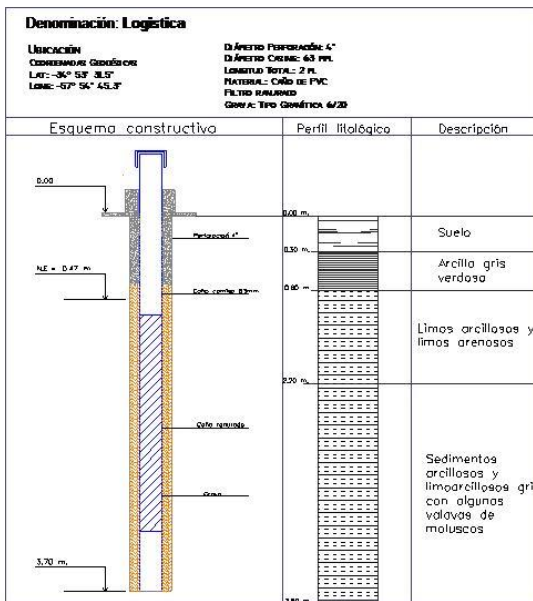
Zuppi G.M.; Sacchi E. 2004. Dynamic processes in the Venice Region outlined by environmental isotopes, Rivista ISOTOPES IN ENVIRONMENTAL AND HEALTH STUDIES, volume 40, pp. 35-44, ISSN 1025-6016. (ISSN 1025-6016)

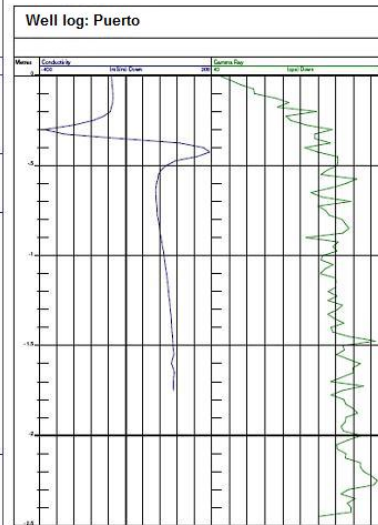
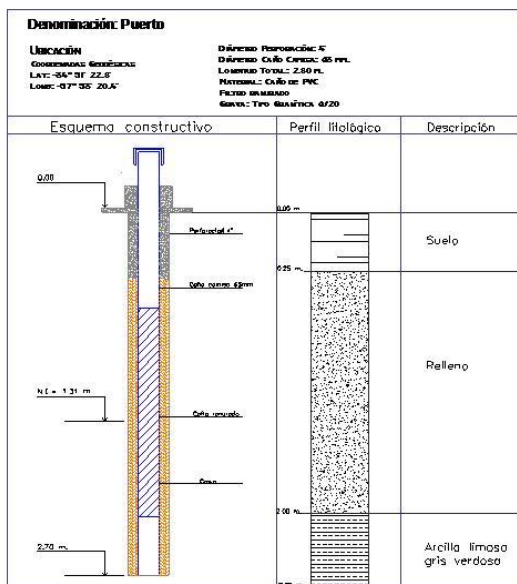
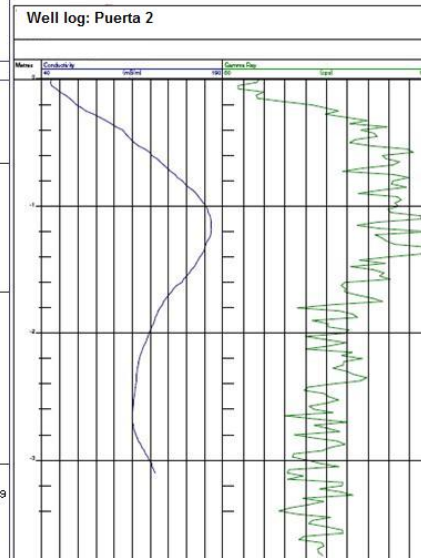
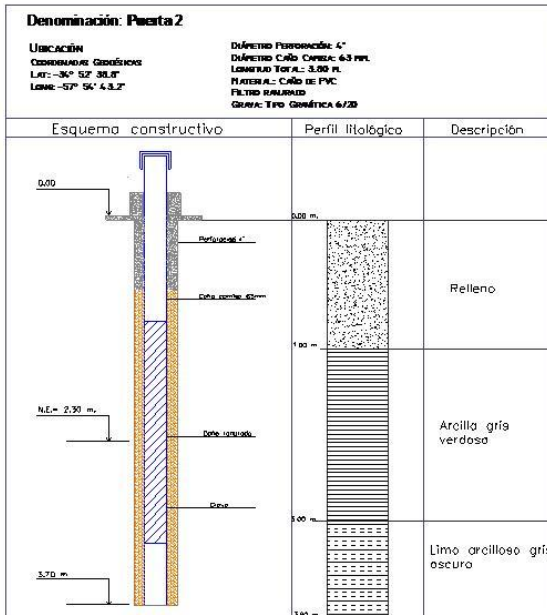
ANNEX 1
Well description

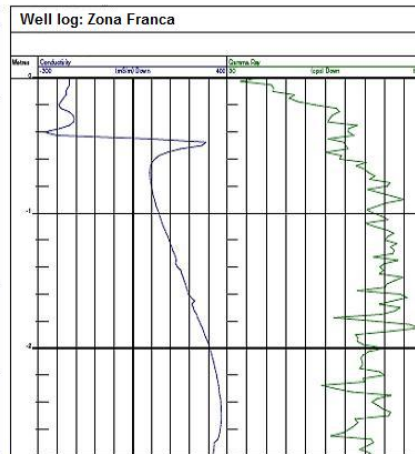
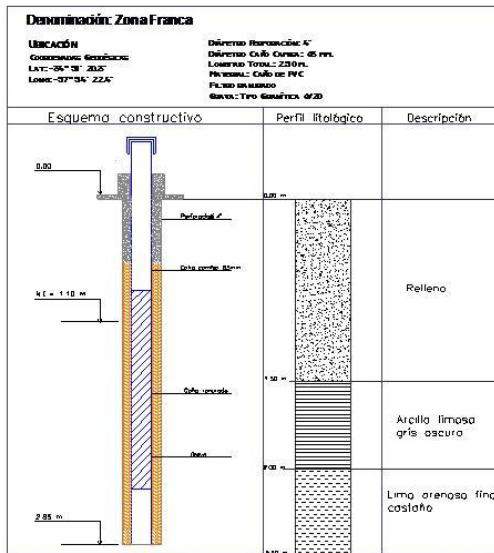
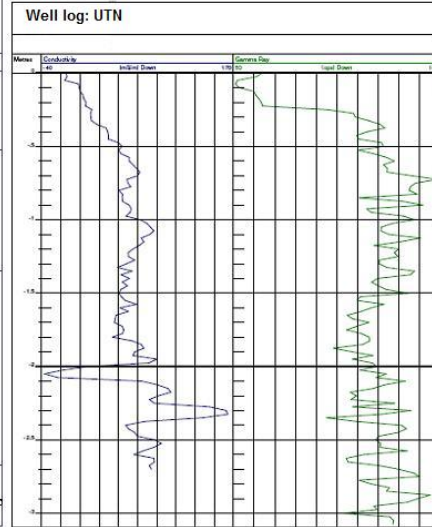
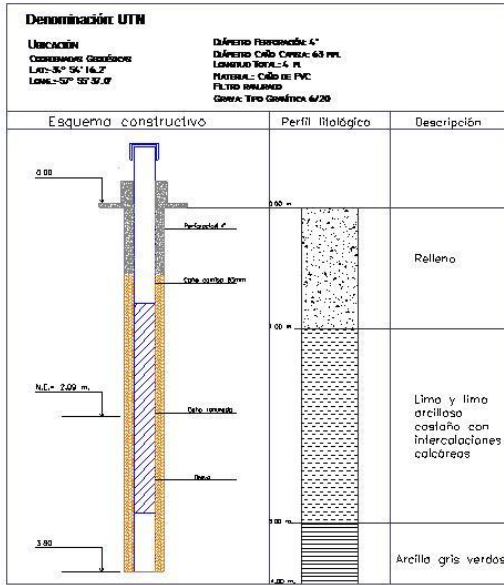












ANNEX 2
Chemical data tables

Pozo	Gas	Astillero	Puerta	Petroken	Parque Rdz.	H Naval	utn	64 y 128	60 y 145	Vivero	Logística	Metodología		
Parámetros	oc06	oc06	oc06	oc06	oc06	oc06	oc06	oc06	oc06	oc06	oc06	de análisis	Unidad	LCM
Arsénico	<0,01	<0,01	<0,01	<0,01	<0,01	<0,01	<0,01	<0,01	<0,01	<0,01	<0,01	SM 3500/3114-C	mg/L	0,01
Benceno	<10,0	<10,0	<10,0	<10,0	<10,0	<10,0	<10,0	<10,0	<10,0	<10,0	<10,0	EPA 8260	mg/L	10
Bicarbonato	574,9	586,9	402,9	597,9	724,9	851,8	795,8	689,9	750,3	643,9	1081,8	SM 2320-B	mg/L	0,5
Cadmio	<0,01	<0,01	<0,01	<0,01	<0,01	<0,01	<0,01	<0,01	<0,01	<0,01	<0,01	SM 3500/3111-B	mg/L	0,01
Calcio	88,8	231,5	93,8	55,9	189,8	172,7	145,7	21,0	45,9	113,8	40,9	SM 3500 Ca-B	mg/L	0,5
Carbonato	<0,5	<0,5	<0,5	<0,5	<0,5	<0,5	<0,5	<0,5	<0,5	<0,5	<0,5	SM 2320-B	mg/L	0,5
Cinc	<0,01	<0,01	<0,01	<0,01	<0,01	<0,01	<0,01	<0,01	<0,01	<0,01	<0,01	SM 3500/3111-B	mg/L	0,01
Cloruro	174,8	167,0	153,2	246,3	273,2	38,3	39,3	76,1	70,3	630,7	41,1	SM 4500 Cl-B	mg/L	1
Cobalto	<0,02	0,025	<0,02	<0,02	0,048	<0,02	<0,02	<0,02	<0,02	0,028	<0,02	SM 3500/3111-B	mg/L	0,02
Cobre	<0,02	<0,02	<0,02	<0,02	<0,02	<0,02	<0,02	<0,02	<0,02	<0,02	<0,02	SM 3500/3111-B	mg/L	0,02
Cond. Elect.	1158,0	1641,7	1109,9	1391,4	2830,6	1374,1	1841,9	1526,8	1405,3	3718,1	2329,1	SM 2510-B	µs/cm	0,1
Cromo	<0,02	<0,02	<0,02	<0,02	<0,02	<0,02	<0,02	<0,02	<0,02	<0,02	<0,02	SM 3500/3111-B	mg/L	0,02
Etilbenceno	<10,0	<10,0	<10,0	<10,0	<10,0	<10,0	<10,0	<10,0	<10,0	<10,0	<10,0	EPA 8260	µg/L	10
Fenoles totales	<0,05	<0,05	<0,05	<0,05	<0,05	<0,05	<0,05	<0,05	<0,05	<0,05	<0,05	SM 5530-C	mg/L	0,05
Fluoruro	0,7	0,7	0,5	1,5	0,9	1,0	0,6	0,1	0,6	0,9	0,8	SM 4110-B	mg/L	0,1
Hidrocarburos totales	< 0.2	< 0.2	< 0.2	< 0.2	< 0.2	< 0.2	< 0.2	< 0.2	< 0.2	< 0.2	< 0.2	EPA 8015	mg/L	0,2
Magnesio	31,8	24,4	21,9	9,4	42,8	44,8	37,8	6,1	12,9	65,7	23,9	SM 3500/3111-B	mg/L	5
Mercurio	0,001	0,003	<0,001	0,005	0,007	0,002	0,003	0,006	<0,001	0,006	0,003	SM 3500/3112-B	mg/L	0,001
Níquel	<0,01	<0,01	<0,01	<0,01	<0,01	<0,01	<0,01	<0,01	<0,01	<0,01	<0,01	SM 3500/3111-B	mg/L	0,01
Nitrato	<5,0	8,8	5,5	<5,0	5,5	6,2	<5,0	<5,0	<5,0	5,5	<5,0	SM 4110-B	mg/L	5
Nitrito	<0,05	<0,05	<0,05	<0,05	<0,05	<0,05	<0,05	<0,05	<0,05	<0,05	<0,05	SM 4110-B	mg/L	0,05
pH	7,3	7,6	7,8	7,5	7,7	7,9	7,7	8,20	7,70	7,80	8,10	SM 4500H*-B	upH	0,01
Plomo	<0,02	<0,02	<0,02	<0,02	<0,02	<0,02	<0,02	<0,02	<0,02	<0,02	<0,02	SM 3500/3111-B	mg/L	0,02
Potasio	8	31	16	8,2	43	37,0	7,0	19,0	16,0	43,0	39,0	SM 3500/3111-B	mg/L	1
Residuo Seco	827,1	1172,6	792,8	993,9	2021,9	981,5	1315,7	1090,6	1003,8	2655,8	1663,6	SM 2540-B	mg/L	1
Sodio	101,0	138,0	74,0	246,0	345,0	51,0	243,0	330,0	181,0	789,0	447,0	SM 3500/3111-B	µg/L	10
Sulfato	10,0	199,8	199,8	19,0	799,3	30,0	299,8	199,8	199,8	719,0	399,7	SM 4500 SO4-E	mg/L	1
Sulfuro	<0,1	<0,1	<0,1	<0,1	<0,1	<0,1	<0,1	<0,1	<0,1	<0,1	<0,1	SM 4500 S D	mg/L	0,1
Tolueno	<10,0	<10,0	<10,0	<10,0	<10,0	<10,0	<10,0	<10,0	<10,0	<10,0	<10,0	EPA 8260	µg/L	10
Xileno	<10,0	<10,0	<10,0	<10,0	<10,0	<10,0	<10,0	<10,0	<10,0	<10,0	<10,0	EPA 8260	µg/L	10

Pozo	Dique (F)	Tiro Federal (F)	Puerto (F)	Dique (PM)	Tiro Federal (PM)	Puerto (PM)	Dique (PU)	Tiro Federal (PU)	Puerto (PU)	Metodología		
Parámetros	oc06	oc06	oc06	oc06	oc06	oc06	oc06	oc06	oc06	de análisis	Unidad	LCM
Arsénico	0,23	<0,01	<0,01	0,09	0,17	0,21	0,04	0,21	0,04	SM 3500/3114-C	mg/L	0,01
Benceno	<10,0	<10,0	<10,0	<10,0	<10,0	<10,0	<10,0	<10,0	<10,0	EPA 8260	µg/L	10
Bicarbonato	209,46	1081,79	130,97	482,91	1368,73	540,89	597,88	1495,71	322,08	SM 2320-B	mg/L	0,5
Cadmio	<0,01	<0,01	<0,01	<0,01	<0,01	<0,01	<0,01	<0,01	<0,01	SM 3500/3111-B	mg/L	0,01
Calcio	27,94	40,92	32,93	33,80	323,35	92,51	85,00	450,00	1239,00	SM 3500 Ca-B	mg/L	0,5
Carbonato	<0,5	<0,5	<0,5	<0,5	<0,5	<0,5	<0,5	<0,5	<0,5	SM 2320-B	mg/L	0,5
Cinc	<0,01	<0,01	<0,01	<0,01	<0,01	<0,01	<0,01	<0,01	<0,01	SM 3500/3111-B	mg/L	0,01
Cloruro	192,22	62,07	47,05	117,13	528,60	2502,82	1296,86	3393,82	12013,54	SM 4500 Cl-B	mg/L	1
Cobalto	<0,02	<0,02	<0,02	<0,02	<0,02	<0,02	<0,02	<0,02	<0,02	SM 3500/3111-B	mg/L	0,02
Cobre	<0,02	<0,02	<0,02	<0,02	<0,02	<0,02	<0,02	<0,02	<0,02	SM 3500/3111-B	mg/L	0,02
Cond. Elect.	1600,00	1579,00	921,20	1700,00	5076,00	7238,00	4500,00	13200,00	23650,00	SM 2510-B	µs/cm	0,1
Cromo	<0,02	<0,02	<0,02	<0,02	<0,02	<0,02	<0,02	<0,02	<0,02	SM 3500/3111-B	mg/L	0,02
Etilbenceno	<10,0	<10,0	<10,0	<10,0	<10,0	<10,0	<10,0	<10,0	<10,0	EPA 8260	µg/L	10
Fenoles totales	<0,05	<0,05	<0,05	<0,05	<0,05	<0,05	<0,05	<0,05	<0,05	SM 5530-C	mg/L	0,05
Fluoruro	1,50	0,80	0,30	0,80	1,40	0,90	0,50	1,30	0,80	SM 4110-B	mg/L	0,1
HCT	< 0.2	< 0.2	< 0.2	< 0.2	< 0.2	< 0.2	< 0.2	< 0.2	< 0.2	EPA 8015	mg/L	0,2
Magnesio	9,75	9,95	11,94	115,43	227,87	117,02	98,01	215,74	646,75	SM 3500/3111-B	mg/L	5
Mercurio	<0,001	<0,001	<0,001	<0,001	<0,001	<0,001	<0,001	<0,001	<0,001	SM 3500/3112-B	mg/L	0,001
Níquel	<0,01	<0,01	<0,01	<0,01	<0,01	<0,01	<0,01	<0,01	<0,01	SM 3500/3111-B	mg/L	0,01
Nitrato	<5,0	<5,0	<5,0	<5,0	<5,0	<5,0	<5,0	<5,0	<5,0	SM 4110-B	mg/L	5
Nitrito	<0,05	<0,05	<0,05	<0,05	<0,05	<0,05	<0,05	<0,05	<0,05	SM 4110-B	mg/L	0,05
pH	7,50	7,20	7,10	7,90	7,20	7,00	7,90	7,70	6,80	SM 4500H*-B	upH	0,01
Plomo	<0,02	<0,02	<0,02	<0,02	<0,02	<0,02	<0,02	<0,02	<0,02	SM 3500/3111-B	mg/L	0,02
Potasio	12,00	39,00	11,00	35,60	86,00	119,00	13,50	42,00	57,00	SM 3500/3111-B	mg/L	1
Residuo Seco	1071,43	1450,00	1785,71	1714,29	1928,30	4357,14	3214,29	9428,57	16892,86	SM 2540-B	mg/L	1
Sodio	361,10	428,00	76,00	319,01	1742,00	1765,00	678,50	2415,00	2998,05	SM 3500/3111-B	µg/L	10
Sulfato	279,77	399,67	55,68	319,73	2997,50	799,33	259,78	1199,00	1600,00	SM 4500 SO4-E	mg/L	1
Sulfuro	<0,1	<0,1	<0,1	<0,1	<0,1	<0,1	<0,1	<0,1	<0,1	SM 4500 S D	mg/L	0,1
Tolueno	<10,0	<10,0	<10,0	<10,0	<10,0	<10,0	<10,0	<10,0	<10,0	EPA 8260	µg/L	10
Xileno	<10,0	<10,0	<10,0	<10,0	<10,0	<10,0	<10,0	<10,0	<10,0	EPA 8260	µg/L	10

Pozo	Gas	Astillero	Puerta	Petroken	Parque Rdz.	H Naval	UTN	64 y 128	60 y 145	Vivero	Logística	Metodología		
Parámetros	ab07	ab07	ab07	ab07	ab07	ab07	ab07	ab07	ab07	ab07	ab07	de análisis	Unidad	LCM
Arsénico	< 0,01	< 0,01	< 0,01	< 0,01	< 0,01	< 0,01		< 0,01	< 0,01	< 0,01	< 0,01	SM 3500/3114-C	mg/L	0,01
Benceno	<10,0	<10,0	<10,0	<10,0	<10,0	<10,0		<10,0	<10,0	<10,0	<10,0	EPA 8260	mg/L	10
Bicarbonato	632,4	645,6	443,2	657,7	797,3	937,0		758,9	823,5	708,3	1190,0	SM 2320-B	mg/L	0,5
Cadmio	<0,01	<0,01	<0,01	<0,01	<0,01	<0,01		<0,01	<0,01	<0,01	<0,01	SM 3500/3111-B	mg/L	0,01
Calcio	97,7	254,7	103,2	61,5	198,8	189,9		23,1	50,5	125,1	45,0	SM 3500 Ca-B	mg/L	0,5
Carbonato	< 0,5	< 0,5	< 0,5	< 0,5	< 0,5	0,05		< 0,5	< 0,5	< 0,5	< 0,5	SM 2320-B	mg/L	0,5
Cinc	<0,01	<0,01	<0,01	<0,01	<0,01	0,05		<0,01	<0,01	<0,01	< 0,02	SM 3500/3111-B	mg/L	0,01
Cloruro	201,0	192,0	176,1	283,2	314,1	44,0		87,5	80,8	725,3	47,3	SM 4500 Cl-B	mg/L	1
Cobalto	< 0,02	0,025	< 0,02	< 0,02	0,048	< 0,02		< 0,02	< 0,02	0,028	< 0,02	SM 3500/3111-B	mg/L	0,02
Cobre	< 0,02	< 0,02	< 0,02	< 0,02	< 0,02	< 0,02		< 0,02	< 0,02	< 0,02	< 0,02	SM 3500/3111-B	mg/L	0,02
Cond. Elect.	1284,4	1834,9	1223,1	1545,6	2952,8	1513,9		1684,1	1548,4	4179,0	2564,5	SM 2510-B	µs/cm	0,1
Cromo	< 0,02	< 0,02	< 0,02	< 0,02	< 0,02	< 0,02		< 0,02	< 0,02	< 0,02	< 0,02	SM 3500/3111-B	mg/L	0,02
Etilbenceno	<10,0	<10,0	<10,0	<10,0	<10,0	<10,0		<10,0	<10,0	<10,0	<10,0	EPA 8260	µg/L	10
Fenoles totales	< 0,05	< 0,05	< 0,05	< 0,05	< 0,05	< 0,05		< 0,05	< 0,05	< 0,05	< 0,05	SM 5530-C	mg/L	0,05
Fluoruro	0,8	0,7	0,6	1,7	1,0	1,1		0,1	0,7	1,0	0,9	SM 4110-B	mg/L	0,1
HCT	< 0,2	< 0,2	< 0,2	< 0,2	< 0,2	< 0,2		< 0,2	< 0,2	< 0,2	< 0,2	EPA 8015	mg/L	0,2
Magnesio	35,0	34,7	24,1	10,3	47,1	49,3		6,7	14,2	72,2	26,3	SM 3500/3111-B	mg/L	5
Mercurio	0,0011	0,0033	<0,001	0,0055	0,0077	0,0022		0,0066	<0,001	0,0066	0,0033	SM 3500/3112-B	mg/L	0,001
Níquel	< 0,01	< 0,01	< 0,01	< 0,01	< 0,01	< 0,01		< 0,01	< 0,01	< 0,01	< 0,01	SM 3500/3111-B	mg/L	0,01
Nitrato	< 5	9,7	6,1	< 5	6,1	6,8		< 5	< 5	6,1	< 5	SM 4110-B	mg/L	5
Nitrito	< 0,05	< 0,05	< 0,05	< 0,05	< 0,05	< 0,05		< 0,05	< 0,05	< 0,05	< 0,05	SM 4110-B	mg/L	0,05
pH	7,3	7,6	7,8	7,5	7,7	7,9		8,20	7,70	7,80	8,10	SM 4500H*-B	upH	0,01
Plomo	< 0,02	< 0,02	< 0,02	< 0,02	< 0,02	< 0,02		< 0,02	< 0,02	< 0,02	< 0,02	SM 3500/3111-B	mg/L	0,02
Potasio	8,8	34,1	17,6	9,02	47,3	40,7		20,9	17,6	47,3	42,9	SM 3500/3111-B	mg/L	1
Residuo Seco	917,4	1310,6	873,6	1104,0	2109,1	1081,4		1202,9	1106,0	2985,0	1831,8	SM 2540-B	mg/L	1
Sodio	111,1	151,8	76,8	270,6	276,0	56,1		363,0	199,1	867,9	491,7	SM 3500/3111-B	µg/L	10
Sulfato	11,0	219,8	219,8	20,9	879,3	33,0		219,8	219,8	839,0	439,6	SM 4500 SO4-E	mg/L	1
Sulfuro	< 0,1	< 0,1	< 0,1	< 0,1	< 0,1	< 0,1		< 0,1	< 0,1	< 0,1	< 0,1	SM 4500 S D	mg/L	0,1
Tolueno	<10,0	<10,0	<10,0	<10,0	<10,0	<10,0		<10,0	<10,0	<10,0	<10,0	EPA 8260	µg/L	10
Xileno	<10,0	<10,0	<10,0	<10,0	<10,0	<10,0		<10,0	<10,0	<10,0	<10,0	EPA 8260	µg/L	10

Pozo	Dique (F)	Tiro Federal (F)	Puerto (F)	Dique (PM)	Tiro Federal (PM)	Puerto (PM)	Dique (PU)	Tiro Federal (PU)	Puerto (PU)	Metodología		
Parámetros	ab07	ab07	ab07	ab07	ab07	ab07	ab07	ab07	ab07	de análisis	Unidad	LCM
Arsénico	0,32	< 0,01	< 0,01	< 0,01	0,04	0,03	0,01	< 0,01	< 0,01	SM 3500/3114-C	mg/L	0,01
Benceno	<10,0	<10,0	<10,0	<10,0	<10,0	<10,0	<10,0	<10,0	<10,0	EPA 8260	mg/L	10
Bicarbonato	292,94	896,70	190,96	656,87	617,88	790,84	483,90	1473,71	275,95	SM 2320-B	mg/L	0,5
Cadmio	<0,01	<0,01	<0,01	<0,01	<0,01	<0,01	<0,01	<0,01	<0,01	SM 3500/3111-B	mg/L	0,01
Calcio	39,12	57,29	47,90	30,94	40,92	50,90	102,79	446,60	1317,37	SM 3500 Ca-B	mg/L	0,5
Carbonato	<0,5	<0,5	<0,5	<0,5	<0,5	<0,5	<0,5	<0,5	<0,5	SM 2320-B	mg/L	0,5
Cinc	<0,01	<0,01	<0,01	<0,01	<0,01	<0,01	<0,01	<0,01	<0,01	SM 3500/3111-B	mg/L	0,01
Cloruro	179,28	56,09	43,67	119,13	548,62	2412,72	1266,83	3103,50	11512,97	SM 4500 Cl-B	mg/L	1
Cobalto	<0,02	<0,02	<0,02	<0,02	<0,02	<0,02	<0,02	<0,02	<0,02	SM 3500/3111-B	mg/L	0,02
Cobre	<0,02	<0,02	<0,02	<0,02	<0,02	<0,02	<0,02	<0,02	<0,02	SM 3500/3111-B	mg/L	0,02
Cond. Elect.	1650,00	1700,00	1010,00	2000,00	6300,00	9100,00	5700,00	15000,00	21000,00	SM 2510-B	µs/cm	0,1
Cromo	<0,02	<0,02	<0,02	<0,02	<0,02	<0,02	<0,02	<0,02	<0,02	SM 3500/3111-B	mg/L	0,02
Etilbenceno	<10,0	<10,0	<10,0	<10,0	<10,0	<10,0	<10,0	<10,0	<10,0	EPA 8260	µg/L	10
Fenoles totales	<0,05	<0,05	<0,05	<0,05	<0,05	<0,05	<0,05	<0,05	<0,05	SM 5530-C	mg/L	0,05
Fluoruro	2,10	1,11	0,43	0,93	0,98	0,58	0,61	1,20	0,75	SM 4110-B	mg/L	0,1
HCT	< 0.2	< 0.2	< 0.2	< 0.2	< 0.2	< 0.2	< 0.2	< 0.2	< 0.2	EPA 8015	mg/L	0,2
Magnesio	13,65	13,93	17,41	14,93	47,76	112,08	97,52	202,00	874,66	SM 3500/3111-B	mg/L	5
Mercurio	<0,001	<0,001	<0,001	<0,001	<0,001	<0,001	<0,001	<0,001	<0,001	SM 3500/3112-B	mg/L	0,001
Níquel	<0,01	<0,01	<0,01	<0,01	<0,01	<0,01	<0,01	<0,01	<0,01	SM 3500/3111-B	mg/L	0,01
Nitrato	<5,0	<5,0	<5,0	<5,0	<5,0	<5,0	<5,0	<5,0	<5,0	SM 4110-B	mg/L	5
Nitrito	<0,05	<0,05	<0,05	<0,05	<0,05	<0,05	<0,05	<0,05	<0,05	SM 4110-B	mg/L	0,05
pH	7,30	7,20	7,10	7,60	7,40	7,30	7,20	6,80	6,80	SM 4500H*-B	upH	0,01
Plomo	<0,02	<0,02	<0,02	<0,02	<0,02	<0,02	<0,02	<0,02	<0,02	SM 3500/3111-B	mg/L	0,02
Potasio	16,80	54,60	16,00	15,00	49,00	84,00	43,00	100,00	152,00	SM 3500/3111-B	mg/L	1
Residuo Seco	1214,29	1214,29	714,29	1428,57	4500,00	6500,00	4071,43	10714,29	15000,00	SM 2540-B	mg/L	1
Sodio	367,31	363,17	111,00	336,00	1100,00	1530,00	632,00	2420,00	3870,00	SM 3500/3111-B	µg/L	10
Sulfato	268,58	86,73	67,94	449,63	1448,79	729,79	424,65	1301,76	1548,71	SM 4500 SO4-E	mg/L	1
Sulfuro	<0,1	<0,1	<0,1	<0,1	<0,1	<0,1	<0,1	<0,1	<0,1	SM 4500 S D	mg/L	0,1
Tolueno	<10,0	<10,0	<10,0	<10,0	<10,0	<10,0	<10,0	<10,0	<10,0	EPA 8260	µg/L	10
Xileno	<10,0	<10,0	<10,0	<10,0	<10,0	<10,0	<10,0	<10,0	<10,0	EPA 8260	µg/L	10

Pozo	Gas	Astillero	Puerta	Petroken	Parque Rdz.	H Naval	utn	64 y 128	60 y 145	Vivero	Logística	Metodología		
Parámetros	oc07	oc07	oc07	oc07	oc07	oc07	oc07	oc07	oc07	oc07	oc07	de análisis	Unidad	LCM
Arsénico	0,02	<0,01	<0,01	<0,01	<0,01	0,060	<0,01	0,020	<0,01	<0,01	0,010	SM 3500/3114-C	mg/L	0,01
Benceno	<10,0	<10,0	<10,0	<10,0	<10,0	<10,0	<10,0	<10,0	<10,0	<10,0	<10,0	EPA 8260	mg/L	10
Bicarbonato	522,9	567,3	316,9	573,4	373,9	504,9	488,9	549,9	846,8	521,9	910,8	SM 2320-B	mg/L	0,5
Cadmio	<0,01	<0,01	<0,01	<0,01	<0,01	<0,01	<0,01	<0,01	<0,01	<0,01	<0,01	SM 3500/3111-B	mg/L	0,01
Calcio	75,8	217,0	66,9	49,9	179,0	96,8	75,8	15,0	52,9	51,9	80,8	SM 3500 Ca-B	mg/L	0,5
Carbonato	<0,5	<0,5	<0,5	<0,5	<0,5	<0,5	<0,5	<0,5	<0,5	<0,5	<0,5	SM 2320-B	mg/L	0,5
Cinc	0,050	0,030	0,020	0,020	0,020	0,12	0,03	<0,01	0,02	<0,01	0,03	SM 3500/3111-B	mg/L	0,01
Cloruro	191,0	182,4	167,3	269,0	298,4	41,8	43,0	83,1	76,8	689,1	44,9	SM 4500 Cl-B	mg/L	1
Cobalto	<0,02	<0,02	<0,02	<0,02	<0,02	<0,02	<0,02	<0,02	<0,02	<0,02	<0,02	SM 3500/3111-B	mg/L	0,02
Cobre	<0,02	<0,02	<0,02	<0,02	<0,02	<0,02	<0,02	<0,02	<0,02	<0,02	<0,02	SM 3500/3111-B	mg/L	0,02
Cond. Elect.	1158,9	1425,8	790,4	1409,2	2219,2	821,4	853,3	1286,7	1518,7	3127,4	1901,1	SM 2510-B	µs/cm	0,1
Cromo	<0,02	<0,02	<0,02	<0,02	<0,02	<0,02	<0,02	<0,02	<0,02	<0,02	<0,02	SM 3500/3111-B	mg/L	0,02
Etilbenceno	<10,0	<10,0	<10,0	<10,0	<10,0	<10,0	<10,0	<10,0	<10,0	<10,0	<10,0	EPA 8260	µg/L	10
Fenoles totales	<0,05	<0,05	<0,05	<0,05	<0,05	<0,05	<0,05	<0,05	<0,05	<0,05	<0,02	SM 5530-C	mg/L	0,05
Fluoruro	0,2	<0,1	<0,1	0,3	0,4	0,6	<0,1	<0,1	<0,1	0,5	0,4	SM 4110-B	mg/L	0,1
HCT	< 0.2	< 0.2	< 0.2	< 0.2	< 0.2	< 0.2	< 0.2	< 0.2	< 0.2	< 0.2	< 0.2	EPA 8015	mg/L	0,2
Magnesio	32,8	23,7	15,9	12,9	7,0	33,8	29,9	8,0	25,9	47,8	42,8	SM 3500/3111-B	mg/L	5
Mercurio	<0,001	<0,001	<0,001	<0,001	<0,001	<0,001	<0,001	<0,001	<0,001	<0,001	<0,001	SM 3500/3112-B	mg/L	0,001
Níquel	<0,01	<0,01	<0,01	<0,01	<0,01	<0,01	<0,01	<0,01	<0,01	<0,01	<0,01	SM 3500/3111-B	mg/L	0,01
Nitrato	<5,0	<5,0	<5,0	12,0	18,0	<5,0	<5,0	48,0	<5,0	31,0	<5,0	SM 4110-B	mg/L	5
Nitrito	<0,05	<0,05	<0,05	<0,05	<0,05	<0,05	<0,05	<0,05	<0,05	<0,05	<0,05	SM 4110-B	mg/L	0,05
pH	6,6	6,5	6,8	6,8	7,2	6,9	6,8	7,60	7,00	6,80	7,00	SM 4500H*-B	upH	0,01
Plomo	0,02	0,04	<0,02	<0,02	0,02	0,02	0,02	0,02	0,02	0,02	0,02	SM 3500/3111-B	mg/L	0,02
Potasio	7	8	9	6	13	20,0	4,0	14,0	12,0	24,0	25,0	SM 3500/3111-B	mg/L	1
Residuo Seco	827,8	1018,4	564,6	1006,6	1585,1	586,7	609,5	919,1	1084,8	2233,8	1357,9	SM 2540-B	mg/L	1
Sodio	135,0	92,0	63,0	253,0	253,0	19,0	60,0	302,0	216,0	526,0	296,0	SM 3500/3111-B	µg/L	10
Sulfato	8,0	87,9	32,0	23,0	744,0	11,0	37,0	137,9	119,9	729,6	259,8	SM 4500 SO4-E	mg/L	1
Sulfuro	<0,1	<0,1	<0,1	<0,1	<0,1	<0,1	<0,1	<0,1	<0,1	<0,1	<0,1	SM 4500 S D	mg/L	0,1
Tolueno	<10,0	<10,0	<10,0	<10,0	<10,0	<10,0	<10,0	<10,0	<10,0	<10,0	<10,0	EPA 8260	µg/L	10
Xileno	<10,0	<10,0	<10,0	<10,0	<10,0	<10,0	<10,0	<10,0	<10,0	<10,0	<10,0	EPA 8260	µg/L	10

Pozo	Dique (F)	Tiro Federal (F)	Puerto (F)	Dique (PM)	Tiro Federal (PM)	Puerto (PM)	Dique (PU)	Tiro Federal (PU)	Puerto (PU)	Metodología		
Parámetros	oc07	oc07	oc07	oc07	oc07	oc07	oc07	oc07	oc07	de análisis	Unidad	LCM
Arsénico	0,15	< 0,01	< 0,01	0,02	0,04	< 0,01	0,01	< 0,01	< 0,01	SM 3500/3114-C	mg/L	0,01
Benceno	<10,0	<10,0	<10,0	<10,0	<10,0	<10,0	<10,0	<10,0	<10,0	EPA 8260	mg/L	10
Bicarbonato	137,68	982,10	211,67	664,87	1567,69	1175,77	587,88	1175,77	391,92	SM 2320-B	mg/L	0,5
Cadmio	<0,01	<0,01	<0,01	<0,01	<0,01	<0,01	<0,01	<0,01	<0,01	SM 3500/3111-B	mg/L	0,01
Calcio	18,39	26,92	22,51	26,95	45,91	31,94	108,78	524,40	1240,52	SM 3500 Ca-B	mg/L	0,5
Carbonato	<0,5	<0,5	<0,5	<0,5	<0,5	<0,5	<0,5	<0,5	<0,5	SM 2320-B	mg/L	0,5
Cinc	<0,01	<0,01	<0,01	<0,01	<0,01	<0,01	<0,01	<0,01	<0,01	SM 3500/3111-B	mg/L	0,01
Cloruro	185,21	56,06	59,57	148,39	904,90	2222,30	1147,72	3370,37	8005,02	SM 4500 Cl-B	mg/L	1
Cobalto	<0,02	<0,02	<0,02	<0,02	<0,02	<0,02	<0,02	<0,02	<0,02	SM 3500/3111-B	mg/L	0,02
Cobre	<0,02	<0,02	<0,02	<0,02	<0,02	<0,02	<0,02	<0,02	<0,02	SM 3500/3111-B	mg/L	0,02
Cond. Elect.	1500,00	2030,00	2500,00	2400,00	3300,00	6100,00	4500,00	13500,00	22500,00	SM 2510-B	µs/cm	0,1
Cromo	<0,02	<0,02	<0,02	<0,02	<0,02	<0,02	<0,02	<0,02	<0,02	SM 3500/3111-B	mg/L	0,02
Etilbenceno	<10,0	<10,0	<10,0	<10,0	<10,0	<10,0	<10,0	<10,0	<10,0	EPA 8260	µg/L	10
Fenoles totales	<0,05	<0,05	<0,05	<0,05	<0,05	<0,05	<0,05	<0,05	<0,05	SM 5530-C	mg/L	0,05
Fluoruro	< 0,1	< 0,1	< 0,1	< 0,1	0,60	1,00	0,40	0,90	0,40	SM 4110-B	mg/L	0,1
HCT	< 0.2	< 0.2	< 0.2	< 0.2	< 0.2	< 0.2	< 0.2	< 0.2	< 0.2	EPA 8015	mg/L	0,2
Magnesio	6,42	6,55	8,18	15,92	59,70	106,27	92,08	236,83	777,15	SM 3500/3111-B	mg/L	5
Mercurio	<0,001	<0,001	<0,001	<0,001	<0,001	<0,001	<0,001	<0,001	<0,001	SM 3500/3112-B	mg/L	0,001
Níquel	<0,01	<0,01	<0,01	<0,01	<0,01	<0,01	<0,01	<0,01	<0,01	SM 3500/3111-B	mg/L	0,01
Nitrato	<5,0	<5,0	6,00	<5,0	<5,0	<5,0	<5,0	<5,0	<5,0	SM 4110-B	mg/L	5
Nitrito	<0,05	<0,05	<0,05	<0,05	<0,05	<0,05	<0,05	<0,05	<0,05	SM 4110-B	mg/L	0,05
pH	7.9	7.7	7.35	7.40	7.10	7.30	6.90	6.60	6.60	SM 4500H*-B	upH	0,01
Plomo	<0,02	<0,02	<0,02	<0,02	<0,02	<0,02	<0,02	<0,02	<0,02	SM 3500/3111-B	mg/L	0,02
Potasio	7,90	25,66	7,52	11,00	30,00	39,00	25,00	56,00	82,00	SM 3500/3111-B	mg/L	1
Residuo Seco	1071,43	1450,00	1785,71	1714,29	2357,14	4357,14	3214,29	9642,86	16071,43	SM 2540-B	mg/L	1
Sodio	388,88	402,50	52,17	303,00	1171,00	1407,00	692,00	2590,00	3138,00	SM 3500/3111-B	µg/L	10
Sulfato	249,12	153,87	48,46	259,78	1498,75	579,92	255,79	1680,00	1598,67	SM 4500 SO4-E	mg/L	1
Sulfuro	<0,1	<0,1	<0,1	<0,1	<0,1	<0,1	<0,1	<0,1	<0,1	SM 4500 S D	mg/L	0,1
Tolueno	<10,0	<10,0	<10,0	<10,0	<10,0	<10,0	<10,0	<10,0	<10,0	EPA 8260	µg/L	10
Xileno	<10,0	<10,0	<10,0	<10,0	<10,0	<10,0	<10,0	<10,0	<10,0	EPA 8260	µg/L	10

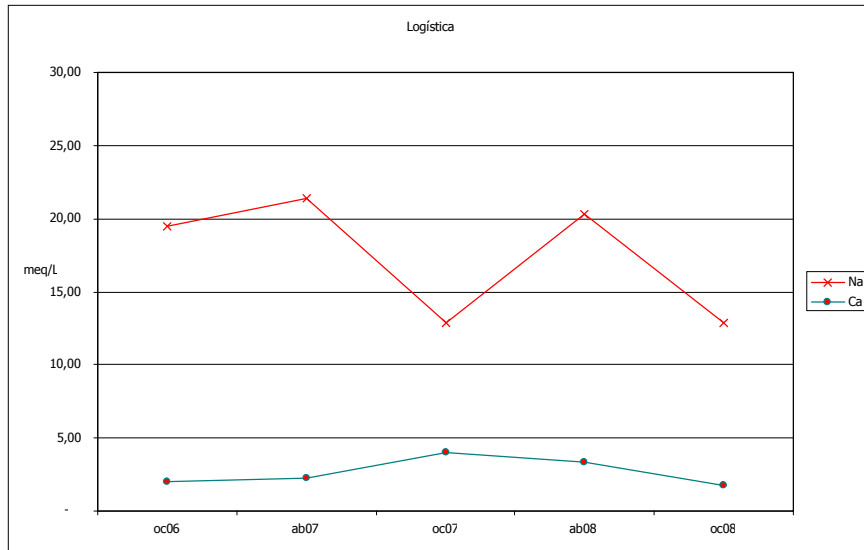
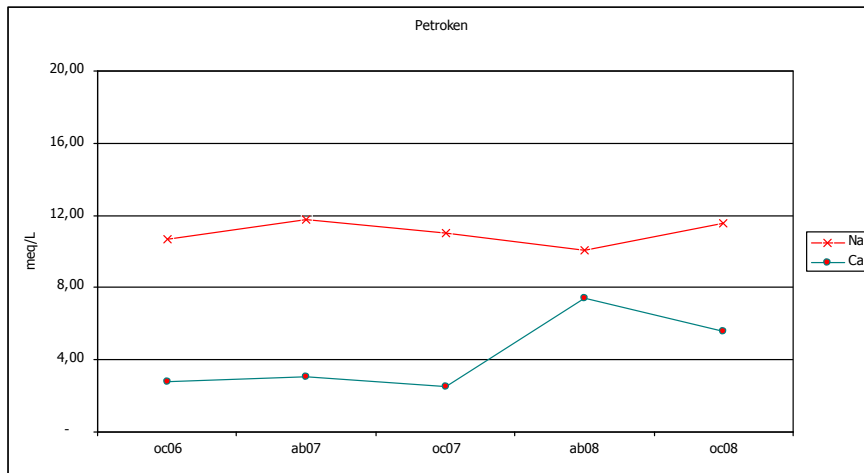
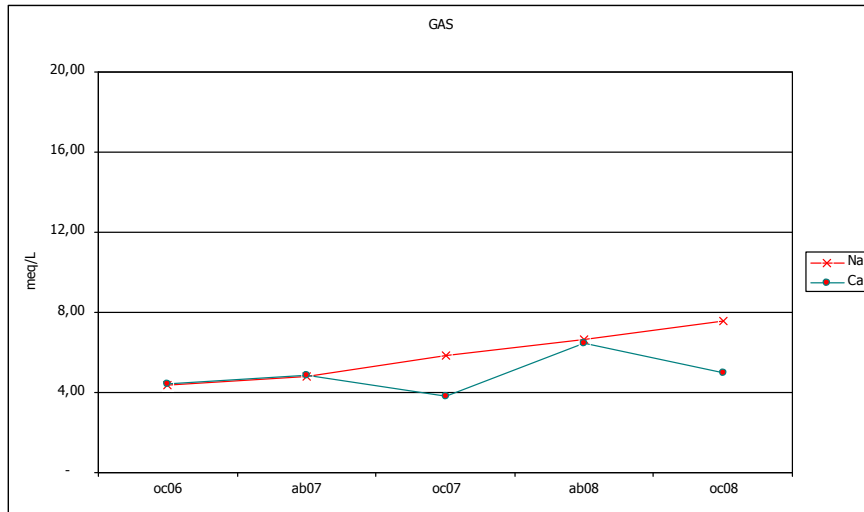
Pozo	Gas	Astillero	Puerta	Petroken	Parque Rdz.	H Naval	UTN	64 y 128	60 y 145	Vivero	Logística	Metodología		
Parámetros	ab08	ab08	ab08	ab08	ab08	ab08	ab08	ab08	ab08	ab08	ab08	de análisis	Unidad	LCM
Arsénico	0,013	<0,01	<0,01	0,063	0,019	0,070	<0,01	0,012	<0,01	<0,01	0,018	SM 3500/3114-C	mg/L	0,01
Benceno	<10,0	<10,0	<10,0	<10,0	<10,0	<10,0	<10,0	<10,0	<10,0	<10,0	<10,0	EPA 8260	mg/L	10
Bicarbonato	644,4	701,5	293,1	518,4	565,7	811,5	642,0	603,2	743,6	835,8	1201,6	SM 2320-B	mg/L	0,5
Cadmio	<0,01	<0,01	<0,01	<0,01	<0,01	<0,01	<0,01	<0,01	<0,01	0,03	<0,01	SM 3500/3111-B	mg/L	0,01
Calcio	129,0	258,0	86,0	148,4	187,2	167,5	159,6	62,4	66,1	146,7	66,2	SM 3500 Ca-B	mg/L	0,5
Carbonato	<0,5	<0,5	<0,5	<0,5	<0,5	<0,5	<0,5	<0,5	<0,5	<0,5	<0,5	SM 2320-B	mg/L	0,5
Cinc	<0,01	<0,01	<0,01	<0,01	0,010	0,20	0,01	<0,01	<0,01	<0,01	<0,01	SM 3500/3111-B	mg/L	0,01
Cloruro	205,6	196,4	159,8	289,7	321,4	45,1	46,3	89,5	82,7	742,0	48,4	SM 4500 Cl-B	mg/L	1
Cobalto	<0,02	<0,02	<0,02	<0,02	<0,02	<0,02	<0,02	<0,02	<0,02	0,04	<0,02	SM 3500/3111-B	mg/L	0,02
Cobre	<0,02	<0,02	<0,02	<0,02	<0,02	<0,02	<0,02	<0,02	<0,02	<0,02	<0,02	SM 3500/3111-B	mg/L	0,02
Cond. Elect.	1433,1	1650,6	865,6	1644,4	2750,1	1309,4	1170,1	1603,5	1577,7	3749,6	2464,6	SM 2510-B	µs/cm	0,1
Cromo	<0,02	<0,02	<0,02	<0,02	<0,02	<0,02	<0,02	<0,02	<0,02	<0,02	<0,02	SM 3500/3111-B	mg/L	0,02
Etilbenceno	<10,0	<10,0	<10,0	<10,0	<10,0	<10,0	<10,0	<10,0	<10,0	<10,0	<10,0	EPA 8260	µg/L	10
Fenoles totales	<0,05	<0,05	<0,05	<0,05	<0,05	<0,05	<0,05	<0,05	<0,05	<0,05	<0,05	SM 5530-C	mg/L	0,05
Fluoruro	0,6	0,3	0,4	0,8	0,3	0,8	0,5	0,9	0,8	0,7	0,3	SM 4110-B	mg/L	0,1
HCT	< 0.2	< 0.2	< 0.2	< 0.2	< 0.2	< 0.2	< 0.2	< 0.2	< 0.2	< 0.2	< 0.2	EPA 8015	mg/L	0,2
Magnesio	38,8	12,3	15,5	26,1	13,3	46,6	39,2	22,5	26,3	114,0	32,1	SM 3500/3111-B	mg/L	5
Mercurio	<0,001	<0,001	<0,001	<0,001	<0,001	<0,001	<0,001	<0,001	<0,001	<0,001	<0,001	SM 3500/3112-B	mg/L	0,001
Níquel	<0,01	<0,01	<0,01	0,01	0,01	0,01	0,01	0,01	<0,01	0,03	<0,01	SM 3500/3111-B	mg/L	0,01
Nitrato	<5,0	<5,0	<5,0	<5,0	<5,0	<5,0	<5,0	8,2	<5,0	8,2	8,2	SM 4110-B	mg/L	5
Nitrito	<0,05	<0,05	<0,05	<0,05	<0,05	<0,05	<0,05	<0,05	<0,05	<0,05	<0,05	SM 4110-B	mg/L	0,05
pH	7,98	7,03	8,01	7,09	7,15	6,81	6,85	7,40	7,22	7,74	7,06	SM 4500H*-B	upH	0,01
Plomo	<0,02	0,07	<0,02	0,02	0,03	0,02	0,03	0,02	0,02	0,09	0,03	SM 3500/3111-B	mg/L	0,02
Potasio	4,3	6,5	9,2	7,8	15,7	24,0	2,8	12,7	14,0	31,2	28,2	SM 3500/3111-B	mg/L	1
Residuo Seco	915,0	556,0	810,0	1435,0	2112,0	1499,0	955,0	1305,0	1040,0	2841,2	2045,0	SM 2540-B	mg/L	1
Sodio	153,0	126,0	78,2	232,2	407,2	40,5	49,1	294,0	190,9	652,0	467,2	SM 3500/3111-B	µg/L	10
Sulfato	15,1	73,0	81,4	114,4	792,0	17,2	54,6	284,8	277,6	484,6	321,8	SM 4500 SO4-E	mg/L	1
Sulfuro	<0,1	<0,1	<0,1	<0,1	<0,1	<0,1	<0,1	<0,1	<0,1	<0,1	<0,1	SM 4500 S D	mg/L	0,1
Tolueno	<10,0	<10,0	<10,0	<10,0	<10,0	<10,0	<10,0	<10,0	<10,0	<10,0	<10,0	EPA 8260	µg/L	10
Xileno	<10,0	<10,0	<10,0	<10,0	<10,0	<10,0	<10,0	<10,0	<10,0	<10,0	<10,0	EPA 8260	µg/L	10

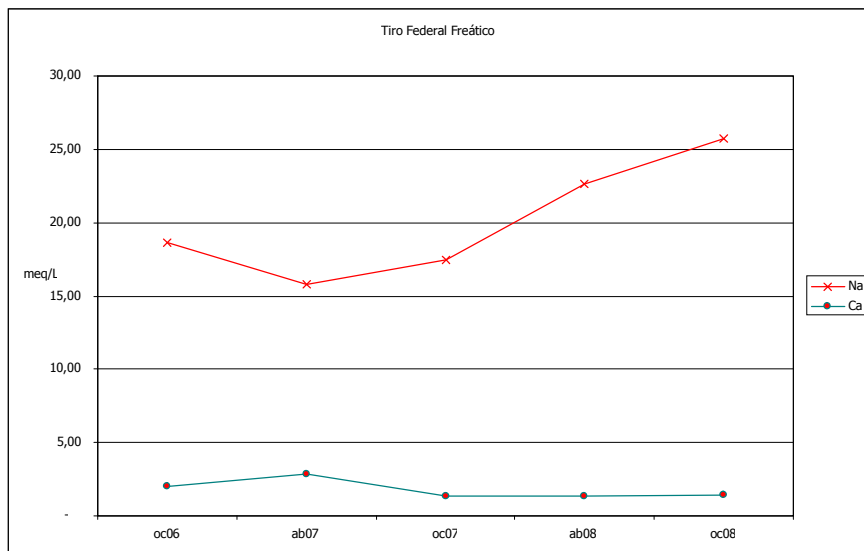
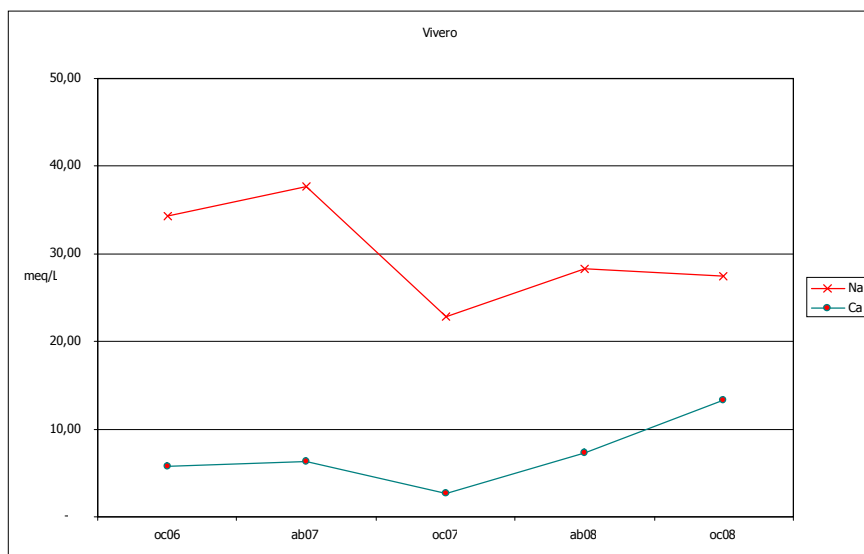
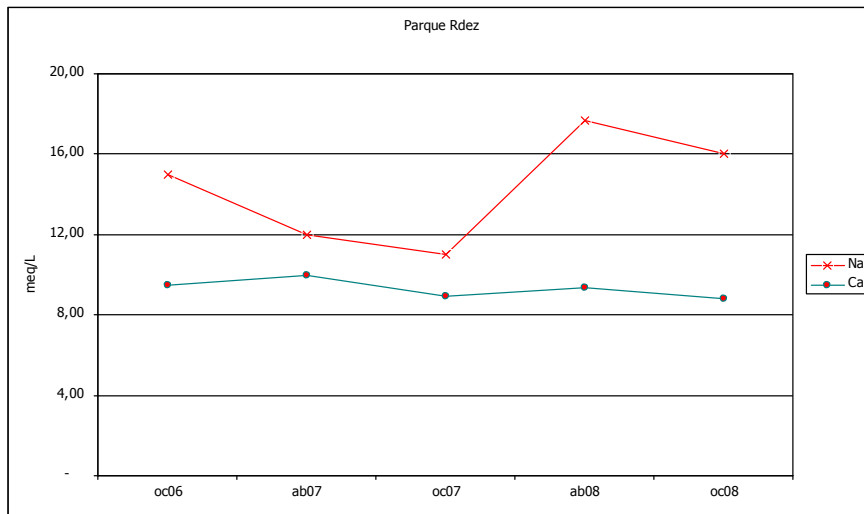
Pozo	Dique (F)	Tiro Federal (F)	Puerto (F)	Dique (PM)	Tiro Federal (PM)	Puerto (PM)	Dique (PU)	Tiro Federal (PU)	Puerto (PU)	Metodología		
Parámetros	ab08	ab08	ab08	ab08	ab08	ab08	ab08	ab08	ab08	de análisis	Unidad	LCM
Arsénico	0,10	< 0,01	< 0,01	0,02	0,02	0,02	0,01	< 0,01	< 0,01	SM 3500/3114-C	mg/L	0,01
Benceno	<10,0	<10,0	<10,0	<10,0	<10,0	<10,0	<10,0	<10,0	<10,0	EPA 8260	mg/L	10
Bicarbonato	344,04	1463,41	283,04	518,20	1370,03	653,27	399,12	1221,16	136,97	SM 2320-B	mg/L	0,5
Cadmio	<0,01	<0,01	<0,01	<0,01	<0,01	<0,01	<0,01	<0,01	<0,01	SM 3500/3111-B	mg/L	0,01
Calcio	49,20	26,25	66,87	52,69	84,63	92,12	165,67	436,00	1275,60	SM 3500 Ca-B	mg/L	0,5
Carbonato	<0,5	<0,5	<0,5	<0,5	<0,5	<0,5	<0,5	<0,5	<0,5	SM 2320-B	mg/L	0,5
Cinc	<0,01	<0,01	<0,01	<0,01	<0,01	<0,01	<0,01	<0,01	<0,01	SM 3500/3111-B	mg/L	0,01
Cloruro	178,20	82,99	38,24	92,70	586,96	2445,18	1360,72	3382,61	10208,50	SM 4500 Cl-B	mg/L	1
Cobalto	<0,02	<0,02	<0,02	<0,02	<0,02	<0,02	<0,02	<0,02	<0,02	SM 3500/3111-B	mg/L	0,02
Cobre	<0,02	<0,02	<0,02	<0,02	<0,02	<0,02	<0,02	<0,02	<0,02	SM 3500/3111-B	mg/L	0,02
Cond. Elect.	2100,00	3140,00	1103,00	2266,67	11100,00	7100,00	4900,00	13900,00	22383,33	SM 2510-B	µs/cm	0,1
Cromo	<0,02	<0,02	<0,02	<0,02	<0,02	<0,02	<0,02	<0,02	<0,02	SM 3500/3111-B	mg/L	0,02
Etilbenceno	<10,0	<10,0	<10,0	<10,0	<10,0	<10,0	<10,0	<10,0	<10,0	EPA 8260	µg/L	10
Fenoles totales	<0,05	<0,05	<0,05	<0,05	<0,05	<0,05	<0,05	<0,05	<0,05	SM 5530-C	mg/L	0,05
Fluoruro	0,50	0,60	1,20	0,40	0,90	0,60	0,50	0,90	0,60	SM 4110-B	mg/L	0,1
HCT	< 0,2	< 0,2	< 0,2	< 0,2	< 0,2	< 0,2	< 0,2	< 0,2	< 0,2	EPA 8015	mg/L	0,2
Magnesio	11,94	27,66	37,12	21,39	84,48	123,05	79,38	289,66	340,31	SM 3500/3111-B	mg/L	5
Mercurio	<0,001	<0,001	<0,001	<0,001	<0,001	<0,001	<0,001	<0,001	<0,001	SM 3500/3112-B	mg/L	0,001
Níquel	<0,01	<0,01	<0,01	<0,01	<0,01	<0,01	<0,01	<0,01	<0,01	SM 3500/3111-B	mg/L	0,01
Nitrato	34,50	<5,0	<5,0	<5,0	<5,0	<5,0	<5,0	<5,0	<5,0	SM 4110-B	mg/L	5
Nitrito	<0,05	<0,05	<0,05	<0,05	<0,05	<0,05	<0,05	<0,05	<0,05	SM 4110-B	mg/L	0,05
pH	7,20	7,37	7,18	7,53	7,30	8,00	7,00	7,00	6,90	SM 4500H*-B	upH	0,01
Plomo	<0,02	<0,02	<0,02	<0,02	<0,02	<0,02	<0,02	<0,02	<0,02	SM 3500/3111-B	mg/L	0,02
Potasio	12,23	39,75	11,51	20,53	27,00	80,67	27,17	66,00	103,00	SM 3500/3111-B	mg/L	1
Residuo Seco	1119,05	1371,43	1428,57	1619,05	7928,57	5071,43	3500,00	9928,57	15988,10	SM 2540-B	mg/L	1
Sodio	430,00	520,03	87,80	371,00	1354,00	1414,00	806,00	2410,00	2784,00	SM 3500/3111-B	µg/L	10
Sulfato	327,13	262,28	135,29	384,88	1370,76	1315,10	409,44	1296,00	3510,07	SM 4500 SO4-E	mg/L	1
Sulfuro	<0,1	<0,1	<0,1	<0,1	<0,1	<0,1	<0,1	<0,1	<0,1	SM 4500 S D	mg/L	0,1
Tolueno	<10,0	<10,0	<10,0	<10,0	<10,0	<10,0	<10,0	<10,0	<10,0	EPA 8260	µg/L	10
Xileno	<10,0	<10,0	<10,0	<10,0	<10,0	<10,0	<10,0	<10,0	<10,0	EPA 8260	µg/L	10

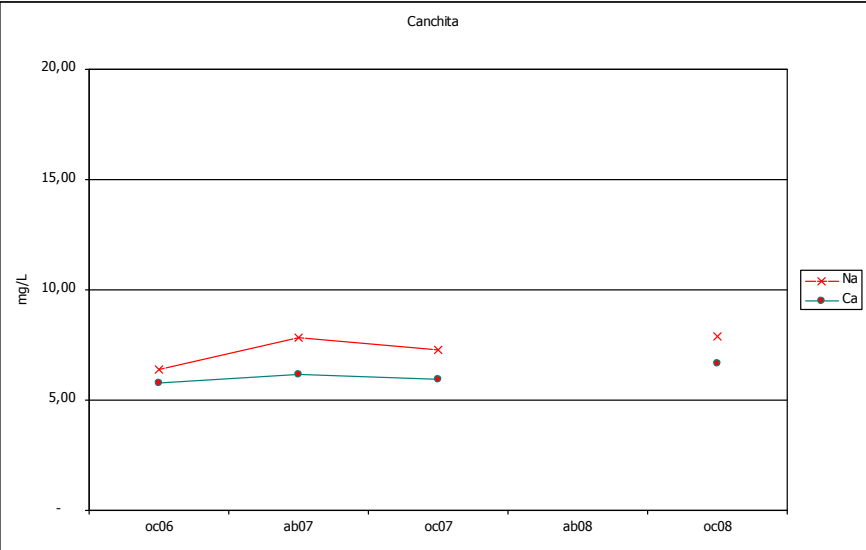
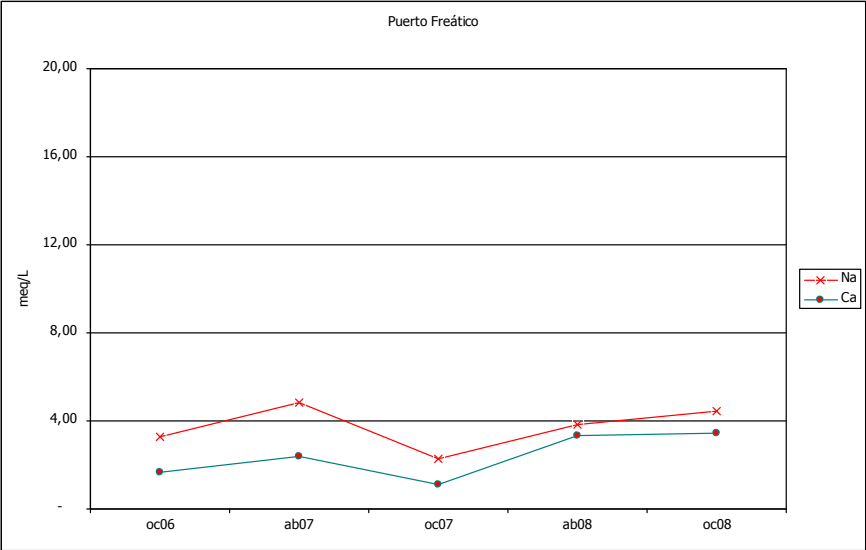
Pozo	Gas	Astillero	Puerta	Petroken	Parque Rdz.	H Naval	UTN	64 y 128	60 y 145	Vivero	Logística	Metodología		
Parámetros	oc08	oc08	oc08	oc08	oc08	oc08	oc08	oc08	oc08	oc08	oc08	de análisis	Unidad	LCM
Arsénico	0,011	<0,01	0,013	0,317	0,017	0,073	<0,01	0,015	<0,01	0,015	0,026	SM 3500/3114-C	mg/L	0,01
Benceno	<10,0	<10,0	<10,0	<10,0	<10,0	<10,0	<10,0	<10,0	<10,0	<10,0	<10,0	EPA 8260	mg/L	10
Bicarbonato	485,6	637,5	309,1	547,4	662,2	644,5	397,3	432,6	783,9	1297,9	856,5	SM 2320-B	mg/L	0,5
Cadmio	<0,01	<0,01	<0,01	<0,01	<0,01	<0,01	<0,01	<0,01	<0,01	0,03	<0,01	SM 3500/3111-B	mg/L	0,01
Calcio	100,0	235,8	97,7	111,4	176,7	143,6	127,4	19,2	69,2	266,3	35,1	SM 3500 Ca-B	mg/L	0,5
Carbonato	<0,5	<0,5	<0,5	<0,5	<0,5	<0,5	<0,5	<0,5	<0,5	<0,5	<0,5	SM 2320-B	mg/L	0,5
Cinc	<0,01	<0,01	<0,01	<0,01	0,010	0,20	0,01	<0,01	<0,01	<0,01	<0,01	SM 3500/3111-B	mg/L	0,01
Cloruro	180,5	194,8	142,0	284,0	303,5	17,0	71,5	182,3	64,4	1158,2	39,3	SM 4500 Cl-B	mg/L	1
Cobalto	<0,02	<0,02	<0,02	<0,02	<0,02	<0,02	<0,02	<0,02	<0,02	0,04	<0,02	SM 3500/3111-B	mg/L	0,02
Cobre	<0,02	<0,02	<0,02	<0,02	<0,02	<0,02	<0,02	<0,02	<0,02	<0,02	<0,02	SM 3500/3111-B	mg/L	0,02
Cond. Elect.	1259,5	1557,3	923,1	1651,3	2635,3	1178,5	1068,5	1588,1	1626,8	5074,8	1914,3	SM 2510-B	µs/cm	0,1
Cromo	<0,02	<0,02	<0,02	<0,02	<0,02	<0,02	<0,02	<0,02	<0,02	<0,02	<0,02	SM 3500/3111-B	mg/L	0,02
Etilbenceno	<10,0	<10,0	<10,0	<10,0	<10,0	<10,0	<10,0	<10,0	<10,0	<10,0	<10,0	EPA 8260	µg/L	10
Fenoles totales	<0,05	<0,05	<0,05	<0,05	<0,05	<0,05	<0,05	<0,05	<0,05	<0,05	<0,05	SM 5530-C	mg/L	0,05
Fluoruro	0,3	<0,1	0,4	0,9	0,2	<0,1	0,3	0,3	0,5	0,6	<0,1	SM 4110-B	mg/L	0,1
HCT	< 0.2	< 0.2	< 0.2	< 0.2	< 0.2	< 0.2	< 0.2	< 0.2	< 0.2	< 0.2	< 0.2	EPA 8015	mg/L	0,2
Magnesio	37,8	12,0	19,7	46,6	56,4	51,4	34,6	8,9	38,1	181,2	23,4	SM 3500/3111-B	mg/L	5
Mercurio	<0,001	<0,001	<0,001	<0,001	<0,001	<0,001	<0,001	<0,001	<0,001	<0,001	<0,001	SM 3500/3112-B	mg/L	0,001
Níquel	<0,01	<0,01	<0,01	0,01	0,01	0,01	0,01	0,01	<0,01	0,03	<0,01	SM 3500/3111-B	mg/L	0,01
Nitrato	<5,0	<5,0	<5,0	<5,0	<5,0	<5,0	<5,0	8,2	<5,0	8,2	8,2	SM 4110-B	mg/L	5
Nitrito	<0,05	<0,05	<0,05	<0,05	<0,05	<0,05	<0,05	<0,05	<0,05	<0,05	<0,05	SM 4110-B	mg/L	0,05
pH	6,72	7,08	7,1	6,93	7,22	7,06	6,92	7,86	7,30	6,99	7,08	SM 4500H*-B	upH	0,01
Plomo	<0,02	0,09	<0,02	<0,02	<0,02	<0,02	<0,02	<0,02	<0,02	<0,02	<0,02	SM 3500/3111-B	mg/L	0,02
Potasio	7,3	10,3	14,8	16,5	40,1	32,1	3,2	14,0	28,2	53,7	32,0	SM 3500/3111-B	mg/L	1
Residuo Seco	1110,0	890,0	590,0	2840,0	6820,0	920,0	970,0	1470,0	1590,0	8430,0	1860,0	SM 2540-B	mg/L	1
Sodio	174,1	129,3	85,2	265,7	368,0	57,9	83,6	390,7	209,3	631,1	296,7	SM 3500/3111-B	µg/L	10
Sulfato	41,7	76,1	103,3	64,7	592,4	78,6	162,8	276,5	249,6	526,5	444,6	SM 4500 SO4-E	mg/L	1
Sulfuro	<0,1	<0,1	<0,1	<0,1	<0,1	<0,1	<0,1	<0,1	<0,1	<0,1	<0,1	SM 4500 S D	mg/L	0,1
Tolueno	<10,0	<10,0	<10,0	<10,0	<10,0	<10,0	<10,0	<10,0	<10,0	<10,0	<10,0	EPA 8260	µg/L	10
Xileno	<10,0	<10,0	<10,0	<10,0	<10,0	<10,0	<10,0	<10,0	<10,0	<10,0	<10,0	EPA 8260	µg/L	10

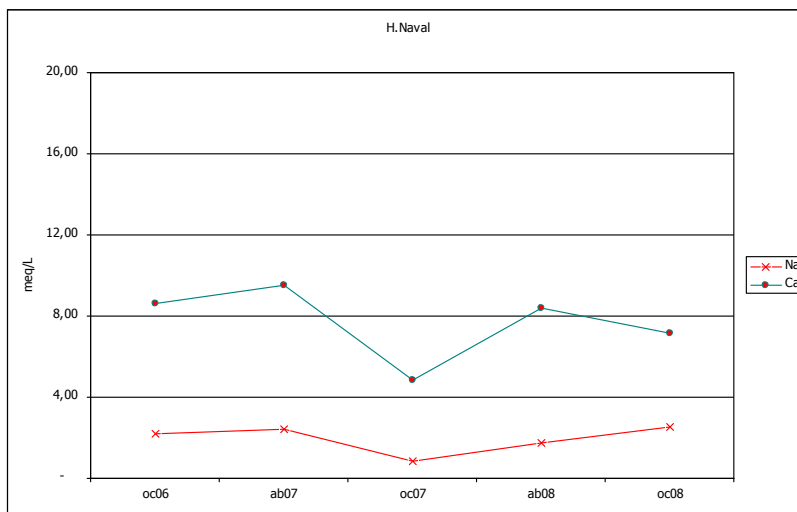
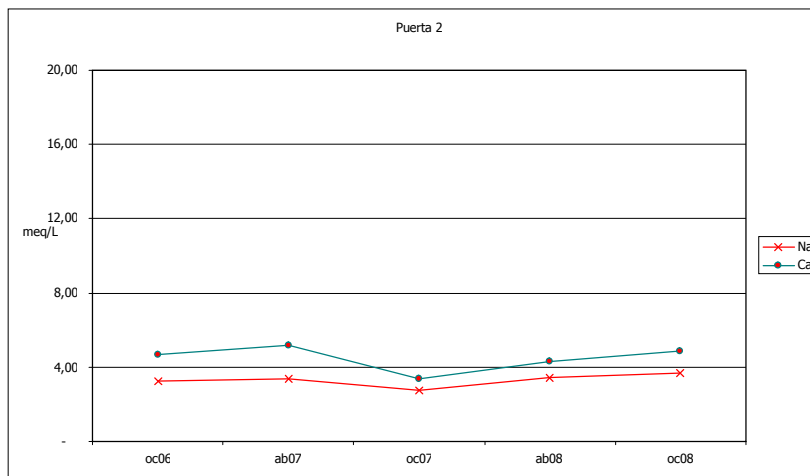
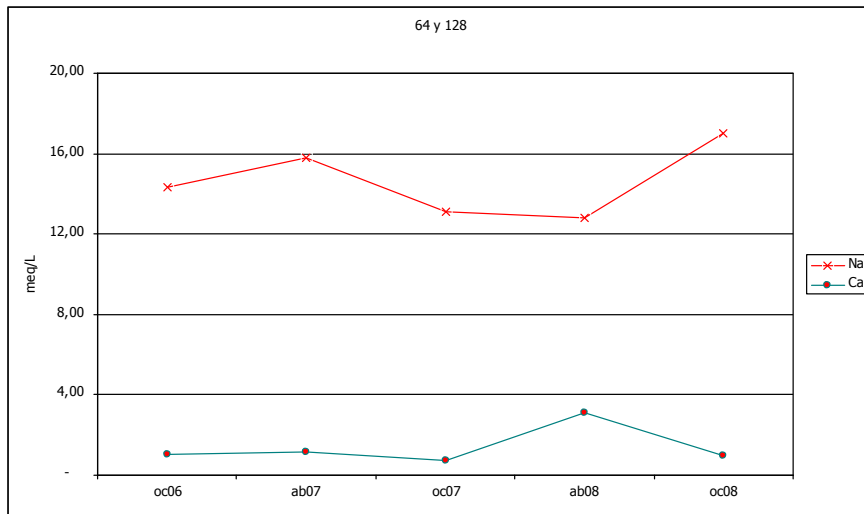
Pozo	Dique (F)	Tiro Federal (F)	Puerto (F)	Dique (PM)	Tiro Federal (PM)	Puerto (PM)	Dique (PU)	Tiro Federal (PU)	Puerto (PU)	Metodología		
Parámetros	oc08	oc08	oc08	oc08	oc08	oc08	oc08	oc08	oc08	de análisis	Unidad	LCM
Arsénico	0,15	< 0,01	< 0,01	<0,01	0,03	< 0,01	0,01	< 0,01	< 0,01	SM 3500/3114-C	mg/L	0,01
Benceno	<10,0	<10,0	<10,0	<10,0	<10,0	<10,0	<10,0	<10,0	<10,0	EPA 8260	mg/L	10
Bicarbonato	330,62	971,29	257,42	441,43	1165,48	547,43	635,74	1094,86	141,25	SM 2320-B	mg/L	0,5
Cadmio	<0,01	<0,01	<0,01	<0,01	<0,01	<0,01	<0,01	<0,01	<0,01	SM 3500/3111-B	mg/L	0,01
Calcio	30,84	28,24	69,36	33,93	48,70	62,38	152,00	436,00	1369,00	SM 3500 Ca-B	mg/L	0,5
Carbonato	<0,5	<0,5	<0,5	<0,5	<0,5	<0,5	<0,5	<0,5	<0,5	SM 2320-B	mg/L	0,5
Cinc	<0,01	<0,01	<0,01	<0,01	<0,01	<0,01	<0,01	<0,01	<0,01	SM 3500/3111-B	mg/L	0,01
Cloruro	139,30	81,29	81,29	134,05	504,07	2310,40	1253,15	3122,58	8721,13	SM 4500 Cl-B	mg/L	1
Cobalto	<0,02	<0,02	<0,02	<0,02	<0,02	<0,02	<0,02	<0,02	<0,02	SM 3500/3111-B	mg/L	0,02
Cobre	<0,02	<0,02	<0,02	<0,02	<0,02	<0,02	<0,02	<0,02	<0,02	SM 3500/3111-B	mg/L	0,02
Cond. Elect.	1566,67	1920,00	2000,00	2266,67	11100,00	7100,00	4900,00	13900,00	22383,33	SM 2510-B	µs/cm	0,1
Cromo	<0,02	<0,02	<0,02	<0,02	<0,02	<0,02	<0,02	<0,02	<0,02	SM 3500/3111-B	mg/L	0,02
Etilbenceno	<10,0	<10,0	<10,0	<10,0	<10,0	<10,0	<10,0	<10,0	<10,0	EPA 8260	µg/L	10
Fenoles totales	<0,05	<0,05	<0,05	<0,05	<0,05	<0,05	<0,05	<0,05	<0,05	SM 5530-C	mg/L	0,05
Fluoruro	<0,1	0,20	0,40	<0,1	0,85	0,72	0,54	1,10	0,63	SM 4110-B	mg/L	0,1
HCT	< 0,2	< 0,2	< 0,2	< 0,2	< 0,2	< 0,2	< 0,2	< 0,2	< 0,2	EPA 8015	mg/L	0,2
Magnesio	7,76	17,21	43,88	17,41	55,82	111,59	80,22	204,39	614,85	SM 3500/3111-B	mg/L	5
Mercurio	<0,001	<0,001	<0,001	<0,001	<0,001	<0,001	<0,001	<0,001	<0,001	SM 3500/3112-B	mg/L	0,001
Níquel	<0,01	<0,01	<0,01	<0,01	<0,01	<0,01	<0,01	<0,01	<0,01	SM 3500/3111-B	mg/L	0,01
Nitrato	<5,0	<5,0	<5,0	<5,0	<5,0	<5,0	<5,0	<5,0	<5,0	SM 4110-B	mg/L	5
Nitrito	<0,05	<0,05	7,10	<0,05	<0,05	<0,05	<0,05	<0,05	<0,05	SM 4110-B	mg/L	0,05
pH	7,50	7,37	7,18	7,53	7,30	7,80	7,10	6,73	6,73	SM 4500H*-B	upH	0,01
Plomo	<0,02	<0,02	<0,02	<0,02	<0,02	<0,02	<0,02	<0,02	<0,02	SM 3500/3111-B	mg/L	0,02
Potasio	12,23	39,75	11,51	20,53	55,00	80,67	27,17	66,00	97,00	SM 3500/3111-B	mg/L	1
Residuo Seco	1119,05	1371,43	1428,57	1619,05	7928,57	5071,43	3500,00	9928,57	15988,10	SM 2540-B	mg/L	1
Sodio	455,70	591,30	101,70	404,40	1334,80	1536,60	683,10	3060,10	3982,00	SM 3500/3111-B	µg/L	10
Sulfato	311,52	636,97	184,95	266,58	1478,97	582,51	349,91	1152,00	2044,10	SM 4500 SO4-E	mg/L	1
Sulfuro	<0,1	<0,1	<0,1	<0,1	<0,1	<0,1	<0,1	<0,1	<0,1	SM 4500 S D	mg/L	0,1
Tolueno	<10,0	<10,0	<10,0	<10,0	<10,0	<10,0	<10,0	<10,0	<10,0	EPA 8260	µg/L	10
Xileno	<10,0	<10,0	<10,0	<10,0	<10,0	<10,0	<10,0	<10,0	<10,0	EPA 8260	µg/L	10

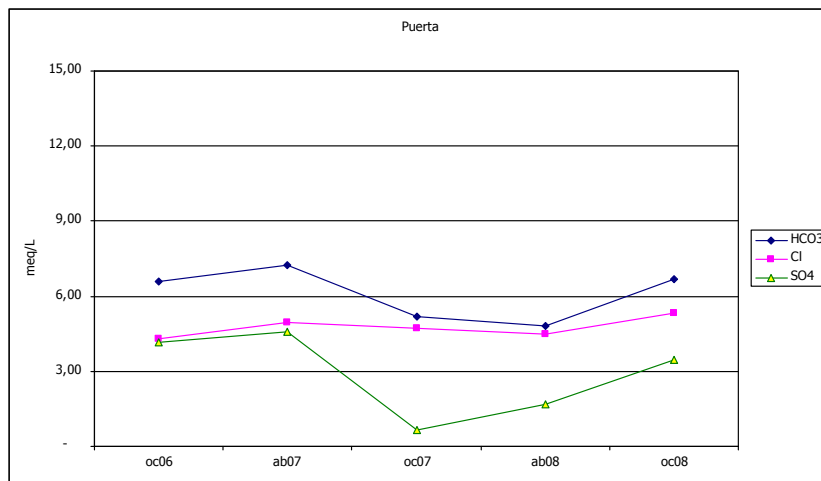
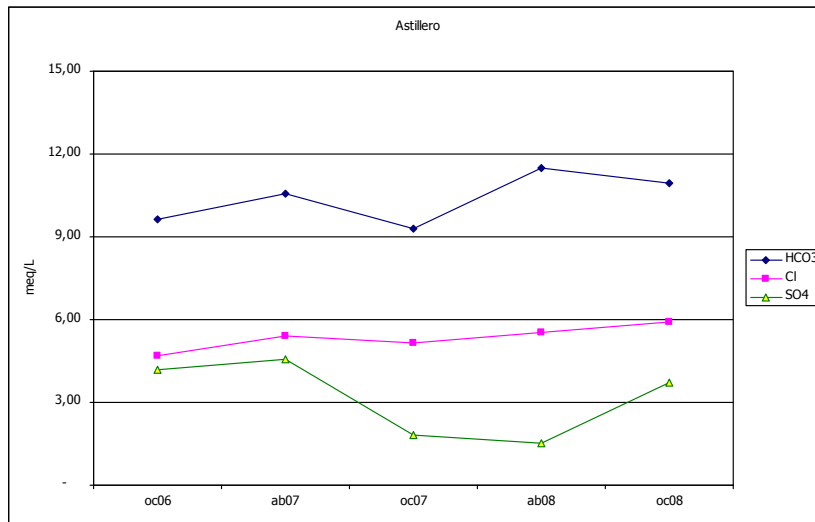
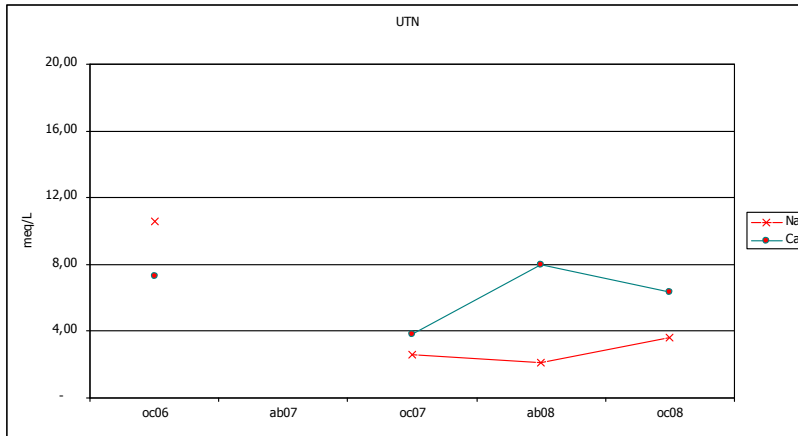
ANNEX 3
Chemical variations plots

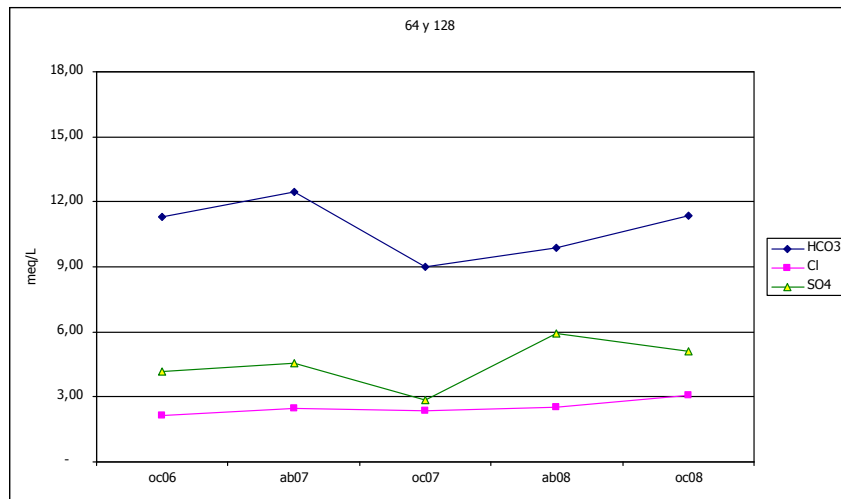
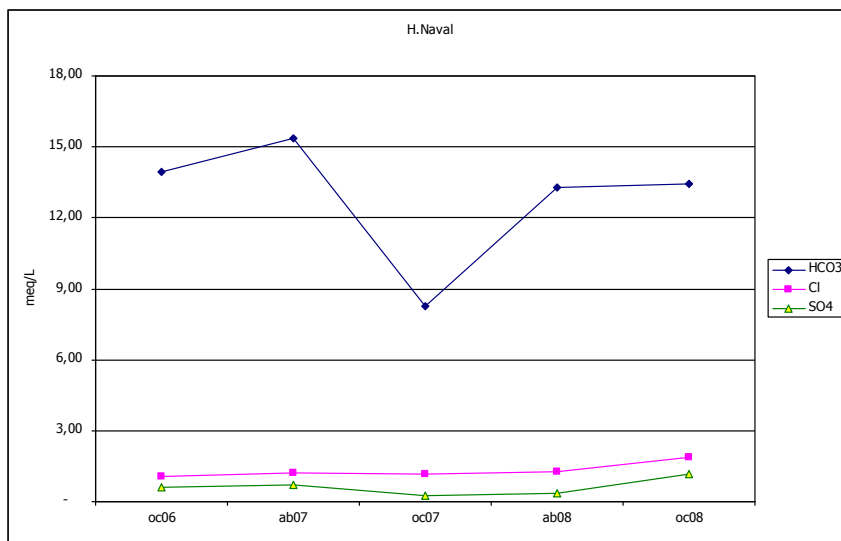
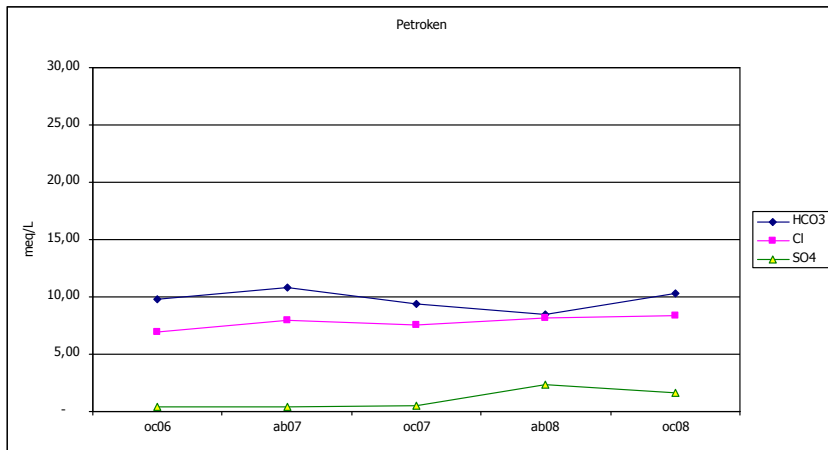


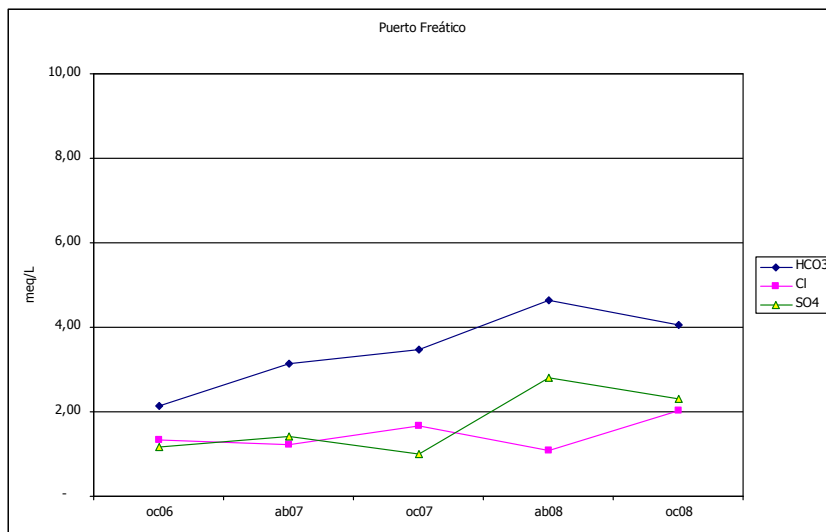
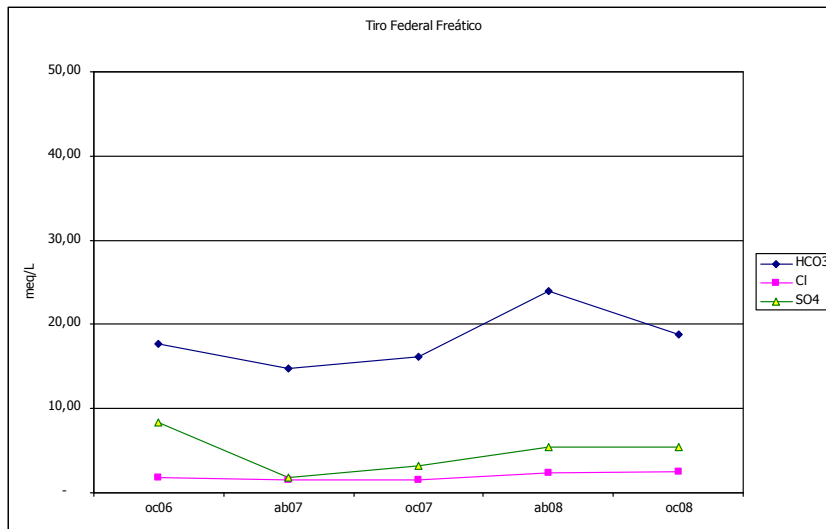
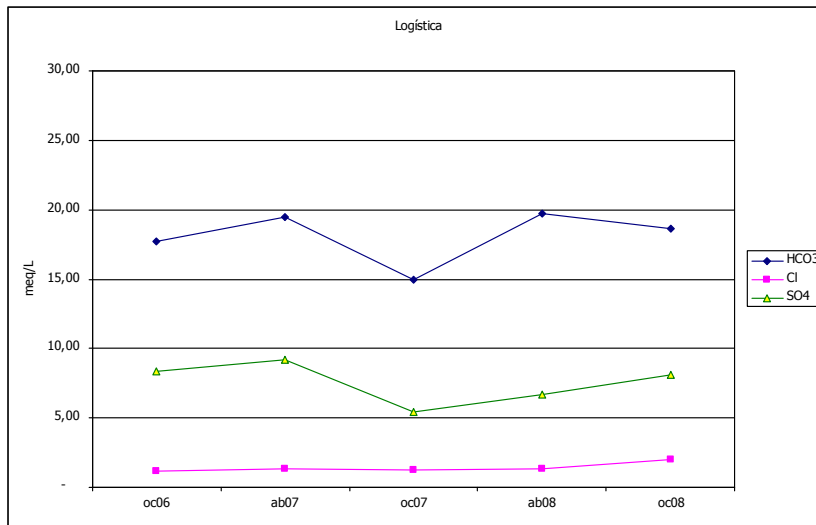


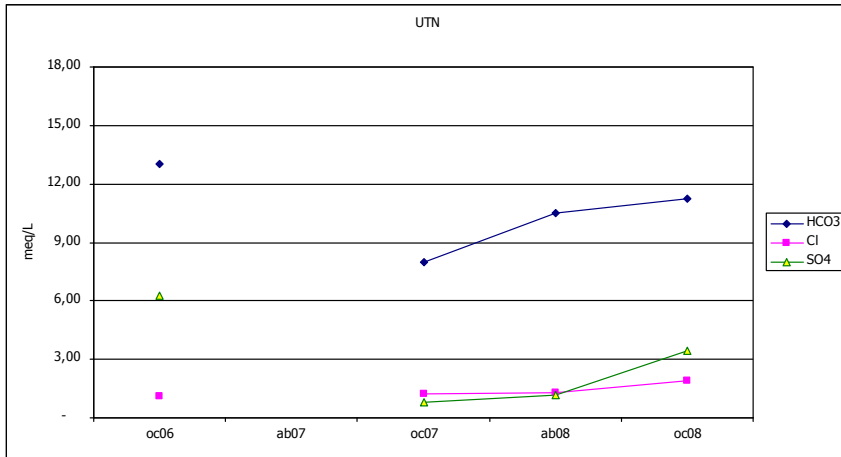
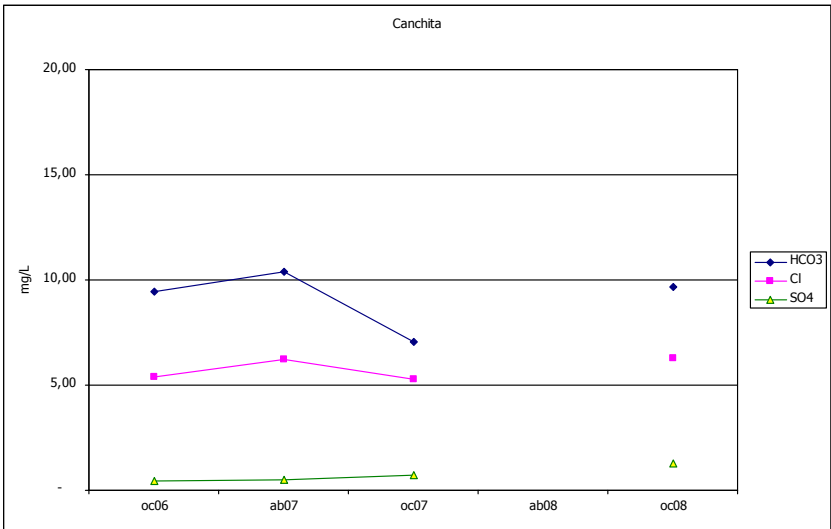
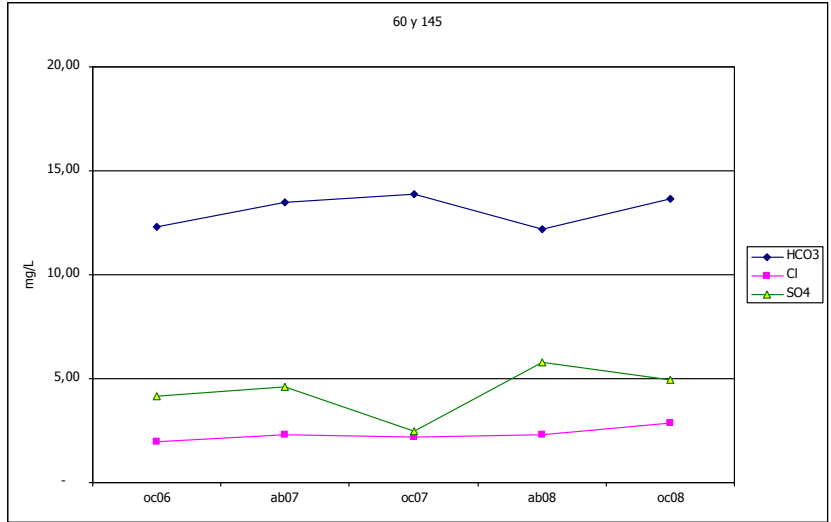


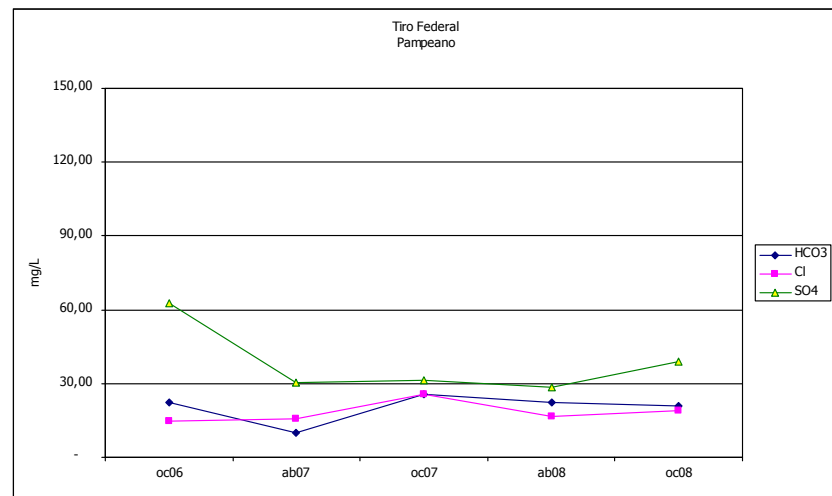
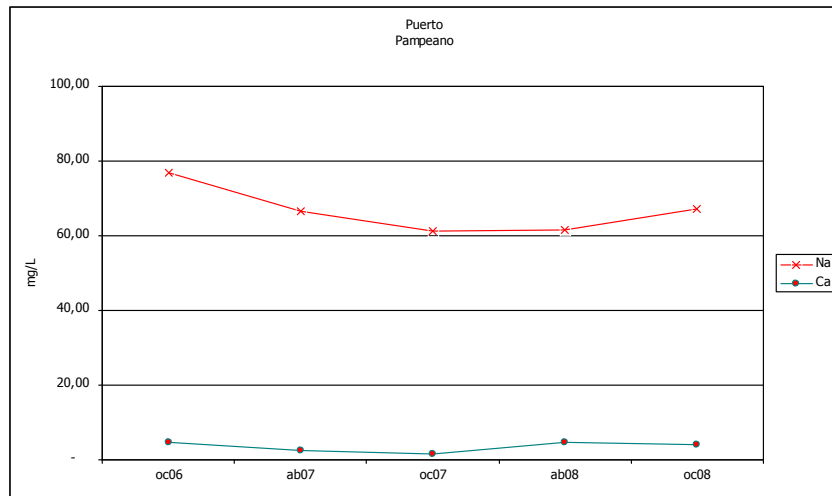
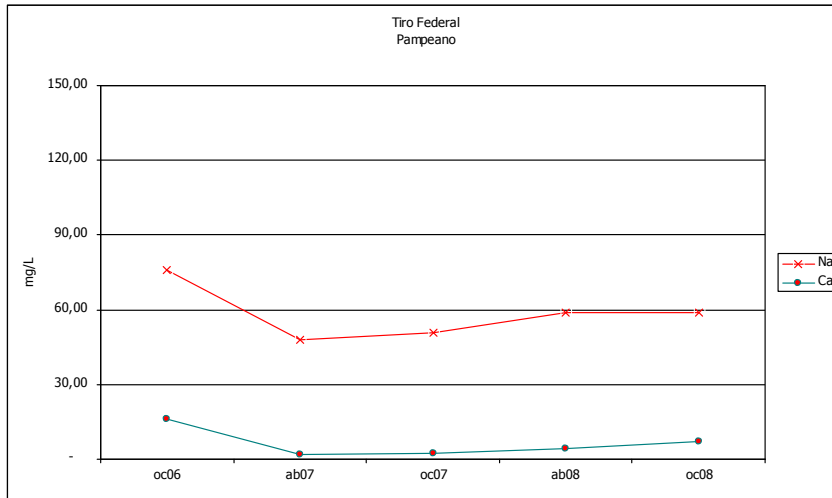


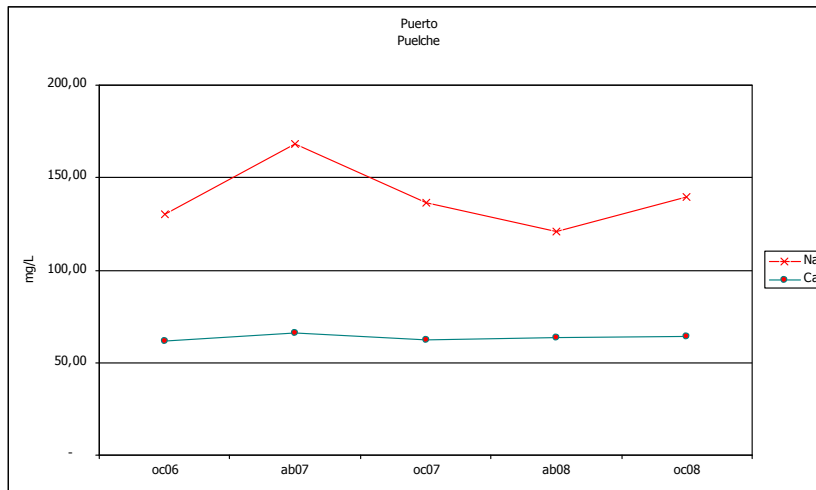
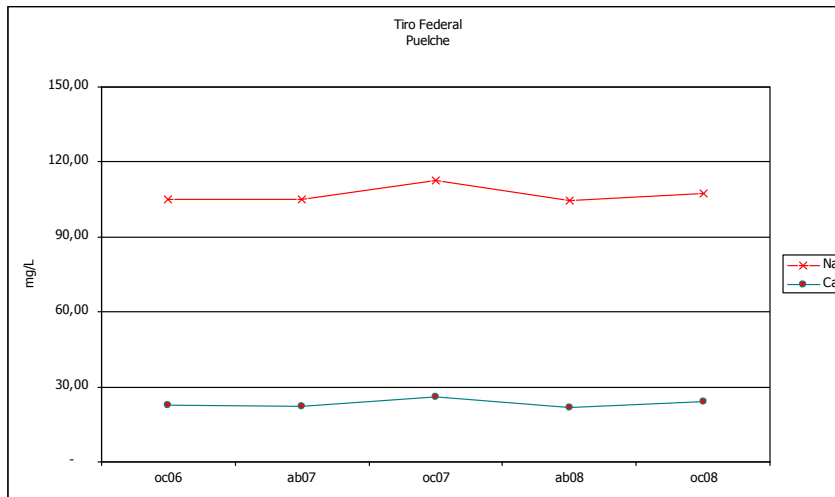
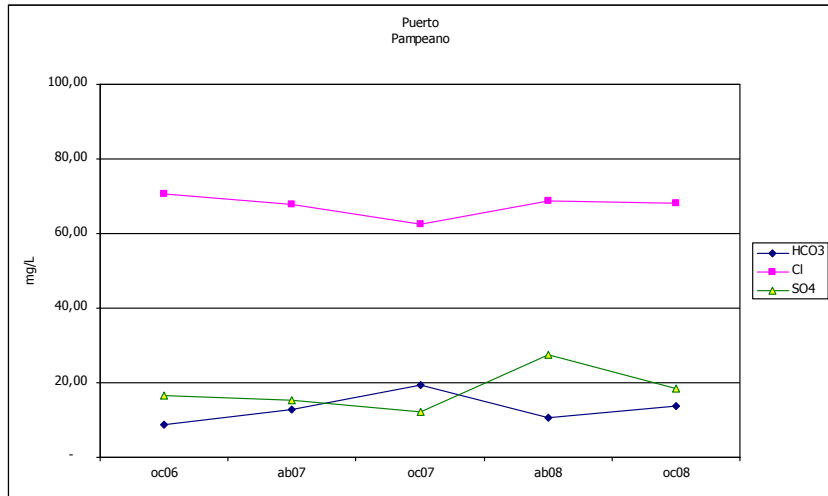


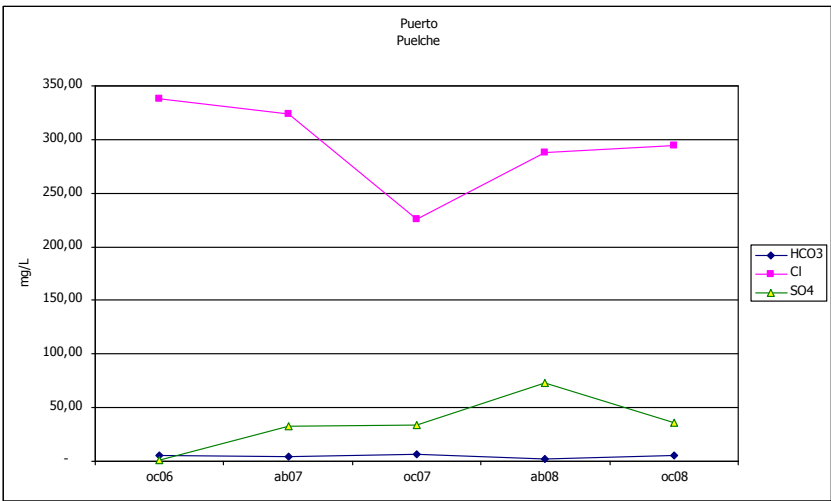
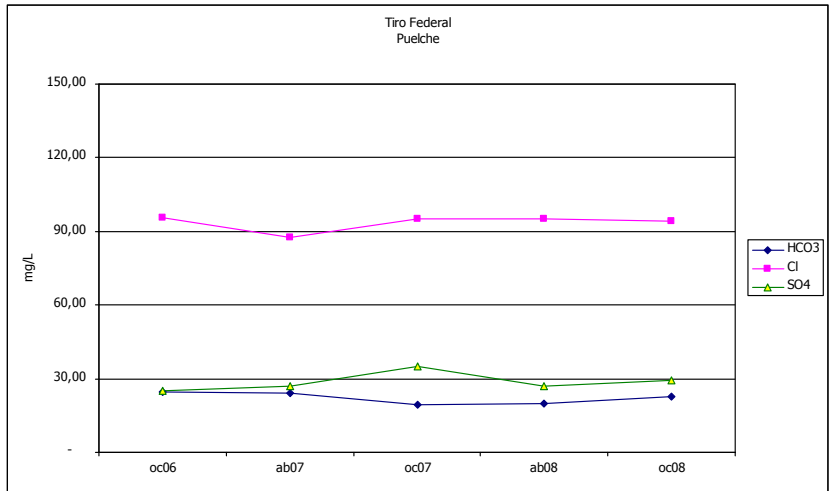












Dichiarazione di riproducibilità

(Legge 22 aprile 1941 n. 633, modificata dalla Legge 21 maggio 2004 n. 128, artt. 12-13)

Il sottoscritto (nome e cognome) Jerónimo Enrique Ainchil matricola 955399
nato a La Plata, Buenos Aires, Argentina il 19 gennaio 1962
iscritto alla Scuola/corso di dottorato di ricerca in Scienze Ambientali

Indirizzo

Autore della tesi di dottorato dal titolo:

COASTAL PLAIN IN NORTHEASTERN BUENOS AIRES PROVINCE:

HYDROGEOLOGICAL CHARACTERISTICS

consapevole delle conseguenze civili e penali derivanti da dichiarazioni mendaci, ai sensi degli artt. 75 e 76 del D.P.R 28/12/2000 n. 445

Dichiara che la propria tesi è:

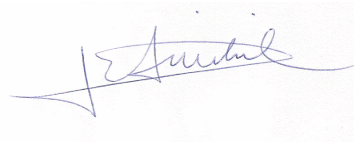
- riproducibile totalmente per motivi di studio
- riproducibile parzialmente, per motivi di studio, per le seguenti parti:
- non riproducibile

Autorizza la pubblicazione della versione digitale della tesi sui siti dell'Ateneo e delle Biblioteche Nazionali:

- sì
- no

Dichiara inoltre:

1. la completa corrispondenza tra la versione elettronica della tesi consegnata e la tesi in formato cartaceo;
2. di essere a conoscenza che l'Ateneo si riserva i diritti di riproduzione per scopi di ricerca e didattici, con citazione della fonte;
3. che il contenuto e l'organizzazione della tesi è opera originale da me realizzata e non compromette in alcun modo i diritti di terzi, ivi compresi quelli relativi alla sicurezza dei dati personali;
4. che pertanto l'Ateneo è in ogni caso esente da responsabilità di qualsivoglia natura civile, amministrativa o penale, e sarà da me tenuta indenne a qualsiasi richiesta o rivendicazione da parte di terzi;
5. che la tesi di dottorato non è il risultato di attività rientranti nella normativa sulla proprietà industriale, non è stata prodotta nell'ambito di progetti finanziati da soggetti pubblici o privati con vincoli alla divulgazione dei risultati, non è oggetto di eventuale registrazioni di tipo brevettale o di tutela.



Venezia, 15 novembre 2009

(firma del richiedente)

Estratto per riassunto della tesi di dottorato

L'estratto (max. 1000 battute) deve essere redatto sia in lingua italiana che in lingua inglese e nella lingua straniera eventualmente indicata dal Collegio dei docenti.

L'estratto va firmato e rilegato come ultimo foglio della tesi.

Studente: Jerónimo Enrique Ainchil _____ matricola: 955399 _____

Dottorato: Scienze Ambientali _____

Ciclo: XXII _____

Titolo della tesi¹ : COASTAL PLAIN IN NORTHEASTERN BUENOS AIRES PROVINCE:
HYDROGEOLOGICAL CHARACTERISTICS

Riassunto:

Tutti gli sforzi indirizzati alla conservazione ed al recupero ambientale richiedono molteplici informazioni per un'attività decisionale. In questo contesto è essenziale comprendere il comportamento delle componenti ambientali e la loro interazione.

L'acquisizione di dati e la elaborazione delle informazioni sono generalmente processi costosi. La tesi qui di seguito esposta prevede una sequenza di passi successivi, in cui ogni passo porta ad una maggiore comprensione dei differenti aspetti della idrologia nella zona costiera in NE di Buenos Aires (Argentina). Questo modello è la base necessaria per l'assunzione delle decisioni relative allo sviluppo economico e sociale dell'area in esame.

Le conclusioni evidenziano il contributo di ogni tecnica adottata alla costruzione di un modello. Alla fine, si può concludere che è fondamentale conoscere le caratteristiche delle risorse naturali per indirizzare le politiche di sviluppo regionale.

Abstract:

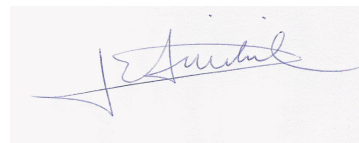
All the efforts aimed at environmental conservation and recovery require information for decision-making. In this context, it is essential to understand the behaviour of environmental components and their interrelation.

Data acquisition and information processing are usually expensive processes. Besides, they can last long periods of time. This thesis involves a sequence in which each step makes it possible to advance in better understanding of the different aspects of the coastal zone in NE of Buenos Aires (Argentina) hydrogeology, concluding in the proposal of a model. This model is the necessary basis for decision-making related to economic and social development of the analysed area. This area included an important industry activity.

The conclusions highlight the contribution of each technique to the construction of a model and the advantages of constructing a model integrating the information processed by the methodologies used.

Finally, it should be noted that it is significant to know the features of natural resources to establish regional development policies.

Firma dello studente



¹ Il titolo deve essere quello definitivo, uguale a quello che risulta stampato sulla copertina dell'elaborato consegnato.